This is to certify that the
dissertation entitled

CARBENE COMPLEXES, BIS(IMIDO) COMPLEXES, AND TITANIUM HYDROAMINATION CATALYSTS

presented by

JAMES THADDEUS CISZEWSKI

has been accepted towards fulfillment
of the requirements for the

Ph.D. degree in Chemistry

Aaron L. Ellis
Major Professor's Signature

12/17/04
Date

CARBENE COMPLEXES, BIS(IMIDO) COMPLEXES, AND TITANIUM ALKYNE HYDROAMINATION CATALYSTS

By

James Thaddeus Ciszewski

A DISSERTATION

Submitted to
Michigan State University
in partial fulfillment of the requirements
for the degree of

DOCTOR OF PHILOSOPHY

Department of Chemistry

2004

ABSTRACT

CARBENE COMPLEXES, BIS(IMIDO) COMPLEXES, AND TITANIUM ALKYNE HYDROAMINATION CATALYSTS

By

James Thaddeus Ciszewski

Several new chelating dipyrrolyl ligands based on *N*,*N*-di(pyrrolyl-α-methyl)-*N*-methylamine (dpma) have been synthesized, including a compound containing a norbornenyl group (H_2dpna) and a compound containing a chiral menthyl group (H_2dpCHIRA). Dipyrrolylmethane derivatives have also been investigated as chelating dipyrrolyl ligands for metal complexes.

The group-6 complexes $M(NBu^t)_2$(dpma), where M = Cr, Mo, and W, have been synthesized and characterized by single-crystal x-ray diffraction, which shows that the axial imido ligand is significantly bent compared to the linear imido group. Variable temperature ^{1}H NMR indicates that the imido ligands remain inequivalent from -80 °C to +80 °C. ^{1}H, ^{13}C, and ^{14}N NMR data have been used to investigate the imido group inequivalencies. DFT calculations have been performed to determine the energies associated with straightening the axial (bent) imido ligand, and indicate that the spectroscopic differences between the two imido ligands is due to the different chemical environments (axial versus equatorial).

The dpma ligand has been incorporated into several different molybdenum and ruthenium alkylidene species. These five-coordinated complexes do not perform metathesis reactions, probably due to steric and electronic effects imposed by the dpma ligand. Another complex containing the 5,5-dimethyldipyrrolylmethane ligand (dmpm), shows metathesis activity at elevated temperatures, but decomposition of the complex at these

temperatures prohibits the use of this complex as a metathesis catalyst.

The first group-6 imido self-tethered alkylidene has been prepared. The tethered complex shows no sign of ring strain. The complex is unstable to alkoxide substitution.

Cyclooctyne has been found to react in a [2+2] manner with molybdenum and tungsten bis(imido) dichloride complexes. The alkylidene product isolated in both cases contains two equivalents of cyclooctyne, and is stable to metathesis conditions. Chemical and thermal decomposition of these complexes results in a novel pyrrole containing the two cyclooctyne molecules. The tungsten complex reacts with 50% aqueous sulfuric acid to yield a dinuclear μ-oxo oxide complex containing the inserted cyclooctyne molecules.

Titanium complexes containing the dpma and dmpm ligands, as well as $Ti(NMe_2)_4$, have been found to be active catalysts for the hydroamination of alkyne with amines. These catalysts exhibit different selectivity, indicating that the active catalysts in each case is different.

Dedicated to the memories of my dad, Richard Thomas Ciszewski,
and my Auntie Verba.

ACKNOWLEDGMENTS

This research was carried out with generous support of Michigan State University, The United States Department of Energy, and The Office of Naval Research. The writer gratefully appreciates the support of the Department of Chemistry at Michigan State University for a Brubaker Fellowship and a Dye Fellowship, as well as the use of instruments and laboratory space.

Thanks also to my Dissertation Committee for the helpful advice with many different things, personal and professional. Thank you to Dr. Wulff, for taking the time to read this dissertation, and to be on my committee. I especially appreciate the help of Prof. James McCusker for listening and putting things into perspective. The time and effort put into my research by Prof. Mitch Smith has been remarkable, and I owe much of what I have been able to accomplish to his dedication and time, especially in Odom/Smith Group Meetings. Also thanks are due to Profs. Beck and Posey for the time and effort they put in on my committee.

The people I have worked with over the last five and one-half years have also played a large part in my success. Angie, my friend and box mate, helped me with this research, made me laugh, made me realize things ('cause it hit me that Montana was really just a leg, and then just like that it all fell into place), and sang with me. Chris and JD, good friends who helped change the catalyst on so many glove boxes so many times, helped me learn to do air-sensitive chemistry, let me use their glassware and, in the case of JD, always walked too fast. Paul (aka Dr. Worm) who helped me learn how to do things in lab, played "The Time is Wrong" with me (although he usually lost), and made me laugh the first couple of years I was here. Yahong, who helped me not get buried with crystal structures, helped when I needed it, and was just a good friend who always had a smile on her face. Dan let me rant when I needed to, and has been a good friend the last few years. Thanks

to Kin, my friend, who I used as an example of how hard to work. Ben helped me purify a few things (especially H_2dpCHIRA) and was always there to talk to. Sarah helped me a lot with various COGS-related things, and the way she stood by me and helped me when I needed help the most, I'll never forget. Amanda, Emily, Andrea, and Kapil have been there to listen and talk to over the last couple of years.

Much thanks goes to Bob Rasico, who helped immensly with getting the new lab in order, and a multitude of other stuff that needed to be fixed and/or changed. Thanks also to Melissa Parsons; Bill Fritz; Manfred Langer and Scott Bankroff in the Glass Shop; Kermit Johnson and Long Lee in the NMR facility; Rui Huang; Don Ward; Glenn Wesley and Tom Bartlett in the Machine Shop; Scott Sanderson and Dave Cedarstaff in the Electronics Shop; Tom Geissenger and Bill Flick in Stores; Karen Maki, Lisa Coye, and Beth McGaw in the Business Office; Nan Murray; Debbie Roper; and Lisa Dillingham.

Much of the work in this dissertation has been done by and with Ms. Angie Turnas, Dr. Changsheng Cao, Mr. Cliff Foster, Mr. Chris Hall, Ms. Shannon Harris, Dr. Yahong Li, Dr. Yanhui Shi, and Dr. Baohan Xie, and I appreciate their assistance. I would like to mention especially the assistance of Prof. James F. Harrison with the computations included in this work.

A special thanks must go to my advisor, Prof. Aaron Odom, for his understanding, patience, and support through this research. I hope that I have done my part in securing his future at Michigan State, as he has done his part in helping me throughout the process of getting this research done and becoming an inorganic (or organometallic) chemist.

Thank you to Laura, for being understanding and encouraging when I decided to return to school.

The encouragement and help of my family is appreciated more than they can know. My mom, who was always patient and supportive, and my sisters Cindy, Kathy, and Sue, who have always been there for me. And thank you also to Dr. Michael Thomas and Rosemary Thomas for their support and generosity over the last two years, and a special thanks

to Rosemary Thomas for proofreading this work.

Finally, I want to thank Carrie for all of her love and support the last two years. I couldn't have finished without her and I'm looking forward to our future together.

PREFACE

The bulk of this work has previously been published elsewhere. Chapter 2 is an expanded version of the article "Investigation of Transition Metal–Imido Bonding in $M(NBu^t)_2$(dpma)", *Inorg. Chem.* **2004**, *43*, 3605-3617 by James T. Ciszewski, James F. Harrison, and Aaron L. Odom.

Chapter 4 is based on "Synthesis of and Structure of an imido-tethered Schrock carbene of molybdenum", *Dalton Trans.* **2004**, 4226-4227 by James T. Ciszewski, Baohan Xie, Changsheng Cao, and Aaron L. Odom.

Chapter 5 is adapted from "Group-6 Imido Activation by a Ring-Strained Alkyne", *Organometallics* **2004**, *23*, 5386-5388 by James T. Ciszewski, Kapil S. Lokare, and Aaron L. Odom.

Chapter 6 is a compilation of the work that appeared in "Titanium η^1-Pyrrolyl Complexes: Electronic and Structural Characteristics Imposed by the *N*,*N*-Di(pyrrolyl-α-methyl)-*N*-methylamine (dpma) Ligand", *Inorg. Chem.* **2001**, *40*, 1987-1988 by Shannon A. Harris, James T. Ciszewski, and Aaron L. Odom; "$Ti(NMe_2)_4$ as a Precatalyst for Hydroamination of Alkynes with Primary Amines", *Organometallics* **2001**, *20*, 3967-3969 by Yanhui Shi, James T. Ciszewski, and Aaron L. Odom; "Hydroamination of Alkynes Catalyzed by a Titanium Pyrrolyl Complex", *Organometallics* **2001**, *20*, 5011-5013 by Changsheng Cao, James T. Ciszewski, and Aaron L. Odom; "Group-4 η^1-Pyrrolyl Complexes Incorporating *N*,*N*-Di(pyrrolyl-α-methyl)-*N*-methylamine", *Inorg. Chem.* **2002**, *41*, 6298-6306 by Yahong Li, Angie Turnas, James T. Ciszewski, and Aaron L. Odom; and "Titanium dipyrrolylmethane derivatives: rapid intermolecular alkyne hydroamination" *Chem. Commun.* **2003**, 586-587 by Yanhui Shi, Christopher Hall, James T. Ciszewski, Changsheng Cao, and Aaron L. Odom.

Images in this dissertation are presented in color.

TABLE OF CONTENTS

LIST OF TABLES

LIST OF FIGURES

LIST OF SCHEMES

LIST OF CHARTS

LIST OF ABBREVIATIONS

dpma: *N*,*N*-di(pyrrolyl-α-methyl)-*N*-methylamine

dpna: *N*,*N*-di(pyrrolyl-α-methyl)-*N*-(1-methyl-norborn-5-ene) amine

dpCHIRA: *N*,*N*-di(pyrrolyl-α-methyl)-*N*-[(1S,2S,5R)-1-(2-isopropyl-5-methyl)-cyclohexyl]amine

dppm: 5,5-di-*n*-propyldipyrrolylmethane

dmpm: 5,5-dimethyldipyrrolylmethane

Bu^t: *tert*-butyl

Ndip: 2,6-diisopropylphenyl

Ar: an aromatic group

ppm: parts per million

DME, dme: 1,2-dimethoxyethane

THF, thf: tetrahydrofuran

CHAPTER 1

CHELATING PYRROLYL LIGANDS

Introduction

Pyrrole is currently undergoing a renaissance as a ligand for early transition metals. Previously, the pyrrole group was used primarily as the building block for macrocylic ligands, i.e. the ubiquitous porphryns and pthalocyanines.[1] Recently, several groups, including the Odom group at Michigan State University, have begun to study smaller pyrrole containing ligands.

This sudden interest in the use of pyrrole in ligands can be attributed to several factors, the primary one being the aromaticity of the pyrrole molecule. While the estimated aromatic stabilization energy of pyrrole, ~23 kcal/mole, is less than that of benzene at ~35 kcal/mole, this stabilization results in the pyrrolyl nitrogen atom being decidedly non-basic, primarily because the lone pair electrons of the nitrogen atom is delocalized in order to complete the 6-electron π-system of pyrrole.[2]

In transition metal complexes, the pyrrolyl π-system and the metal center can compete for the lone pair of electrons on the nitrogen atom, allowing for the stablization of both high and low oxidation-state metal centers (eq 1-1). Low oxidation-state metal

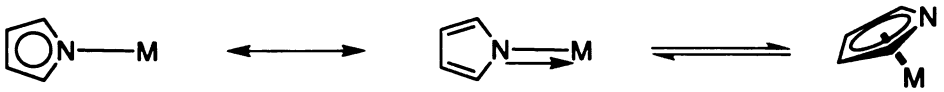

(1-1)

centers would be expected not to compete as effectively for the lone pair electrons as the π-system, resulting in an η^1 linkage through a deprotonated pyrrole nitrogen atom. High oxidation-state metal centers would be expected to be more competitive for the lone pair electrons, either disrupting the aromatic system, or bonding through it.

Additionally, pyrrole is an attractive building block for ligand synthesis because it readily undergoes substitution chemistry, making it easily incorporated into complex ligands.[3] For example, the Mannich reaction between pyrrole, formaldehyde, and a wide variety of aliphatic amines (vide infra) gives high yields of tridentate dipyrrolyl ligands.

There are also many ways of introducing substituents to the pyrrole ring itself, affording an easy way of altering the electronics of the aromatic π-system.

Syntheses of several multi-dentate ligands incorporating the pyrrole ring has been accomplished. These syntheses, as well as the use of these compounds as ligands in early transition metal chemistry, are detailed below.

Results and Discussion

Ligands derived from amines. *N,N*-Di(pyrrolyl-α-methyl)-*N*-methylamine (H_2dpma, **1**) is synthesized as shown in eq 1-2. Carrying out the reaction at a lower temperature, 55 °C, decreases side products and eliminates the need for chromatography. This results in a higher yield than the preparation of Raines.[4] The ORTEP diagram obtained by single-crystal x-ray analysis is shown in Figure 1-1.

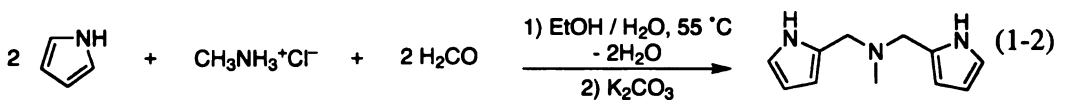

1 (1-2)

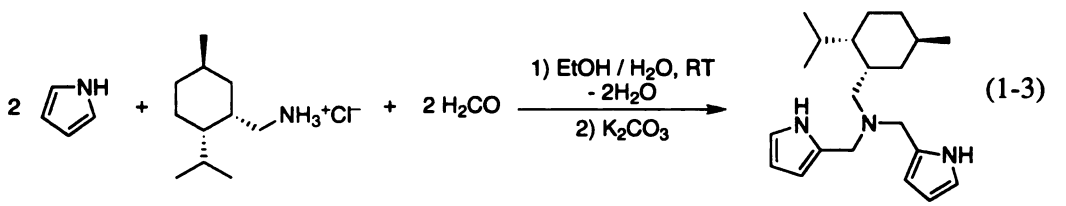

2 (1-3)

Interestingly, the methylamine hydrochloride can be replaced by a wide variety of amine hydrochlorides. This enables the synthesis of a variety of ligands with widely varying steric and electronic properties, while still retaining the chelating dipyrrole properties of the parent ligand. For example, the inclusion of a chiral menthol group in the ligand, eq 1-3, results in a ligand, H_2dpCHIRA (**2**). Alternatively, a functional group may be introduced into the ligand this way, as in the synthesis of H_2dpna (**3**), eq 1-4. Several of these novel ligands have been prepared.

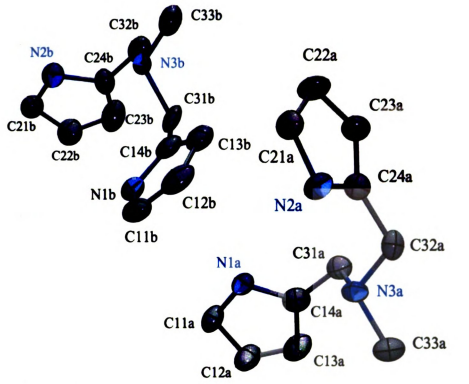

Figure 1-1. The ORTEP representation (50% probability ellipsoids) of H_2dpma, **1**, obtained by single-crystal x-ray diffraction, showing the two indistingishable molecules in the asymmetric unit.

However, a few amines did not yield the desired ligands. For example, *t*-butylamine hydrochloride yielded only the product where the *t*-butylamine was monosubstituted, and attempts to produce a ligand based on 4-(ethylamine)-styrene were unsuccessful, yielding only thick, intractable oils.

Single crystal x-ray analysis of two of these ligands, H_2dpma (Figure 1-1) and H_2dpna (Figure 1-2), shows the connectivity of the atoms. The bond lengths and bond

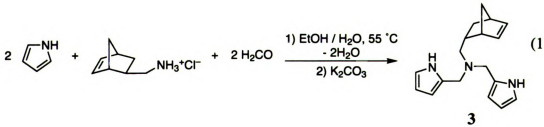

(1-4)

3

angles in these structures are unremarkable. Structural parameters of the crystal structures of H_2dpma and H_2dpna are given in Table 1-1.

Reaction of these ligands with slightly more than two equivalents of *n*-butyl lithium generates, in excellent yields, the dilithium salts of the ligands. These salts can be used in substitution chemistry with metal halides as an effective means of introducing the ligand to a metal center.

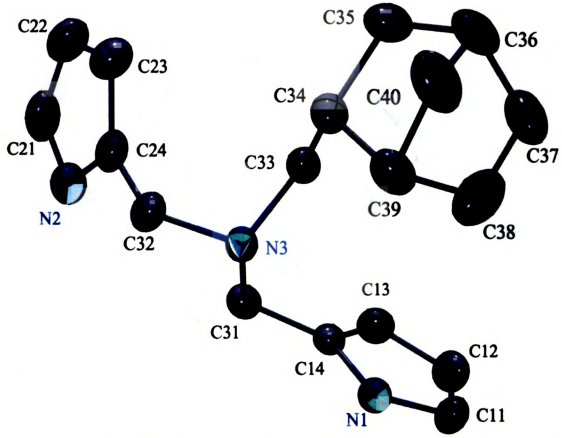

Figure 1-2. The ORTEP representation (50% probability ellipsoids) of H_2dpna (**3**), obtained by single-crystal x-ray diffraction.

Ligands derived from ketones. In order to change the electronic and steric properties of the H_2dpma-type ligands, a slightly altered dipyrrolyl ligand without the donor amine group was envisioned. The work of Lindsey's group with dipyrrolylmethanes gave the appropriate ligands.[5] The acid-catalyzed condensation of two equivalents of pyrrole

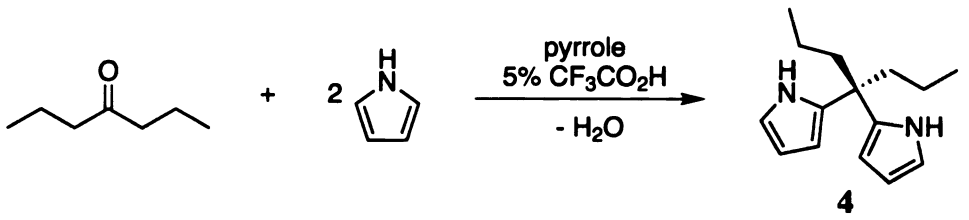

(1-5)

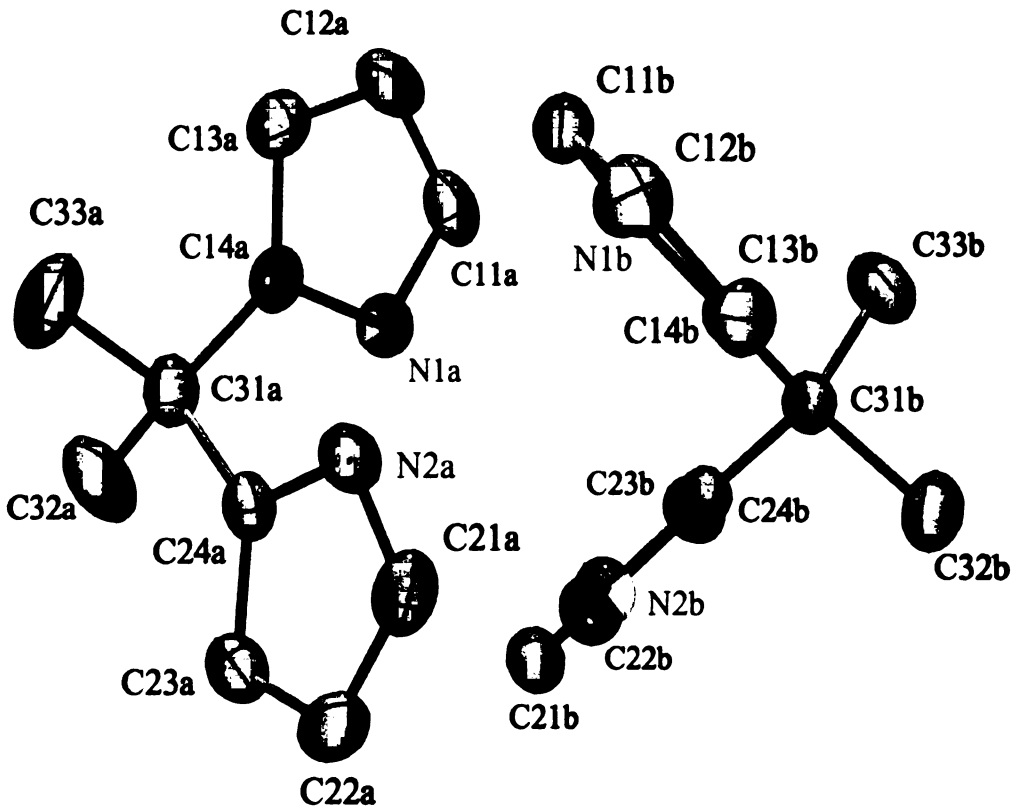

Figure 1-3. The ORTEP representation (50% probability ellipsoids) of 5,5–dimethyl-dipyrrolylmethane (H_2dmpm) obtained by single-crystal x-ray diffraction, showing the two chemically equivalent molecules in the asymmetric unit.

with aldehydes or ketones rapidly form the dipyrrolylmethane derivatives, for example the synthesis of 5,5–di-*n*-propyldipyrrolylmethane (H_2dppm, **4**), eq 1-5. The aldehyde or ketone used may be varied extensively, including aliphatic and aromatic compounds.

Single-crystal x-ray analysis of 5,5–dimethyl-dipyrrolylmethane (H_2dmpm) (Figure 1-3), shows the connectivity of the atoms. As in the case of H_2dpma and H_2dpna, the bond

Table 1-1. Structural parameters for H_2dpma (**1**), H_2dpna (**3**), and H_2dmpm from single–crystal x-ray diffraction.

	H_2dpma	H_2dpna	H_2dmpm
Formula	$C_{11}H_{15}N_3$	$C_{18}H_{23}N_3$	$C_{22}H_{28}N_4$
Formula weight	189.26	281.39	348.48
Space Group	P3(1)	P–1	P–1
a (Å)	14.094(4)	7.6219(9)	8.434(3)
b (Å)	14.094(4)	9.8910(12)	9.197(3)
c (Å)	9.288(3)	10.9370(13)	13.232(4)
α (°)	90	72.509(2)	99.838(7)
β (°)	90	83.640(2)	95.449(7)
γ (°)	120	77.710(3)	97.257(7)
Volume (Å^3)	1597.7(8)	767.41(16)	996.0(6)
Z	6	2	2
μ (mm^{-1})	0.073	0.073	0.070
$D_{calc.}$ (g cm^{-3})	1.180	1.218	1.162
$R(F_0)$ (I > 2s)	0.0988	0.0536	0.0405
$R_w(F_0)$ (I > 2s)	0.2636	0.1209	0.0811

lengths and the bond angles of the pyrrole rings in H_2dmpm are unremarkable. Structural parameters are included in Table 1-1.

As in the case of the H_2dpma derivatives, the dipyrromethanes react with *n*-butyl lithium to give the dilithium salts, which enables the introduction of the ligands to a wide variety of metal centers.

Experimental

General considerations. All manipulations were carried out in an MBraun drybox under a purified nitrogen atmosphere unless stated otherwise. Anhydrous ether

was purchased from Columbus Chemical Industries, Inc. and freshly distilled from purple sodium benzophenone ketyl. Toluene was purchased from Spectrum Chemical Mfg. Corp. and purified by refluxing over molten sodium under nitrogen for at least 2 days. Pentane (Spectrum Chemical Mfg. Corp.), tetrahydrofuran (JADE Scientific), 1,2-dimethyoxyethane (DME, Aldrich Chemical Company), and benzene (EM Science) were distilled from purple sodium benzophenone ketyl. Dichloromethane (EM Science) and acetonitrile (Spectrum Chemical) were distilled from calcium hydride. Deuterated solvents were dried over purple sodium benzophenone ketyl (C_6D_6) or P_2O_5 ($CDCl_3$) and distilled under nitrogen. 1-(methylamine)-5-norbornene[6] and (1*S*, 2*S*, 5*R*)-1-cyano-2-isopropyl-5-methylcyclohexane[7] were synthesized as reported. Other compounds were purchased from commercial sources. Liquids were distilled under purified nitrogen or in vacuo prior to use.

^1H and ^{13}C spectra were recorded on Varian spectrometers at the Max T. Rogers NMR facility at Michigan State University. ^1H and ^{13}C assignments were confirmed with the use of two-dimensional ^1H–^1H and ^{13}C–^1H correlation NMR experiments when necessary. All spectra were referenced internally to residual protiosolvent (^1H) or solvent (^{13}C) resonances. Chemical shifts are quoted in ppm and coupling constants in Hz. Common coupling constants are not reported. ^{14}N NMR spectra were collected on a VXR-500 spectrometer and are referenced to external neat CH_3NO_2. ^{14}N NMR spectra can also be internally referenced to dissolved natural abundance $^{14}N_2$, which was invariably noticeable in our samples prepared under purified nitrogen, at –72 ppm ($\nu_{1/2}$ = 50-80 Hz) in C_6D_6 versus neat nitromethane. ^{14}N NMR spectra were deconvoluted using Varian software, and data reported are from the spectral deconvolutions.

General considerations for x-ray diffraction. Crystals grown at –35 °C were moved quickly from a scintillation vial to a microscope slide containing Paratone N. Samples were selected and mounted on a glass fiber in wax and Paratone. The data collections were carried out at a sample temperature of 173(2) K on a Bruker AXS three-circle goniometer with a

CCD detector. The data were processed and reduced utilizing the program SAINTPLUS supplied by Bruker AXS. The structures were solved by direct methods (SHELXTL v5.1, Bruker AXS) in conjunction with standard difference Fourier techniques.

***N,N*-di(pyrrolyl-α-methyl)-*N*-methylamine (H_2dpma, 1).** This preparation is a modification of the literature procedure. To a solution of methylamine hydrochloride (6.7 g, 99 mmol) in 100 mL of absolute ethanol heated in a 55 °C oil bath was added aqueous formaldehyde solution (37%, 16.2 g, 200 mmol). After most of the methylamine hydrochloride was dissolved, pyrrole (13.4 g, 200 mmol) was added to the reaction mixture. The resulting mixture was refluxed at 55 °C for 4 h, and volatiles were removed under reduced pressure yielding a viscous oil. The oil was triturated with ether to give a white solid. The solid was then dissolved in water, basified with 5% K_2CO_3, and extracted with ether. Additional K_2CO_3 was added if needed, and the aqueous phase was extracted twice more with ether. The organic layers were combined, and volatiles were removed in vacuo. The resulting oil was crystallized from benzene/hexanes at –35 °C yielding the product as a white solid, m 70–72 °C (lit 74–76 °C).[4] Yield: 13.7 g (72%). ^{1}H NMR (300 MHz, $CDCl_3$): δ = 8.38 (m, 2H, N(*H*)-pyrrole), 6.59 (m, J_1 = 0.97 Hz, J_2 = 1.47, J_3 = 1.22 Hz, 2H, 5-C_4H_3N), 6.01 (m, J_1 = 2.68 Hz, J_2 = 3.18, 2H, 4-C_4H_3N), 5.93 (m, 2H, 3-C_4H_3N), 3.37 (s, 4H, $C_4H_3NCH_2N$), 2.07 (s, 3H, $C_4H_3NCH_2NMe$). ^{13}C NMR ($CDCl_3$): δ = 127.53 (2-C_4H_3N), 117.95 (5-C_4H_3N), 108.50 (4-C_4H_3N), 107.86 (3-C_4H_3N), 53.37 ($C_4H_3NCH_2N$), 41.52 (dpma-N*Me*). ^{14}N NMR (C_6D_6): δ = –234 ($\nu_{1/2}$ = 1160 Hz).

Li_2dpma. A solution of H_2dpma (5.00 g, 26.4 mmol) in approximately 100 mL of toluene was cooled to near frozen in a liquid nitrogen cold well within the dry box. To the stirring cold solution, 1.6 M *n*-butyl lithium (35 mL, 56 mmol, 2.12 equiv.) was slowly added by pipette. The product precipitated as a white solid during addition. When addition was complete, the solution was stirred for 5 min, then 100 mL of pentane was added. The solid was collected on a frit and was washed repeatedly with pentane. Drying in vacuo yielded Li_2dpma (5.30 g, 26.4 mmole, >99.9 %), mp 148 °C dec. ^{1}H NMR (300 MHz,

THF-d_8): δ = 6.66 (s, 2H), 5.91 (s, 2H), 5.83 (s, 2H), 3.55 (br s, 4H, $C_4H_3NCH_2N$), 2.24 (s, 3H, $C_4H_3NCH_2N$*Me*). ^{13}C NMR ($CDCl_3$): δ = 139.44, 126.93, 107.61, 105.50, 58.81 ($C_4H_3NCH_2N$), 42.87 (dpma-N*Me*).

***N,N*-di(pyrrolyl-α-methyl)-*N*-(1-methyl-norborn-5-ene)amine (H_2dpna, 2).** To a solution of 16.0 g 1-(methylamine)-5-norbornene hydrochloride (0.100 mol) in 200 mL of 95% ethanol in a 55 °C oil bath was added 16.2 g 37% formalin solution (5.99 g formaldehyde, 0.200 mol), causing most of the solid to dissolve. To this solution was added 13.4 g pyrrole (0.2000 mol), and the reaction was stirred for 5 h. After cooling overnight, the solution was poured into 400 mL 5% aqueous K_2CO_3, then extracted four times with 200 mL portions of diethyl ether. The combined ether layers were decolorized with activated carbon, dried with Mg_2SO_4, and filtered. The volatiles were removed on a rotary evaporator, and then on a Schlenk line in vaccuo to yield 20.3 g of a tan solid (72.1 mmol, 72.1%), m 74–76 °C. Single crystals suitable for x-ray diffraction were grown from benzene/hexane. ^1H NMR (500 MHz, $CDCl_3$): δ = 8.26 (s, 2H, N(*H*)-pyrrole), 6.75 (m, J_1 = 2.45 Hz, J_2 = 1.46 Hz, 2H, 5-C_4H_3N), 6.15 (m, J_1 = 2.45 Hz, J_2 = 2.93 Hz, 2H, 4-C_4H_3N), 6.06 (dd, J_1 = 2.93 Hz, J_2 = 5.86 Hz, 1H), 6.04 (m, J = 3.42 Hz, 2H, 3-C_4H_3N), 5.63 (dd, 1H), 3.63 (d, J = 14.16 Hz, 2H, $C_4H_3NCH_2N$), 3.45 (d, J = 14.16 Hz, 2H, $C_4H_3NCH_2N$), 2.87 (s, 1H), 2.77 (s, 1H), 2.30 (m, J_1 = 2.93 Hz, J_2 = 3.42 Hz, J_3 = 3.91 Hz, 1H), 2.16 (m, J_1 = 8.79 Hz, J_2 = 3.91 Hz, J_3 = 6.35 Hz, J_4 = 5.86 Hz, J_5 = 6.83 Hz, 2H), 1.83 (m, J_1 = 5.37 Hz, J_2 = 1.47 Hz, J_3 = 2.44 Hz, J_4 = 4.88 Hz, J_5 = 3.91 Hz, 1H), 1.41 (dq, J_1 = 4.40 Hz, J_2 = 1.96 Hz, 1H), 1.24 (d, J = 8.30 Hz, 1H), 0.50 (m, J_1 = 2.45 Hz, J_2 = 1.96 Hz, J_3 = 4.39 Hz, J_4 = 2.93 Hz, J_5 = 1.47 Hz, 1H,). ^{13}C NMR ($CDCl_3$): δ = 137.14, 132.22, 129.19 (2-C_4H_3N), 117.03 (5-C_4H_3N), 108.11 (4-C_4H_3N), 107.34(3-C_4H_3N), 58.19, 50.67, 49.33, 44.77, 42.29, 36.97, 30.97.

[(1S,2S,5R)-1-(2-isopropyl-5-methyl)cyclohexyl]amine hydrochloride. A suspension of 11.3g of $LiAlH_4$ (298 mmol) in 800 mL dry tetrahydrofuran was placed into a 2 L 3-neck flask in an ice bath. The flask was fitted with a mechanical stirrer, nitrogen

inlet, and an addition funnel. Through the addition funnel was slowly added a solution of 24.4g (1*S*, 2*S*, 5*R*)-1-cyano-2-isopropyl-5-methylcyclohexane (148 mmol) in 500 mL dry tetrahydrofuran. After stirring for 12 h, 500 g ice and 1 L tetrahydrofuran were slowly added to the flask. The white solid was filtered off, and the volatiles removed on a rotary evaporator. 250 mL water was added, and the solution was extracted with three 250 mL portions of ethyl acetate. The combined organic layers were dried with Na_2SO_4, filtered, and the volatiles were removed on a rotary evaporator. An ethereal solution of 1M HCl was added until precipitation of the title compound ceased.The white solid was collected on a frit, washed with –35 °C hexanes, and dried in vacuo. The yield was 10.5 g (51 mmol, 34.5%), m 194 °C dec. ^{1}H NMR (300 MHz, $CDCl_3$): δ = 8.4 (br s, 3H), 3.0 (br s, 1H), 2.4 (br s, 1H), 2.1 (br d, 1H), 1.7 (br d, 2H), 1.6 (br s, 1H), 1.25 (br m, 1H), 1.05 (br m, 3H), 1.0 (br m, 8H). ^{13}C NMR ($CDCl_3$): δ = 46.74, 37.04, 35.85, 35.19, 34.00, 29.41, 25.84, 25.22, 22.27, 21.53, 20.86. Anal. Calcd for $C_{11}H_{24}NCl$: C, 64.21; H, 11.76; N, 6.81. Found: C, 63.83; H, 12.17; N, 6.61.

***N*,*N*-di(pyrrolyl-α-methyl)-*N*-[(1S,2S,5R)-1-(2-isopropyl-5-methyl)-cyclohexyl]amine (H_2dpCHIRA, 3).** To a solution of 2.5 g [(1S,2S,5R)-1-(2-isopropyl-5-methyl)cyclohexyl]amine hydrochloride (12.2 mmol) in 250 mL 95% ethanol was added 1.61 g pyrrole (24.0 mmol) and 2.0 g 37% formalin solution (0.74 g formaldehyde, 24.6 mmol). The solution was stirred for 5 d, basified with a saturated solution of K_2CO_3 in water, and extracted thrice with 200 mL portions of diethyl ether. The combined ether layers were dried with Mg_2SO_4, filtered, and the volatiles removed by rotary evaporation. Flash chromatography (silica gel, 5% ethyl acetate in hexanes), afforded 1.69 g of the title compound (5.15 mmol, 42.2%) as a light yellow oil. ^{1}H NMR (300 MHz, $CDCl_3$): δ = 8.16 (s, 2H, N(*H*)-pyrrole), 6.70 (m, 2H, 5-C_4H_3N), 6.11 (m, 2H, 4-C_4H_3N), 6.01 (m, 2H, 3-C_4H_3N), 3.67 (d, 2H), 3.29 (d, 2H), 2.55 (t, 1H), 2.03 (m, 5H), 1.60 (m, 3H), 1.25 (m, 3H), 0.85 (m, 9H). ^{13}C NMR ($CDCl_3$): δ = 129.49, 117.04, 108.09, 107.34, 51.15, 50.24, 38.18, 35.62, 32.91, 29.03, 25.75, 25.35, 21.77, 21.06.

Li_2dpCHIRA. To a thawing solution of 1.69 g H_2dpCHIRA (5.16 mmol) in 50 mL pentane was added 7.0 mL 1.6 M *n*-butyl lithium (12.6 mmol), and the solution was stirred for 5 min. Removal of the volatiles in vacuo, trituration with toluene, removal of the volatiles in vacuo, trituration with pentane, and removal of the volatiles in vacuo yielded 1.43 g (4.21 mmol, 81.7 %) of the title compound as a light orange solid, mp 140 °C dec. ^{1}H NMR (300 MHz, THF-d_8): δ = 6.69 (t, *J*=1.62 Hz, 2H), 5.93 (t, *J*=2.49 Hz, 2H), 6.01 (m, J_1=1.18 Hz, J_2 = 1.32 Hz, 2H), 3.83 (d, *J*=13.5 Hz, 2H, $C_4H_3NCH_2N$), 3.56 (d, *J*=13.5 Hz, 2H, $C_4H_3NCH_2N$), 2.81 (t, *J*=13.2 Hz, 1H), 2.31 (s, 1H), 1.98 (br d, *J*=10.8 Hz, 1H), 1.70-1.52 (br m, 2H), 1.50-1.35 (br m, 3H), 1.30 (br s, 2H), 0.87 (dd, J_1=6.5 Hz, J_2=1.2 Hz, 12H), 0.69 (d, *J*=6.3 Hz, 3H). ^{13}C NMR (THF-d_8): δ = 140.06, 126.87, 107.83, 105.23, 57.87, 53.83, 49.66, 39.50, 36.90, 35.73, 29.92, 27.02, 23.09, 21.66.

5,5-di-*n*-propyldipyrrolylmethane (H_2dppm, 4). To a solution of 75 mL pyrrole and 8.0 mL of 4-heptanone (6.5 g, 57 mmol) in an oven-dried 250 mL Schlenk flask flushing with argon was added 0.5 mL trifluoroacetic anhydride. After stirring for 18 h, the solution was made basic with 300 mL of 0.3 M NaOH. The mixture was twice extracted with 300 mL portions of diethyl ether, and the combined organic layers were washed with two 200 mL portions of water. After drying with $MgSO_4$, the solution was filtered, and the volatiles were removed by rotary evaporation. Sublimation of the solid yielded 4.88 g (21.1 mmol, 37.2%) of the title compound as a white solid, m 101–103 °C. ^{1}H NMR (300 MHz, $CDCl_3$): δ = 7.60 (s, 2H, N(*H*)-pyrrole), 6.58 (m, J_1=1.71 Hz, J_2=0.98 Hz, J_3=1.47 Hz, 2H, 5-C_4H_3N), 6.13 (m, 2H, 4-C_4H_3N), 6.11 (m, 2H, 3-C_4H_3N), 1.89 (m, J_1=4.64 Hz, J_2=3.17 Hz, J_3=3.91 Hz, J_4=0.98 Hz, J_5=4.15 Hz, 4H, $(C_4H_3N)_2C(CH_2CH_2Me)_2$), 1.08 (m, J_1=4.40 Hz, J_2=3.17 Hz, J_3=1.71 Hz, J_4=2.68 Hz, J_5=3.42 Hz, 4H, $(C_4H_3N)_2C(CH_2CH_2Me)_2$), 0.86 (t, *J*=7.33 Hz, 6H, $(C_4H_3N)_2C(CH_2CH_2CH_3)_2$). ^{13}C NMR ($CDCl_3$): δ = 137.27 (2-$C_4H_3N$), 116.80 (5-$C_4H_3N$), 107.30 (4-$C_4H_3N$), 105.51 (3-$C_4H_3N$), 42.74 ($(C_4H_3N)_2C(CH_2CH_2Me)_2$), 39.88 ($(C_4H_3N)_2C(CH_2CH_2Me)_2$), 17.11

$((C_4H_3N)_2C(CH_2CH_2Me)_2)$, 14.50 $((C_4H_3N)_2C(CH_2CH_2CH_3)_2$.

Li_2dmpm. To a thawing solution of 1.04 g H_2dmpm (5.97 mmol) in 20 mL pentane was added 10.0 mL 1.6 M *n*-butyl lithium (16 mmol). A white solid quickly formed. After stirring for 5 min, the solid was collected on a frit and washed with copious quantities of pentane. Drying in vacuo gave 1.10 g of the title compound (5.91 mmol, 99.0%) as a white solid, mp 153 °C dec. ^{1}H NMR (300 MHz, THF-d_8): δ = 6.54 (br s, 2H), 5.90 (m, J_1=1.5 Hz, J_2=1.3 Hz, J_3=2.4 Hz, J_4=2.9 Hz, J_5=2.1 Hz, 4H), 1.55 (s, 6H). ^{13}C NMR (THF-d_8): δ = 1.44.97, 106.73, 102.83 (br), 32.98, 15.69.

CHAPTER 2

AN INVESTIGATION OF TRANSITION METAL–IMIDO BONDING IN $M(NR)_2$(dpma)

Introduction

Transition metal imido chemistry has become popular in the last several years. The imido group is an important supporting ligand in many catalytic reactions,[8] including C–H bond activation,[9] hydroamination of alkynes with titanium imido intermediates,[10] and other processes.[11] There is a large number of group–6 bis(imido) compounds, offering a rich chemistry that has been the subject of much research, both for the basic knowledge obtained as well as these compounds' utility as precatalyts or intermediates.[12]

Often, the two imido ligands in these group–6 compounds are inequivalent in the solid state, with one imido ligand being substantially more bent than the other, as in $Mo(NPh)_2(S_2CNEt_2)_2$.[13] The Mo–N–Ph bond angles in the solid state are substantially different, with one being 169.4(4)° and the other 139.4(4)°. While it is quite common to find these inequivalent imido group geometries in the solid state, it is rare to find bis(imido) compounds in which the imido ligands do not either equilibrate rapidly in or become equivalent in solution, as evidenced by one type of imido group in the NMR spectra.[14,15]

A statistical analysis of the bis(imido) structures of the Group-6 transition elements from the Cambridge Structural Database is shown in Figure 2-1. The imido–metal bond angles were summed to avoid arbitrary definitions of what was considered a "linear" bond, and what constituted a "bent" bond. The complex with the lowest sum of bond angles is the aforementioned $Mo(NPh)_2(S_2CNEt_2)_2$ at 309°.[13] The average sum of imido bond angles was 328° with a standard deviation of 8°. It was expected that 4– and 5–coordinate compounds would have a larger sum of bond angles than 6–coordinate complexes, due to the ability of the lower coordinate compounds to form formal triple bonds to the imido ligands, whereas the 6–coordinate complexes would be expected to have formal metal–imido bond orders of, at most, 2.5. However, this is not true; that is, 6–coordinate complexes are no

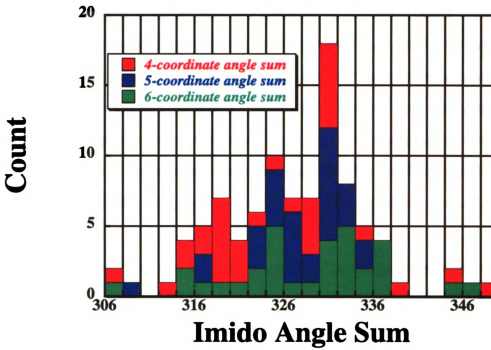

Figure 2-1. Statistics on the bis(imido) complexes of Group-6 from the Cambridge Structural Database. Each entry is the sum of the two imido bond angles in a complex.

more likely to have smaller imido–metal angles than the 4– and 5–coordinate complexes. This can be rationalized by the effects that other ligands on the metal centers have on the ability of the imido ligands to participate in π–bonding with the metal center.[16] Of the bis(imido) complexes examined, 30% had at least one imido with a bond angle of 155° or less; however, the reasons behind this behavior could not be elucidated from the statistical analysis.

This study attempts to determine the underlying reasons that many bis(imido) complexes show imido bending, i.e., is the underlying reason for the bending the electronics of the system and, if so, are the electronics associated with electronegativity changes at the metal center and bond polarity?

The three common valence bond structures which have been used to qualitatively explain metal-imido bonding (**Chart 2-1**)[12,17] can give some insights into the metal-imido bond. In Structure **I**, which can be identified unambiguously in the solid state, an sp^2

hybridized nitrogen atom donates two electrons to the metal center (using the neutral method of electron counting), resulting in a bent bond. Structure **II** is a linear imido, with an *sp*-hybridized nitrogen atom also donating two electrons to the metal center, with the lone pair of electrons in a nitrogen 2*p* orbital. In Structure **III**, the *sp* hybridized nitrogen atom donates four electrons to the metal, the lone pair interacting with a π-acceptor orbital on the metal center. Even though structures **II** and **III** will be difficult to differentiate based on bond lengths and angles, they have completely different effects on the electronics of the compound.

Various research groups have used orbital symmetry arguments to differentiate between structures **II** and **III**. Bercaw and co-workers, for example, have used structure **II** to describe the imido bonding in the complex $Ta(Cp^*)_2(NPh)H$.[18] In the similar niobium phenylimido complex $Nb(Me_3SiCp)_2(NPh)Cl$, the Nb–N–C(ipso) angle is somewhat bent

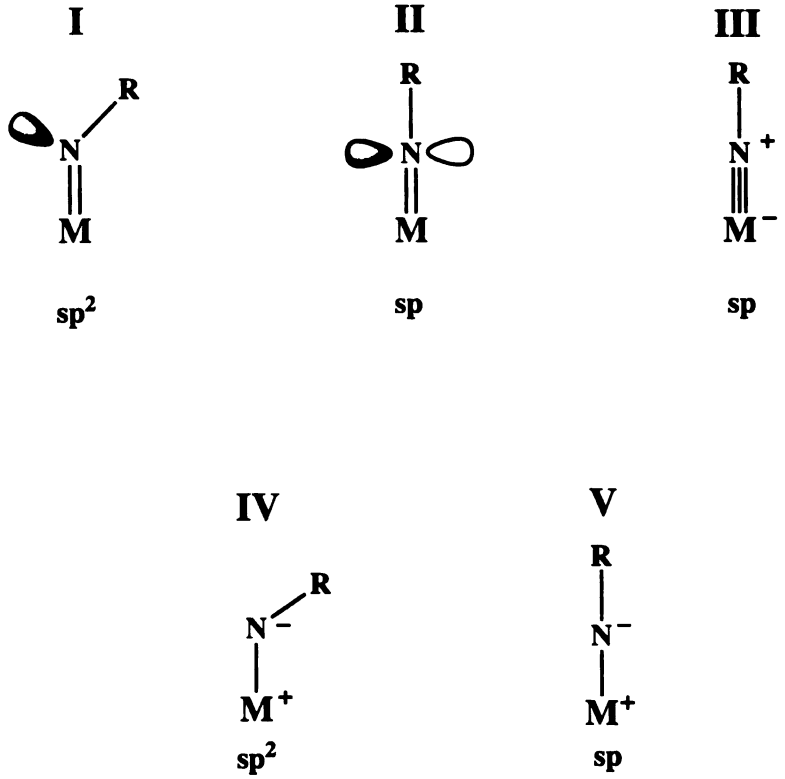

Chart 2-1. A few of the pertinent valence bond structures for a transition metal bound imido ligand.

at 165°; calculations suggest that the potential energy surface describing imido bending is essentially flat to a bond angle of 140°.[19] Jørgenson has suggested, in theoretical work, that the aromatic rings in phenyl imido complexes can accept electron density from the imido nitrogen atom, reducing imido π-bonding and flattening the potential energy surfaces associated with imido bending.[20] On the other hand, since $Nb(Cp)_2(NBu^t)Cl$ has a relatively short Nb–N(imido) bond and a linear Nb–N–C(ipso) angle, structure **III** is a more reasonable approximation.[21]

Unlike more covalent nitrogen double-bonds, such as in organic imines,[22] calculations indicate that energy differences between bent and linear imido bonds in metal complexes are fairly small.[19,20] In fact, the "lateral shift" mechanism for imine isomerization involves a transition state very similar to structure **II**.[23] In more covalent systems, such as organic imines, a less likely mechanism is one that involves polarization of the C–N double bond, resulting in a zwitterionic transition state. These zwitterionic forms, **IV** and **V**, should be much larger participants in the structure of transition metal imido complexes, where the metal-imido bond is more highly polarized.[17] The bond angle would change dramatically during interconversion of these structures, but the electron density at the nitrogen atom and at the metal center would remain relatively constant. The polarity of metal-nitrogen bonds increases when descending a triad (vide infra),[24] so that the polar structures **IV** and **V** should play a larger role in the description of heavier congeners as compared to structures **I**, **II** and **III**.

It appears that, oftentimes, in complexes which have a tridentate, dianionic ligand and two monodentate ligands on a transition metal, the two monodentate ligands will not rapidly exchange, at least on the NMR time scale.[25,26] A prime example of this is the complex $Cr(NBu^t)_2\{[Bu^tNC(O)]_2NBu^t\}$, prepared by Wilkinson and coworkers,[27] which exhibits two nonequivalent imido environments on the NMR timescale in solution.[28]

Three bis(*tert*-butyl) imido complexes have been prepared spanning the group-6 metals (chromium, molybdenum, and tungsten) which incorporate the tridentate, dianionic

ligand *N,N*-di(pyrrolyl-α-methyl)-*N*-methylamine (dpma), $M(NBu^t)_2$(dpma). These complexes are very closely related structurally, and contain inequivalent imido groups both in the solid state and in solution on the NMR time scale, and thus can be used to study metal-imido bonding interactions. Any spectroscopic differences between these molecules, since they are so closely related structurally, can be attributed to the electronic differences of the Group-6 metals. Also prepared was $Mo(Ndip)_2$(dpma), useful for comparisons between alkyl and aryl substituents, which will be briefly discussed, as well as $Mo(NBu^t)_2$(dpCHIRA).

These compounds were studied by ^1H NMR, ^{13}C NMR, CP-MAS ^{13}C NMR, ^{14}N NMR, and x-ray diffraction. Although these data provide information about imido ligands in differing environments on the same metal, the experimental data cannot determine if these differences are induced by different bond angles in the imido ligands or simply because of the inherent electronic differences between axial and equatorial imido ligands Therefore, Density Functional Theory was used to explore the electronic energy associated with imido bending.

Results and Discussion

Syntheses and structures. Reaction of $Cr(NBu^t)_2(Br)_2(py)$[29] and Li_2dpma in diethyl ether yields dark red $Cr(NBu^t)_2$(dpma) (**5**) (eq 2-1). The two imido groups in the solid-state structure are inequivalent, with one being substantially bent at 151.10(16)°, and the other being linear at 175.28(16)°. The bond angles around the chromium center in the solid-state structure are not those expected for either a trigonal bipyramid or a square pyramid; the complex is best described (vide infra) as a pseudo-square pyramid with the bent imido group in the axial position (Figure 2-2). The fact that the two imido groups are different in the solid state is not unusual, but what is unusual is that the two imido ligands don't equilibrate in solution to give a single NMR resonance.[14,15] There are two sharp, distinct *tert*-butyl resonances observed in the solution ^1H NMR of **5** from –80 °C to 80 °C

$$CrBr_2(py)(NBu^t)_2 + Li_2dpma \xrightarrow[-2\ LiBr\ -\ pyridine\ 34\%]{Et_2O} Cr(NBu^t)_2(dpma)\ \mathbf{5} \quad (2\text{-}1)$$

$$MoCl_2(NBu^t)_2(dme) + Li_2dpma \xrightarrow[-2\ LiCl\ 38\%]{Et_2O} Mo(NBu^t)_2(dpma)\ \mathbf{6} \quad (2\text{-}2)$$

$$W(NHBu^t)_2(NBu^t)_2 + H_2dpma \xrightarrow[-2\ H_2NBu^t\ 50\%]{Et_2O} W(NBu^t)_2(dpma)\ \mathbf{7} \quad (2\text{-}3)$$

$$MoCl_2(Ndip)_2(dme) + Li_2dpma \xrightarrow[-2\ LiCl\ 38\%]{Et_2O} Mo(Ndip)_2(dpma)\ \mathbf{8} \quad (2\text{-}4)$$

$$MoCl_2(NBu^t)_2(dme) + Li_2dpCHIRA \xrightarrow[-2\ LiCl\ 15\%]{Et_2O} Mo(NBu^t)_2(dpCHIRA)\ \mathbf{9} \quad (2\text{-}5)$$

(Figure 2-3). This unexpected behavior can be attributed to the chelating dpma ligand.

As shown in eq 2-2 and 2-3, the molybdenum and tungsten analogs of **5**, $Mo(NBu^t)_2(dpma)$ (**6**) and $W(NBu^t)_2(dpma)$ (**7**), have been synthesized. The molybdenum bis(imido) **6** is readily prepared from $Mo(NBu^t)_2Cl_2(dme)$[30] and Li_2dpma. The tungsten analog **7** was prepared by transamination on $W(NBu^t)_2(NHBu^t)_2$[31] with H_2dpma. As in the case of **5**, these complexes also display two different resonances due to the *tert*-butylimido groups that do not equilibrate on the ^1H NMR timescale even at 80 °C.

As can be seen in Table 2-1 and in Figure 2-4, the solid-state structures for **5-6** are very similar. In fact, the largest differences are found in the chromium complex **5**, and these differences, although slight, can be attributed to the smaller atomic radius of the chromium atom. The two imido angles in **5** measure 151.1(2)° and 175.3(2)°, and the Cr–N(imido) bond distances are statistically different at 1.626(2) Å and 1.641(2) Å for

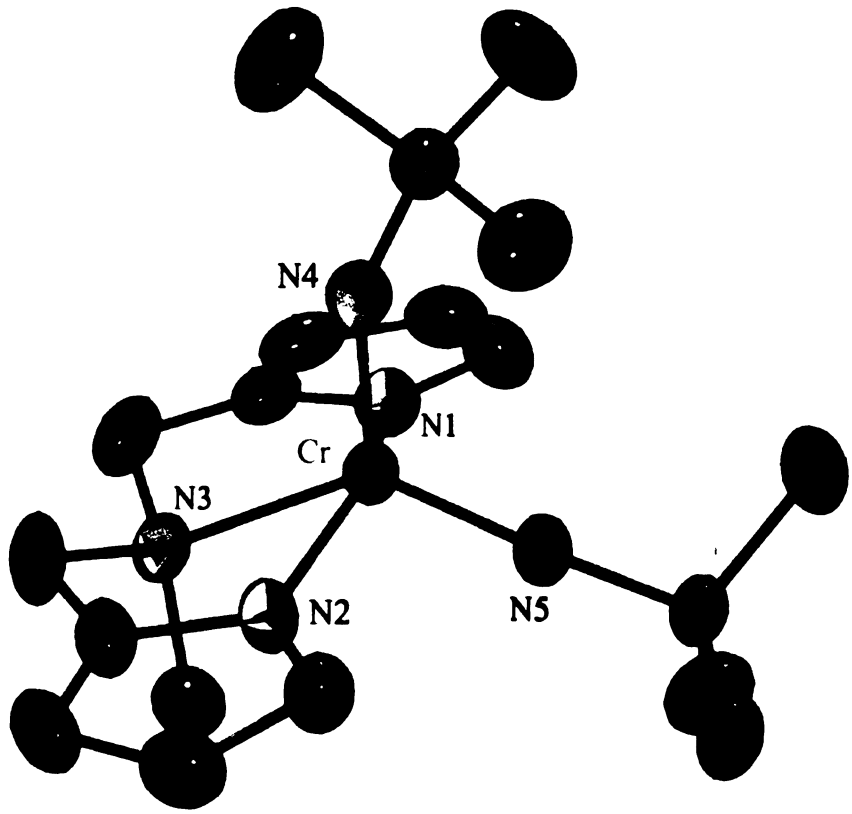

Figure 2-2. The ORTEP representation (50% probability elipsoids) of Cr(dpma)$(NBu^t)_2$ (**5**).

linear and bent, respectively. In the tungsten structure (**7**), the W–N(imido) distances are statistically equivalent at 1.748(3) Å and 1.757(3) Å; the bond distances and angles in the molybdenum bis(imido) **6** are within statistical errors of those in tungsten complex **7**.

The continuous symmetry parameter, $\tau = (\alpha - \beta)/60$ (where α and β are the largest and second largest angles around the metal center, respectively) can be used to quantify the accuracy of describing a complex as either a square pyramid ($\tau = 0$) or as a trigonal bipyramid ($\tau = 1$).[32] For complexes **5-7**, τ is computed as 0.28, 0.22, and 0.19, respectively, indicating that all three compounds are better described as square pyramidal.

Arylimido Mo$(Ndip)_2$(dpma) (**8**) was prepared from Mo$(Ndip)_2Cl_2(dme)$[30] and Li_2dpma in 35% yield (eq 2-4). The structure of **8**, as determined by x-ray crystallography, is remarkably similar to the *tert*-butylimido derivative **6**. Arylimido **8** has bent and linear imido angles of 155.8(5)° and 175.2(5)°, the bent imido bond angle being slightly larger

Figure 2-3. The variable temperature ^1H NMR of Mo(dpma)$(NBu^t)_2$ (**6**).

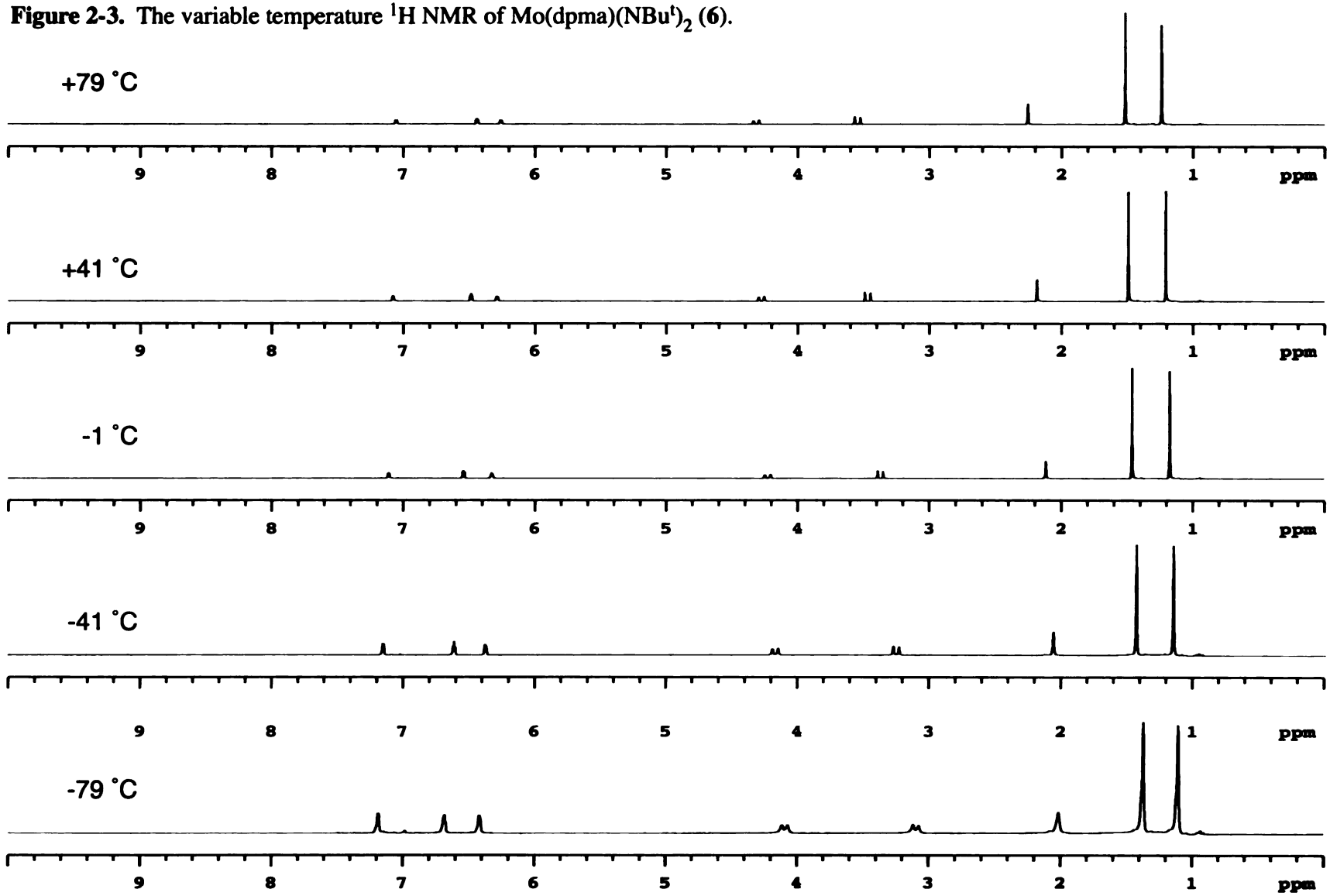

Table 2-1. Selected bond distances and angles from x-ray diffraction on complexes **5–9**. For the numbering scheme, see Figure 2-2.

Distances and Angles (Å/°)	$Cr(NBu^t)_2$(dpma) (5)	$Mo(NBu^t)_2$(dpma) (6)	$W(NBu^t)_2$(dpma) (7)	$Mo(Ndip)_2$(dpma) (8)	$Mo(NBu^t)_2$(dpCHIRA) (9)
M-N(4)	1.6256(18)	1.731(6)	1.748(3)	1.751(5)	1.750(7)
M-N(5)	1.6409(18)	1.732(6)	1.757(3)	1.728(4)	1.745(5)
M-N(pyrrolyl) ave.	1.996(2)	2.068(6)	2.067(3)	2.073(5)	2.071(6)
M-N(3)	2.1717(18)	2.339(7)	2.321(3)	2.290(5)	2.331(6)
M-N(4)-C	151.10(16)	156.5(6)	158.2(3)	155.8(5)	155.2(6)
M-N(5)-C	175.28(16)	171.6(5)	170.4(3)	175.2(5)	177.7(6)
N(4)-M-N(5)	112.48(9)	110.5(3)	111.40(14)	111.2(2)	111.2(3)
N(pyrrolyl)-M-N(4) ave	99.35(8)	104.2(3)	103.57(13)	103.4(2)	100.3(3)
N(pyrrolyl)-M-N(5) ave	96.64(8)	99.3(3)	99.32(12)	98.1(2)	100.4(3)
N(3)-M-N(4)	113.64(8)	98.5(3)	98.89(12)	106.9(2)	98.2(3)
N(3)-M-N(5)	133.88(8)	150.8(3)	149.51(12)	141.8(2)	150.6(3)
N(pyrrolyl)-M-N(3) ave	76.05(8)	72.6(3)	72.57(11)	72.79(18)	73.5(3)

than in the bis(*tert*-butylimido) complex. The Mo–N(imido) bond distances do vary with statistical significance at 1.728(4) Å and 1.751(5) Å. These bond lengths are very similar to those found in bis(*tert*-butylimido) complex **6**. The largest differences between the bis(2,6-diisopropylphenylimido) structure and the bis(*tert*-butylimido) structure is in the angles between the imido substituents and the donor amine of the dpma ligand, and appear to be a consequence of the steric bulk of the isopropyl groups on the aromatic rings. Bis(arylimido) **8** has a structure that closely resembles a square pyramid as judged by the τ-parameter of 0.01 for the solid-state structure. An additional complex, $Mo(NBu^t)_2$(dpCHIRA) (**9**), was synthesized by the reaction of $Mo(NBu^t)_2Cl_2$(dme) with Li_2dpCHIRA. This complex is very similar to $Mo(NBu^t)_2$(dpma) (**6**), although imido-molybdenum bond lengths are very

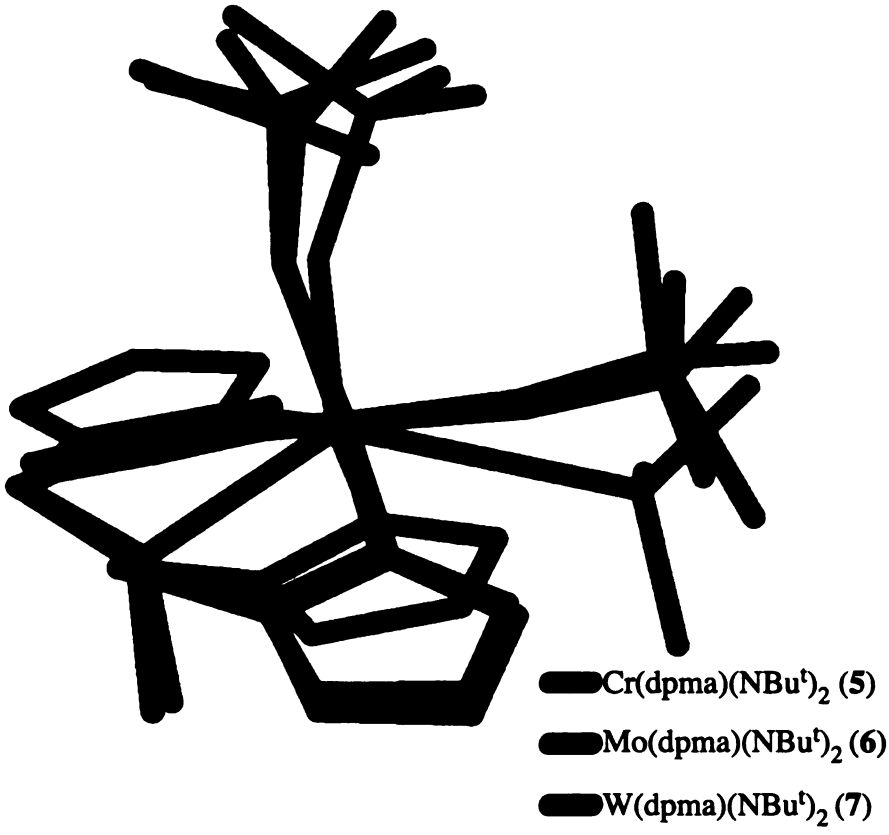

Figure 2-4. Superposition of the crystal structures of $Cr(dpma)(NBu^t)_2$ (**5**), $Mo(dpma)(NBu^t)_2$ (**6**), and $W(dpma)(NBu^t)_2$ (**7**).

slightly longer at 1.750(5) Å and 1.745(5) Å for the linear and the bent metal-imido bonds, respectively. The equatorial bond angle is slightly larger at 177.7(6)°, and the axial bond angle is similar (although statistically different by 0.1°) at 155.2(6)°. This structure, with a τ of 0.13, can also be viewed as more closely approximated as square pyramidal.

Since τ is significantly smaller in the case of the bis(arylimido) complex **8** than in any of the bis(*tert*-butylimido) structures, it is tempting to attribute this to electronic effects imposed by the arylimido groups versus the alkylimido groups. Figure 2-5 is a histogram of all of the group-6, five coordinate bis(imido) complexes from the CSD, along with complexes **5-9**, showing how τ varies with the type of substituent on the imido ligands. As can be seen, there appears to be little correlation between τ and the character of the imido group, although 26 of the 35 compounds (74%) do have a τ value less than 0.30. It appears that for some reason, perhaps electronic, group-6 bis(imido) complexes tend

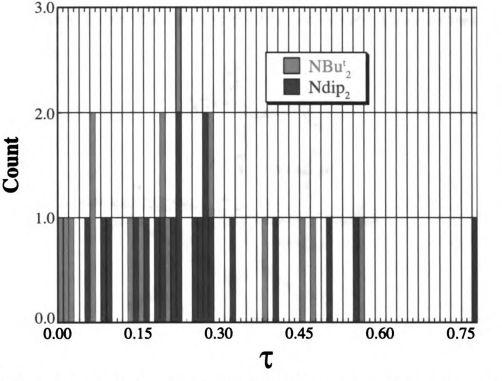

Figure 2-5. Statistics on the five coordinate bis(imido) complexes of group-6 from the Cambridge Structural Database showing the type of imido ligand versus τ.

towards square pyramidal geometry rather than trigonal bipyramidal geometry.

The $M(imido)_2$ core is remarkably similiar across the entire series as exemplified by the N(4)–M–N(5) bond angles, which are between 110.5° and 112.5° in all five complexes.

^{1}H and ^{13}C NMR spectroscopy. The ^{1}H and ^{13}C NMR of $M(NBu^t)_2(dpma)$, where M = Cr, Mo, and W, display inequivalent *tert*-butyl resonances. nOe experiments (Figure 2.6) were used to determine that the overall solid-state geometries were retained in solution, and we were also able to unambiguously assign the *t*-butyl ^{1}H resonances to the bent (axial) and linear (equatorial) imido ligands. (^{1}H,^{13}C)-HMQC and (^{13}C,^{13}C)-HMBC spectroscopy[33] was used to assign all of the proton and carbon resonances in the corresponding ^{13}C spectra; the full assignments for all of the (*tert*-butylimido)(dpma) complexes can be found in the experimental section. Since the axial (bent) imido nitrogen atom is expected to be more electron-rich, the resonances associated with this ligand are expected to be more shielded than the corresponding atoms on the equatorial (linear) imido

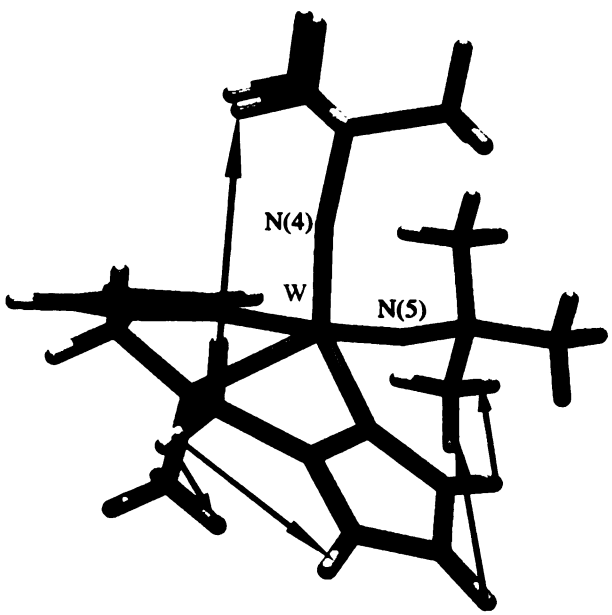

Figure 2-6. The relavent nOe enhancements used to assign the ^{1}H NMR resonances in $W(dpma)(NBu^t)_2$; the arrowhead points to the proton that is enhanced by excitation of the proton at the end of the arrow.

ligand. This expectation is confirmed by the nOe experiments.

The ^{13}C NMR chemical shifts of the *tert*-butylimido groups can be very informative as to the M–N bonding in bis(*t*-butylimido) complexes;[34] specifically $\Delta\delta_{\alpha\beta} = \delta C_\alpha - \delta C_\beta$, where C_α and C_β are the quaternary and primary carbon atoms, respectively, in the *tert*-butylimido groups. Large $\Delta\delta_{\alpha\beta}$ values are often attributed to the most covalent metal-nitrogen bonds, i.e., those with the most triple bond character (structure **III** in Chart 2-1), whereas more polarized bonding interactions (structures **I**, **II**, **IV**, or **V**) exhibit smaller values of $\Delta\delta_{\alpha\beta}$. Since the polarity of the metal-imido bond will increase down a transition metal triad, *ceteris paribus*, the corresponding $\Delta\delta_{\alpha\beta}$ values will decrease. This trend is consistent with greater participation of structures **IV** and **V** in the overall description of the bonding of the imido ligands. Similary, decreasing $\Delta\delta_{\alpha\beta}$ values reflect increasing polarity in these systems as one proceeds from chromium to molybdenum to tungsten with values of 47.17 ppm, 38.54 ppm, and 34.17 ppm, respectively.[35]

Although comparisons between the different transition metal congeners of bis(imido) complexes using $\Delta\delta_{\alpha\beta}$ values are intriguing, similar comparisons between bis(imido) complexes containing different supporting ligands have the potential to be very informative about the electronics of the ligands. As will be shown, the results are qualitatively what is expected from various common ligands.

It is not unusual for a linear correlation to exist between chemical shifts and electronegativities[36]; many such studies have appeared in the literature.[37] Many of the reported values for ^{13}C NMR chemical shift differences correlate well with the estimated electronegativities of the Group-6 metals in the +6 oxidation state,[38] and thus to expected polarity changes in the metal-nitrogen bonds. Plots of $\Delta\delta_{\alpha\beta}$ versus estimated electronegativity of the metal center for four different bis(*tert*-butylimido) systems are found in Figure 2-7. The four different systems are $M(Tp^*)Cl(NBu^t)_2$,[39] $M(OSiR_3)_2(NBu^t)_2$,[34,40] $M(Cp)Me(NBu^t)_2$,[29,41] and $M(dpma)(NBu^t)_2$, where M = Cr, Mo, and W. Suggestive that metal electronegativity is, indeed, an important factor in imido nitrogen electron density,

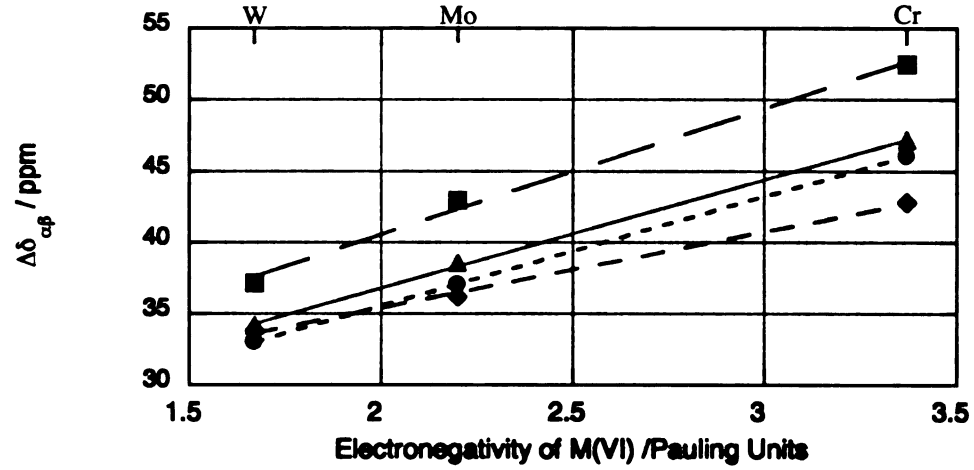

Figure 2-7. Plot of bis(tert-butylimido) complexes of group-6 $\Delta\delta_{\alpha\beta}$ values versus Sanderson electronegativity values for the metals in the +6 oxidation state.

■ : $M(Tp^*)Cl(NBu^t)_2$, y = 22.785 + 8.8668x R = 0.9974;

▲ : $M(dpma)(NBu^t)_2$, y = 21.613 + 7.6024x R = 0.99963;

● : $M(OSiR_3)_2(NBu^t)_2$, y = 20.194 + 7.6545x R = 0.99999;

◆ : $M(Cp)(Me)(NBu^t)_2$, y = 24.696 + 5.3457x R=0.99852.

the linear fits of all four lines are excellent. The linear fits also suggest that $\Delta\delta_{\alpha\beta}$ values are a reasonable measure of imido nitrogen electron density, at least in isostructural systems. *The good linear fits do not necessarily indicate that Sanderson's electronegativities for M(VI) are accurate but suggest only that the effective electronegativity* ***differences*** *are accurately portrayed within each set of complexes.* Indeed, the electronegativity of the metal center should vary as the supporting ligands are varied. Since the Sanderson electronegativities were calculated from complexes containing ligands that are both more electronegative and poorer π-donors than those included in Figure 2-7, they will overestimate the electronegativity of the metal centers. Essentially, the plots in Figure 2-7 need to be referenced so as to give the "true" effective electronegativities on the Pauling scale. As the ligands become more electron-deficient, they would be expected to cause

greater changes in the effective electronegativity of the metal center, and therefore have increasing slopes to the lines as plotted in Figure 2-7. The most electron-rich ligand sets should have the smallest slope. The slopes of the lines in Figure 2-7 follow this trend. The ligand set that is expected to be the least electron-donating, (Tp*)(Cl) (which can be viewed as a having a zwitterionic structure with a formal positive charge on the metal center in the complex, and a formal negative charge on the boron atom), has the largest slope at 8.87. The $OSiR_3$ ligands and the dpma ligand are expected to be similar to each other and more electron donating than the (Tp*)(Cl) set, and the slopes of the lines corresponding to these ligands are 7.65 and 7.60, respectively. The ligand set (Cp)(Me), with two very electron-rich ligands, has the smallest linear slope at 5.35.

There is no way of referencing the $\Delta\delta_{\alpha\beta}$ plots to the Pauling scale, but an arbitrary reference value can be used. The obvious choice for (*tert*-butyl)imido complexes is *trans*-bis(*tert*-butyl)diazene, $Bu^tN{=}NBu^t$ ($\Delta\delta_{\alpha\beta}$ = 39.0 ppm), since there is expected to be no bond polarity in the nitrogen-nitrogen bond. Referencing the data in Figure 2-7 to bis(*tert*-butyl)diazene results in the plot shown in Figure 2-8, and allows estimation of the relative electron-withdrawing abilities of metal centers with very dissimilar ligand sets. Positive values would be expected for complexes, with large contributions from structure **III** in Chart I, that would be withdrawing more electron-density from the imido nitrogen atom compared to the reference compound. Complexes with significant contributions from structures **IV** and **V** would be expected to give rise to negative values compared to bis(*tert*-butyl)diazene. According to this technique, chromium with the ligand sets studied is always more electron-withdrawing than (*t*-butyl)imido and tungsten is always less electron-withdrawing, whereas molybdenum varies from more to less electron-withdrawing depending on the ligand set.

Examination of a larger set of ligands, X, in $X_2Cr(NBu^t)_2$ is informative. For X_2 = $(neophyl)_2$,[29] $(neopentyl)_2$,[29] $(benzyl)_2$,[42] $(OSiMe_3)_2$,[29,34] dpma, and Cl_2,[29] the electronic changes from altering the ligands result in $\Delta\delta_{\alpha\beta}$ values that range over 14.8 ppm.[43] Remarkably, this implies that changing the supporting ligand can have as large an effect

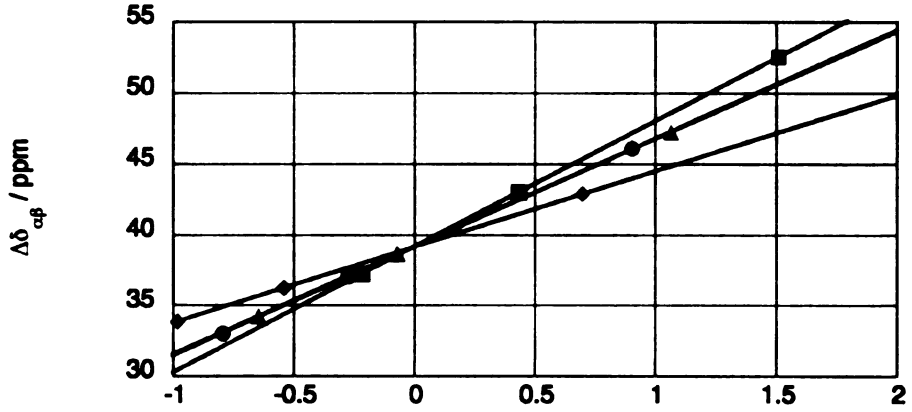

Ligands on $M(NBu^t)_2$	Cr	Mo	W
Cp(Me) : ◆	0.70	–0.54	–0.98
$OSiR_3$: ●	0.91	–0.26	–0.79
dpma : ▲	1.07	–0.07	–0.64
Tp(Cl) : ■	1.51	0.44	–0.21

Figure 2-8. Estimation of electron-withdrawing ability of various ligand sets on $M(NBu^t)_2$. Values are in arbitrary units with bis(tert-butyl)diazene as reference of 0. Metal centers estimated to be more electron-withdrawing than the reference are positive.

on the electron densities of the imidio nitrogen atoms as changing the metal centers from chromium to molybdenum to tungsten. It can be seen from these data that the donor ability of the dpma ligand is similar to dichloride and bis(trialkylsiloxy).[44]

For $Mo(NR)_2(S_2CNEt_2)_2$ complexes, the differences in the solid-state ^{13}C NMR resonances have been correlated to imido bonding.[14a] In solution, the difference in chemical shift, $\Delta\delta_{l-b}$, for the quaternary carbons on the axial (linear) *tert*-butyl groups minus the equatorial (bent), i.e. $\Delta\delta_{l-b} = C(\alpha)_{(linear)} - C(\alpha)_{(bent)}$, was found to change as Cr > W > Mo with $\Delta\delta_{l-b}$ equal to 2.1 ppm, 1.3 ppm, and 0.8 ppm, respectively, in the dpma complexes studied.[45] Although it is not clear why the numbers trend in this way, the overall

magnitude of $\Delta\delta_{l-b}$ is informative. Despite the large difference in bond angles for the linear imido ligands compared to the bent imido ligands (>25°), and the different coordination environments of the two imido ligands, the effect of these changes on the values of $\Delta\delta_{l-b}$ observed is significantly less than is the effect that changing the metal center or supporting ligands has on $\Delta\delta_{\alpha\beta}$. The electron density of the imido nitrogen atoms is clearly influenced substantially by changes in the metal center and the other ligands on the metal center, and less so by the imido group environment.

Solid-state ^{13}C NMR spectroscopy. Since the solid-state structure is not necessarily the structure adopted in solution, the solution-state NMR data was compared to the CP-MAS ^{13}C NMR spectral data. The data correlate amazingly well as can be seen in Figure 2-9 and Table 2-2; however, there are a few differences.

Unlike in the solution-state spectra, the ordering of the $\Delta\delta_{l-b}$ values was found to be Cr > Mo > W in the solid-state, with values of 4.0 ppm, 0.9 ppm, and 0.8 ppm, respectively, which is similar to the results found with ^{14}N NMR (vide infra).

^{14}N NMR spectroscopy. ^{14}N NMR can also be used to investigate metal-imido bonding, and this use of ^{14}N NMR has been thoroughly discussed by Bradley and coworkers

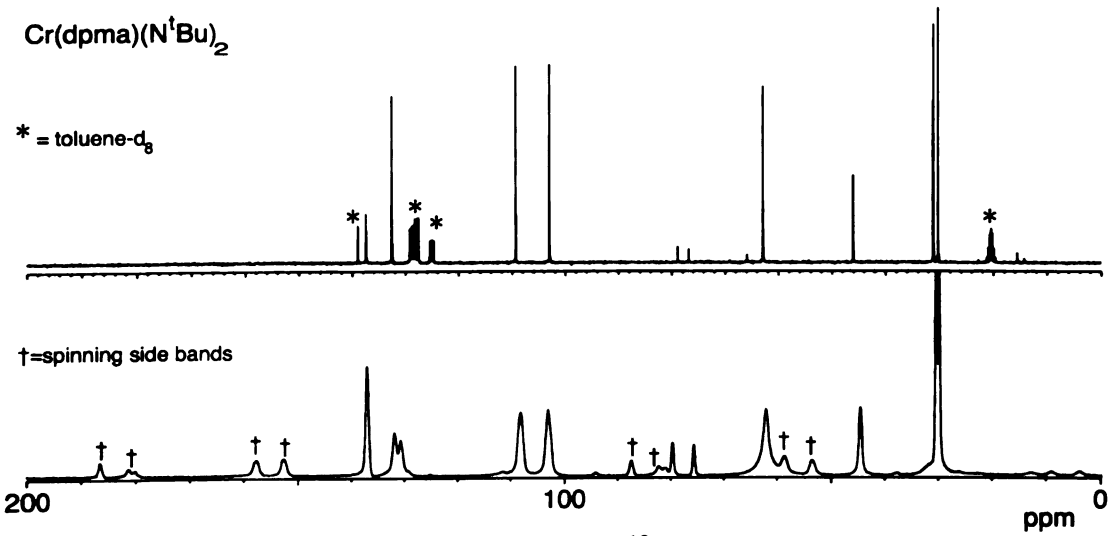

Figure 2-9. The solution state (top) and CP-MAS ^{13}C NMR (bottom) spectra of Cr(dpma)(NBu^t)$_2$ (**5**).

Table 2-2. Comparison of solution and solid-state ^{13}C NMR data from compounds **5–7**.

	Cr(dpma)(NBu^t)$_2$ (5)	Mo(dpma)(NBu^t)$_2$ (6)	W(dpma)(NBu^t)$_2$ (7)
C(CH_3)$_3$ bent			
solution	30.2	31.0	32.5
solid	30.0	31.0	32.2
C(CH_3)$_3$ linear			
solution	31.1	31.7	33.1
solid	30.6	32.3	33.6
CMe_3 bent			
solution	76.8	69.5	66.8
solid	75.8	69.2	66.8
CMe_3 linear			
solution	78.9	70.3	68.1
solid	79.8	70.1	67.6
CH_2			
solution	62.9	60.7	60.9
solid	62.3	60.3	59.3
NCH_3			
solution	46.0	44.6	44.7
solid	44.6	45.2	42.3
Pyrrole-4-*C*			
solution	103.0	105.0	105.7
solid	103.2	103.7	106.8
Pyrrole-3-*C*			
solution	109.3	110.0	111.0
solid	108.3	109.3	108.9
Pyrrole-2-*C*			
solution	132.6	133.4	134.3
solid	132.0	132.4	134.1
Pyrrole-1-*C*			
solution	138.9	139.0	139.8
solid	137.1	139.3	140.3

and by others.[15] Osborn and Le Ny, for example, reported the ^{14}N NMR of several axially symmetric, trigonal bipyramidal tungsten mono(imido) complexes.[46] Because these complexes were highly symmetric, the ^{14}N NMR resonances were relatively narrow ($\Delta\nu_{1/2}$ <100 Hz). Broader resonances are observed in the ^{14}N NMR spectra of the dpma systems studied because of the lower symmetry of these compounds; however, all of the resonances corresponding to the nitrogen atoms of the complexes are readily observed, Figure 2-10.

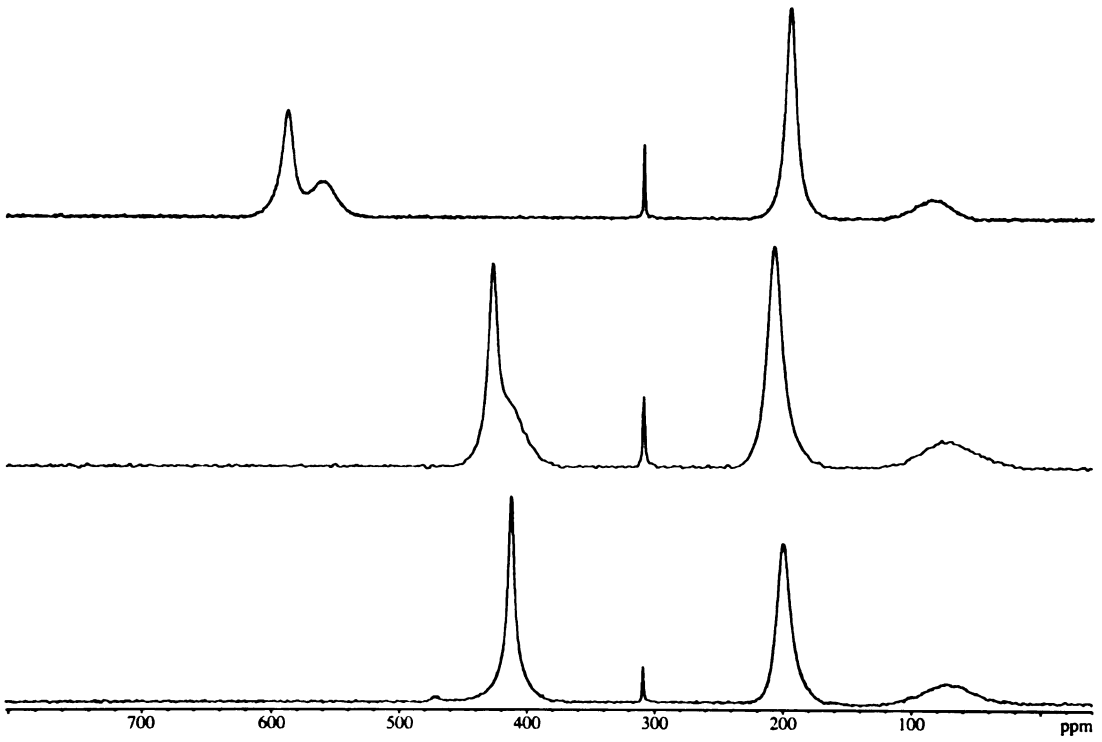

Figure 2-10. The ^{14}N NMR spectra of $Cr(NBu^t)_2(dpma)$ (**5**) (top), $Mo(NBu^t)_2(dpma)$ (**6**) (middle), and $W(NBu^t)_2(dpma)$ (**7**) (bottom).

47

$$\sigma = \sigma_D + \sigma_p \qquad (2\text{-}7)$$

The Ramsey equation, eq 2-7, describes the shielding of a nucleus in terms of a diamagnetic component, σ_D, and a paramagnetic component, σ_P; the paramagnetic term predominates in nitrogen NMR.[48] As one descends a column in the periodic table, imido group resonances in nitrogen NMR shield significantly, primarily due to the higher negative charge on the nitrogen atom as the M-N(imido) bond polarity increases as well as the increase in ΔE because of larger ligand field splittings.[15] Bending in imido-metal bonds is expected to decrease ΔE because of lower energy $n \rightarrow \pi^*$ circulations,[15] compared to

linear imido-metal bonds, and this will decrease the shielding of the bent imido nitrogen resonances.

The ^{14}N NMR (Figure 2-10) spectra of compounds **5** – **8** are unlike the crystal structures and the ^{1}H and ^{13}C NMR spectra of these compounds in that only $Cr(NBu^t)_2(dpma)$ (**5**) clearly shows two distinct imido resonances. The spectrum of **5** has one relatively sharp peak at 588 ppm ($\Delta\nu_{1/2}$ = 382 Hz) corresponding to the axial (bent) imido nitrogen atom[14b] and a broader resonance at 560 ppm ($\Delta\nu_{1/2}$ = 688 Hz) for the equatorial (linear) imido nitrogen atom. The molybdenum derivative, $Mo(NBu^t)_2(dpma)$ (**6**), exhibits two unresolved resonances at 472 ($\Delta\nu_{1/2}$ = 248 Hz) and 458 ppm ($\Delta\nu_{1/2}$ = 1100 Hz). The tungsten congener, $W(NBu^t)_2(dpma)$ (**7**), appears to have a single imido resonance at ~413 ppm; however, deconvolution of the spectrum requires two resonances at 415 ($\Delta\nu_{1/2}$ = 808 Hz) and 413 ppm ($\Delta\nu_{1/2}$ = 190 Hz) to explain the shape of the peak. The imido nitrogen atom resonances do shift upfield as expected as the shielding increases down the triad, going from **5** to **7**. This shielding increase is dramatic at >150 ppm down the triad. Similar trends are seen in the nitrogen NMR of nitrido[49] complexes.[50]

Imido substituent effects can be seen by comparing the ^{14}N resonances of complexes **6** and **8**. While alkyl imido **6** displays two resonances for the imido groups, aryl imido **8** has a single Lorentzian peak in the ^{14}N NMR for the imido nitrogen atoms at 429 ppm ($\Delta\nu_{1/2}$ = 648 Hz), which cannot be deconvoluted into two distinct resonances.

Increases in the M-N(imido) bond polarity may result in decreased sensitivity of the corresponding chemical shifts to imido nitrogen environment.[38] This is seen experimentally; the more covalent chromium complex **5** shows higher sensitivity to imido nitrogen environment than do the molybdenum and tungsten analogs, so much so that in the tungsten compound the resonances are separated by only 2 ppm. Assuming that one of the imido substituents is more electron-rich than the other substituent (consistent with the ^{13}C NMR data), the two imido ligands should react differently when the electronegativity of the metal center is decreasing on going from chromium to molybdenum to tungsten.

This increase in bond polarity going down the group decreases the differences caused by having the nitrogen atoms in different environments. This also seems to be a reasonable explanation for the differences seen between alkyl imido **6** and aryl imido **8**, that is, the aryl substituents on the imido nitrogen atoms of **8** result in more electronegative imido nitrogen atoms and higher Mo-N(imido) bond polarity. The result is the unresolvable resonances for the two different imido nitrogen atoms of **8**. The aryl group will also resonance stabilize the imido lone pair electrons, leading to an increase in ΔE for $n \rightarrow \pi^*$ paramagnetic circulations, shielding the aryl imido nitrogen atom by ~30 ppm compared to the *tert*-butyl derivative.

If one assumes that the ^{14}N NMR chemical shift differences are predominantly caused by the imido bond angle differences, an alternative explanation evolves. This would require that the ^{1}H and ^{13}C NMR chemical shifts are more sensitive to other factors. In this case, the more polar M-N(imido) bonds, those where M are molybdenum and especially tungsten, have a lower energy barrier to bending and straightening the M-N(imido)-C bonds. This lowered energy barrier would result in fluxional processes which equilibrate the imido bond angles on the ^{14}N NMR time scale. The solid-state structures and Density Functional Theory calculations (vide infra) suggest that while the minima of the imido bond angle bending potential energy surfaces are similar, the energies required for a specific bond angle deformation change with the metal center. Variable temperature ^{14}N might be useful to determine if the compounds are fluxional; there should be a low temperature limit at which the two different imido environments "freeze out," becoming inequivalent. In these compounds, unfortunately, lowering the temperature quickly broadens the resonances, eliminating any possibility of observing two distinct peaks. Increasing the temperature of solutions of $Mo(NBu^t)_2$(dpma) (**6**) resulted in clearer, sharper resonances with some shifting, although this shifting was insignificant over the temperature range available. Thus, it appears that there is no interchange of the imido ligands on the NMR time scale evident in the ^{14}N NMR spectra of these compounds, consistent with what is seen in the

^{1}H NMR spectra.

A few conclusions may be drawn from the ^{14}N NMR spectra of complexes **6–8**. The first is that the imido nitrogen resonances become more shielded as the metal is changed from chromium to molybdenum to tungsten. Secondly, decreasing the electronegativity of the metal center appears to reduce the differences between the axial and the equatorial imido ligands. As in the case of the $\Delta\delta_{l-b}$ values (vide supra), the differences between the resonances due to the axial (bent) and equatorial (linear) imido ligands followed the trend Cr > Mo ~ W. The shifts of the resonance positions on changing the metal down the triad were much larger than the shifts of the resonance positions resulting from electronic differences between the two imido ligand environments.

Typical of the chemical shifts seen for other amine complexes, the ^{14}N NMR resonances corresponding to the amine donors of the dpma ligand are found at 84 ppm ($\Delta\nu_{1/2}$ = 1024 Hz), 74 ppm ($\Delta\nu_{1/2}$ = 1594 Hz), 79 ppm ($\Delta\nu_{1/2}$ = 1750 Hz), and 42 ppm ($\Delta\nu_{1/2}$ = 3132 Hz) for compounds **5–8**, respectively.

Concerning the ^{14}N NMR chemical shifts of the pyrrolyl nitrogen atoms, there appears to be a link between pyrrolyl nitrogen chemical shifts and the π-electron density in the pyrrole ring.[51] For free azoles, the ^{14}N chemical shifts vary linearly with the calculated π-charge densities (SCF-PPP-MO method) of the aromatic ring. The possibility of being able to correlate the ^{14}N chemical shifts of pyrrolyl nitrogen atoms and the π-acceptor strength of a metal center is indeed exciting, and these systems offer a change to evaluate the extent of metal center-aromatic system competition in these complexes.

The ^{14}N NMR chemical shift for the pyrrolyl nitrogen atoms in Cr(NBu^t)$_2$(dpma) (**5**) is 195 ppm ($\Delta\nu_{1/2}$ = 125 Hz); the corresponding chemical shifts in the molybdenum and tungsten complexes are 198 ppm ($\Delta\nu_{1/2}$ = 372 Hz) and 201 ppm ($\Delta\nu_{1/2}$ = 421 Hz), respectively. This slight deshielding as one preceeds down the triad is consistent with slightly more π-bonding between the metal centers and the pyrrolyl nitrogen atom changing from chromium to molybdenum to tungsten. The arylimido complex **8** has a pyrrolyl

nitrogen atom resonance at 206 ppm ($\Delta\nu_{1/2}$ = 895 Hz); apparently, the less electron-donating arylimido groups lead to additional pyrrolyl nitrogen electron-density being donated to the metal center than in the alkylimido complex **6**. Since the chemical shift differences in these compounds are so small, the effects mentioned are undoubtedly small also. The size of the chemical shift changes observed might be related to competition for the π-acceptor orbital between the axial imido ligand and the pyrrolyl nitrogen lone pair electrons. For example, in the compounds Ti(dpma)$_2$, Zr(dpma)$_2$, and Hf(dpma)$_2$, the pyrrolyl ^{14}N chemical shifts vary almost linearly with the electronegativities of the metals in the +4 oxidation state over a 47 ppm range.[25] This is due to the pyrrolyl p-electrons not having to compete with the strongly p-donating imido ligands found in complexes **5–9**.

Examination of M(NBu^t)$_2$(dpma) using DFT. Geometry optimizations of the M(NBu^t)$_2$(dpma) complexes at the SCF level, utilizing the LANL2dz effective core potential and the associated 3s3p3d basis set for the transition metals and the all electron 3-21g basis set for the main group elememts, yield bond lengths and angles that are in remarkable agreement with the geometries obtained from single-crystal x-ray diffraction experiments. Figure 2-11 shows the experimental and calculated M–N–C bond angles and metal-ligand bond distance for complexes **5–7**. As in the x-ray diffraction data, the chromium–imido bond distances are essentially the same in the calculated structure. Correlations between bond distance and bond order rarely work well; bond distances appear to be the result of many different factors.[16] Rothwell and coworkers, for example, have shown experimentally that metal alkoxide bond angles have no apparent correlation to metal alkoxide bond lengths.[52] A similar conclusion can be drawn from the data presented here; i.e., the two M–N(imido) bonds in each molecule seem quite similar despite their different environments.

The structure optimization calculations yield atomic charges; we can obtain the "net charge" of the two M–N imido bonds in each of the three compounds examined by subtracting the atomic charge of the nitrogen atom from the atomic charge of the metal atom. Subtracting the "net charge" of the axial (bent) metal–imido bond from the "net

Figure 2-11. Comparison of selected bond angles and bond lengths from the crystal strucures (top) and calculated geometries (bottom) of $M(dpma)(NBu^t)_2$.

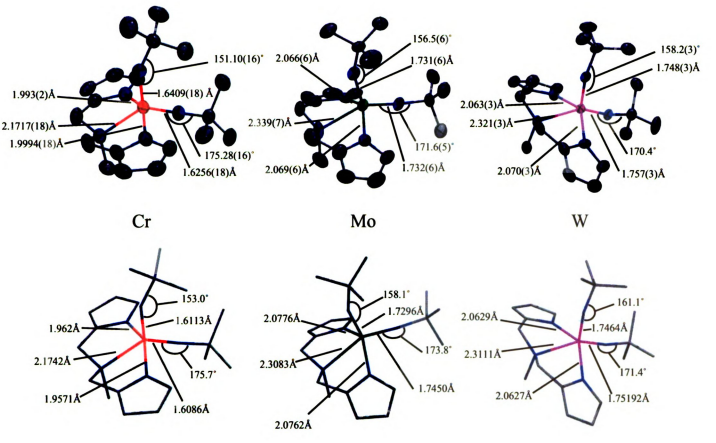

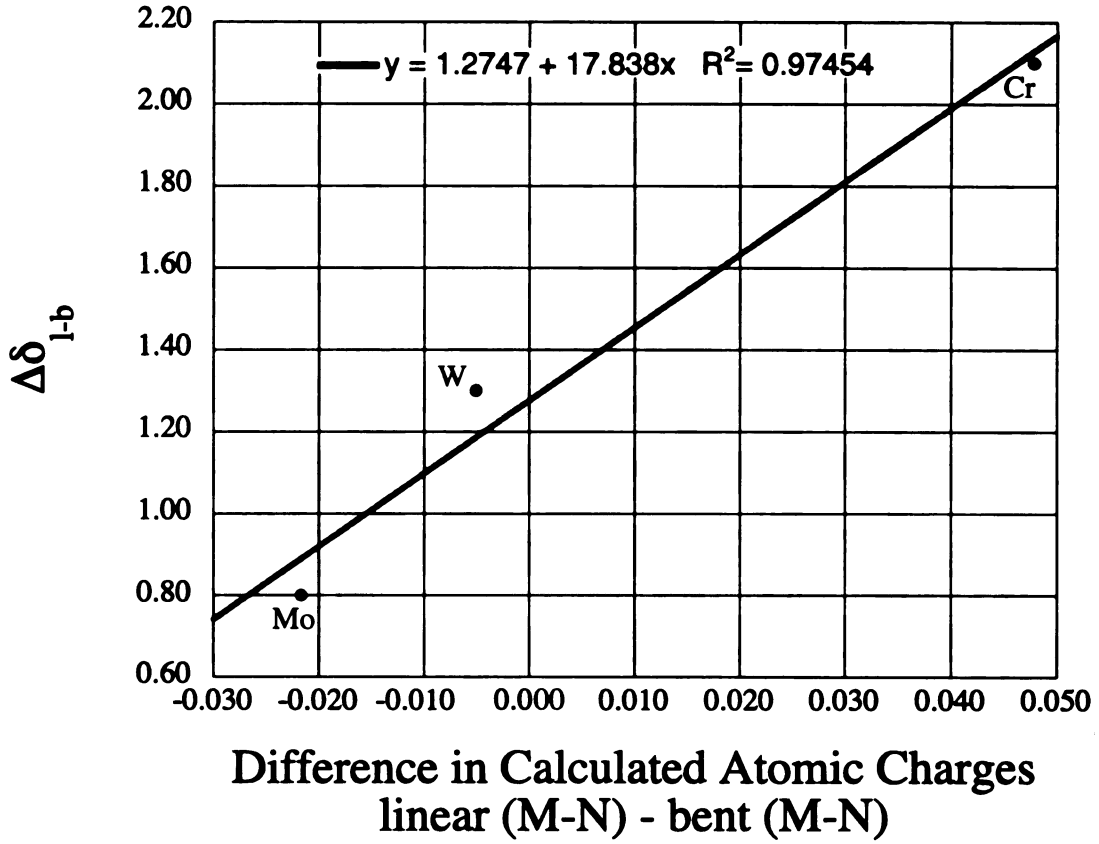

Figure 2-12. Plot of the differences of the calculated atomic charge differences between linear and bent imido bonds versus $\Delta\delta_{l\text{-}b}$ for compounds **5–7**.

charge" of the equitorial (linear) metal–imido bond should give an estimation of the polarity difference between the two imido bonds. Graphing these values for the three complexes versus the observed solution-state $\Delta\delta_{l\text{-}b}$ for complexes **5–7** (vide supra), Figure 2-12, results in a straight line. The results indicitate that the axial (bent) metal–imido bond in complex **5** is less polar than the equatorial (linear) metal–imido bond. The opposite is true in the case of the molybdenum complex **6**; that is, the axial (bent) metal–imido bond is more polar than the equatorial (linear) metal–imido bond. In complex **7**, the axial (bent) metal–imido bond is more polar than the equatorial (linear) metal–imido bond, but the two bonds are more similar in polarity than in either complexes **5** or **7**. Why the calculated imido bond polarities trend the same way as does the solution-state $\Delta\delta_{l\text{-}b}$ rather than the solid-state $\Delta\delta_{l\text{-}b}$ is unknown.

Since the spectroscopic techniques discussed above cannot explain the factors leading to the resonance differences seen for the two imido substituents, the energy barriers associated with straightening the axial (bent) imido ligand from the solid-state angles to 175° (the approximate bond angle of the equatorial imido ligand) were calculated using Density Functional Theory, utilizing the LANL2dz effective core potential and the associated 3s3p3d basis set for the transition metals and the all electron 3-21g basis set for the main group elememts. In order to minimize computational expense as well as to avoid adding additional complications, these calculations involved simply changing the axial imido angle and determining the energy, without optimizing the rest of the structure. Because of this, the energies obtained are best viewed as upper limits. The energy associated with straightening the axial imido ligand for the chromium complex **5** was calculated as 4.5 kcal/mol (Figure 2-13). Legzdins and coworkers found, in a similar calculation for imido bending in Cr(O)(NMe)(Me)(NPr^i_2), an energy of 4.4 kcal/mol associated with the deformation of the Cr–N–C angle.[53] The energies calculated for straightening the axial imido bonds in complexes **6** and **7** are 2.7 kcal/mol and 2.0 kcal/mol, respectively. These energies are small enough that the M–N(imido)–C bond angles should be changing rapidly on the NMR timescale in room temperature solutions, so the differences between the two imido ligands seen in the NMR spectra (supra infra) are probably a result of the overall coordination environment of the different ligands and the equilibrium bond angles.

Plotting the calculated angle deformation energies versus the estimated electronegativity in the +6 oxidation state[38] of the associated metal results in a straight line, Figure 2-14, suggesting that the angular deformation energy is related to the M–N(imido) bond polarity. Additional factors involved in the bond angle deformation would be expected to cause this plot to deviate from linearity.

The ultimate question that arises from these systems is why the axial imido ligand is bent in the solid-state structures. The molecular orbitals (Figure 2-15) might yield some insight into this question, for if the pyrrolyl ligands were purely σ-only donors, the axial

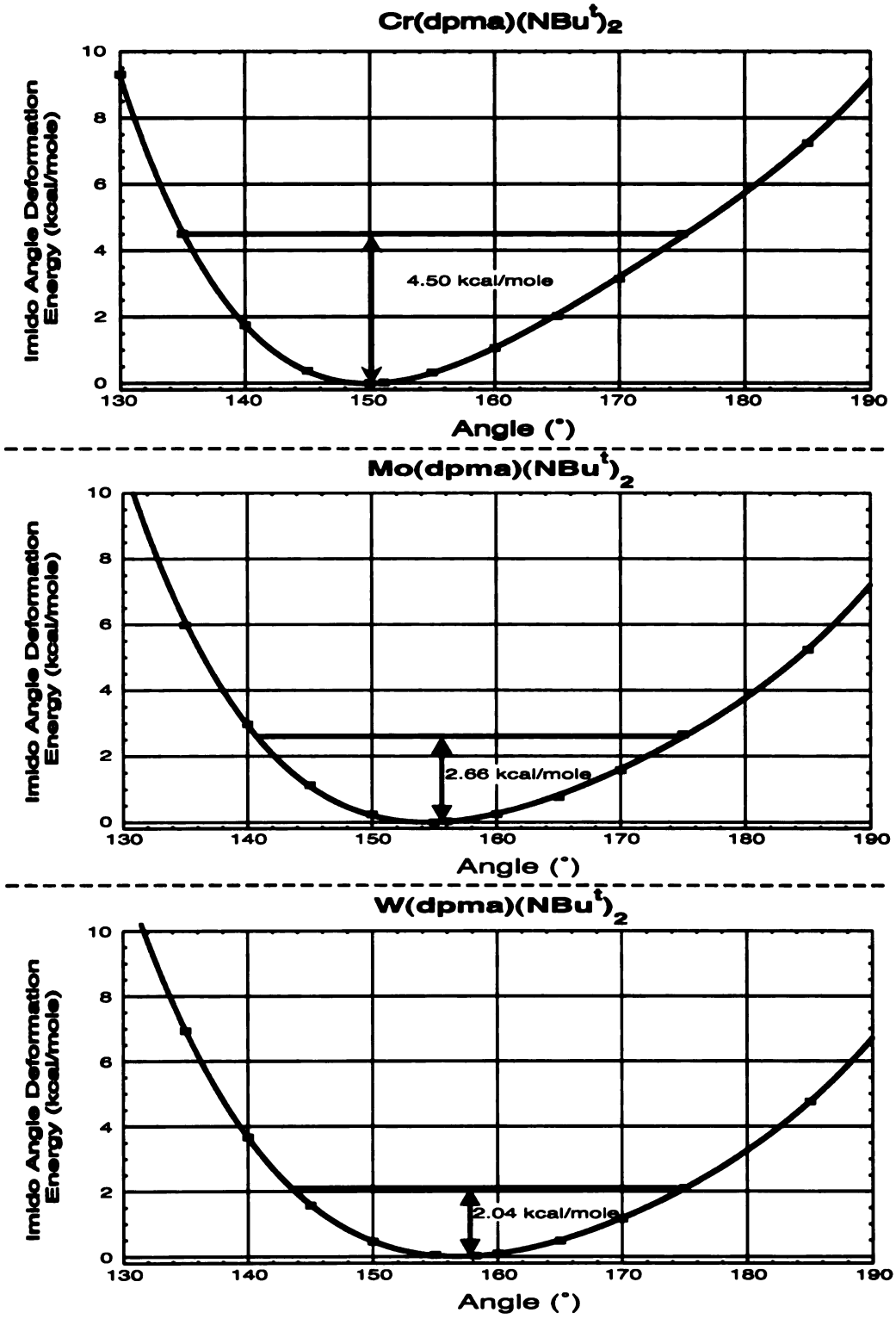

Figure 2-13. Plots of calculated energies versus angle for the axial imido ligand of compounds **5-7**.

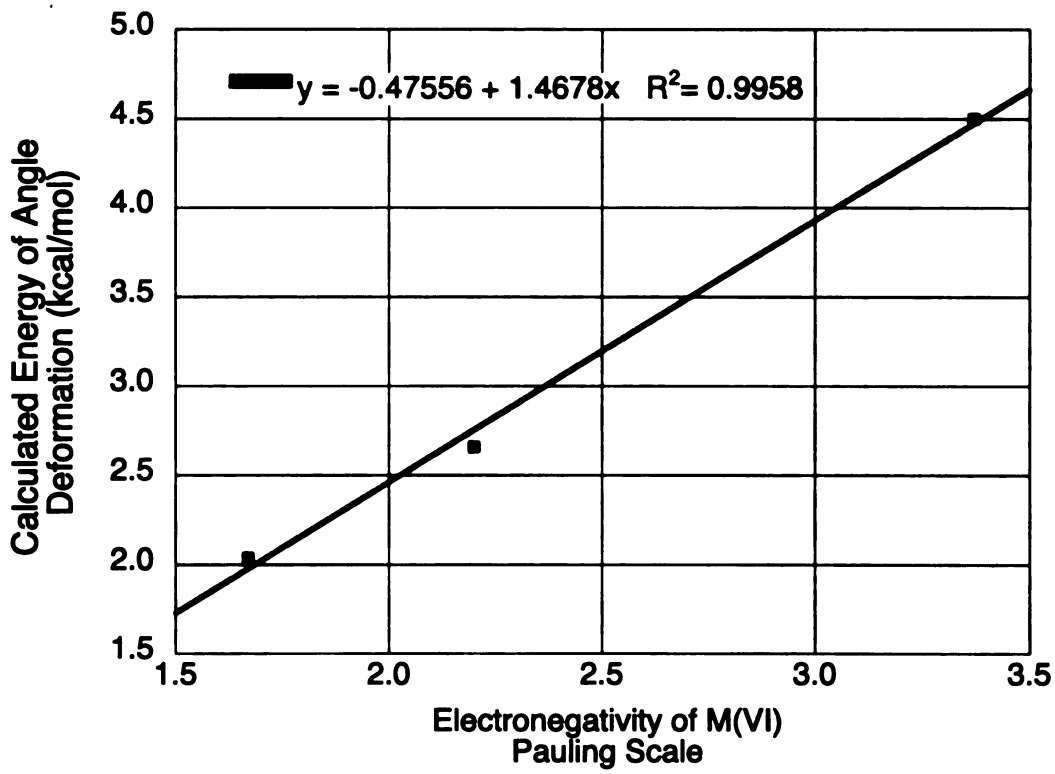

Figure 2-14. Plot of calculated energy difference from minimum to 175° in axial imido angle versus estimated electronegativities on the Pauling Scale.

imido ligand ought to be linear. However, any π-bonding from the pyrrolyl ligands could compete with axial imido π-bonding, resulting in a bent imido ligand. Several molecular orbitals were found with contributions from the pyrrolyl π-systems and the axial imido consistent with this postulate, and the ^{14}N NMR resonances for the pyrrolyl nitrogen are suggestive of attenuated π-bonding to those substituents due to competition with the imido ligand (vide supra).

Conclusions

It was attempted to quantify the relationship between electronegativity and imido angle bond deformation in these interesting complexes. Although none of the data described above is convincing alone, the overall picture created by the range of experimental and computational techniques described leads to several conclusions concerning these

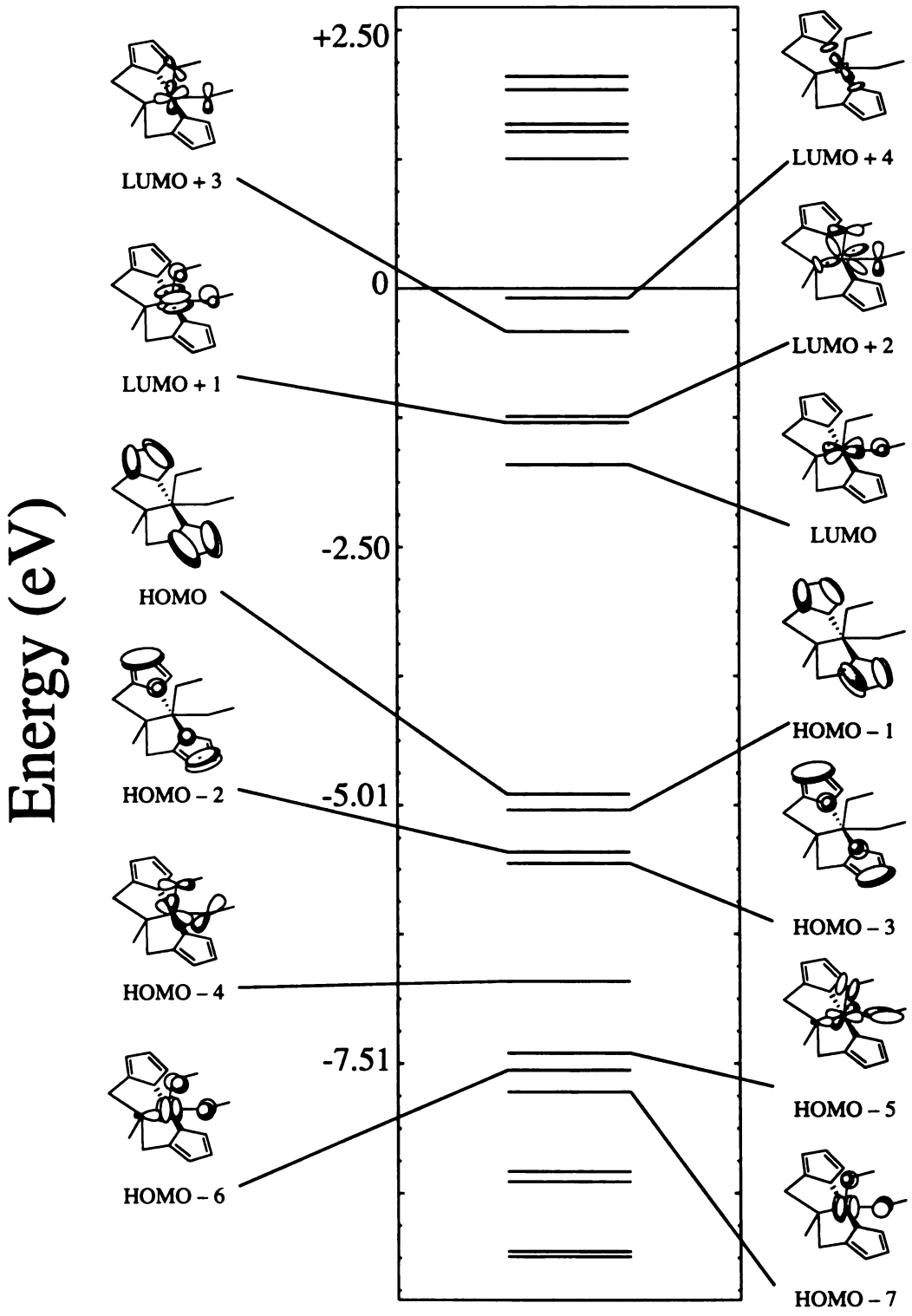

Figure 2-15. Plot of some of the calculated molecular orbital of $Cr(dpma)(NBu^t)_2$ (**5**). For ease of viewing, atom labels and *tert*-butyl methyl groups have been omitted.

bis(imido) complexes.

The ^{14}N NMR and the ^{13}C solid-state NMR data indicate that the axial imido ligands in the studied complexes are bent (solution and solid) and that they are more electron-rich than are the equatorial imido ligand. However, it cannot be shown that the axial ligand is electron-rich *because* it is bent rather than being electron-rich because it is in the axial position. However, if the canonical forms in Chart 2-1 are reasonable descriptors of the bonding in these complexes, and assuming that imido ligands will form triple bonds when able (Structrue **III**, Chart 2-1), it is reasonable to say that the axial imido ligand is bent due to the larger amount of electron-density (or vice-versa). Assuming that imido ligand bond angle and electron density are related, the following conclusions can be drawn.

The spectroscopic evidence, including ^{1}H, ^{13}C, and ^{14}N NMR data, suggests that the imido substituents in the $M(NBu^t)_2$(dpma) complexes do not exchange on the NMR timescale. Thus, it is possible to study the environmental differences of the two imido ligands via spectroscopy. For example, the more shielded *tert*-butyl resonances were found to be from the apparently more electron-rich axial (bent) imido ligands in complexes **5-7**. The calculated bond deformation energies indicate that the axial imido ligand angle is changing in solution, and that the observed differences in the two imido substituents is due to different equilibrium bond angles and different environments, i.e., axial vs. equatorial.

The fact that $\Delta\delta_{l-b}$ is nonzero indicates that the electron-densities on the two different imido nitrogen atoms are not the same. The value of $\Delta\delta_{l-b}$ in solution and in the solid-state changed as Cr > Mo ~ W, similar to differences between imido nitrogen chemical shifts in the ^{14}N NMR.[54] However, the effect of changing the other ligands on the metal centers can be larger than changing the imido environment, as indicated by the $\Delta\delta_{\alpha\beta}$ values. Therefore, imido environment on the metal center is likely less important to imido bonding than these metal-nitrogen polarity issues.[55]

A relatively simple description of imido bonding for this series of complexes is

apparent with these points in mind.[56] There will be a contribution to bonding from polar structures such as **IV** and **V**, and since these zwitterionic contributors both have a M–N(imido) bond order of one, rehybridization involving exchange between these structures will not greatly affect the bonding or nitrogen atom electron-density. The barrier to straightening or bending an imido bond in this model will be determined by the energy required to exchange bent imido structure **I** with linear forms **II** and **III**, the extent to which the polar forms **IV** and **V** participate, and any steric effects. Thus, as the M–N(imido) bond becomes more covalent for metal centers with relatively high electronegativity, e.g. chromium(VI) with very electron-withdrawing groups, the barrier to nitrogen rehybridization (bending or straightening) should increase. The DFT calculations on these complexes found that the chromium complex **5** has a higher barrier to imido angle deformation than the more polar, isostructural tungsten complex **7**, consistent with this assertion. The linear relationship between the calculated deformation barriers and the estimated electronegativity suggests that bond polarity is a major factor in determining imido ligand deformation energies.

The barrier to isomerization in highly covalent systems could approach those in organic imines, which typically range from 15 kcal/mol to >23 kcal/mol.[22,23] Thus, the conclusions on these systems are consistent with the results of other studies that have observed[14] and calculated[57] differences in imido bonding associated with imido ligand bending, which are typically small. Additionally, studies of these systems indicate that larger barriers to imido angle deformation due to electronic structure may be found for chromium(VI) or other transition metals where the effective electronegativity more closely approximates that of nitrogen and where the bending is required[16] by the electronics of the system, rather than by sterics[58] or some other effect.

Experimental

General considerations. All manipulations of air-sensitive materials were carried out in an MBraun glove box under an atmosphere of purified nitrogen. Ethereal solvents

Table 2-3. Structural parameters for compounds **5–9** from single–crystal x-ray diffraction.

	$Cr(dpma)(NBu^t)_2$ (5)	$Mo(dpma)(NBu^t)_2$ (6)	$W(dpma)(NBu^t)_2$ (7)	$Mo(Ndip)_2(dpma)$ (8)	$Mo(NBu^t)_2(dpCHIRA)$ (9)
Formula	$C_{19}H_{31}CrN_5$	$C_{19}H_{31}MoN_5$	$C_{19}H_{31}WN_5$	$C_{35}H_{47}MoN_5$	$C_{29}H_{49}MoN_5$
Formula weight	381.49	425.43	513.34	633.72	563.67
Space Group	P21/c	P2(1)/n	P2(1)/n	Fdd2	P2(1)2(1)2(1)
a (Å)	10.2007(2)	9.451(5)	9.4181(11)	19.415(5)	9.852(3)
b (Å)	9.4695(3)	10.175(5)	10.2171(12)	61.473(17)	16.642(4)
c (Å)	21.7312(5)	22.217(11)	22.190(3)	11.280(3)	18.190(5)
α (°)	90	90	90	90	90
β (°)	94.638(2)	93.569(9)	93.271(2)	90	90
γ (°)	90	90	90	90	90
Volume ($Å^3$)	2092.26(9)	2132.4(17)	2131.8(4)	13463(6)	2982.4(13)
Z	4	4	4	16	4
μ (mm^{-1})	0.557	0.626	5.429	0.419	0.464
$D_{calc.}$ ($g\ cm^{-3}$)	1.211	1.325	1.599	1.251	1.255
$R(F_0)$ (I > 2s)	0.0433	0.0723	0.0192	0.0431	0.0640
$R_w(F_0)$ (I > 2s)	0.0961	0.1020	0.0466	0.0886	0.1077

and pentane were purchased from Aldrich Chemical Co. and distilled from purple sodium benzophenone ketyl. Toluene was purchased from Aldrich Chemical Co., refluxed over molten sodium for at least 2 d, and distilled. Dichloromethane was purchased from Spectrum Chemical Co., refluxed with calcium hydride for at least 2 d, and distilled. NMR solvents were purchased from Cambridge Isotopes Laboratories, Inc. Deuterated benzene was distilled from purple sodium benzophenone ketyl. Deuterated toluene was degassed and dried with neutral activated alumina. NMR solvents were stored in sealed containers equipped with a Teflon stopcock in the dry box prior to use. Spectra were taken on Varian instruments located in the Max T. Rogers Instrumentation Facility. Routine coupling constants are not reported. Alumina, silica, and Celite were dried at >200 °C under dynamic vacuum for at least 12 h, then stored under inert atmosphere. $Cr(NBu^t)_2(Br)_2(py)$,[29] $Mo[N(2,6\text{-}Pr^i_2C_6H_3)]_2Cl_2(dme)$,[30] $W(NBu^t)_2(NHBu^t)_2$,[31] and $Mo(NBu^t)_2Cl_2$(1,2-dimethoxyethane)[30] were prepared by literature methods. Bis(*tert*-butyl)diazene was purchased from Aldrich Chemical Co., and spectroscopic examinations were carried out in d_7-toluene by ^1H [δ = 1.18 (s, Bu^t)] and ^{13}C NMR [σ = 65.95 $C(CH_3)_3$, 26.90 $C(CH_3)_3$]. Combustion analyses were performed by Oneida Research Services in Whitesboro, NY.

Procedure for Density Functional Theory calculations. The calculated molecular structures were obtained by geometry optimizations at the SCF level using the LANL2dz effective core potential and the associated 3s3p3d basis set[59] for the transition metals Cr, Mo, and W while the all electron 3-21g basis[60] was used for the main group elements (H, C, O and N). The potential energy curves for the axial imido angle were calculated at the DFT level using the B3LYP functional.[61] As the angle was varied, the remainder of the molecule was kept at the optimal SCF geometry, a procedure that may overestimate the barrier for imido angle deformation. All calculations used the Gaussian 98-program[62] as implemented on the Chemistry Department's Silicon Graphics Origin 3400 computer.

$Cr(NBu^t)_2$(dpma) (5). A solution of Li_2dpma (0.1006 g, 0.500 mmol) in 5 mL ether was cooled to near frozen in a liquid nitrogen cold well. This was added to a cold

solution of $Br_2Cr(NBu^t)_2(py)$ (0.2163 g, 0.499 mmol) in 5 mL ether. The resulting solution was allowed to warm to box temperature and stirred for 2 h. The solids formed were filtered off, and ether was removed *in vacuo*. The residue was recrystallized from ether/pentane, yielding **1** as a dark red powder in 34% yield (0.0655 g, 0.172 mmol), m 128-130 °C ^{1}H NMR (toluene-d_8): δ = 6.97 (s, 2H, pyrrole-5-H), 6.60 (m, J_1=2.44 Hz, J_2=2.93 Hz 2H, pyrrole-4-H), 6.37 (m J_1=1.22 Hz, J_2=1.71, 2H, pyrrole-3-H), 4.37 (d, *J*=12.7 Hz, 2H, N-C*H*H-pyrrole, *anti* to methyl), 3.57 (d, *J*=12.7 Hz, 2H, N-CH*H*-pyrrole, *syn* to methyl), 2.41 (s, 3H, NCH_3), 1.47 (s, 9H, $NC(CH_3)_3$, linear), 1.14 (s, 9H, $NC(CH_3)_3$, bent). ^{13}C NMR (toluene-d_8): δ = 138.95 (pyrrole-1-C), 132.56 (pyrrole-2-C), 109.33 (pyrrole-3-C), 103.00 (pyrrole-4-C), 78.89 ($NCMe_3$, linear), 76.78 ($NCMe_3$, bent), 62.88 (methine CH_2), 46.03 (NCH_3), 31.12 ($NC(CH_3)_3$, linear), 30.22 ($NC(CH_3)_3$, bent). ^{14}N NMR (benzene-d_6): δ = 587.90 ($\Delta\nu_{1/2}$ = 382.27 Hz), 559.80 ($\Delta\nu_{1/2}$ = 688 Hz), 194.84 ($\Delta\nu_{1/2}$ = 327 Hz), 83.66 ($\Delta\nu_{1/2}$ = 1024 Hz). Anal. Calcd for $C_{19}H_{31}N_5Cr$: C, 59.82; H, 8.19; N, 18.36. Found: C, 60.20; H, 8.22; N, 17.98.

$Mo(NBu^t)_2$(dpma) (6). A solution of Li_2dpma (0.2014 g, 1.00 mmol) in a mixture of 5 mL toluene and 1 mL ether was cooled in a liquid nitrogen temperature cold well to near frozen. This solution was added to a cold, stirring solution of $Cl_2Mo(NBu^t)_2$(dme) (0.4007 g, 1.00 mmol) in 5 mL toluene. The reaction solution was allowed to warm to box temperature and stirred for 2 h. The solution was filtered, and volatiles were removed *in vacuo*. The resulting brown solid was recrystallized from pentane giving **2** as a yellow solid in 38% yield (0.161 g, 0.378 mmol), m 86 °C dec. ^{1}H NMR (toluene-d_8): δ = 7.09 (s, 2H, pyrrole-5-H), 6.51 (m, J_1=0.73 Hz, J_2=2.44, 2H, pyrrole-4-H), 6.31 (m, *J*=2.44, 2H, pyrrole-3-H), 4.28 (d, *J*=12.7 Hz, 2H, N-C*H*H-pyrrole, *anti* to methyl), 3.46 (d, *J*=12.7 Hz, 2H, N-CH*H*-pyrrole, *syn* to methyl), 2.17 (s, 3H, NCH_3), 1.49 (s, 9H, $NC(CH_3)_3$, linear), 1.21 (s, 9H, $NC(CH_3)_3$, bent). ^{13}C NMR (toluene-d_8): δ = 139.00 (pyrrole-1-C), 133.37 (pyrrole-2-C), 110.04 (pyrrole-3-C), 104.96 (pyrrole-4-C), 70.29 ($NCMe_3$, linear), 69.51 ($NCMe_3$, bent), 60.67 (CH_2), 44.61 (NCH_3), 31.69 ($NC(CH_3)_3$, linear), 31.04 ($NC(CH_3)_3$,

bent). ^{14}N NMR (23 °C, benzene-d_6): δ = 472 ($\Delta\nu_{1/2}$ = 248 Hz), 458 ppm ($\Delta\nu_{1/2}$ = 1100 Hz), 198.30 ($\Delta\nu_{1/2}$ = 372 Hz), 73.75 ($\Delta\nu_{1/2}$ = 1594 Hz). ^{14}N NMR (59 °C, toluene-d_8): δ = 427.03 ($\Delta\nu_{1/2}$ = 273 Hz), 412.98 ($\Delta\nu_{1/2}$ = 792 Hz), 206.76 ($\Delta\nu_{1/2}$ = 432.76 Hz), 69.58 ($\Delta\nu_{1/2}$ = 1981 Hz). Anal. Calcd for $C_{19}H_{31}N_5Mo$: C, 53.64; H, 7.34; N, 16.46. Found: C, 53.50; H, 7.23; N, 16.38. $Mo(NBu^t)_2Cl_2$[63] may also be used in the preparation of **6** with similar results.

$W(NBu^t)_2$(dpma) (7). A solution of H_2dpma (0.1902 g, 1.00 mmol) in 5 mL toluene was cooled to near frozen. The cold solution of ligand was added to a cold solution of $W(NBu^t)_2(NHBu^t)_2$ (0.4702 g, 1.00 mmol) in 5 mL toluene. The resulting solution was allowed to warm to box temperature and stirred for 2 h. Volatiles were removed *in vacuo* to yield a brown oil. To the oil, 2 mL of pentane was added. The solution was stirred for several min. Volatiles were again removed, which resulted in a yellow solid. Recrystallization from pentane gave **3** as a tan solid in 50% yield (0.255 g, 0.499 mmol), mp 78 °C dec. ^{1}H NMR (toluene-d_8): δ = 7.16 (s, 2H, pyrrole-5-H), 6.38 (t, J_1=3.17, J_2=2.45, 2H, pyrrole-4-H), 6.20 (m, J_1=1.46, 2H, pyrrole-4-H), 4.48 (d, J=12.6 Hz, 2H, N-C*H*H-pyrrole, *anti* to methyl), 3.46 (d, J=12.6 Hz, 2H N-CH*H*-pyrrole, *syn* to methyl), 1.94 (s, 3H, NCH_3), 1.45 (s, 9H, $NC(CH_3)_3$, linear), 1.12 (s, 9H, $NC(CH_3)_3$, bent). ^{13}C NMR (toluene-d_8): δ = 139.76 (pyrrole-1-C), 134.35 (pyrrole-2-C), 111.00 (pyrrole-3-C), 105.73 (pyrrole-4-C), 68.06 ($NCMe_3$, linear), 66.81 ($NCMe_3$, bent), 60.87 (CH_2), 44.658 (NCH_3), 33.08 ($NC(CH_3)_3$, linear), 32.51 ($NC(CH_3)_3$, bent). ^{14}N NMR (benzene-d_6): δ = 415.21 ($\Delta\nu_{1/2}$ = 808 Hz), 412.70 ($\Delta\nu_{1/2}$ = 190 Hz), 201.44 ($\Delta\nu_{1/2}$ = 421 Hz), 78.71 ($\Delta\nu_{1/2}$ = 1750 Hz). Anal. Calcd for $C_{19}H_{31}N_5W$: C, 44.46; H, 6.09; N, 13.64. Found: C, 43.99; H, 5.86; N, 13.69.

$Mo(Ndip)_2$(dpma) (8). A solution of Li_2dpma (1.001 g, 4.97 mmol) in 25 mL ether was cooled to near frozen. This cold solution was added to $Cl_2Mo(Ndip)_2(dme)$ (3.038 g, 5.00 mmol) in 25 mL ether. The resulting solution was allowed to warm to box temperature and stirred overnight. Lithium chloride was filtered off, and ether was removed *in vacuo*. The resulting brown solid was recrystallized from ether/pentane, which gave **4** as a tan

solid in 35% yield (1.10 g, 1.74 mmol). ^{1}H NMR (benzene-d_6): δ = 6.93-7.02 (m, 6H), 6.91 (m, 2H), 6.40 (m, J_1=2.69, J_2=2.44, 2H), 6.26 (m, 2H), 4.43 (d, J = 13.0 Hz, 2H), 3.90 (h, J = 6.7 Hz, 2H), 3.46 (d, J = 13.0 Hz, 2H), 3.18 (h, J = 6.7 Hz, 2H), 2.23 (s, 3H), 1.05 (d, J = 6.7 Hz, 9H), 1.04 (d, J = 6.7 Hz, 9H). ^{13}C NMR (benzene-d_6): δ = 153.22, 151.90, 147.91, 143.43, 139.20, 131.26, 129.55, 128.29, 128.29, 128.19, 127.81, 126.65, 122.95, 122.35, 111.06, 110.99, 105.84, 60.56, 45.46, 28.88, 28.80, 23.58, 23.42. ^{14}N NMR (benzene-d_6): δ = 429.32 ($\Delta\nu_{1/2}$ = 648 Hz), 205.85 ($\Delta\nu_{1/2}$ = 895 Hz), 42.49 ($\Delta\nu_{1/2}$ = 3132 Hz). Anal. Calcd for $C_{35}H_{47}N_5Mo$: C, 66.34; H, 7.48; N, 11.05. Found: C, 66.39; H, 7.42; N, 11.03.

Mo(NBu^t)$_2$(dpCHIRA) (9). A solution of Li_2dpma (0.0856 g,0.252 mmol) in a mixture of 5 mL ether was cooled in a liquid nitrogen temperature cold well to near frozen. This solution was added to a cold, stirring solution of $Cl_2Mo(NBu^t)_2$(dme) (0.1009 g, 0.253 mmol) in 5 mL ether. The reaction solution was allowed to warm to box temperature and stirred for 1 h. The solution was filtered, and volatiles were removed in vacuo. The resulting brown solid was recrystallized from pentane giving **9** as a yellow solid in 15% yield (0.0215 g, 0.0391 mmol), mp 108 °C dec. ^{1}H NMR (toluene-d_8): δ = 7.09 (s, 2H, pyrrole-5-H), 6.48 (m, 2H, pyrrole-4-H), 6.28 (m, 2H, pyrrole-3-H), 4.32 (t, 2H, N-C*H*H-pyrrole), 3.92 (dd, 2H, N-CH*H*-pyrrole), 3.00 (m, 1H), 2.60 (d, 1H,), 1.80 (m, 2H), 1.49 (d, 2H), 1.43 (s, 9H, CCH_3), 1.2-1.4 (m, 7H), 1.10 (s, 9H, CCH_3), 0.84 (d, 3H), 0.75 (d, 3H), 0.64 (d, 3H) . ^{13}C NMR (toluene-d_8): δ = 139.81, 139.47 (pyrrole-1-C), 133.40, 133.36 (pyrrole-2-C), 109.92, 109.88 (pyrrole-3-C), 105.09, 104.80 (pyrrole-4-C), 70.58 (N*C*Me$_3$), 69.91 (N*C*Me$_3$, bent), 58.72, 57.65, 50.79, 49.13,40.12, 35.63, 31.91, 31.38, 31.15, 28.70, 26.06, 24.88, 22.81, 21.65. Anal. Calcd for $C_{29}H_{49}N_5Mo$: C, 61.79; H, 8.76; N, 12.42. Found: C, 61.33 H, 9.18; N, 11.94.

General considerations for single crystal x-ray diffraction. Single crystals of **1-4** were grown at –35 °C in an MBraun inert atmosphere glove box. All but a small portion of the mother liquor was removed, and the crystals were removed from the glovebox in a sealed vial. The crystals were rapidly coated in Paratone N and mounted

on a glass fiber. The mounted crystal was placed under a cold stream of nitrogen from an Oxford "Cryostream" low-temperature device. Data were collected on a Bruker-AXS, Inc. SMART CCD diffractometer utilizing a PC running Windows NT. The data collection was done on a Bruker-AXS, Inc. 3-circle goniometer (χ set to 54.78°). The source was a water-cooled Mo x-ray tube (λ = 0.71073 Å) operating at 50 kV/40 mA. A single crystal graphite monochromator selected the wavelength of light prior to being columated. The cell was determined using ω–θ scans (–0.3° scan width) with 3 sets of 20 frames. The initial cell was found by repeated least squares and Bravais lattice analysis. Full data sets were collected using ω–θ scans in four runs. The fourth run duplicates the first 50 frames of the first run to allow analysis of peak intensity changes resulting from crystal degradation; no correction was necessary for any of the structures reported. Absorption corrections were applied to the data. Using the initial cell, data were integrated to hkl/ intensity data using the Bruker-AXS, Inc. program package SAINT. The final unit cell was determined by SAINT using all the observed data. The structures were solved and refined using the SHELXTL program developed by G. M. Sheldrick and Bruker-AXS, Inc. A full listing of atomic coordinates, bond lengths, bond angles, and thermal parameters for all the structures have been deposited at the Cambridge Crystallographic Data Centre and can be found in the Appendix I. Additional data pertaining to the collection and processing of the four structures can be found in Table 2-3. In Table 2-3, $R1 = \Sigma||F_0|-|F_c||/\Sigma|F_o|$ and $wR2 = \{\Sigma w(F_0^2-F_c^2)^2/\Sigma w(F_o^2)^2\}^{1/2}$. A partial listing of geometrical parameters for all four data sets may be found in Table 2-3.

CHAPTER 3

TRANSITION METAL ALKYLIDENES CONTAINING DIPYRROLYL LIGANDS

Introduction

In the last decade, Schrock carbenes (alkylidenes) have found extensive use as carbon-carbon double bond metathesis catalysts in both polymer and small-molecule synthesis. The substantial work of Schrock and coworkers has resulted in highly active, readily prepared, and commercially available molybdenum imido alkylidene catalysts.[64,65] Schrock, Hoveyda, and coworkers have introduced catalysts with chiral ancillary ligands and with polymer-supported ligands.[66-72] These ancillary ligands are typically alkoxide or aryloxide ligands; electron-withdrawing ligands result in more highly-active catalysts than electron-donating ligands. Little success in making active catalysts has resulted from the use of other types of ligands, such as aryldiamido ligands.[73,74]

The introduction of ruthenium-based metathesis catalysts by Grubbs and coworkers has allowed the use of less-stringent anaerobic conditions during double-bond metathesis.[75] There have been many successful advances in these ruthenium catalysts, most notably the use of N-heterocyclic carbenes (Ardeungo carbenes) as ancillary ligands.[76-83] Modification of the ruthenium-based catalysts to enable asymmetric ring-closing metathesis catalysts and polymer-supported catalysts has been less straightforward than with the molybdenum-based catalysts, primarily due to the difficulty involved with ancillary ligand substitution of the ruthenium catalysts. Alkoxide substitution of the chlorides has been shown to result in substantial decrease of reactivity of these complexes as metathesis catalysts.[84]

Dipyrrolyl ligands offer several advantages as ligands. They are readily synthesized in high yield. Many functional groups, including chiral centers, can be incorporated into the ligands through the use of appropriate starting materials. These ligands have already seen widespread use in titanium-based hydroamination catalysts[85] (Chapter 6), and it was anticipated that their incorporation into metathesis catalysts could result in novel catalysts with interesting symmetric and asymmetric properties. With this in mind, several new

molybdenum– and ruthenium–based alkylidenes have been synthesized.

Results and Discussion

Reaction of Li_2dpma with one equivalent of $(OTf)_2Mo(Ndip)(=CHCMe_2Ph)$ yields, after work-up, Mo(dpma)(Ndip)(=$CHCMe_2Ph$) (**10**, eq 3-1), as a mixture of two isomers. Since one isomer is more soluble in pentane than is the other, a partial separation of the two isomers may be carried out. The crystal structure of one of these isomers, the less pentane soluble isomer, is shown in Figure 3-1 and selected bond lengths and bond angles are shown in Table 3-1. As can be seen, the imido ligand is axial and the neophylidene ligand is equatorial in this structure.

Although the molybdenum–carbon alkylidene bond distance in complex **10** of 1.898(2) Å is in the typical range reported for molybdenum neophylidene complexes (1.881 – 1.963 Å), and the downfield position of the alkylidene proton (12.4 ppm) is in the usual range of alkylidene proton resonances, the molecule is unreactive towards the typical metathesis substrates (norbornene, diethyl diallyl malonate). In fact, Mo(dpma)(Ndip)(=$CHCMe_2Ph$) (**10**) is air stable in the solid state and in solution for longer than 12 h. Surprisingly, the isomers were found to slowly interconvert in solution; at 65 °C (C_6D_6), 15% of the pentane insoluble isomer converts to the other isomer in approximately 12 h.

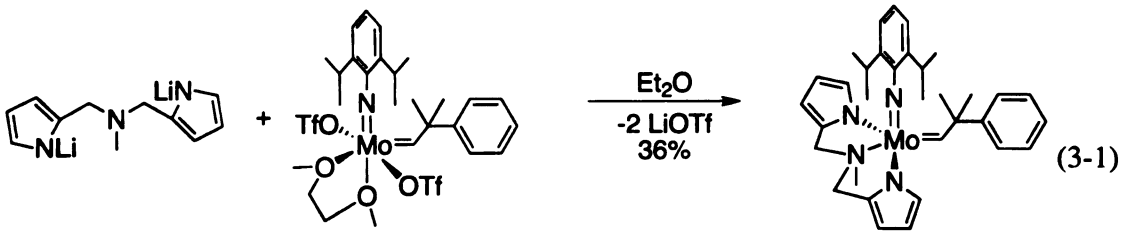

(3-1)

10

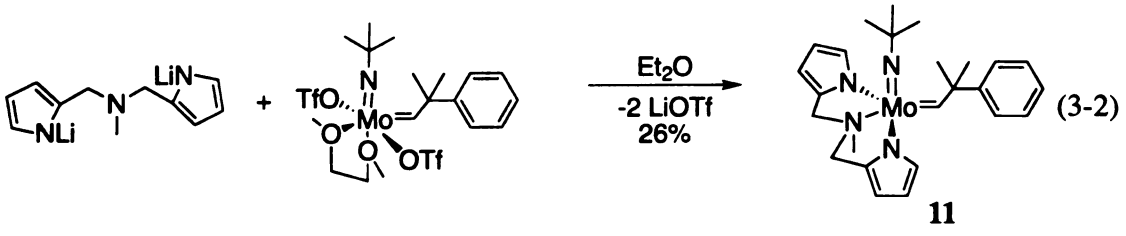

(3-2)

11

Table 3-1. Selected bond distances and angles from x-ray diffraction on complexes **10** and **11**. For the numbering scheme, see Figure 3-1.

Distances and Angles (Å/°)	Mo(Ndip)(dpma) (=CHCMe$_2$Ph) (10)	Mo(NBu^t)(dpma) (=CHCMe$_2$Ph) (11)
Mo-N(4)	1.716(2)	1.693(5)
Mo-C(5)	1.898(2)	1.871(6)
Mo-N(1)	2.089(2)	2.100(5)
Mo-N(2)	2.0789(19)	2.106(5)
Mo-N(3)	2.303(2)	2.277(5)
Mo-N(4)-C(41)	172.83(17)	163.9(5)
Mo-C(5)-C(51)	143.84(19)	147.2(6)
N(4)-Mo-C(5)	103.45(10)	104.0(3)
N(1)-Mo-N(4)	107.04(8)	101.1(2)
N(2)-Mo-N(4)	103.53(8)	101.9(2)
N(1)-Mo-C(5)	99.16(9)	97.8(2)
N(2)-Mo-C(5)	96.60(9)	98.9(2)
N(3)-Mo-N(4)	114.05(8)	128.2(2)
N(3)-Mo-C(5)	142.38(9)	127.7(2)
N(1)-Mo-N(2)	141.04(8)	147.1(2)
N(1)-Mo-N(3)	73.35(8)	73.5(6)
N(2)-Mo-N(3)	72.45(7)	73.9(2)

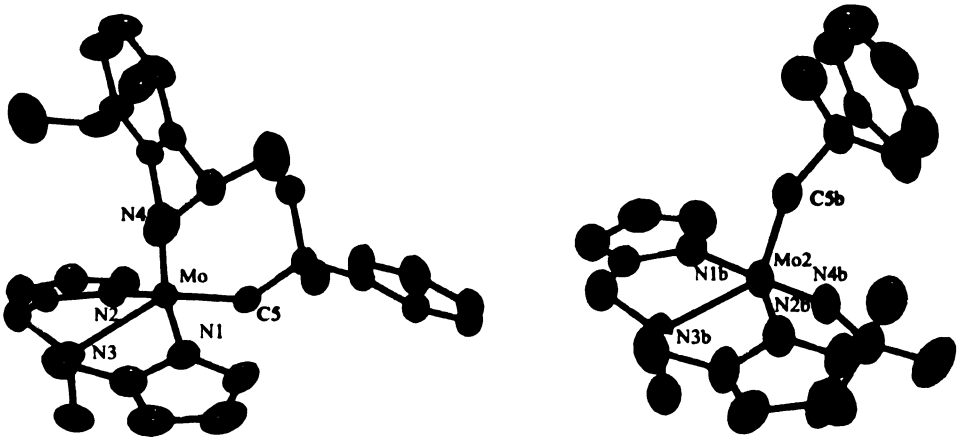

Figure 3-1. The ORTEP representation (50% probability ellipsoids) of Mo(dpma)(Ndip) (=CHCMe$_2$Ph) (**10**) (left) and Mo(dpma)(NBu^t)(=CHCMe$_2$Ph) (**11**) (right).

The space-filling model of Mo(dpma)(Ndip)(=CHCMe$_2$Ph), (**10**), Figure 3-2, shows a possible explanation for the remarkable lack of reactivity of this complex, i.e., the steric requirements of the dpma ligand prevent the substrates from reaching the metal center. In order to test this theory, Mo(dpma)(NBu^t)(=CHCMe$_2$Ph), **11**, was synthesized from (OTf)$_2$Mo(NBu^t)(=CHCMe$_2$Ph) and Li$_2$dpma, eq 3-2, resulting in a mixture of two different isomers. It was anticipated that there would be less steric crowding around the metal center due to the smaller (*t*-butyl)imido ligand. The solid-state structure obtained from single-crystal x-ray diffraction is shown in Figure 3-1, and selected bond lengths and bond angles are shown in Table 3-1. The space-filling model derived from the solid-state structure (Figure 3-2) indicates that there is less steric bulk around the molybdenum center than in the arylimido complex **10**. However, complex **11** also shows a lack of reactivity towards metathesis chemistry. Thus, it appears that the lack of in complexes **10** and **11** is due to electronic effects. It would not be suprising if the molybdenum orbitals needed to perform metathesis would be involved in bonding with the dpma ligand.

The obvious difference between the solid-state structures of the two dpma complexes is that in the (*t*-butyl)imido derivative the imido group is equatorial and the neophylidene group is axial. This results in a slight bending of the Mo–N(imido)–C bond to 163.9°; otherwise the only other substantial differences are seen in the N(3)–Mo–N(imido) and the N(3)–Mo–C(neophylidene) bond angles, resulting in complex **11** being better described as a square pyramidal structure than the arylimido complex (τ = 0.02 and τ = 0.32 for the (*t*-butyl)imido and arylimido complexes, respectively).

While nOe experiments were unable to differentiate the two isomeric species, it seems reasonable to suggest that the two different orientations seen in the solid-state structures of **10** and **11** are the two isomers produced in the syntheses, however only one isomer has been isolated from each reaction. It also seems reasonable to suggest that the two isomers interconvert via a Berry pseudo-rotation mechanism, Scheme 3-2.

Compound **12**, Mo(dmpm)(Ndip)(=CHCMe$_2$Ph) (Figure 3-5), obtained by

Figure 3-2. The space-filling representation of Mo(dpma)(Ndip)(=CHCMe$_2$Ph) (**10**) (left) and Mo(dpma)(NBu^t)(=CHCMe$_2$Ph) (**11**) (right), with the ligands color-coded.

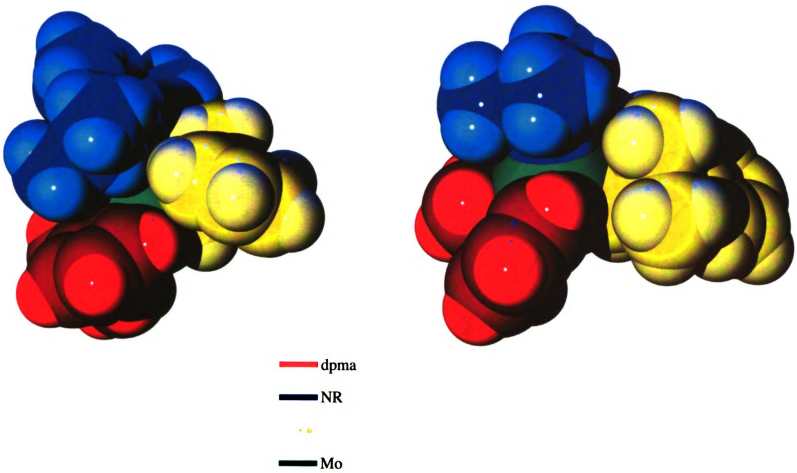

Scheme 3-1. Interconversion of the axial imido ligand with the equatorial neophylidene ligand through a Berry pseudo-rotation mechanism.

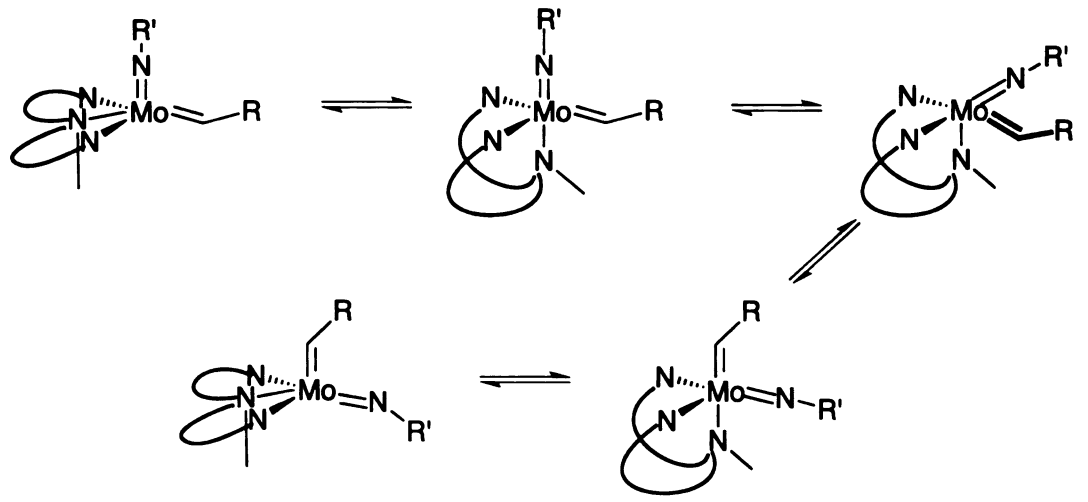

reaction of Li_2dmpm with $(OTf)_2$Mo(Ndip)(=CHCMe$_2$Ph) (eq 3-3), was prepared to determine the influence of the dpma donor amine on the reactivity of complexes **10** and **11**. Selected bond lengths and bond angles from single-crystal x-ray diffraction are shown in Table 3-2. As in the case of Mo(dpma)(NR)(=CHCMe$_2$Ph), the molybdenum-carbon alkylidene bond length is typical at 1.925(9) Å, although longer than in the dpma complexes **10** and **11**. The corresponding alkylidene proton resonance at 12.97 ppm is in the typical range. Unfortunately, complex **12** also shows very little metathesis activity.

In the solid-state structure, the dmpm ligand in this molecule adopts an η^1,η^5 coordination geometry, similar to the coordination of this ligand in Ti(dmpm)$(NMe_2)_2$ (Chapter 6). However, the room temperature ^{1}H and ^{13}C NMR spectra are indicative of slow η^5-pyrrolyl to η^1-pyrrolyl exchange. The free energy of activation associated with

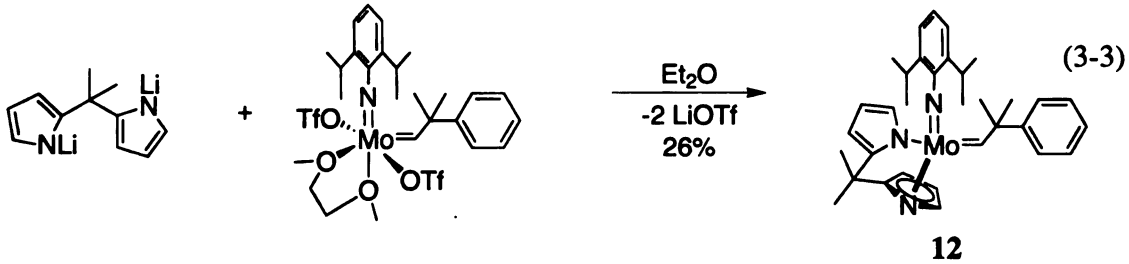

(3-3)

12

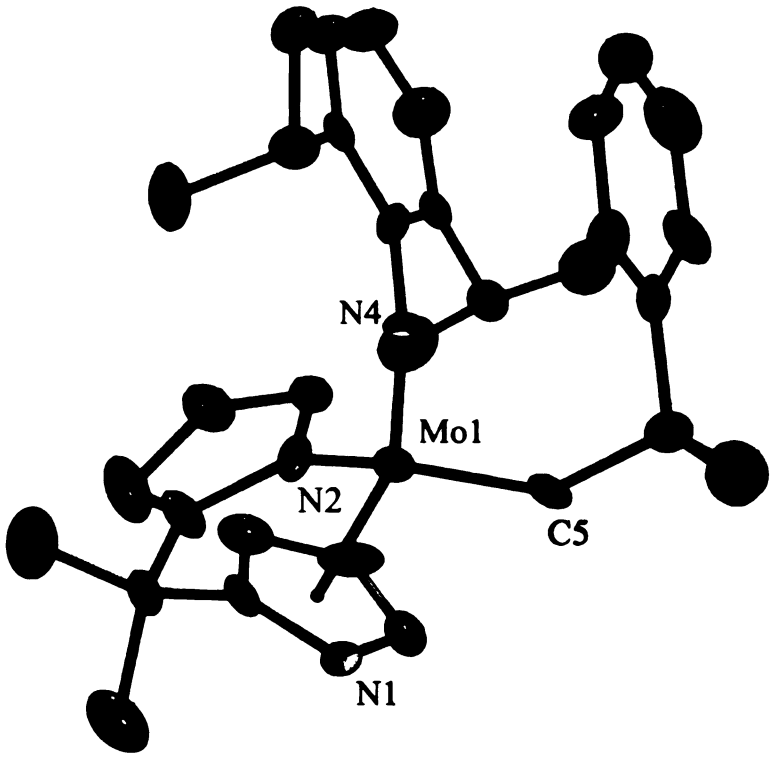

Figure 3-3. The ORTEP representation (50% probability ellipsoids) of Mo(dmpm)(Ndip) (=CHCMe$_2$Ph) (**12**).

Table 3-2. Selected bond distances and angles from x-ray diffraction for complex **12**. For the numbering scheme, see Figure 3-3.

Distances and Angles (Å/°)	Mo(Ndip)(dmpm) (=CHCMe$_2$Ph) (12)
Mo-N(4)	1.731(6)
Mo-C(5)	1.925(9)
Mo-centroid	2.083
Mo-N(2)	2.083(8)
Mo-N(4)-C(41)	169.7(6)
Mo-C(5)-C(51)	141.0(7)
N(4)-M-C(5)	102.0(4)
centroid-Mo-N(4)	126.3
N(2)-Mo-N(4)	105.9(3)
centroid-Mo-C(5)	117.0
N(2)-Mo-C(5)	100.4(3)

Figure 3-4. *The variable temperature ^{1}H NMR spectra of Mo(dmpm)(Ndip)(=CHCMe$_2$Ph), (13).*

Figure 3-4. The variable temperature ^{1}H NMR spectra of Mo(dmpm)(Ndip)(=CHCMe$_2$Ph), (**12**).

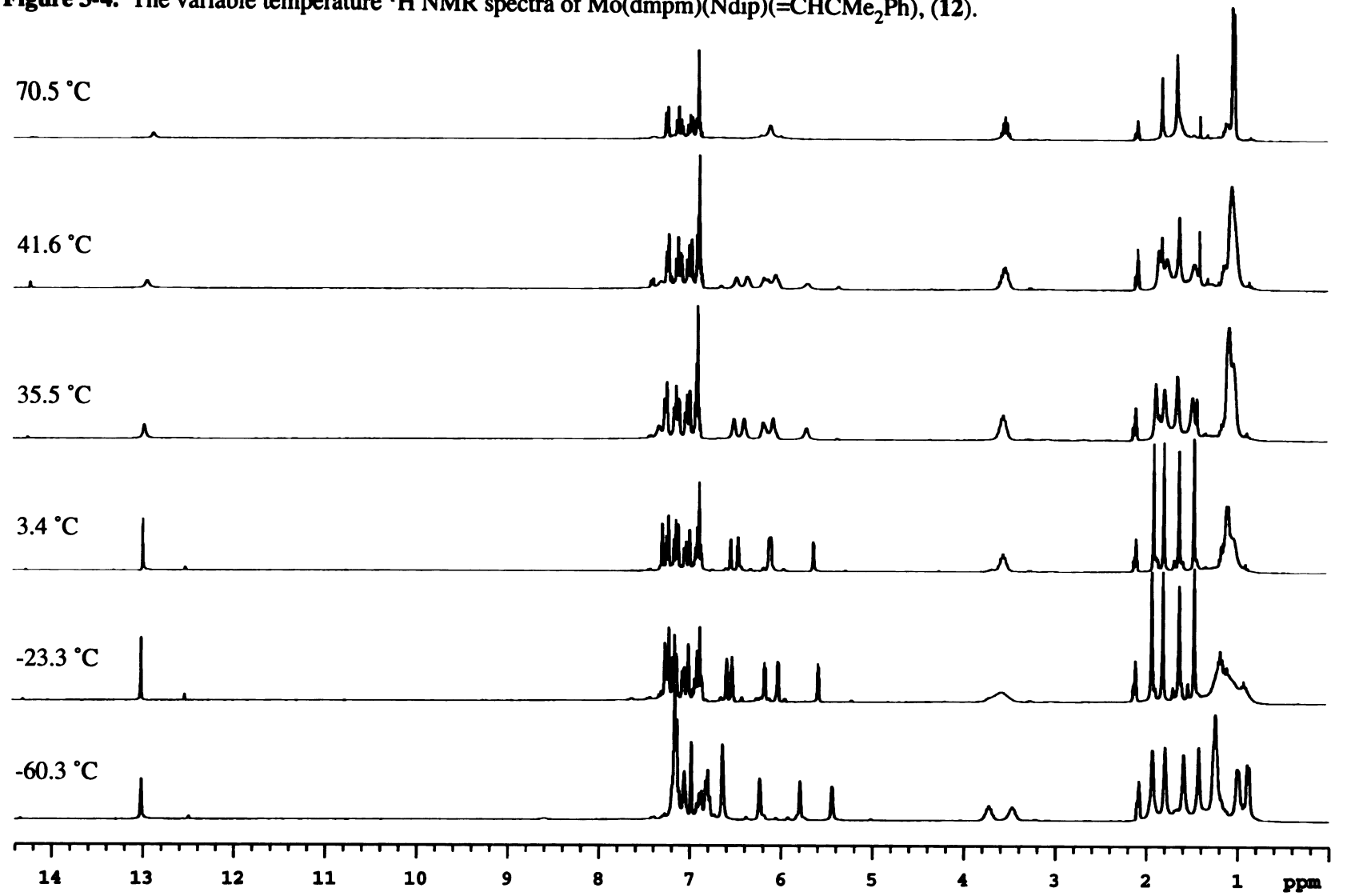

this exchange was determined by variable temperature ^{1}H NMR to be 16.0 kcal/mole in toluene-d_8 at 41.6 °C (Figure 3-7).

It is believed that the lack of reactivity of this complex is due, in large part, to the high temperatures (> 40°C) required for the dmpm ligand to adopt an η^1,η^1 coordination geometry in this complex. At these elevated temperatures, ^{1}H NMR clearly shows a rapid disappearance of the alkylidene proton resonance in the presence of either diethyl diallyl malonate or 1,7-ocatdiene, after production of a few percent ring-closing product.

Frustrated by the lack of reactivity of these complexes, complexes **13**, Ru(dpm a)(PCy_3)(=CHCH=CMe_2) (eq 3-4), and **14**, Ru(dpma)(PCy_3)(=CHPh) (eq 3-5), were synthesized in the expectation that these ruthenium alkylidenes would exhibit greater metathesis reactivity. Figure 3-7 shows the structure of complex **13** obtained from single-crystal x-ray diffraction; selected bond lengths and angles are shown in Table 3-3. The ruthenium–carbon alkylidene bond distance of 1.854(11) Å is similar to the ruthenium–carbon bond distance seen in other Grubbs' catalysts derivatives, and the alkylidene proton resonance at 19.09 ppm is consistent with what is seen in other derivatives of Grubbs' catalyst. However, as in the case of the molybdenum complexes (vide supra), the ruthenium

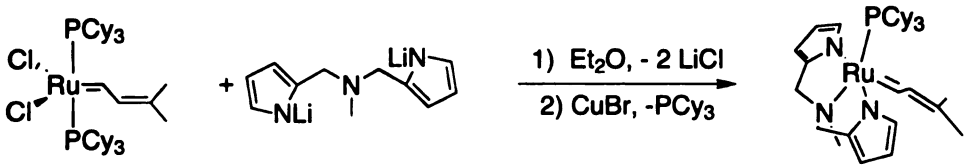

(3-4)

13

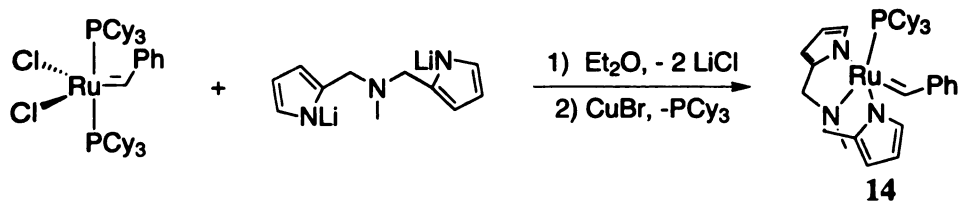

(3-5)

14

Table 3-3. Selected bond distances and angles from x-ray diffraction on Ru(dpma)(PCy_3)(=CHCH=CMe_2), (**13**). For the numbering scheme, see Figure 3-5.

Distances and Angles (Å/°)	Ru(dpma)(PCy_3)(=CHCH=CMe_2) (**13**)
Ru-P	2.313(3)
Ru-C(1)	1.854(11)
Ru-N(1)	2.078(10)
Ru-N(2)	2.092(9)
Ru-N(3)	2.141(9)
Ru-C(1)-C(2)	129.5(9)
P-Ru-C(1)	98.7(3)
N(1)-Ru-P	97.4(3)
N(2)-Ru-P	99.0(2)
N(3)-Ru-P	152.0(3)
N(1)-Ru-C(1)	89.5(4)
N(2)-Ru-C(1)	98.2(4)
N(3)-Ru-C(1)	109.1(4)
N(1)-Ru-N(3)	80.4(4)
N(2)-Ru-N(3)	80.2(4)

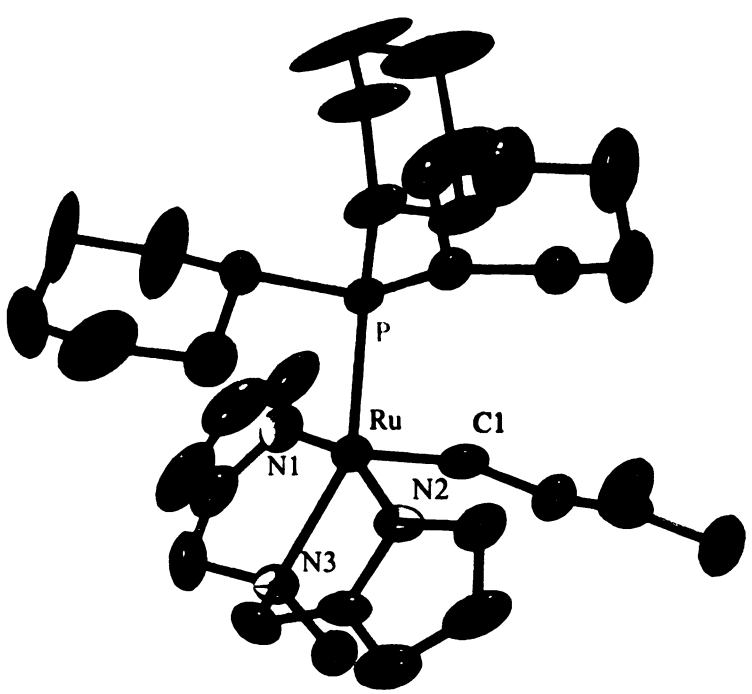

Figure 3-5. The ORTEP representation (50% probability ellipsoids) of Ru(dpma)(PCy_3)(=CHCH=CMe_2) (**13**).

compounds also show no metathesis activity, even at elevated temperatures and with CuBr added to promote tricyclohexylphosphine dissociation from the metal center.

Conclusions

Several new molybdenum and ruthenium alkylidene complexes have been synthesized and structurally which contain dipyrrolyl ligands. While structural and spectroscopic evidence indicate that these compounds are typical Schrock-type carbenes, they do not react as do typical Schrock carbenes. The lack of reactivity of the dpma-containing complexes **10**, **11**, **13**, and **14** appears to be due to a combination of steric and electronic effects imposed by the tridentate ligand, whereas the lack of reactivity of the dmpm complex **12** appears to be the inaccesablity of the η^1,η^1-coordinated complex at room temperature.

Experimental

General considerations. All manipulations of air-sensitive materials were carried out in an MBraun glove box under an atmosphere of purified nitrogen. Ethereal solvents and pentane were purchased from Aldrich Chemical Co. and distilled from purple sodium benzophenone ketyl. Toluene was purchased from Aldrich Chemical Co., refluxed over molten sodium for at least 2 d, and distilled. Dichloromethane was purchased from Spectrum Chemical Co., refluxed with calcium hydride for at least 2 d, and distilled. NMR solvents were purchased from Cambridge Isotopes Laboratories, Inc. Deuterated benzene was distilled from purple sodium benzophenone ketyl. Deuterated toluene was degassed and dried with neutral activated alumina. NMR solvents were stored in sealed containers equipped with a Teflon stopcock in the dry box prior to use. Spectra were taken on Varian instruments located in the Max T. Rogers Instrumentation Facility. Routine coupling constants are not reported. Alumina, silica, and Celite were dried at >200 °C under dynamic vacuum for at least 12 h, then stored under inert atmosphere. $RuCl_2(PCy_3)(=CHPh)$ was purchased

from Strem Chemical, and used as received. $Mo(Ndip)(=CHCMe_2Ph)(OTf)_2(dme)$[86] and $RuCl_2(PCy)_3(=CHCH=CMe_2)$[87,88] were prepared by literature methods. Combustion analyses were performed in-house at the Michigan State University Chemistry Department.

General considerations for single crystal x-ray diffraction. Single crystals of **1-4** were grown at –35 °C in an MBraun inert atmosphere glovebox. All but a small portion of the mother liquor was removed, and the crystals were removed from the glovebox in a sealed vial. The crystals were rapidly coated in Paratone N and mounted on a glass fiber. The mounted crystal was placed under a cold stream of nitrogen from an Oxford "Cryostream" low-temperature device. Data were collected on a Bruker-AXS, Inc. SMART CCD diffractometer utilizing a PC running Windows NT. The data collection was done on a Bruker-AXS, Inc. 3-circle goniometer (χ set to 54.78°). The source was a water-cooled Mo x-ray tube (λ = 0.71073 Å) operating at 50 kV/40 mA. A single crystal graphite monochromator selected the wavelength of light prior to being columated. The cell was determined using ω–θ scans (–0.3° scan width) with 3 sets of 20 frames. The initial cell was found by repeated least squares and Bravais lattice analysis. Full data sets were collected using ω–θ scans in four runs. The fourth run duplicates the first 50 frames of the first run to allow analysis of peak intensity changes resulting from crystal degradation; no correction was necessary for any of the structures reported. Absorption corrections were applied to the data. Using the initial cell, data were integrated to hkl/intensity data using the Bruker-AXS, Inc. program package SAINT. The final unit cell was determined by SAINT using all the observed data. The structures were solved and refined using the SHELXTL program developed by G. M. Sheldrick and Bruker-AXS, Inc. A full listing of atomic coordinates, bond lengths, bond angles, and thermal parameters for all the structures have been deposited at the Cambridge Crystallographic Data Centre and can be found in the Supporting Information. Additional data pertaining to the collection and processing of the four structures can be found in Table 3-4. In Table 3-4, $R1 = \Sigma||F_0|-|F_c||/\Sigma|F_o|$ and wR2 =

Table 3-4. Structural parameters for compounds **10–13** from single–crystal x-ray diffraction.

	Mo(Ndip)(dpma) (=CHCMe$_2$Ph) (10)	2Mo(NBu^t) (dpma)(=CHCMe$_2$Ph) •Et$_2$O•DME (11)	Mo(Ndip)(dmpm) (=CHCMe$_2$Ph) (12)	Ru(dpma)(PCy$_3$) (=CHCH=CMe$_2$)•toluene (13)
Formula	$C_{33}H_{42}MoN_4$	$C_{22.4}H_{33.6}Mo_{0.8}N_{3.2}O_{0.8}$	$C_{33}H_{41}MoN_3$	$C_{41}H_{62}N_3PRu$
Formula weight	590.65	437.28	575.63	728.98
Space Group	P2(1)/n	P–1	Pna2(1)	P–1
a (Å)	9.7242(17)	12.0651(19)	26.218(6)	9.6514(12)
b (Å)	16.088(2)	14.139(2)	11.061(2)	13.3909(16)
c (Å)	19.984(3)	19.318(3)	10.104(2)	19.128(2)
α (°)	90	96.541(3)	90	69.938(2)
β (°)	100.005(12)	102.773(3)	90	76.147(2)
γ (°)	90	114.526(3)	90	74.182(2)
Volume (Å^3)	3078.7(8)	2844.3(8)	2930.0(11))	2204.9(5)
Z	4	5	4	2
μ (mm^{-1})	0.453	0.486	0.473	0.419
$D_{calc.}$ (g cm^{-3})	1.274	1.276	1.305	1.098
$R(F_0)$ (I > 2s)	0.0252	0.0575	0.0571	0.0980
$R_w(F_0)$ (I > 2s)	0.0600	0.1223	0.0871	0.2979

$\{\Sigma w(F_0^2-F_c^2)^2/\Sigma w(F_o^2)^2\}^{1/2}$. A partial listing of geometrical parameters for all four data sets may be found in Table 3-4.

Mo(dpma)(Ndip)(=CHCMe$_2$Ph) (10). A solution of Li_2dpma (0.2020 g, 1.00 mmol) in a mixture of 20 mL toluene and 5 mL ether was cooled in a liquid nitrogen temperature cold well to near frozen. This solution was added to a cold, stirring solution of (OTF)$_2$Mo(Ndip)(=CHCMe$_2$)(dme) (0.7922 g, 1.00 mmol) in 40 mL toluene. After stirring the reaction for 18 h, the volatiles were removed in vacuo, and the solid dissolved in 40 mL toluene. The volatiles were again removed in vacuo, and the brown solid was dissolved in 20 mL toluene and filtered. The brown-red solid obtained after removal of volatiles in vacuo was recrystallized from toluene/pentane, to yield **10** as a brown solid in 35.9% yield (0.2123 g, 0.359 mmol) in two crops, m 78 °C dec. Anal. Calcd for $C_{33}H_{42}N_4Mo$: C, 67.11; H, 7.17; N, 9.49. Found: C, 66.63; H, 7.34; N, 957. More pentane soluble isomer: ^{1}H NMR (benzene-d$_6$): δ = 12.42 (s, 1H, Mo=C*H*CMe$_2$Ph), 7.44 (d, *J*=8.1 Hz, 2H), 7.20 (t, *J*=6.78 Hz, 2H), 7.06 (m, *J*=7.67 Hz, 1H), 6.95 (d, *J*=1.77 Hz, 3H), 6.68 (br s, 2H), 6.42 (m, *J*=2.8 Hz, 2H), 6.18 (m, *J*=2.95 Hz, 2H), 3.93 (d, *J*=13.1 Hz, 2H, N-CH*H*-pyrrole), 3.45 (sept, *J*=6.93 Hz, 2H, Ph[C*H*(CH$_3$)$_2$]$_2$), 3.22 (d, *J*=13.1 Hz, 2H, N-CH*H*-pyrrole), 1.90 (s, 3H, NC*H*$_3$), 1.78 (s, 6H, Mo=CHC(C*H*$_3$)$_2$Ph), 1.07 (d, *J*=6.93 Hz, 12H, Ph[CH(C*H*$_3$)$_2$]$_2$). ^{13}C NMR (benzene-d$_6$): 296.81 (Mo=C*H*CMe$_2$Ph), 152.36, 147.92, 140.03, 135.28, 128.78, 127.35, 126.61, 126.32, 122.95, 110.75, 105.56, 60.26, 55.15, 43.69, 30.92, 28.51, 23.50. Less pentane soluble isomer: ^{1}H NMR (benzene-d$_6$): δ = 12.63 (s, 1H, Mo=C*H*CMe$_2$Ph), 7.37 (d, *J*=7.4 Hz, 2H), 7.21 (t, *J*=7.4 Hz, 2H), 7.06 (t, *J*=7.0 Hz, 1H), 6.94 (d, *J*=0.73 Hz, 3H), 6.70 (m, *J*=1.33 Hz, 2H), 6.42 (m, J_1=3.4 Hz, J_2=0.89 Hz, 2H), 6.19 (m, J_1=2.1 Hz, J_2=1.2 Hz, 2H), 3.70 (sept, *J*=6.78 Hz, 2H, Ph[C*H*(CH$_3$)$_2$]$_2$), 3.56 (d, *J*=14.0 Hz, 2H, N-CH*H*-pyrrole), 3.35 (d, *J*=14.0 Hz, 2H, N-CH*H*-pyrrole), 2.23 (s, 3H, NC*H*$_3$), 1.72 (s, 6H, Mo=CHC(C*H*$_3$)$_2$Ph), 1.09 (d, *J*=6.78 Hz, 12H, Ph[CH(C*H*$_3$)$_2$]$_2$) . ^{13}C NMR (benzene-d$_6$): 304.40 (Mo=C*H*CMe$_2$Ph), 153.39, 147.84, 147.30, 141.86, 139.81, 136.22, 129.28, 126.38, 123.29, 111.56, 106.03, 58.32, 55.92, 48.89, 30.78, 28.51, 23.57.

$Mo(NBu^t)_2(CH_2CMe_2Ph)_2$. A solution of $Cl_2Mo(NBu^t)_2$(dme) (2.82 g, 7.06 mmol) in 100 mL ether was cooled in a liquid nitrogen temperature cold well to near frozen. To this solution was added 34 mL of 0.5M $ClMgCH_2CMe_2Ph$ in tetrahydrofuran. After stirring at box temperature for 14 h, the suspension was filtered through celite. The volatiles were removed from the filtrate in vacuo, leaving a brown oil which was used without further purification. ^1H NMR (benzene-d_6): δ = 7.32 (d, 4H), 7.17 (s, 2H), 7.12 (d, 2H), 7.02 (m, 2H), 1.58 (s, 4H), 1.43 (s, 12H), 1.24 (s, 18H). ^{13}C NMR (benzene-d_6): 152.26, 128.37, 126.15, 125.66, 72.71, 67.47, 39.74, 33.36, 32.33.

$Mo(NBu^t)(=CHCMe_2Ph)(OTf)_2$(dme). The crude $Mo(NBu^t)_2(CH_2CMe_2Ph)_2$ oil obtained above was dissolved in 100 mL 1,2-dimethoxyethane and cooled in a liquid nitrogen temperature cold well to near frozen. A cold solution of 3.19 g triflic acid (21.3 mmol) in 10 mL 1,2-dimethoxyethane was added. The solution was allowed to warm to box temperature, and was stirred for 16 h. Removal of the volatiles in vacuo left a brown oil, which was washed well with 50 mL portions of pentane (discarded) until a brown solid formed. This solid was dissolved in ether, and placed in the -35 °C freezer overnight. The solid *t*-butyl ammonium triflate was filtered off, and the volatiles were removed in vacuo. Recrystallization from ether/pentane gave 0.8636 g of a brown solid (1.26 mmol, 17.8%) as a mixture of seven isomers, m. 72 °C dec. ^1H NMR (benzene-d_6): δ = 15.27 (s, 0.10H), 14.91 (s, .051H), 14.87 (s, 0.07H), 14.84 (s, 0.09H), 14.32 (s, 0.20H), 13.79 (s, 0.21H), 13.42 (s, 0.25H), 7.30 (d, 1.1H), 7.39 (t, 3.2H), 7.35-7.1 (m, 6.8H), 7.06 (m, 5.5H), 3.57 (br s, 0.73H), 3.36 (br s, 2.4H), 3.17(br s, 15.3H), 2.90 (br s, 1.8H), 2.84 (0.93H), 2.14 (s, 1.2H), 1.93 (s, 2.8H), 1.84 (s, 4.2H), 1.79 (s, 1.7H), 1.69 (s, 5.0H), 1.60 (br m, 3.2), 1.57 (s, 1.5H), 1.54 (s, 0.75H), 1.51 (s, 1.44H), 1.39 (s, 9.78H), 1.36 (s, 2.2H), 1.32 (s, 9.0H), 1.23 (s, 3.0H), 1.21 (s, 2.9H), 1.18 (br s, 3.2H), 0.91 (br s, 7.5H), 0.86 (br s, 1.0H), 0.83 (s, 1.5H). ^{13}C NMR (benzene-d_6): 333.93, 332.89, 329.52, 326.66, 318.26, 317.28, 309.90, 150.97, 150.41, 150.07, 149.87, 149.06, 147.26, 139.12, 128.93, 128.79, 128.62, 128.17, 127.44, 127.33, 127.05, 126.79, 126.62, 126.46, 126.34, 125.81, 125.73, 122.53, 122.19,

118.29, 117.98, 87.17, 78.89, 77.85, 76.59, 75.66, 71.31, 70.38, 69.71, 61.28, 60.84, 60.39, 59.74, 55.16, 53.96, 41.91, 40.45, 41.91, 40.45, 34.36, 32.03, 31.91, 31.60, 31.32, 31.24, 30.93, 30.79, 30.45, 30.31, 30.26, 29.58, 29.30, 29.13, 27.79, 27.06, 22.62, 14.20.

Mo(dpma)(NBu^t)(=CHCMe$_2$Ph) (11). A solution of Li_2dpma (0.0305 g, 0.152 mmol) in 5 mL diethyl ether was cooled in a liquid nitrogen temperature cold well to near frozen. This solution was added to a cold, stirring solution of $(OTF)_2$Mo(NBu^t)(=CHC Me_2)(dme) (0.1.005 g, 0.146 mmol) in 5 mL diethyl ether. After stirring the reaction for 2 h, the volatiles were removed in vacuo, and the solid dissolved in 5 mL toluene. This was repeated twice. The volatiles were again removed in vacuo, and the brown solid was dissolved in 10 mL toluene and filtered. The brown-red solid obtained after removal of volatiles in vacuo was recrystallized from toluene/pentane, to yield **11** as a red-brown solid in 32.2% yield (0.0229 g, 0.0471 mmol), m. 82°C dec. This compound is isolated as a mixture of four isomers, one of which predominates. H NMR (benzene-d_6): δ = 12.22 (s, 1H), 7.5 (m, 1H), 7.22 (m, 2H), 7.07 (m, 2H), 6.79 (s, 2H), 6.50 (t, J_1=2.42 Hz, J_2=2.85 Hz, 2H), 6.28 (m, J_1=1.54 Hz, 2H), 3.96 (d, J=13.3 Hz, 2H), 3.25 (d, J=13.3 Hz, 2H), 1.91 (s, 6H), 1.90 (s, 3H), 1.00 (s, 9H). ^{13}C NMR (benzene-d_6): 292.03, 148.74, 138.93, 135.48, 133.24, 132.65, 128.75, 126.51, 126.42, 110.38, 104.95, 60.81, 43.74, 31.92, 30.89.

Mo(dmpm)(Ndip)(=CHCMe$_2$Ph) (12). A solution of Li_2dmpm (0.1860 g, 0.999 mmol) in 5 mL ether was cooled in a liquid nitrogen temperature cold well to near frozen. This solution was added to a cold, stirring solution of $(OTF)_2$Mo(Ndip)(=CHCMe$_2$)(dme) (0.7921 g, 1.00 mmol) in 40 mL toluene. After stirring at box temperature for 20 h, the volatiles were removed in vacuo, and the solid dissolved in 10 mL pentane and filtered. The brown-red solid obtained after removal of volatiles in vacuo was recrystallized from toluene/pentane, to yield 0.1507 g **11** as a yellow solid (0.262 mmol, 26.2%) in two crops, m 58 °C dec. ^{1}H NMR (toluene-d_8, 25 °C): δ = 12.97 (s, 1H, Mo=C*H*CMe$_2$Ph), 7.31 (s, 1H), 7.23 (d, J=7.6 Hz, 2H), 7.11 (m, J_1=7.5 Hz, J_1=8.6 Hz, 2H), 6.51 (s, 1H), 6.41 (m, 1H), 6.15 (m, 1H), 6.08 (s, 1H), 5.67 (m, 1H), 3.54 (sept, J_1=6.3 Hz, 2H, Ph[C*H*$(CH_3)_2]_2$), 1.88 (s,

3H), 1.79 (s, 3H), 1.63 (s, 3H), 1.47 (s, 3H), 1.09 (d, J_1=6.3 Hz, 6H, Ph[CH(CH_3)$_2$]$_2$), 1.01 (d, J_1=6.3 Hz, 6H, Ph[CH(CH_3)$_2$]$_2$). ^{13}C NMR (toluene-d_8): δ = 305.88 (Mo=*C*HCMe$_2$Ph) 166.81, 165.01, 151.75, 150.15, 131.80, 127.75, 123.18, 121.64, 109.81, 108.00, 106.89, 104.09, 55.22, 39.56, 31.81, 30.32, 29.72, 28.19, 24.31, 23.50.

Ru(dpma)(PCy$_3$)(=CHCH=CMe$_2$) (13). To a near frozen solution of 0.5205 g Cl$_2$Ru(PCy$_3$)$_2$(=CHPh) (0.650 mmol) in 5 mL diethyl ether was added a near frozen solution of 0.1308 g Li$_2$dpma in 3 mL ether. After stirring at box temperature for 16 h, 1.0 g CuBr was added. The suspension was stirred for 24 h. Filtering off the solid left a red solid, from which the volatiles were removed in vacuo, giving a red powder. Recrystallization from toluene gave 0.1498 g (0.235 mmol, 36.2%) of the title compound as a red solid (a mixture of four isomers), m. 46°C, dec. ^{1}H NMR (benzene-d_6): δ = 19.85 (m, J_1 = 5.71 Hz, J_2 = 4.76 Hz, 0.66H), 19.33 (m, J_1 = 6.66 Hz, J_2 = 4.76 Hz, 0.57H), 19.22 (m, J_1 = 5.71 Hz, J_2 = 4.76 Hz, 0.35H), 18.88 (m, J_1 = 7.61 Hz, J_2 = 2.86 Hz, 0.89H), 10.05 (s, 0.21H), 9.89 (s, 0.07H), 9.79 (s, 0.32H), 9.10 (s, 0.10H), 7.96 (d, 0.09H), 7.89 (d, 0.16H), 7.61 (d, 0.86H), 6.98 (s, 1.4H), 6.93 (s, 0.72H), 6.75 (s, 1.8H), 6.68 (s, 0.97H), 6.60 (s, 0.88H), 6.56 (s, 0.69H), 6.52 (d, 2.0H), 6.44 (s, 1H), 6.41 (d, 0.48H), 6.40-6.10 (br m, 3.0H), 6.00 (s, 1.8H), 4.64 (d, 0.56H), 4.50 (d, 0.56H), 4.43 (d, 0.39H), 4.32 (d, 1.69H), 3.83 (d, 0.71H), 3.53 (d, 0.74), 3.43 (dd, 1.7H), 3.17 (d, 1.1H), 2.91 (d, 0.76H), 2.8-2.5 (br m, 3.5H), 2.50 (s, 0.58H), 2.46 (s), 2.42 (s), 2.38 (s), 2.34 (s, 4.6H), 2.18 (s, 2.4H), 2.10 (s, 1.2H), 2.03 (br m, 7.0H), 1.84 (br m, 8.9H), 1.8-1.5 (br m, 25.5H), 1.5-1.0 (br m, 38.5H), 0.85 (br m, 5.1H), 0.63 (br m, 2.3H), 0.27 (s, 8.5H). ^{13}C NMR (benzene-d_6): δ = 297.05 (d), 295.90 (d), 294.52 (q), 290.92 (q), 148.22, 146.79, 146.58, 145.29, 144.91, 141.48, 141.08, 137.95, 137.81, 135.80, 135.40, 134.52, 133.62, 131.86, 130.78, 130.46, 129.43, 129.27, 126.74, 125.61, 124.57, 124.48, 123.59, 121.74, 121.63, 118.77, 118.36, 112.99, 112.19, 111.92, 109.44, 109.09, 108.88, 108.68, 108.58, 108.14, 107.50, 107.45, 105.27, 104.92, 104.67, 104.38, 104.31, 63.23, 60.67, 56.18, 55.75, 49.99, 42.82, 42.76, 41.37, 36.58, 36.33, 35.82, 35.56, 35.29, 34.79, 34.52, 34.38, 34.30, 31.00, 30.94, 30.81, 30.68, 30.43, 30.23, 30.14,

30.02, 29.55, 28.139, 28.07, 27.99, 27.93, 27.89, 27.79, 27.65, 27.56, 27.34, 26.82, 26.66, 26.42, 26.11, 22.66, 20.68, 20.34, 20.28, 18.28, 1.37. Anal. Calcd for $C_{34}H_{54}N_3PRu$: C, 64.12; H, 8.55; N, 6.60. Found: C, 64.76; H, 8.79; N, 6.40.

Ru(dpma)(PCy_3)(=CHPh) (14). A solution of Li_2dmpm (0.3966 g, 1.97 mmol) in 5 mL diethyl ether was cooled in a liquid nitrogen temperature cold well to near frozen. This solution was added to a cold, stirring solution of $Cl_2Ru(PCy_3)_2$(=CHPh) (1.620 g, 1.97 mmol) in 50 mL diethyl ether. After stirring at box temperature for 2 h, 2.1 g CuBr was added. The suspension was stirred for 30 m, then placed in a –35 °C freezer for 16 h. Filtering off the solid left a red liquid, from which the volatiles were removed in vacuo, giving a red powder. ^1H and ^{31}P NMR indicated the presence of $Cl_2Ru(PCy_3)_2$(=CHPh), so the powder was dissolved in 100 mL ether, and 0.1188 g Li_2dpma (0.591 mmol) was added. The solution was stirred for 14 h, 1.0g CuBr was added and the solution was stirred for an additional hour. The solid was filtered off and the volatiles were removed in vacuo, giving 1.27 g of **13** as a mixture of two isomers (1.93 mmol, 98.0%), which was used as obtained, 58 °C, dec. ^1H NMR (benzene-d_6): δ = 19.09 (d, *J*=12.37 Hz,1H, Ru=C*H*Ph), 7.21 (m, 2H), 7.19 (m, 1H), 7.04 (d, 2H), 6.87 (m, 2H), 6.80 (m, 2H), 6.56 (m, 2H), 4.31 (d, *J*=12.9 Hz, 2H, N-CH*H*-pyrrole), 3.44 (d, *J*=12.9 Hz, 2H, N-CH*H*-pyrrole), 3.27 (s, 1H), 2.45 (q, 4H), 2.02 (s, 3H), 0.9–1.9 (m, 28H, $P(C_6H_{11})_3$). ^{13}C NMR (benzene-d_6): δ = 298.34 (d), 298.16 (d), 152.57, 152.53, 141.22, 129.67, 129.42, 129.33, 128.87, 128.53, 109.61, 105.39, 63.10, 54.43, 48.52, 42.08, 34.853, 34.58, 30.78, 30.12, 29.67, 27.77, 27.64, 26.76, 26.61.HRMS(FAB$^+$): 659.2957, expected for $C_{36}H_{52}N_3PRu$: 659.2953.

CHAPTER 4

SELF-TETHERED MOLYBDENUM ALKYLIDENES

Introduction

Molybdenum carbon-carbon double bond metathesis catalysts have proven very useful, with the pioneering work of Schrock and coworkers.[89-95] Fürstner and coworkers synthesized several ruthenium alkylidenes tethered to *N*-heterocylic carbene ancillary ligands (eq 4-1), and investigated these complexes for ring-closing metathesis reactivity, with the thought that these catalysts might be more stable than current ruthenium metathesis catalysts. The intent was to produce a catalyst that, when all of the substrate was consumed from a reaction, would regenerate the tethered alkylidene preferentially over the unstable methylidene complex.[96] Subsequently, Grubbs and co-workers used these catalysts for the selective cyclo-polymerizations of olefins by ring-opening metathesis polymerization.[97] Since the tether remains attached to the metal center, the chance of a metathesis reaction resulting in regeneration of the starting catalyst and a macrocyclic polymer are increased

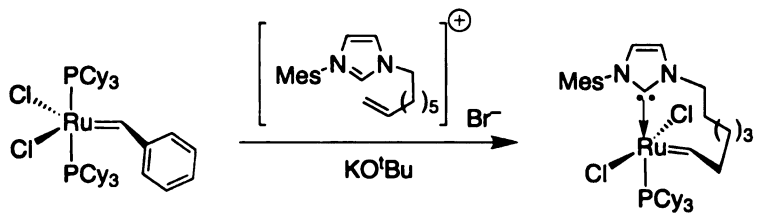

(4-1)

dramatically compared to a chain-termination step that would result in a linear polymer, Scheme 4-1

The chemistry of tethered molybdenum alkylidene complexes, with the alkylidene attached to the molybdenum center through an ancillary ligand, is being explored. It is believed that this will result in increased catalyst reusability, as in the ruthenium case, by eliminating the methylidene intermediates formed. In addition, the work of Schrock, Hovyeda, and co-workers in producing polymer-supported molybdenum metathesis catalysts would likely benefit from any increase in catalyst reusability derived from tethering the alkylidene to the metal center, Scheme 4-1.[98] The use of self-tethered

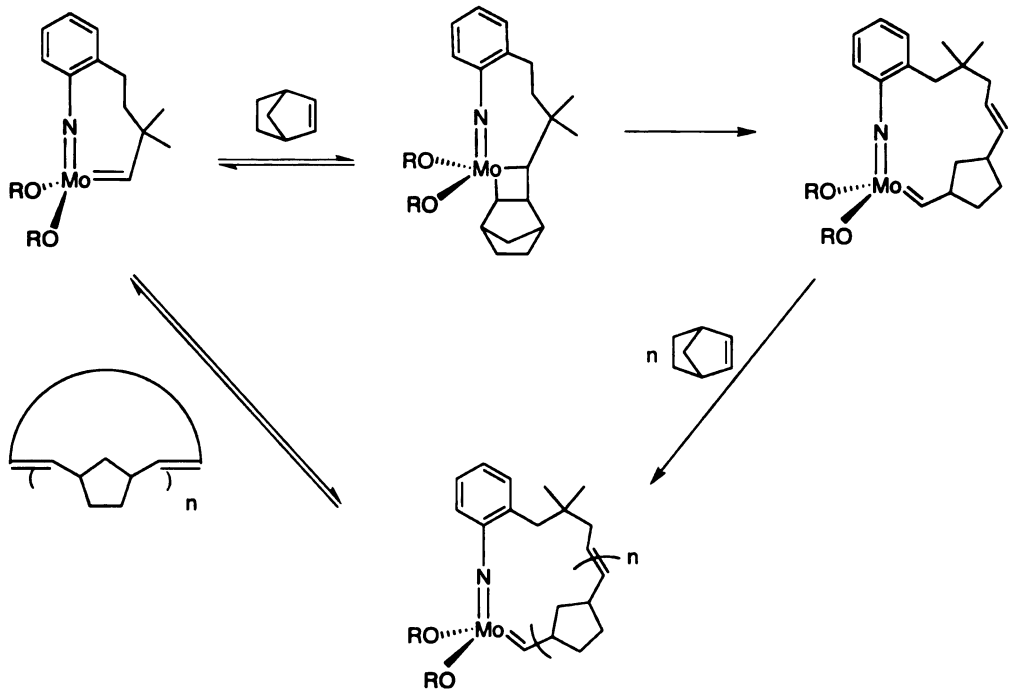

Scheme 4-1. The cyclic polymerization of norbornylene using a self-tethered metathesis catalyst.

molybdenum catalysts for the synthesis of novel cyclo-oligomerization products for use in high-performance materials is also envisioned.

There are very few examples of complexes containing two molybdenum metal-ligand bonds tethered to form a metallacycle. A few examples of mutually tethered di-carbenes have been reported, typically prepared via oligomerization of alkynes by reduced metal complexes.[99] The Zeigler-Natta polymerization activity of tethered group-6 bis(imido), *ansa*-di(organoimido) (analogs of *ansa*-metallocenes of the Group-4 elements) has been studied.[100] Computer models, based on reported molybdenum crystal structures, indicated that the optimum ring size of the tether was 7-8 atoms. This is consistent with the typical ring sizes used to generate tethered organoimidos. Thus, a tether that would produce a ring size in this regime was envisioned.

Originally, an alkene-substituted dpma ligand was going to be used as the tethering ligand, as it was fairly straight-forward to synthesize ligands such as H_2dpna (**3**). However,

as discussed in Chapter 3, the dpma ligand inactivates molybdenum alkylidenes to metathesis reactions. Linkages through the alkoxides were tried, but resulted in reduced metal species. A linkage via the imido substituent has been adopted as an alternative, and has resulted in the first imido-tethered group-6 alkylidene.

Results and Discussion

The ligand which was ultimately successful in producing the imido-tethered alylidene was an arylamine with a alkene attached at the *ortho*-position, generating an 8-membered azametallocycle when the catalyst was ultimately synthesized. Scheme 4-2 outlines the synthetic route to the aniline derivative; commercially available phenethyl bromide is first converted to the alkyl zinc by reaction with Reike zinc. The copper-mediated S_N2' addition of the alkyl zinc to 3,3-dimethylallylbromide[101] (~9:1 S_N2' : S_N2 isomers) results in 97% yield of the combined isomers,[102] which was nitrated under standard conditions without purification.[103] The high-yielding nitration generates a near equimolar ratio of the *ortho* and *para* isomers, which was reduced without separation of the isomeric products.[104] Column chromatography of the reduced product mixture gave the desired *ortho*-substituted aniline **15** in 22% yield, based on the crude mixture of the nitro isomers.

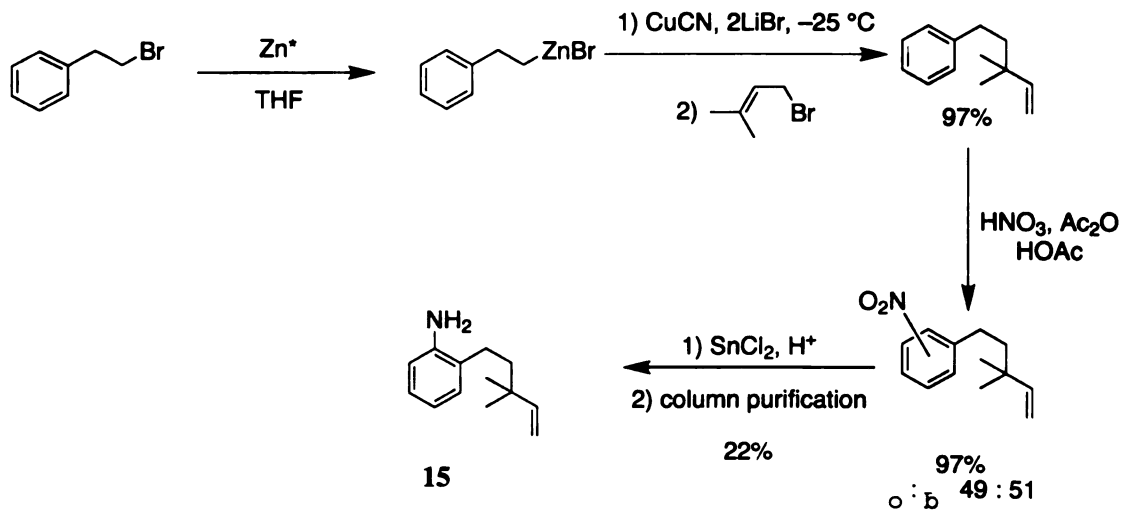

Scheme 4-2. Synthesis of 2-(3,3-dimethylpent-4-enyl)aniline.

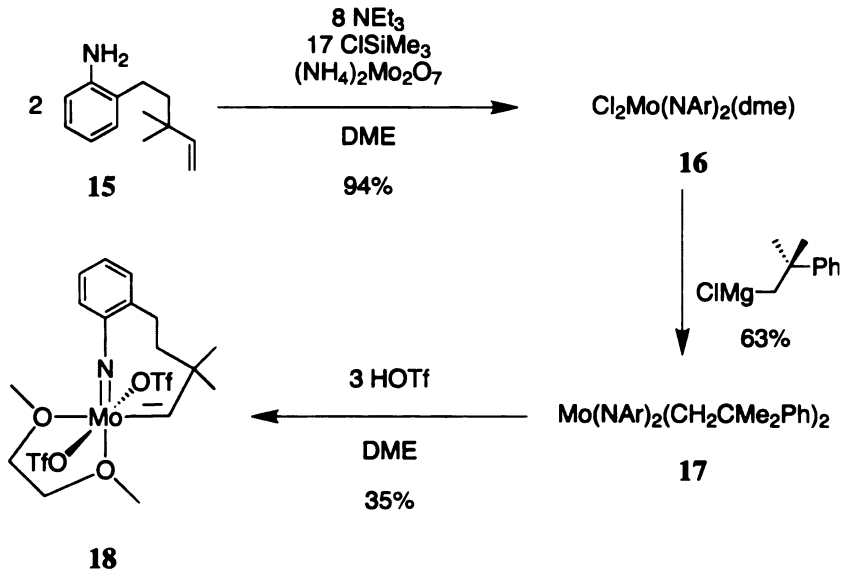

Scheme 4-3. Synthesis of the tethered carbene.

A modification of the standard literature molybdenum alkylidene synthesis procedure was used to produce the desired tethered alkylidene (Scheme 4-3).[93] Reaction of **15** (H_2NAr) with NEt_3, $ClSiMe_3$, and $(NH_4)_2Mo_2O_7$ in DME provided 94% yield of $Mo(NAr)_2(Cl)_2(DME)$ (**16**), although twice the normal molar equivalents of $(NH_4)_2Mo_2O_7$ were required. Otherwise, the reaction appeared to yield exclusively a mono(imido) complex (characterized only by NMR), even after heating for longer than 30 days. When the amount of $(NH_4)_2Mo_2O_7$ was doubled, the reaction was complete in 12 hours. Alkylation of **16** with 2 equiv. of neophylmagnesium chloride in diethyl ether/tetrahydrofuran afforded $Mo(CH_2CMe_2Ph)_2(NAr)_2$ (**17**) in 64% yield. The final step, reaction with three equivalents of triflic acid in DME protonates off one of the imido ligands, and presumably generates the intermediate neophylidene bis(triflate) (not observed) via loss of 2-methyl-2-phenylbutane. This molybdenum neophylidene rapidly cyclizes with the alkene substituent on the remaining imido ligand, producing the desired tethered carbene in 35% isolated yield. Three isomers of the product, as evidenced in the ^1H and ^{13}C NMR spectra (THF-d_8), were present in solution, a complication also observed in untethered systems.[92]

The resulting bis(triflate) **18** is only slightly soluble in many common

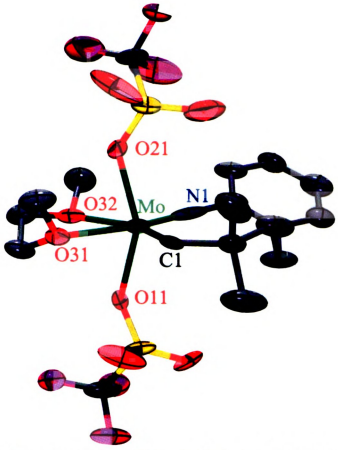

Figure 4-1. The ORTEP representation (25% probability ellipsoids) of the tethered carbene (**18**).

Table 4-1. Selected bond distances and angles from x-ray diffraction of the tethered carbene. For the numbering scheme, see Figure 4-1.

Distances and Angles (Å/°)	Mo(Ar)(OTf)$_2$(dme) (18)
Mo-N(1)	1.714(18)
Mo-C(5)	1.828(19)
Mo-O(11)	2.168(11)
Mo-O(21)	2.125(11)
Mo-N(1)-C(10)	172.9(14)
Mo-C(1)-C(2)	140.0(12)
Mo-O(11)-S(1)	124.2(7)
Mo-O(21)-S(2)	132.3(7)
N(1)-Mo-C(1)	100.2(8)
O(11)-Mo-O(21)	152.7(4)
N(1)-Mo-O(21)	98.4(5)

solvents; however, crystals suitable for x-ray diffraction study were obtained. The solid-state isomer obtained is drawn in Scheme 3-2, and the ORTEP representation is shown in Figure 4-2. Selected bond lengths and angles are shown in Table 4-1. Comparison of the structure of tethered alkylidene **18** with the reported structure of $Mo(OTf)_2$(Ndip)(neopentylidene)(DME),[105] indicates that no ring strain is present in the metallacycle as judged by comparison of bond distances and angles. The bond angles and lengths are all typical of what is seen in other molybdenum neophylidene bis(triflate) complexes, as are the ^1H and ^{13}C NMR spectra (vide supra).

Reactions to produce alkoxide derivatives of tethered neophylidene **18** resulted in reduced metal species, presumably because the imido ligand does not have a second bulky *ortho* substituent, a synthesis that is currently being pursued.

Experimental

General considerations. All manipulations of air-sensitive materials were carried out in an MBraun glove box under an atmosphere of purified nitrogen. Ethereal solvents and pentane were purchased from Aldrich Chemical Co. and distilled from purple sodium benzophenone ketyl. Toluene was purchased from Aldrich Chemical Co., refluxed over molten sodium for at least 2 d, and distilled. Dichloromethane was purchased from Spectrum Chemical Co., refluxed with calcium hydride for at least 2 d, and distilled. NMR solvents were purchased from Cambridge Isotopes Laboratories, Inc. Deuterated benzene was distilled from purple sodium benzophenone ketyl. Deuterated toluene was degassed and dried with neutral activated alumina. NMR solvents were stored in sealed containers equipped with a Teflon stopcock in the glove box prior to use. Spectra were taken on Varian instruments located in the Max T. Rogers Instrumentation Facility. Routine coupling constants are not reported. Alumina, silica, and Celite were dried at >200 °C under dynamic vacuum for at least 12 h, then stored under inert atmosphere. 3,3-dimethyl-5-phenyl-1-pentene was prepared by the method of Reike and co-workers.[103] Combustion analyses

were performed in-house at the Michigan State University Chemistry Department.

General considerations for single crystal x-ray diffraction. Single crystals of **1-4** were grown at –35 °C in an MBraun inert atmosphere glove box. All but a small portion of the mother liquor was removed, and the crystals were removed from the glovebox in a sealed vial. The crystals were rapidly coated in Paratone N and mounted on a glass fiber. The mounted crystal was placed under a cold stream of nitrogen from an Oxford "Cryostream" low-temperature device. Data were collected on a Bruker-AXS, Inc. SMART CCD diffractometer utilizing a PC running Windows NT. The data collection was done on a Bruker-AXS, Inc. 3-circle goniometer (χ set to 54.78°). The source was a water-cooled Mo x-ray tube (λ = 0.71073 Å) operating at 50 kV/40 mA. A single crystal graphite monochromator selected the wavelength of light prior to being columated. The cell was determined using ω–θ scans (–0.3° scan width) with 3 sets of 20 frames. The initial cell was found by repeated least squares and Bravais lattice analysis. Full data sets were collected using ω–θ scans in four runs. The fourth run duplicates the first 50 frames of the first run to allow analysis of peak intensity changes resulting from crystal degradation; no correction was necessary for any of the structures reported. Absorption corrections were applied to the data. Using the initial cell, data were integrated to hkl/intensity data using the Bruker-AXS, Inc. program package SAINT. The final unit cell was determined by SAINT using all the observed data. The structures were solved and refined using the SHELXTL program developed by G. M. Sheldrick and Bruker-AXS, Inc. A full listing of atomic coordinates, bond lengths, bond angles, and thermal parameters for all the structures have been deposited at the Cambridge Crystallographic Data Centre and can be found in the Supporting Information. Additional data pertaining to the collection and processing of the four structures can be found in Table 4-2. In Table 4-2, $R1 = \Sigma||F_0|-|F_c||/\Sigma|F_o|$ and $wR2 = \{\Sigma w(F_0^2-F_c^2)^2/\Sigma w(F_o^2)^2\}^{1/2}$. A partial listing of geometrical parameters for all four data sets may be found in Table 4-2.

Table 4-2. Structural parameters for compound **18** from single–crystal x-ray diffraction.

	Mo(NAr)(=CHCMe$_2$Ph)(OTf)$_2$(dme) (18)
Formula	$C_{18}H_{25}F_6MoNO_8S_s$
Formula weight	657.45
Space Group	P2(1)/n
a (Å)	12.694(15)
b (Å)	15.77(3)
c (Å)	12.87(2)
α (°)	90
β (°)	92.93(16)
γ (°)	90
Volume (Å^3)	2573(8)
Z	4
μ (mm^{-1})	0.758
$D_{calc.}$ (g cm^{-3})	1.697
$R(F_0)$ (I > 2s)	0.1008
$R_w(F_0)$ (I > 2s)	0.2300

2-(3,3-dimethylpent-4-enyl)nitrobenzene. In a flask was loaded fuming HNO_3 (18.7 mL, 90%, d = 1.5), HOAc (18 mL), and Ac_2O (14 mL), which was allowed to cool to room temperature before proceeding. This solution was added dropwise to 3,3-dimethyl-5-phenyl-1-pentene (45.8 g, 0.263 mol) in Ac_2O (120 mL). The reaction was kept between 0 and –5 °C during the addition. After the addition, the mixture was stirred at 0 °C for 12 h. The reaction mixture was poured into crushed ice (300 g). The product was extracted with ethyl ether (3 × 200 mL), and the combined organic layers were washed with portions of saturated $NaHCO_3$ (~300 mL total) until no gas formed on addition of the basic aqueous solution. The organic solution was filtered, and the separated solids were washed with ether (50 mL). The combined aqueous layers were extracted with ether (3 × 200 mL). The combined ether solutions were dried with $MgSO_4$. The volatiles were removed in vacuo providing the product as a yellow oil in 97% yield (55.95 g) as a mixture of 49:51

mixture of *ortho:para* isomers, as determined by GC/FID analysis. The compound was used without further purification.

2-(3,3-dimethylpent-4-enyl)aniline. In a 2000 mL round-bottomed three-necked flask with a thermometer and a mechanical stirrer was loaded $SnCl_2 \cdot 2H_2O$ (270 g, 1.056 mol) and ethanol (500 mL). The mixture was heated to 55 °C, and the crude mixture of nitroarenes prepared in the previous step (55.95 g, 0.26 mol) was added very carefully so that the temperature was kept between 65 °C and 70 °C. After addition, the reaction mixture was stirred at 70 °C for 7 h. After cooling to room temperature, water (200 mL) was added. The pH of the solution was adjusted to 12 by addition of 40% NaOH. Extraction with hexane: ethyl acetate (v:v = 1:1) was carried out until the extract was colorless (~5 × 500 mL). The combined extracts were dried with $MgSO_4$. Removing volatiles in vacuo provided 44.8 g of crude product as a red oil. GC/FID analysis show that the ratio of *ortho* to *para* products was 40:60. Column separation (silica gel, 250 ~ 400 mesh, 6:1 hexane:ethyl acetate) gave 2-(3,3-dimethylpent-4-enyl)aniline (**1**) in 22 % yield (8.8 g) as a red oil. M = 189.30 g/ mol. ^{1}H NMR (300 MHz, $CDCl_3$): δ = 7.02 (m, 2H, -C_6H_4-), 6.62-6.80 (m, 2H, -C_6H_4-), 5.78-5.96 (m, 1H, -C*H*=CH_2), 5.03 (dd, J_1=3 Hz, J_2=5 Hz, 1H, CH=CH_2), 4.99 (dd, J_1=3 Hz, J_2=5 Hz, 1H, -CH=CH_2), 3.56 (s, br, 2H, -NH_2), 2.31-2.46 (m, 2H, -$C_6H_4CH_2CH_2$-), 1.48-1.66 (m, 2H, -$C_6H_4CH_2CH_2$-), 1.08 (s, 6H, -CH_3). ^{13}C NMR ($CDCl_3$): δ = 147.8, 143.9, 129.2, 127.1, 126.8, 118.8, 115.4, 111.2, 41.7, 36.7, 26.6, 26.4. Elemental Analysis: Calc. For $C_{13}H_{19}N$: C, 82.48; H, 10.12; N, 7.40. Found: C, 82.71; H, 10.23; N, 7.56. MS (EI) *m/z* = 189 (M^+). The other isomer of 4-(3,3-dimethylpent-4-enyl)aniline was isolated in 40% yield (16.0 g). ^{1}H NMR (300 MHz, $CDCl_3$): δ = 7.02 (dd, 2H, *J*=208 Hz, 8 Hz, -C_6H_4-), 6.69 (dd, 2H, *J* = 6 Hz, 4 Hz, -C_6H_4-), 5.80-6.01 (m, 1H, -C*H*=CH_2), 5.07 (m, 2H, -CH=CH_2), 3.58 (s, br, 2H, -NH_2), 2.42-2.58 (m, 2H, -$C_6H_4CH_2CH_2$-), 1.56-1.70 (m, 2H, -$C_6H_4CH_2CH_2$-), 1.13 (s, 6H, -CH_3). ^{13}C NMR (C_6D_6): δ = 163.1, 148.4, 144.8, 132.9, 129.3, 115.3, 110.8, 45.6, 36.8, 30.7, 26.8. Elemental Analysis: Calc. For $C_{13}H_{19}N$: C, 82.48; H, 10.12; N, 7.40. Found: C, 82.43; H, 9.57; N, 7.45. MS (EI) m/z = 189 (M^+).

$Mo(NAr)_2Cl_2(DME)$ (16). In a 250 mL Schlenk flask was loaded ammonium dimolybdate (0.529 g, 2.70 mmol), 100 mL 1,2-dimethoxyethane (DME), and a stir bar. To the suspension was added triethylamine (4.37 g, 43.2 mmol), chlorotrimethylsilane (10.0 g, 92.0 mmol), and 1 (1.02 g, 5.40 mmol). The suspension was stirred at 70 °C for 12 h. After cooling to room temperature, the solution was filtered. The volatiles of the filtrate were removed in vacuo to give 1.60 g of $Mo(NAr)_2Cl_2(DME)$ (**16**) as a red solid (2.53 mmol, 93.8%), which was used without further purification. ^1H NMR (299.9 MHz, C_6D_6): δ = 7.73 (d, *J*=7.62 Hz, 2H), 6.94 (d, *J*=7.03 Hz, 2H), 6.88 (t, *J*=7.62 Hz, 2H), 6.75 (t, *J*=7.03 Hz, 2H), 5.97 (m, 2H, =C*H*), 5.04 (m, 4H, CH_2=), 3.46 (s, 4H, O-CH_2), 3.19 (s, 6H, O-CH_3), 2.85 (m, 4H), 1.72 (m, 4H, CH_2), 1.15 (s, 12H, CH_3). ^{13}C NMR (75 MHz, C_6D_6): δ = 156.14 (N–*C*(ipso)) 148.74, 135.84 C(ipso)-CH_2), 128.82, 127.23 (=*C*H), 126.53, 110.77 (CH_2=), 71.11 (O-CH_2), 63.02 (CMe_2), 44.30 (O-CH_3), 37.16 (ArCH_2), 34.51 (CMe_2Ph), 27.80 (ArCH_2CH_2), 26.95 (CMe_2).

$Mo(NAr)_2(CH_2CMe_2Ph)_2$ (17). To a –90 °C solution of $Mo(NAr)_2Cl_2(DME)$ (**16**) (4.80 g, 7.60 mmol) in 300 mL THF was added 34 mL 0.5 M solution of neophyl magnesium chloride (17 mmol, 2.2 equiv.) The solution was allowed to reach room temperature, and then stirred for 18 h. Removal of the volatiles in vacuo left a red solid, which was dissolved in toluene and filtered to remove the magnesium chloride. The volatiles were removed from the toluene solution in vacuo, leaving a red solid which was recrystallized from ether at –35 °C to give 3.50 g of 3 (4.75 mmol, 62.5%). ^1H NMR (299.9 MHz, C_6D_6): δ 7.3 (m, 4H), 7.1 (m, 6H), 7.0 (m, 5H), 6.8 (m, 3H), 5.7 (m, 2H, =CH), 4.9 (m, 4H, $=CH_2$), 2.7 (m, 4H), 1.90 (s, 4H, Mo-CH_2), 1.6 (m, 4H, -CH_2CH_2-), 1.46 (s, 12H, CH_2CMe_2Ph), 1.00 (s, 12H, imido-CH_3). ^{13}C NMR (75.4 MHz, C_6D_6): δ = 155.46 (N–*C*(ipso)), 151.16, 148.35, 135.40, 128.90, 128.62, 126.51, 126.38, 126.23, 125.62, 111.07 (=CH_2), 78.63 (Mo-CH_2), 43.58 (ArCH_2), 40.82 (CMe_2Ph), 36.93(CMe_2), 32.75 (CMe_2Ph), 27.38 (ArCH_2CH_2), 26.94 (CMe_2). Anal. Calc. for $C_{46}H_{60}N_2Mo$: C, 74.97; H, 8.21; N; 3.80. Found: C, 74.93; H, 8.44; N, 3.77.

Tethered carbene (18). A thawing solution of 2.05 g triflic acid (13.7 mmol, 3.0 equiv.) in DME (10 mL) was added to a thawing solution of $Mo(NAr)_2(CH_2CMe_2Ph)_2$ (**17**) (3.32 g, 4.35 mmol) in DME (300 mL). This solution was stirred for 22 h, and then volatiles were removed in vacuo. The anilinium triflate was precipitated from a minimal amount of toluene, and removed by filtration. The remaining dark solid was recrystallized from ether/pentane, giving 1.01 g of a yellow 4 (1.52 mmol, 35.0%), m 83 °C dec. In fluid solution, the compound apparently exists as 3 different isomers, which made definitive assignment of many of the peaks difficult. There is dependence on temperature to the NMR spectra, and the relative amounts of each isomer changes with temperature. Schrock and coworkers have reported similar observations, including the fact that the two minor isomers are more prevalent in polar solvents. However, the tethered carbene has low solubility in most solvents except THF. The spectra reported here were taken at room temperature. Assignments, where they could be definitively made, are given. ^{1}H NMR (299.9 MHz, THF-d_8): δ = 14.30, 14.27, 13.65, 8.15 (d), 7.0-7.6 (m), 3.43 (s, 4H, OCH_2), 3.40 (m), 3.27 (s, 6H, OCH_3) 2.47 (m), 2.31 (s), 1.08 (m). ^{13}C NMR (75.4 MHz, THF-d_8): δ 333.83, 330.83, 326.96, 155.64, 154.83, 154.62, 149.77, 149.44, 148.55, 138.43, 130.801, 130.39, 129.67, 129.42, 129.21, 129.21, 129.11, 128.91, 128.29, 127.42, 126.90, 126.80, 126.29, 126.03, 122.39, 118.18, 72.75, 66.30, 59.92, 59.59, 59.52, 58.90, 45.98, 45.85, 45.00, 30.16, 29.74, 29.30, 28.51, 27.85, 21.48, 15.68. ^{19}F (282.2 MHz, THF-d_8): –78.45, –78.58, –79.56, –79.64. Anal. Calc. for $C_{18}H_{25}F_6MoNO_8S_2$: C, 32.98; H, 3.83; N; 2.13. Found: C, 33.43; H, 4.07; N, 2.12.

CHAPTER 5

CYCLOOCTYNE ADDITION TO GROUP-6 IMIDO COMPLEXES

Introduction

Schrock carbenes (alkylidenes) have impacted synthetic and polymer chemistry tremendously.[106,107] A concise, simple preparation for alkylidenes has been the target of some exploration since the initial discovery by Schrock and co-workers. Nugent and coworkers, for example, have devised a readily prepared, tetraethyl lead activated tungsten mono(oxo) bis(aryloxy) dichloride system that rapidly and catalytically performs ring-closing metathesis of a number of functionalized dienes.[108] Grubbs and co-workers have introduced a method of forming alkylidenes from tungsten bis(imido) dichloride phosphine adducts through reaction with disubstituted cyclopropenes.[109] Despite this, the best synthetic route to molybdenum imido alkylidene metathesis catalysts continues to be that of Schrock's, which was used to prepare the imido-tethered carbene described in Chapter 4.

Research into the use of titanium imido (Chapter 6) and hydroazido(2–) complexes as alkyne hydroamination catalysts[110,111] and related processes[112] has raised interest in [2+2] cycloadditions of alkynes with metal-imido bonds.[113] This type of cycloaddition (Scheme 5-1) typically results in the formation in azametallacyclobutenes (Stucture **A**).[114] Contemplation of the other resonance form, Structure **B**, led to speculation that this form could be favored with the proper choice of metal and ligands.

While searching for such a metal complex, it seemed a necessity that the metal center should readily form stable M=C bonds; a high oxidation state where dπ–pπ bonding

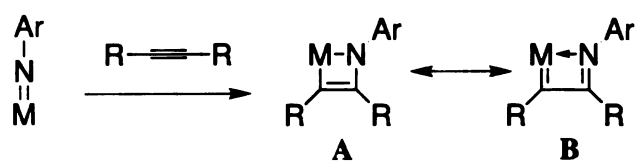

Scheme 5-1. [2+2] Cycloaddition of an alkyne with an imido ligand and resonance forms of the products.

is encouraged should stabilize Structure **B**. The prevalence of molybdenum complexes containing ligand-metal multiple bonds, such as imido alkylidene complexes, made it an atractive starting point (molybdenum has the most metal–ligand multiple bond complexes known of any metal). [115]

Thus, the starting material of choice to form a new molybdenum imido alkylidene is a bis(imido) molybdenum (VI) complex, the synthesis of which is readily carried out on large scales from amines and ammonium molybdate.[116] Reaction of molybdenum(VI) bis(imido) complexes with alkynes has the potential to form the desired product. Unfortunately, molybdenum(VI) bis(imido) complexes are unreactive towards most alkynes under mild conditions, where the alkylidenes would be stable. For example, treatment of $Mo(NAr)_2(Cl)_2(DME)$, where Ar = 2,6-diisopropylphenyl, with a large excess of 3-hexyne at 75 °C overnight results in no reaction.

Results and Discussion

In order to overcome this lack of reactivity, the reaction between $M(NAr)_2(Cl)_2(dme)$, where M = Mo and W, with a highly reactive, ring-strained alkyne, cyclooctyne,[117] was examined. In ethereal solution, $M(NAr)_2(Cl)_2(DME)$ readily reacts with cyclooctyne, forming a slightly soluble yellow complex (Scheme 5-2). Single-crystal x-ray analysis (Figure 5-1) of crystals of the product showed that two equivalents of cyclooctyne reacted with the metal bis(imido) complex. This product, $M(=C_8H_{12}=C_8H_{12}=NAr)(NAr)Cl_2$, may result from [2 + 2] cycloaddition of the metal-imido bond with cyclooctyne, followed by insertion of alkyne into alkylidene **B**. The M = Mo (**19**) and W (**20**) complexes were isolated in 90% and 93% yield, respectively, through this synthetic strategy.

Selected bond lengths and angles of metallacycles **19** and **20** are listed in Table 5-1; the two structures are identical within error. As anticipated, the bond lengths of the metallacycles are more consistent with alkylidene-imine Structure **B** than with the alkyl-amido structure **A**. The Mo=C distance in **19**, 1.933(6) Å, is well within the typical range

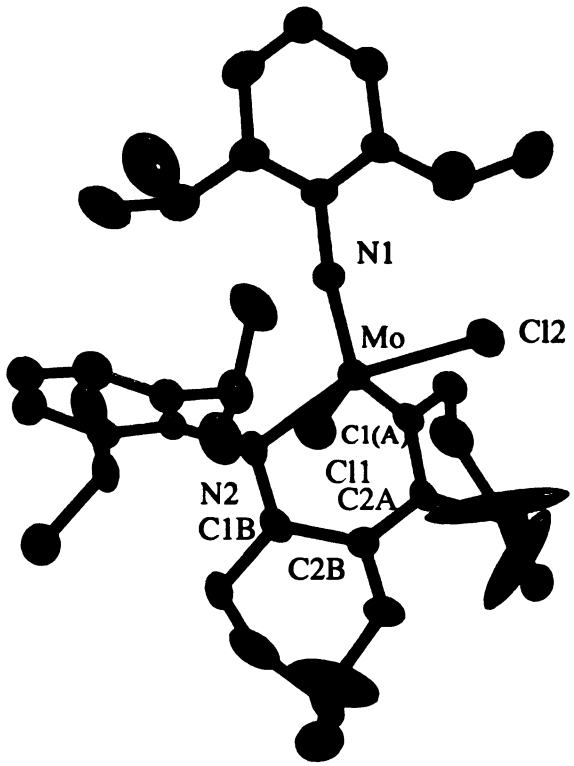

Figure 5-1. The ORTEP representation (25% probability ellipsoids) of azametallacycle **19**.

Table 5-1. Selected bond distances and angles from x-ray diffraction of the double insertion product. For the numbering scheme, see Figure 5-1.

Distances and Angles (Å/°)	Mo(=C_8H_{12}=C_8H_{12}=Ndip)(Ndip)Cl_2 (19)	W(=C_8H_{12}=C_8H_{12}=Ndip)(Ndip)Cl_2 (20)
Mo-N(1)	1.7365(5)	1.736(3)
Mo-C(1A)	1.933(6)	1.944(4)
Mo-N(2)	2.155(5)	2.120(3)
Mo-Cl(1)	2.4479(17)	2.4120(10)
Mo-Cl(2)	2.4192(18)	2.4095(10)
Mo-N(1)-C(11)	166.5(4)	168.6(3)
N(1)-Mo-C(1A)	104.9(2)	107.30(14)
C(1A)-Mo-N(2)	84.5(2)	86.94(13)
N(1)-Mo-N(2)	106.1(2)	100.81(12)
N(1)-Mo-Cl(2)	94.61(16)	94.70(9)
N(1)-Mo-Cl(1)	119.40(15)	122.11(10)
C(1A)-Mo-Cl(2)	91.85(7)	93.04(11)

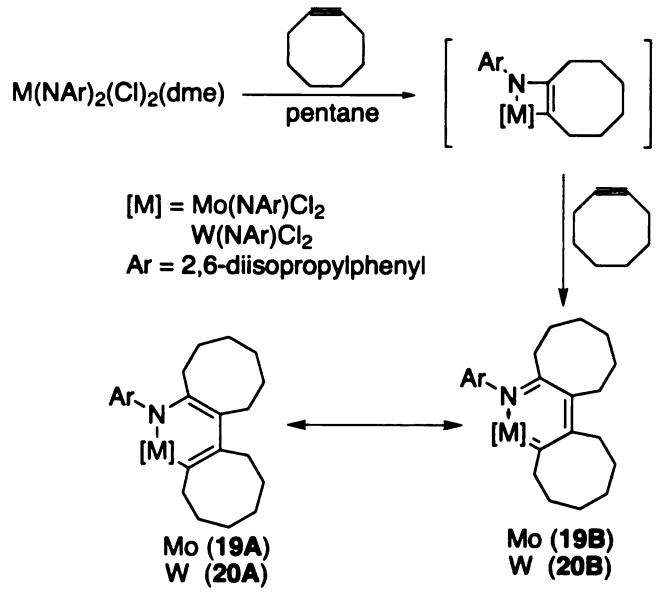

Scheme 5-2. Reactions of $M(NAr)_2Cl_2(dme)$ with cyclooctyne.

seen for Mo=C bonds in alkylidenes; this distance also compares favorably with the Mo=C bond length of 1.878(9) Å seen in the PMe_3 adduct of Schrock's catalyst, Mo(NAr)[=C(H)CMe_2Ph][$OC(CF_3)_2Me]_2(PMe_3)$.[119] For comparison, the average Mo–C single bond distance in $Mo(NAr)_2(neophyl)_2$ is 2.128(5) Å.[115]

The carbon-carbon bonds in the metallacycle are equally informative. For the carbene-imine structure **19A**, the C(2A)–C(2B) bond should have a bond order of 2; the bond length observed in **19** is 1.394(8) Å, slightly longer than the C=C distance of 1.336 Å in butadiene.[120] The C(1A)–C(2A) and C(1B)–C(2B) distances average 1.463(7) Å, and the C–C single bond distance in butadiene is 1.465 Å.[119] Thus, although the bond lengths in these metallacycles are consistent with structure **B**, the alkyl-imido structure **A**, does participate in the bonding. The Mo–N(2) distance in **19** is 2.155(5) Å.

The ^{13}C NMR spectroscopy of complexes **19** and **20** exhibit resonances consistent with the alkylidene character. The molybdenum compound **19** exhibits the resonance for C(1) at 309 ppm; the corresponding resonance in Mo(NAr)[=C(H)CMe_2Ph][$OC(CF_3)_2$Me]$_2$ has a chemical shift of 288 ppm.[118] The tungsten compound **20** has the alkylidene carbon resonance at 278 ppm; in W(NAr)[=C(H)CMe_2Ph][$OC(CF_3)_2Me]_2$, the analogous

resonance occurs at 254 ppm.[121] This data leads to the conclusion that the reaction in Scheme 5-2 constitutes a novel direct conversion of an imido ligand to an alkylidene-like ligand.

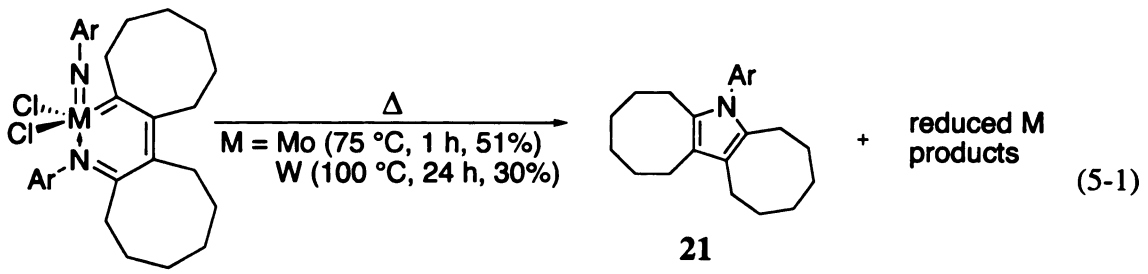

M = Mo (19)
W (20)

21

(5-1)

These metallacyclic complexes undergo an interesting, yet very frustrating, reaction. Thermolysis of both **19** and **20** results in the formation of novel pyrrole **21**, eq 5-1. This product may be formed via reductive elimination from the alkyl-amido structure **A** (Scheme 5-2), or by intramolecular nucleophilic attack of the imine on the alkylidene carbon atom in the alkylidene-imine structure **B**. The tungsten containing complex **20** decomposes more slowly than does the molybdenum derivative **19**, as would be expected for a reduction of the metal center.

The propensity for the molybdenum complex to form pyrrole **21** is remarkable indeed. Most of the attempts to derivatize compound **19** into an active metathesis catalyst have resulted in the formation of the pyrrole decomposition product, as indicated by NMR evidence. For example, reaction of complex **19** with 2 equivalents of LiO^tBu_{F6} in diethyl ether results in formation of resonances in the ^1H NMR spectrum that correspond to those of the pyrrole product. The same reaction carried out with KO^tBu_{F6}, however, resulted in a solution that had no pyrrole present by ^1H NMR; the ^1H NMR is consitent with a species containing one type of diisopropylimido group. Addition of norbornene to this solution in the NMR tube resulted in polymer formation; the polymers formed have resisted characterization due to their low solubility in common solvents. Activation of complexes

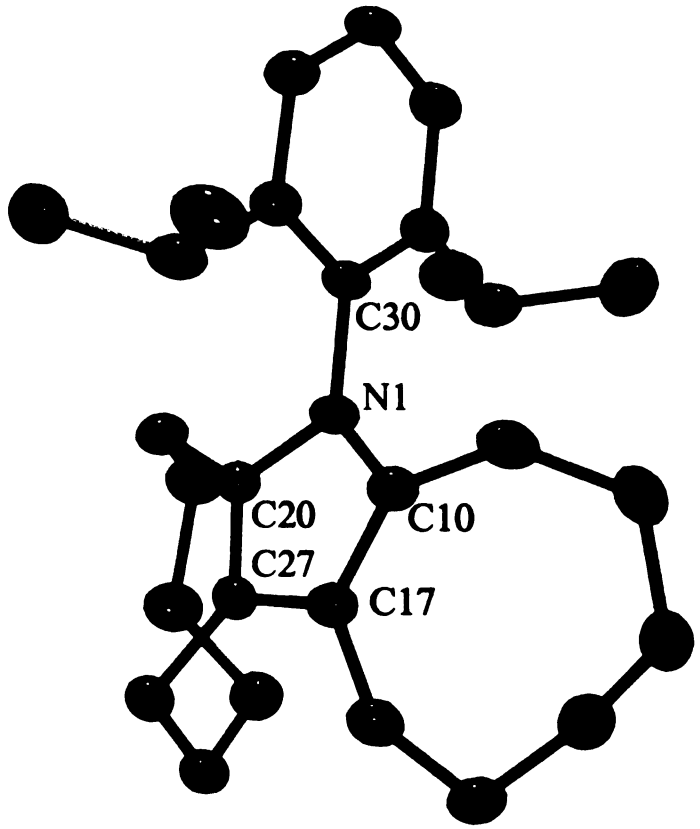

Figure 5-2. The ORTEP representation (25% probability ellipsoids) of pyrrole **21** formed from decomposition of molybdenum complex **19**.

19 and **20** with $AlCl_3$ also results in mixtures that polymerize norbornene.[122] It is hoped that a simple procedure will be found to generate isolable metathesis catalysts from these complexes.

These complexes, while unstable to pyrrole formation, do not participate in any kind of metathesis reaction unless activated (vide supra), likely because of resonance stabilization of the metallacycle. They are oxygen tolerant, and reaction of a toluene solution with 50% aqueous H_2SO_4 results in a metal complex with the metallacycle still present. The product of this reaction (eq 5-2) with the tungsten complex **20** has been structurally characterized by single-crystal x-ray diffraction, and is shown in Figure 5-3, with selected bond lengths and angles shown in Table 5-2. Replacement of all of the non-metallacycle ligands in this

Table 5-2. Selected bond distances and angles from x-ray diffraction of the double insertion product **22**. For the numbering scheme, see Figure 5-3.

Distances and Angles (Å/°)	[W(=C_8H_{12}=C_8H_{12}=Ndip)(O)(μ-O)]$_2$ (22)
W-O(1)	1.696(3)
W-O(2)	1.940(2)
W-C(1A)	2.010(4)
W-N	2.021(3)
O(1)-W-O(2)	124.84(120
O(1)-W-O(2)#1	99.07(11)
O(2)-W-O(2)#1	77.15(11)
O(1)-W-C(1A)	111.38(14)
O(2)-W-C(1A)	123.69(13)
O(1)-W-N	100.55(12)
O(2)-W-N	85.54(11)

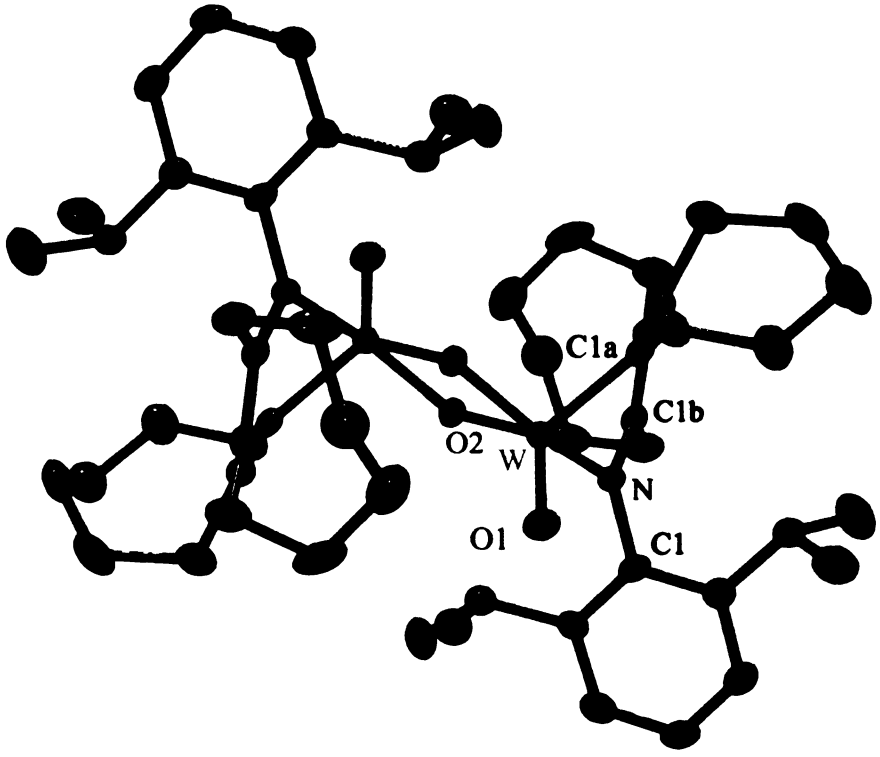

Figure 5-3. The ORTEP representation (25% probability ellipsoids) of tungsten μ-oxo complex **22**.

way results in μ-oxo complex **22.**

Tungsten μ-oxo **22** is apparently less alkylidene-like in its properties. The W–C(1A) distance increases from 1.944(4) Å in imido complex **20** to 2.010(4) Å in **22.** Indeed all the distances in the metallacycle are consistent with greater participation of the amido-

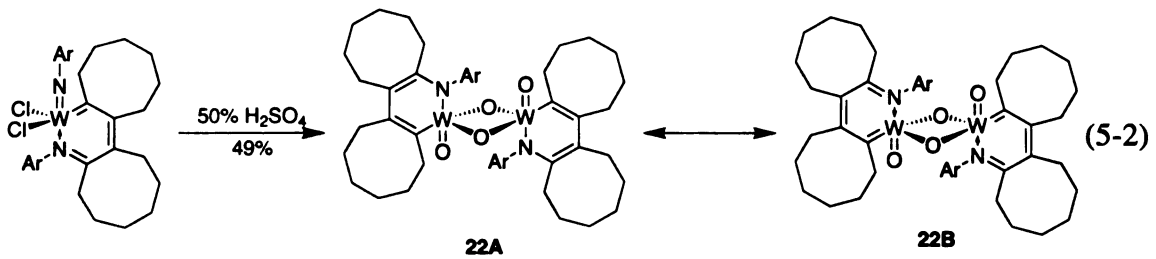

(5-2)

alkyl resonance form (**22A**, eq 5-2) than in the imido derivative. For example, the W–N distance in the metallacycle of **22** shrinks to 2.021(3) Å from 2.120(3) Å in imido **20,** consistent with increased alkyl-amido resonance form participation. Also consistent with this assertion, the ^{13}C NMR resonance for C_α is shielded significantly to 238 ppm in **22** from 278 ppm in **20.**

As can be seen by comparing the bond distances of the metallacycles in tungsten

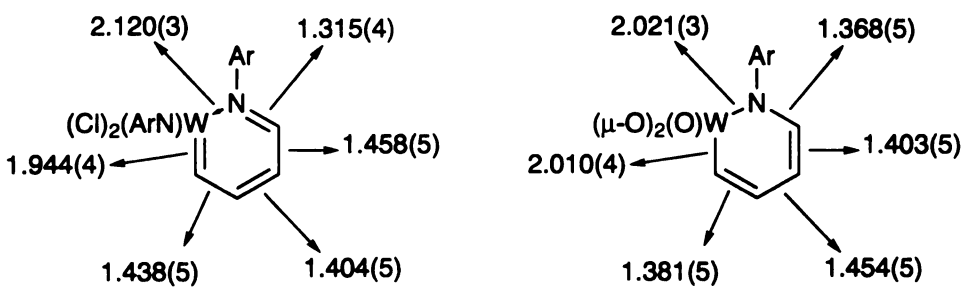

Figure 5-4. Simplified structure comparison between **20** (left) and **22** (right) illustrating the difference in bond length alternation due to changing ligand sets.

imido **20** and oxo **22,** the other ligands on the metal are having a dramatic effect on the favored resonance form (Figure 5-4). While both resonance forms undoubtedly participate in both complexes, changing the ligands on tungsten can affect whether the alkylidene-

imine or alkyl-amido form is favored.

Experimental

General considerations. All manipulations of air-sensitive materials were carried out in an MBraun glove box under an atmosphere of purified nitrogen. Ethereal solvents, pentane, and toluene were purchased from Aldrich Chemical Co. and purified by passing through alumina columns to remove water after sparging with N_2 to remove oxygen. NMR solvents were purchased from Cambridge Isotopes Laboratories, Inc. Deuterated benzene was distilled from purple sodium benzophenone ketyl. Deuterated chloroform was distilled from CaH_2 under dry N_2. NMR solvents were stored in sealed containers equipped with a Teflon stopcock in the dry box prior to use. Spectra were taken on Varian instruments located in the Max T. Rogers Instrumentation Facility. Routine coupling constants are not reported. Many of the assignments are tentative due to the large number of overlapping peaks. The ^{13}C NMR assignments are based on decoupled ^{13}C, peak heights for overlapping signals and DEPT experiments. Alumina, silica, and Celite were dried at >200 °C under dynamic vacuum for at least 12 h, then stored under an inert atmosphere. Mo[N(2,6-$Pr^i_2C_6H_3$)]$_2Cl_2$(dme),[123] W[N(2,6-$Pr^i_2C_6H_3$)]$_2Cl_2$(DME),[121] and Mo(NAr)$_2$(neophyl)$_2$[116] were prepared by literature methods. Cyclooctyne was prepared using the procedure of Brandsma.[124] Combustion analyses were performed by facilities in the Department of Chemistry at Michigan State University.

General considerations for single crystal x-ray diffraction. Single crystals of **19** were grown at ambient temperature in an MBraun inert atmosphere glovebox. Single crystals of **20-22** were grown at –35 °C in an MBraun inert atmosphere glovebox. All but a small portion of the mother liquor was removed, and the crystals were removed from the glovebox in a sealed vial. The crystals were rapidly coated in Paratone N and mounted on a glass fiber. The mounted crystal was placed under a cold stream of nitrogen from an Oxford "Cryostream" low-temperature device. Data were collected on a Bruker-AXS, Inc. SMART CCD diffractometer utilizing a PC running Windows NT. The data collection

Table 5-3. Structural parameters for compounds **19 – 22** from single–crystal x-ray diffraction.

	Mo(=C_8H_{12}=C_8H_{12}=Ndip)(Ndip)Cl_2	W(=C_8H_{12}=C_8H_{12}=Ndip)(Ndip)Cl_2	Pyrrole 21	[W=(C_8H_{12}=C_8H_{12}=Ndip)(O)(μ-O)]$_2$
Formula	$C_{40}H_{58}Cl_2MoN_2$	$C_{40}H_{58}Cl_2MoN_2$	$C_{28}H_{41}N$	$C_{16}H_{25}N_{0.50}O_{1.50}W$
Formula weight	733.72	820.63	391.62	340.29
Space Group	P2(1)/n	Pbca	P–1	P–1
a (Å)	10.487(3)	17.040(3)	10.929(3)	11.1553(16)
b (Å)	17.824(3)	19.421(3)	11.094(3)	12.7101(7)
c (Å)	20.347(7)	22.704(3)	12.388(3)	13.1510(14)
α (°)	90	90	74.760(5)	118.851(9)
β (°)	100.66(4)	90	64.335(4)	98.755(8)
γ (°)	90	90	60.577(4)	99.161(12)
Volume (Å^3)	3737.8(17)	7513.3(19)	1176.8(6)	1554.8(3)
Z	4	8	2	4
μ (mm^{-1})	0.523	3.247	0.062	3.745
$D_{calc.}$ (g cm^{-3})	1.304	1.451	1.105	1.454
$R(F_0)$ (I > 2s)	0.0520	0.0206	0.0308	0.0219
$R_w(F_0)$ (I > 2s)	0.0898	0.0460	0.0712	0.0471

was done on a Bruker-AXS, Inc. 3-circle goniometer (χ set to 54.78°). The source was a water-cooled Mo x-ray tube (λ = 0.71073 Å) operating at 50 kV/40 mA. A single crystal graphite monochromator selected the wavelength of light prior to being columated. The cell was determined using ω–θ scans (–0.3° scan width) with 3 sets of 20 frames. The initial cell was found by repeated least squares and Bravais lattice analysis. Full data sets were collected using ω–θ scans in four runs. The fourth run duplicates the first 50 frames of the first run to allow analysis of peak intensity changes resulting from crystal degradation; no correction was necessary for any of the structures reported. Absorption corrections were applied to the data. Using the initial cell, data were integrated to hkl/intensity data using the Bruker-AXS, Inc. program package SAINT. The final unit cell was determined by SAINT using all the observed data. The structures were solved and refined using the SHELXTL program developed by G. M. Sheldrick and Bruker-AXS, Inc. A full listing of atomic coordinates, bond lengths, bond angles, and thermal parameters for all the structures have been deposited at the Cambridge Crystallographic Data Centre and can be found in the Supporting Information. Additional data pertaining to the collection and processing of the four structures can be found in Table 5-3. In Table 5-3, $R1 = \Sigma||F_0|-|F_c||/\Sigma|F_o|$ and $wR2 = \{\Sigma w(F_0^2-F_c^2)^2/\Sigma w(F_o^2)^2\}^{1/2}$. A partial listing of geometrical parameters for all four data sets may be found in Table 5-3.

Mo(=C_8H_{12}=C_8H_{12}=NAr)(NAr)Cl_2 (19). To a stirred solution of $Cl_2Mo(Ndip)_2(DME)$ (250 mg, 0.411 mmol, 1 equiv) in 5 mL pentane was added cyclooctyne (112 mg, 1.03 mmol, 2.5 equiv). After 3 h, the yellow precipitate was isolated by decanting the liquid, washed with pentane, and dried in vacuo to give pure **19** (271 mg, 0.369 mmol, 90%), m 142 °C dec. ^{1}H NMR ($CDCl_3$) δ = 7.27 (dd, J_1=1.46 Hz, J_2 = 7.76 Hz, 1H), 7.16 (t, J = 7.76 Hz, 1H), 7.03 (m, J_1=6.45 Hz, J_2 = 2.34 Hz, 1H), 6.93 (m, J_1=6.88 Hz, J_2 = 1.61 Hz, J_3=4.69 Hz, J_4 = 1.46 Hz, 1H 3H), 4.85 (dt, J_1=3.99 Hz, J_2 = 17.71 Hz, 1H), 4.16 (m, J_1=4.25 Hz, J_2 = 7.61 Hz, J_3=4.83 Hz, J_4 = 5.42 Hz, J_5=7.46 Hz, 1H), 3.53 (sept, J=6.73 Hz, 2H), 3.37 (sept, J=6.59 Hz, 1H), 3.10 (dt, J_1=4.54 Hz, J_2 =

15.0 Hz, 1H), 2.5 – 2.9 (m, 6H), 1.9 – 2.2 (m, 6H), 1.5 – 1.9 (m, 10H), 1.35 (d, *J*=6.44 Hz, 3H), 1.23 (d, *J*=6.88 Hz, 3H), 1.20 (d, *J*=6.88 Hz, 6H), 0.93 (d, *J*=6.73 Hz, 6H), 0.90 (d, *J*=6.88 Hz, 3H), 0.78 (d, *J*=6.88 Hz, 3H). ^{13}C NMR ($CDCl_3$) δ 309.31 (C_α), 177.14 (N=C), 153.75 (C), 147.32 (2 overlapping C), 143.71 (C), 141.87 (C), 139.74 (C), 133.91 (C), 130.96 (C), 128.69 (CH), 128.13 (CH), 125.44 (CH), 124.10 (CH), 122.55 (2 overlapping CH), 44.21 (CH_2), 32.38 (CH_2), 31.06 (CH_2), 28.72 (Pr^i-CH), 28.59 (2 overlapping Pr^i-CH and overlapping CH_2), 28.34 (Pr^i-CH), 28.15 (CH_2), 28.03 (CH_2), 27.38 (CH_2), 26.30 (CH_2), 26.02 (Pr^i-CH_3), 25.98 (CH_2), 25.44 (Pr^i-CH_3), 25.20 (CH_2), 25.13 (CH_2), 24.80 (CH_2), 24.51(Pr^i-CH_3), 24.38 (Pr^i-CH_3), 24.29 (Pr^i-CH_3), 22.80 (Pr^i-CH_3). Anal. Calcd. for $C_{40}H_{58}Cl_2N_2Mo$: C, 65.48; H, 7.97; N, 3.82. Found: C, 65.59; H, 8.20; N, 3.87.

W(=C_8H_{12}=C_8H_{12}=NAr)(NAr)Cl_2(20). To a stirred solution of $Cl_2W(Ndip)_2(DME)$ (1.00 g, 1.44 mmol, 1 equiv) in 10 mL pentane was added cyclooctyne (389 mg, 3.595 mmol, 2.5 equiv). After 12 h, the green-yellow precipitate was collected on a frit, washed with cold pentane, and dried in vacuo to give pure **2** (1.1 g, 1.34 mmol, 93%), m 122 °C dec. ^{1}H NMR (C_6D_6) δ = 7.07 (dd, 1H), 7.03 (t, 1H), 6.94 (m, 1H), 6.85 (m, 3H), 4.82 (m, 1H), 4.61 (m, 1H), 4.31 (sept, 2H), 3.98 (sept, 1H), 2.72 (m, 1H), 2.65 – 2.21 (m, 6H), 1.69 – 1.87 (m, 6H), 1.43 – 1.68 (m, 10H), 1.37 (d, 3H), 0.1.26 (d, 3H), 1.24 (d, 6H), 1.20 (d, 6H), 0.97 (d, 3H), 0.73 (d, 3H). ^{13}C NMR ($CDCl_3$) δ = 280.89 (C_α), 169.19 (N=C), 150.80 (C), 146.85 (2 overlapping C), 144.68 (C), 143.44 (C), 140.68 (C), 137.76 (C), 128.45 (CH), 127.76 (CH), 127.35 (C), 125.30 (CH), 124.22 (CH), 122.35 (2 overlapping CH), 122.35 (2 overlapping CH), 41.88 (CH_2), 31.34 (CH_2), 30.92 (CH_2), 29.73 (CH_2), 29.44 (CH_2), 29.35 (CH_2), 29.12 (CH_2), 28.59 (2 overlapping CH), 27.94 (2 overlapping CH and one overlapping CH_2), 26.30 (CH_2), 25.84 (CH_3), 25.64 (CH_2), 25.59 (CH_2), 25.50 (2 overlapping CH_3) 25.27 (CH_3), 25.05 (CH_2) 24.88 (2 overlapping CH_3), 24.72 (CH_3), 23.52 (CH_3). Anal. Calcd. for $C_{40}H_{58}Cl_2N_2W$: C, 58.46; H, 7.13; N, 3.41. Found: C, 58.40; H, 7.06; N, 3.46.

Pyrrole 21. From **19**. In a pressure tube, $Cl_2Mo(Ndip)(=C_8H_{12}=C_8H_{12}=Ndip)$ (0.100 g, 0.136 mmol) was dissolved in toluene (20 mL). The sealed pressure tube was heated at 75 °C in an oil bath for 90 min. The volatiles were removed in vacuo, and the black solid was dissolved in 5 mL diethyl ether and passed through a short column of silica gel. Removal of the volatiles in vacuo yielded a yellow solid. Recrystallization from pentane gave 27 mg (0.0702 mmol, 51.6%) of the pyrrole decomposition product as light yellow crystals. From **20**. In a pressure tube, $Cl_2W(Ndip)(=C_8H_{12}=C_8H_{12}=Ndip)$ (0.100 g, 0.122 mmole) was dissolved in toluene (20 mL). The sealed pressure tube was heated at 100 °C in an oil bath for 24 h. The volatiles were removed in vacuo, and the black solid was dissolved in 5 mL diethyl ether and passed through a short column of silica gel. Removal of the volatiles in vacuo yielded a solid, which was recrystallized from pentane giving 14 mg (0.0357 mmol, 30%) of the pyrrole as light yellow crystals, m 114-116 °C. ^1H NMR ($CDCl_3$) δ = 7.35 (dd, 1H, p-H), 7.18 (app dd, 2H, m-H), 2.62-2.57 (m, 4H), 2.39 (sept, *J* = 6.9 Hz, 2H, $CHMe_2$), 2.26-2.32 (m, 4H), 1.56-1.66 (m, 4H), 1.45-1.38 (m, 12H), 1.10 (d, 12H, *J* = 6.9 Hz, $CH(CH_3)_2$). ^{13}C NMR ($CDCl_3$) δ = 148.27 (C–Pr^i), 134.34 (ipso-C), 128.59 (p-C), 128.40 (pyrrole-2-C), 123.63 (m-C), 116.96 (pyrrole-3-C), 29.82 (CH_2), 29.49 (CH_2), 27.42 ($CHMe_2$), 26.33 (CH_2), 25.46 (CH_2), 25.17 (CH_2), 24.61 ($CH(CH_3)_2$), 22.31 (CH_2). Anal. Calcd. for $C_{28}H_{41}N$: C, 85.87; H, 10.55; N, 3.58. Found: C, 85.97; H, 10.88; N, 3.71.

$[W(=C_8H_{12}=C_8H_{12}=NAr)(O)(\mu\text{-}O)]_2$ (22). In a separatory funnel, $Cl_2W(Ndip)(=C_8H_{12}=C_8H_{12}=Ndip)$ (400 mg, 0.487 mmol) was dissolved in 200 mL toluene outside the glovebox. To this, 400 mL of 50% H_2SO_4 was added, and the mixture was shaken for 5 min. The toluene layer was separated and dried with K_2CO_3. The volatiles were removed in vacuo to yield an orange-red solid, m 172 dec. Recrystallization from pentane gave 223 mg of pure **3** (0.1835 mmol, 38%). The ^1H was exhibited characteristics of a fluxional species. Anal. Calcd. for $C_{56}H_{82}N_2O_4W_2$: C, 55.35; H, 6.82; N, 2.31. Found: C, 55.67; H, 6.83; N, 2.61.

CHAPTER 6

HYDROAMINATION OF ALKYNES USING TITANIUM CATALYSTS

Introduction

Imines are most often synthesized via the condensation of aldehydes or ketones with primary amines with the loss of water. While many imines can be made in this way, a more atom-economical way to synthesize imines is through the hydroamination of alkynes with amines, Scheme 6-1. One of the advantages of this method is that water is not formed in hydroamination, so that the resulting imine solution is amenable to further reaction with water-sensitive reagents. Hydroamination of alkynes is currently being studied with the goal that improved catalysts for olefin hydroamination, a major synthetic challenge, can be developed. [125]

Catalysts for the reaction can be based on alkali metals[126], early transition metals[127], late transition metals,[128] actinides,[129] or lanthanides.[130] Until recently, most early transition metal catalysts have been metallocene-based titanium and zirconium based; Bergman and coworkers have convincingly shown these hydroaminations to involve imido intermediates.[131] Generally, these Cp-based group-4 catalysts lead to *anti*-Markovnikov addition of amines to alkynes,[127] whereas late transition metal catalsysts favor Markovnikov products.[125,128]

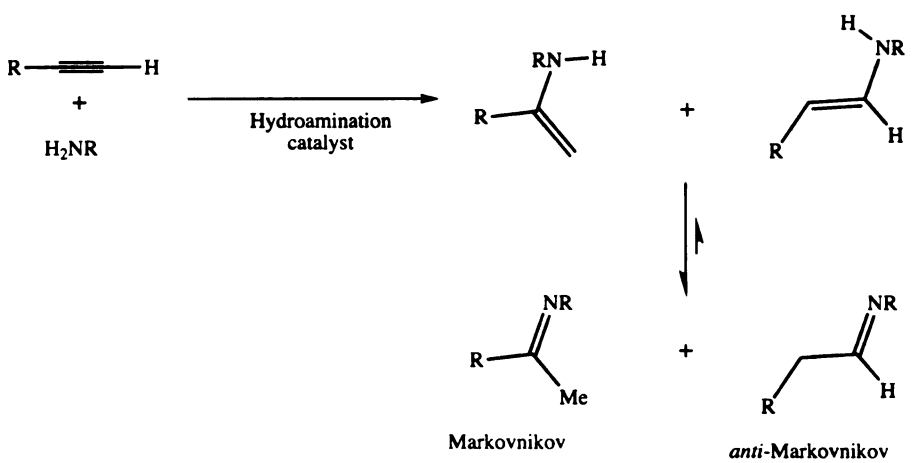

Scheme 6-1. Possible imine products from terminal alkyne hydroamination.

There are currently many titanium hydroamination catalysts known, and several groups are working on this chemistry. The initial work involving titanium catalysis were the intramolecular reactions of Livinghouse and co-workers,[132] as well as early (and often overlooked) observations by Rothwell and co-workers.[133] The Doye,[134] Bergman,[135] and Beller[136] groups have investigated Cp-based systems, and Ackermann and Bergman described a titanium sulfonamide complex for intramolecular hydroaminations.[137] The list of viable catalysts grows weekly.

It was discovered that hydroamination can be catalyzed by non-metallocene titanium systems. The regioselectivity of alkyne hydroamination can also be altered quite effectively by utilizing different ligands on the titanium center.

Results and Discussion

Catalyst design and synthesis. Reaction of $Ti(NMe_2)_4$ with one equivalent of H_2dpma results in the formation of $Ti(dpma)(NMe_2)_2$, **23**, in 97% yield (eq 6-1.) The structure obtained from single-crystal x-ray diffraction is shown in Figure 6-1; selected bond lengths and angles are given in Table 6-1. As can be seen, the structure of the compound is pseudo-trigonal bipyramidal, with the dpma ligand facially orientated. Ti–NMe_2 bond lengths are relatively short compared to previously reported Ti–NMe_2 bonds. The axial Ti–NMe_2 bond length is 1.888(3) Å; the equatorial Ti–NMe_2 bond length is 1.859(3) Å. The Ti-N(pyrrole) bond are longer, averaging 2.016(3) Å, than the Ti-amide bonds by 0.143Å. This is indicative of decreased Ti–N π-bonding with the pyrrolyl nitrogen atoms compared to the dimethyl amide nitrogen atoms. The Ti–N(3) (donor amine) bond length

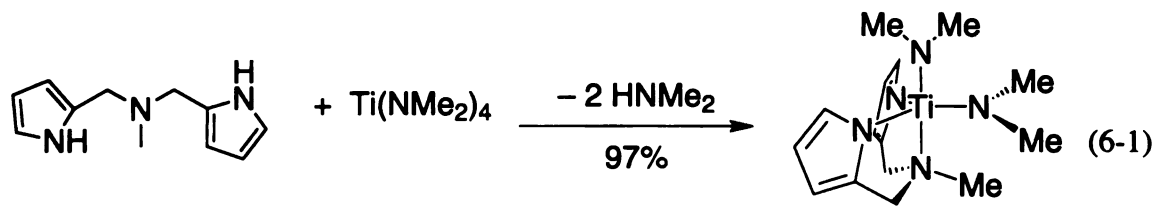

(6-1)

23

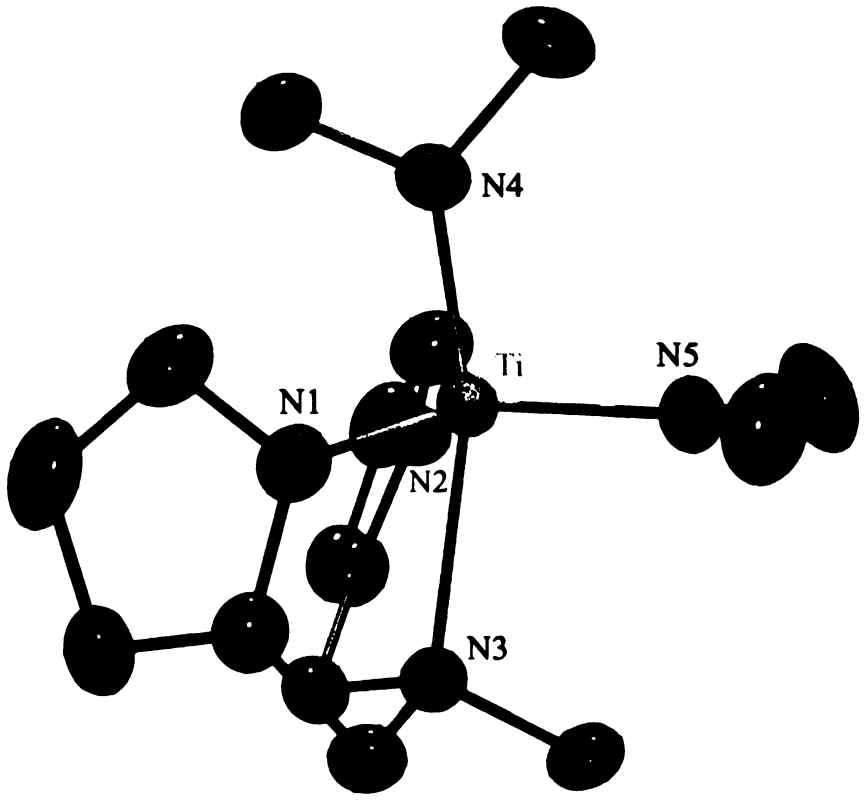

Figure 6-1. The ORTEP representation (25% probability ellipsoids) of Ti(dpma)$(NMe_2)_2$ (**23**).

Table 6-1. Selected bond distances and angles from x-ray diffraction of Ti(dpma)$(NMe_2)_2$(**23**). For the numbering scheme, see Figure 6-1.

Distances and Angles (Å/°)	Ti(dpma)$(NMe_2)_2$ (23)
Ti-N(1)	2.015(3)
Ti-N(2)	2.017(3)
Ti-N(3)	2.312(3)
Ti-N(4)	1.888(3)
Ti-N(5)	1.859(3)
N(1)-Ti-N(2)	120.37(12)
N(1)-Ti-N(3)	76.16(12)
N(1)-Ti-N(4)	97.88(14)
N(1)-Ti-N(5)	115.95(14)
N(2)-Ti-N(3)	75.67(12)
N(2)-Ti-N(4)	94.96(13)
N(4)-Ti-N(5)	100.74(13)

is quite large at 2.312(3) Å.

NMR spectroscopy of Ti(dpma)$(NMe_2)_2$ exhibits some interesting features. The solution state spectrum exhibits no fluxional behavior between 25 °C and 90 °C in C_6D_6; the two dimethylamide ligand resonances are separated by 0.242 ppm. NOE and proton-carbon correlation spectroscopy (gHMQC and gHMBC), indicate that the resonance for the axial dimethylamide ligand is shifted downfield relative to the resonance due to the equatorial dimethylamide ligand. Surprisingly, this difference in chemical shift is not observed in $CDCl_3$, where the two resonances are separated by less than 0.002 ppm.

Ti(dpma)$(NMe_2)_2$ is a very good catalyst for the hydroamination of alkynes with aromatic amines (vide infra). The sluggishness of this complex in hydroamination chemistry, as well as the low yield seen using alkyl amines and internal alkynes as substrates, has led to a search for more active catalysts. The dpma ligand does make the catalyst better in many ways than Ti$(NMe_2)_4$, and we were interested in keeping the benefits of the pyrrole groups. It was reasoned that the donor amine was inhibiting the hydroamination by making the titanium center electron-rich; thus, alkyne coordination to the titanium should be enhanced by making the titanium center less electron-rich. Previous experience with group-6 complexes containing the dpma ligand (vide supra) led to the conclusion that the dpma was a very restrictive ligand in that complexes containing dpma tend to be very rigid and nonfluxional, a characteristic that it currently believed to limit the flexibility of potential catalysts. Thus, interest in a dipyrrolyl ligand that did not contain any other donor groups developed, and the use of H_2dmpm as a ligand was viewed favorably.

Reaction of 1 equivalent of H_2dmpm with Ti$(NMe_2)_4$ (eq 6-2) results in Ti(dmpm)$(NMe_2)_2$ (**24**), in good yield. Because of the low solubility of **24** in common organic solvents, compound **25**, Ti(dppm)$(NMe_2)_4$, was synthesized; the propyl groups on the ligand enhances solubility of the titanium complex in toluene. The structure of **24** obtained via single-crystal x-ray diffraction is shown in Figure 6-1. Selected bond lengths and angles for compounds **24** and **25** are summarized in Tables 6-2. The structure of

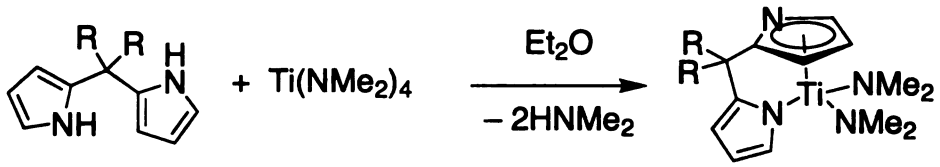

(6-2)

R = Me **24**
R= Pr^n **25**

complex **24** was reported by Love and co-workers[138] as these experiments were progressing. A similar complex, $Ti(C_5H_4CH_2C_4H_3N)(NMe_2)_2$, containing a cycolpentadienyl group in place of one of the pyrrole rings, has been reported by Park and coworkers.[139]

Metal-ligand bond lengths are similar to those seen in $Ti(dpma)(NMe_2)_2$. For example, the Ti–NMe_2 bond lengths average 1.879(5) Å in $Ti(dmpm)(NMe_2)_2$, 1.877(6) Å in $Ti(dppm)(NMe_2)_2$, and 1.874(3) Å in $Ti(dpma)(NMe_2)_2$. As can be seen in the crystal structures for complex **24**, the pyrrole rings adopted a η^1,η^5–bonding mode to the titanium center. The Ti–N(η^1-pyrrole) bond distance averages 2.025(5) Å in $Ti(dmpm)(NMe_2)_2$ and 2.046(7) in $Ti(dppm)(NMe_2)_2$; the average Ti–N(pyrrole) bond length in $Ti(dpma)(NMe_2)_2$ is identical within error at 2.016(3) Å. The structures of **24** and **25** are identical within error to that of $Ti(C_5H_4CH_2C_4H_3N)(NMe_2)_2$.

The NMR behavior of $Ti(dmpm)(NMe_2)_2$ and $Ti(dppm)(NMe_2)_2$ are strikingly different than that of $Ti(dpma)(NMe_2)_2$. Although the pyrrolyl groups are inequivalent in the solid-state structure of both complexes, the room temperature solution-state ^1H NMR is consistent with fast pyrrolyl exchange. Cooling a solution of $Ti(dmpm)(NMe_2)_2$ provided spectra consistent with an η^1,η^5-dmpm complex. Variable temperature ^1H NMR was used to determine the energy of activation associated with η^5-pyrrolyl to η^1-pyrrolyl exchange as 10.2 kcal/mol in CD_2Cl_2 at -60.2 °C (Figure 6-3).

Hydroamination. Complex **24**, $Ti(dpma)(NMe_2)_2$, catalyzes the hydroamination of alkynes with amines, Scheme 6-1. The reaction of aniline or cyclohexylamine with several different alkynes (diphenylacetylene, phenylacetylene, 1-phenylpropyne, 1-hexyne, and 3-hexyne) catalyzed by 10 mol % **24** was investigated, and the results are found in Table

Table 6-2. Selected bond distances and angles from x-ray diffraction of Ti(dmpm)$(NMe_2)_2$ and Ti(dppm)$(NMe_2)_2$. For the numbering scheme, see Figure 6-2.

Distances and Angles (Å/°)	Ti(dmpm)$(NMe_2)_2$ (24)	Ti(dppm)$(NMe_2)_2$ (25)
Ti-Centroid	2.025	2.015(3)
Ti-N(2)	2.025(5)	2.017(3)
Ti-N(4)	1.883(6)	1.888(3)
Ti-N(5)	1.875(5)	1.859(3)
Centroid-Ti-N(2)	105.3	120.37(12)
Centroid-Ti-N(4)	124.0	76.16(12)
Cenroid-Ti-N(5)	111.9	97.88(14)
N(2)-Ti-N(4)	101.5(2)	115.95(14)
N(2)-Ti-N(5)	107.8(2)	75.67(12)
N(4)-Ti-N(5)	104.0(2)	100.74(13)

Figure 6-2. The ORTEP representation (25% probability ellipsoids) of Ti(dmpm)$(NMe_2)_2$ **(25)**.

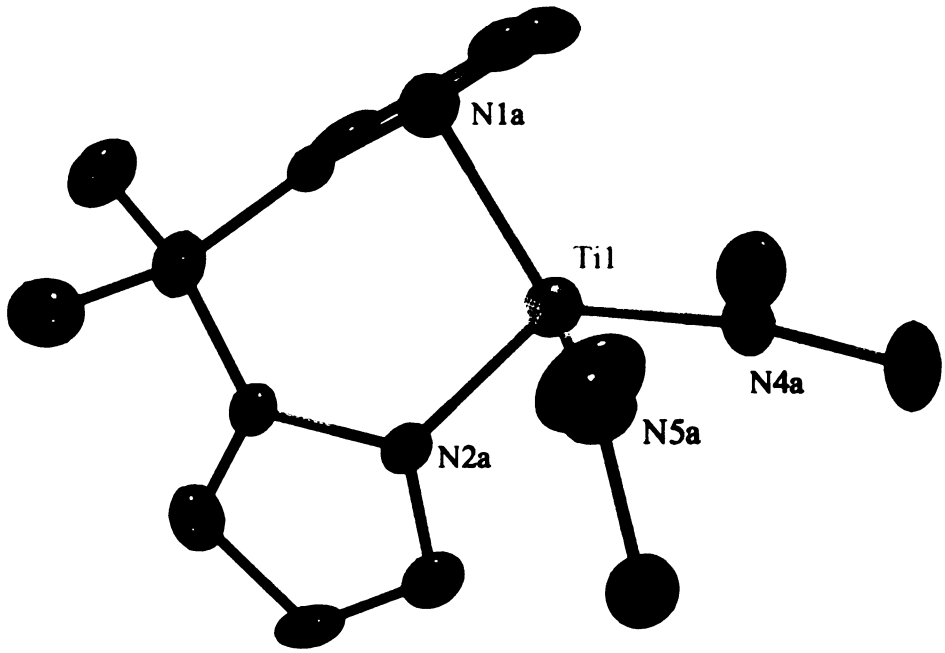

Figure 6-3. The variable temperature ^1H NMR spectra of Ti(dmpm)$(NMe_2)_2$ (**25**).

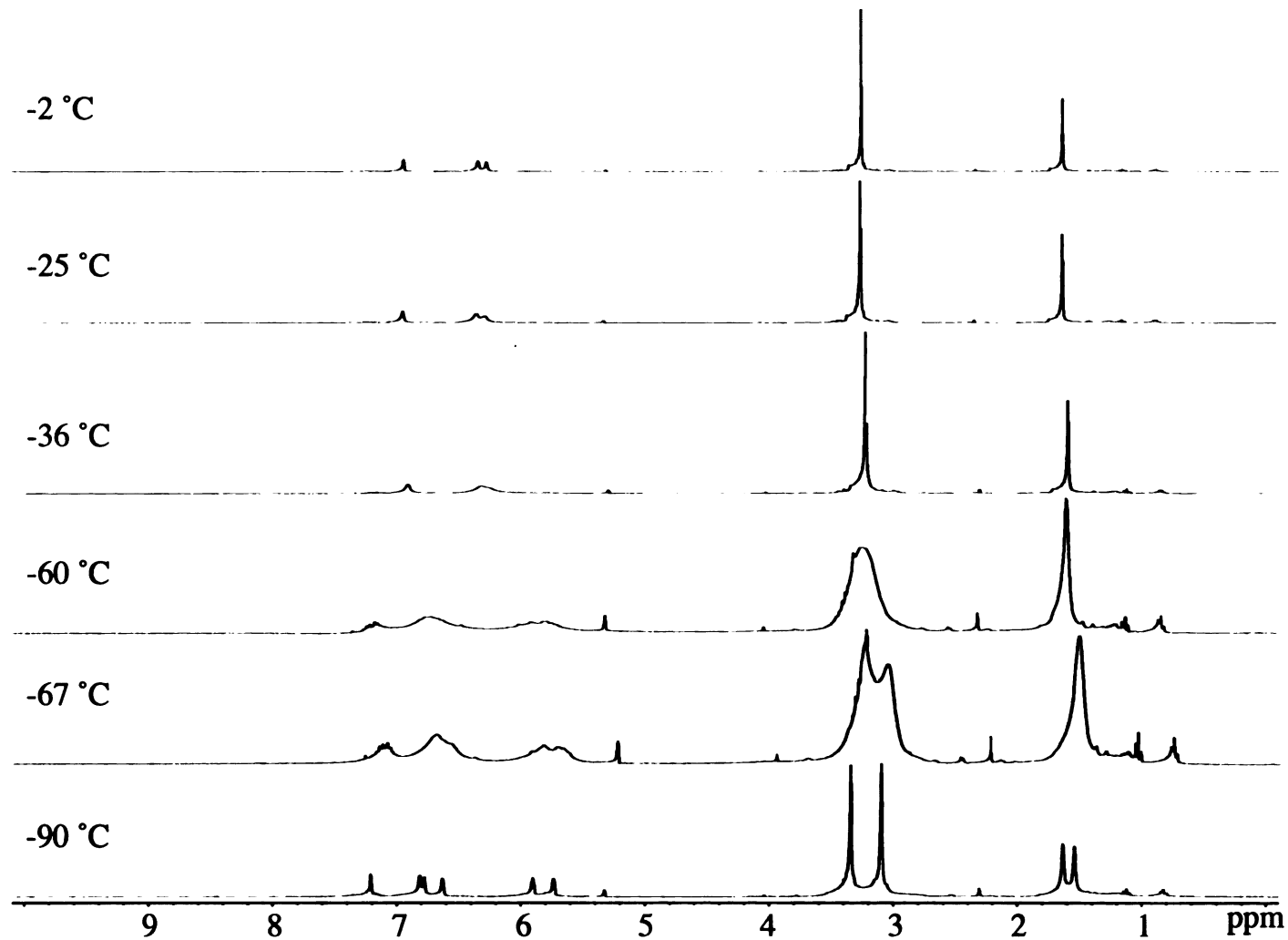

6-3. All reactions were carried out at 75 °C; however higher yields and faster reactions occurred at higher temperatures. In general, terminal alkynes react much more quickly than internal alkynes, and aniline reacted much faster and with more regiochemical selectivity than cyclohexylamine. Hydroamination of 1-phenylpropyne yields predominantly anti-Markovnikov selectivity (nitrogen attachment occurs β to the phenyl group); this is also the product seen with Me_2TiCp_2 as product.[140]

A number of the catalytic reactions were slow at 75 °C, resulting in only low conversions after days of reaction time. Hydroaminations of internal alkynes with cyclohexylamine were usually very slow. Raising the reaction temperature to 130 °C often gave high yields of products in a reasonable time period (<30 h). The yields obtained at 130 °C are shown in brackets in Table 6-3.

Phenylactylene undergoes polymerization/oligomerization with $Ti(dpma)(NMe_2)_2$, (**23**) which lowers the yields of hydroamination products. Polymerization was not seen with other alkynes. A number of different oligomers of phenylactylene were evident in the analysis of reaction mixtures. Treatment of an excess of phenylacetylene (150 equiv) with $Ti(dpma)(NMe_2)_2$ (1 equiv) in toluene at 75 °C resulted in several different oligomers that were separable by column chromatography. The major product, isolated in 45% yield, was 1,3,5-triphenylbenzene.[141]

Pre-catalyst **24** was found to promote the hydroamination of 1-hexyne with a number of different amines (Table 6-4). All of these reactions show that the Markovnikov product is favored, often in excesss of 50:1, over the *anti*-Markovnikov product. Hydroamination did not occur with amines containing nitro or *o*-methoxy substituents. The hydroamination of 1-hexyne with *m*-anisidine or *p*-anisidine occurred with high regioselectivities and yields. Many other functional groups were tolerated, including halogenated anilines.

Electronic effects were observed; reactions involving very electron deficient aromatic amines, such as 2,3,4,5,6-pentafluoroaniline, took days instead of hours to reach completion. Steric effects, however, are negligible. For example, 2,6-diethylaniline and

Table 6-3. Alkyne hydroamination results.

Amine	Alkyne	Catalyst	Time(h)	Yield (M : anti-M)
$PhNH_2$	$Bu^nC{\equiv}CH$	$Ti(dpma)(NMe_2)_2$	6	90 (>50:1)[a]
		$Ti(NMe_2)_4$	2	90 (3 : 1)[a]
		$Ti(dmpm)(NMe_2)_2$	5 min (25 °C)	57 (40:1)[d]
	EtC≡CEt	$Ti(dpma)(NMe_2)_2$	72	73 (2:1)[a]
		$Ti(NMe_2)_4$	17	87[a]
		$Ti(dmpm)(NMe_2)_2$	24 (50 °C)	94[d]
	PhC≡CH	$Ti(dpma)(NMe_2)_2$	8	38 (2 : 1)[c]
		$Ti(NMe_2)_4$	2	49 (2:1)[c]
		$Ti(dmpm)(NMe_2)_2$	5 min (25 °C)	41 (3.6:1)[c]
	PhC≡CPh	$Ti(dpma)(NMe_2)_2$	72[74]	31 [99][a]
		$Ti(NMe_2)_4$	57	92[a]
		$Ti(dmpm)(NMe_2)_2$	24	84[c]
	PhC≡CMe	$Ti(dpma)(NMe_2)_2$	144 [24]	99 (1:24) [96 (1:19)][a]
		$Ti(dmpm)(NMe_2)_2$	6 (50 °C)	50:1[d]
Bu^tNH_2	$Bu^nC{\equiv}CH$	$Ti(NMe_2)_4$	48	0
	EtC≡CEt	$Ti(NMe_2)_4$	48	0
	PhC≡CH	$Ti(NMe_2)_4$	10	53 (1:50)[d]
	PhC≡CPh	$Ti(NMe_2)_4$	48	0
$CyNH_2$	$Bu^nC{\equiv}CH$	$Ti(dpma)(NMe_2)_2$	72	73 (2:1)[a]
	EtC≡CEt	$Ti(dpma)(NMe_2)_2$	72 [24]	3 [57][a]
		$Ti(dmpm)(NMe_2)_2$	48	73[d]
	PhC≡CH	$Ti(dpma)(NMe_2)_2$[e]	20	50 (1:6)[d]
		$Ti(dmpm)(NMe_2)_2$	10 min (25 °C)	54 (1:6)[d]
	PhC≡CPh	$Ti(dpma)(NMe_2)_2$	72 [24]	0 [70][a]
		$Ti(dmpm)(NMe_2)_2$[e]	48 (100 °C)	72[c]
	PhC≡CMe	$Ti(dpma)(NMe_2)_2$	95 [29]	trace [99 (1:4)][a]
		$Ti(dmpm)(NMe_2)_2$	24	93[d]

All reactions with $Ti(dpma)(NMe_2)_2$ and $Ti(NMe_2)_4$ carried out with 10 mol % catalyst in toluene at 75 °C; times and yields in brackets are at 130 °C. Reactions with $Ti(dmpm)(NMe_2)_2$ were carried out in chlorobenzene with 5 mol% catalyst, except as noted.

[a]Results are for aldehyde or ketone hydrolysis products, as determined by GC-FID.

[b]Results are for imine products, as determined by GC-FID.

[c]Isolated yield after reduction with $LiAlH_4$.

[d]Isolated yield of imine.

[e]10 mol % $Ti(dmpm)(NMe_2)_2$ used.

aniline hydroaminated 1-hexyne with comparable rates.

With pre-catalyst **24**, the hydroamination of 1-hexyne with benzylamine or benzhydrylamine proceeded in 70-90% yield and was complete in <48 h at 75 °C. Regioselectivity is poor with benzyhydryl amine, with the Markovnikov product being favored only 3:1. Benzylamine gives very high Markovnikov selectivity.

The reaction of *p*-toluidine with 1-hexyne (eq 6-6) was carried out on a 5 g scale using 2 mol% Ti(dpma)$(NMe_2)_2$. Reduction of the imine product with $LiAlH_4$ gave racemic MeCH[NH(*p*-tol)]Bu^n in 82% (9.4 g) yield. The product obtained had ^1H NMR resonances consistent with literature[142] values.

To be sure that the dpma ligand was not coming off of the metal center during the course of the hydroamination, reactions were carried out with $Ti(NMe_2)_4$, in anticipation that this complex would not be a productive catalyst. However, $Ti(NMe_2)_4$ does catalyze the hydroamination of alkynes with amines; some results are shown in Table 6-3. With terminal alkynes, the Markovnikov product is the favored or exclusive product of hydroamination. As is the case with Ti(dpma)$(NMe_2)_2$, aniline generally gives better yields and faster rates. $Ti(NMe_2)_4$ also appears to catalyze the oligomerization of phenylacetylene, as does Ti(dpma)$(NMe_2)_2$.

The results of $Ti(NMe_2)_4$ catalyzed hydroamination of 1-hexyne with a number of different amines is shown in Table 6-4. As is the case with Ti(dpma)$(NMe_2)_2$, the favored product is the Markovnikov product; most of the reactions with arylamines were complete (in yields >70%) in less than 2h.

$Ti(NMe_2)_4$ is a poorer catalyst for the hydroamination of 1-hexyne with both benzylamine and benzhydrylamine than is complex **24**. In addition, titanium with Cp as ancillary ligand is a poor catalyst for hydroaminations involving benzylamine but was successful with benzhydrylamine.[127d]

Comparison of the catalytic ability of Ti(dpma)$(NMe_2)_2$ and $Ti(NMe_2)_4$ leads to several conclusions. First, the active catalytic species has to be different for each complex.

Table 6-4. Results of hydroamination of 1-hexyne with amines.

Amines	Catalyst	Time (h)	Yield (% M : % anti-M)‡
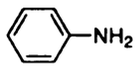	$Ti(NMe_2)_4$	2	90 (3:1)
	$Ti(dpma)(NMe_2)_2$	6	90 (>50:1)
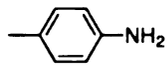	$Ti(NMe_2)_4$	2	87 (4:1)
	$Ti(dpma)(NMe_2)_2$	6	94 (>50:1)
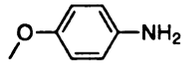	$Ti(NMe_2)_4$	2	93 (6:1)
	$Ti(dpma)(NMe_2)_2$	6	99 (>50:1)
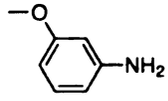	$Ti(NMe_2)_4$	2	82 (40:1)
	$Ti(dpma)(NMe_2)_2$	6	83 (>50:1)
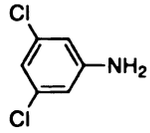	$Ti(NMe_2)_4$	2	72 (23:1)
	$Ti(dpma)(NMe_2)_2$	6	78 (>50:1)
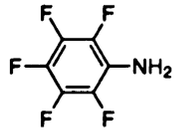	$Ti(NMe_2)_4$	96	75 (37:1)
	$Ti(dpma)(NMe_2)_2$	72	51 (>50:1)
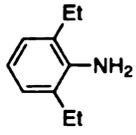	$Ti(NMe_2)_4$	2	57 (9:1)
	$Ti(dpma)(NMe_2)_2$	9	99 (13:1)
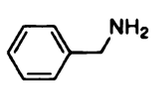	$Ti(NMe_2)_4$	8	17 (5:1)
	$Ti(dpma)(NMe_2)_2$	48	71 (>50:1)
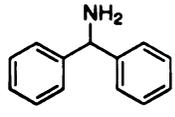	$Ti(NMe_2)_4$	8	17 (5:1)
	$Ti(dpma)(NMe_2)_2$	26	89 (3:1)

Since the regioselectivity of the catalysts are very different, it was concluded that a dpma-containing species is involved in the catalysis with complex **24**. An example of this different regioselectivity is seen in the hydroamination of 1-hexyne with aniline, where $Ti(NMe_2)_4$ gives a 3:1 Markovnikov to *anti*-Markovnikov product ratio, compared with the >50:1 Markovnikov to *anti*-Markovnikov product ratio seen with $Ti(dpma)(NMe_2)_4$. Second, $Ti(dpma)(NMe_2)_2$ is a much more general catalyst than is $Ti(NMe_2)_4$, and yields products with a larger variety of substrates. Alkylamines give poor yields with $Ti(NMe_2)_4$, but can give excellent yields with complex **24**. Third, the pyrrolyl complex **24** generally is more selective for Markovnikov products than is $Ti(NMe_2)_4$.

The use of $Ti(dmpm)(NMe_2)_2$ (**25**) as catalysts for hydroamination results in excellent yields and moderate to high selectivities, as can be seen in Table 6-3. In fact, catalyst **25** was such an active pre-catalyst for hydroamination that solutions of **25** with 1-hexyne and aniline rapidly become hot to the touch, an observation not seen with either $Ti(dpma)(NMe_2)_2$ (**24**) or with $Ti(NMe_2)_4$.

Table 6-5 gives kinetic measurements of the hydroamination of 1-phenylpropyne with aniline, a reaction that is often very clean and moderate in rate and yields predominantly the imine of phenylacetylene. The kinetic measurements were carried out under pseudo-first order kinetics with 10 equiv. of aniline to 1 equiv. of 1-phenylpropyne. The reaction utilizing catalyst **25**, $Ti(dmpm)(NMe_2)_2$, was carried out in chlorobenzene due to low solubility of this catalyst in toluene. Under these conditions with these substrates, it was observed that $Cp_2Ti(Me_3Si{=}SiMe_3)$ was about a factor of two faster than $Ti(dpma)(NMe_2)_2$ (**24**). Still more rapid was commercially available $Ti(NMe_2)_4$. Dipyrrolylmethane complexes **25** and **26** were an order of magnitude faster than the well-explored Cp- and dpma-based catalysts. Reaction rates were consistently slower in chlorobenzene than in toluene.

The Cp-pyrrole complex of Park and coworkers was compared due to its structural similarities to complex **25**, and was found to be a relatively poor catalyst, with reaction rates on the order of 100 times slower than **25**. It is believed that the dipyrrolyl complex **25** can

Table 6-5. Comparison of rate constants for selected catalysts.

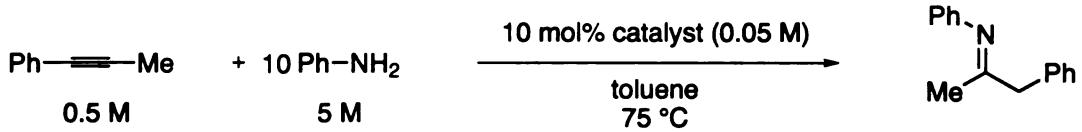

$$-\frac{d[\text{1-phenylpropyne}]}{dt} = k_{obs}\,t$$

Precatalyst	k_{obs} x 10^{-6} s^{-1}
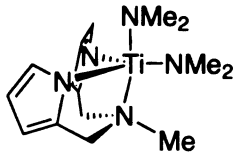	11 [7][a]
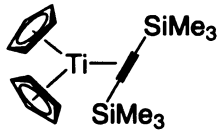	20 [16][a]
$Ti(NMe_2)_4$	76
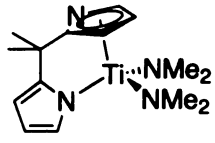	[157][a]
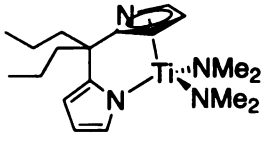	208 [178][a]
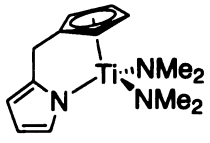	1

[a] Values in brackets are with chlorobenzene as solvent.

more readily access an η^1,η^1-configuration that the Cp-based system, and this contributes to the faster reaction rates.

Conclusions

Dipyrrolyl ligand containing complexes **24**, **25**, and **26** catalyze the hydroamination of alkynes with amines very well. These catalysts often offer better selectivity and higher yields in less time than $Ti(NMe_2)_4$, implying that the pyrrolyl ligands remain attached to the metal center during the course of the hydroamination reaction. Removal of the donor amine group from the dipyrrolyl ligand by using dipyrolylmethane derivatives results in complexes (**25** and **26**) that catalyze hydroamination reactions much more rapidly than the dpma complex **24** does.

Experimental

General considerations. All manipulations of air-sensitive materials were carried out in an MBraun glove box under an atmosphere of purified nitrogen. Ethereal solvents, pentane, and toluene were purchased from Aldrich Chemical Co. and purified by passing through alumina columns to remove water after sparging with N_2 to remove oxygen. NMR solvents were purchased from Cambridge Isotopes Laboratories, Inc. Deuterated benzene was distilled from purple sodium benzophenone ketyl. Deuterated chloroform was distilled from CaH_2 under dry N_2. NMR solvents were stored in sealed containers equipped with a Teflon stopcock in the dry box prior to use. Spectra were taken on Varian instruments located in the Max T. Rogers Instrumentation Facility. Routine coupling constants are not reported. Alumina, silica, and Celite were dried at >200 °C under dynamic vacuum for at least 12 h, then stored under inert atmosphere. Combustion analyses were performed by facilities in the Department of Chemistry at Michigan State University, by Oneida Research Services in Whitesboro, NY, and by Desert Analytics in Tucson, Az.

$Ti(NMe_2)_2$(dpma) (24). $Ti(NMe_2)_4$ (1.098 g, 3.1704 mmol) was dissolved in Et_2O

Table 6-6. Structural parameters for compounds **24** - **26** from single–crystal x-ray diffraction.

	$Ti(dpma)(NMe_2)_2$ (24)	**$Ti(dmpm)(NMe_2)_2$ (25)**	**$Ti(dppm)(NMe_2)_2$ (26)**
Formula	$C_{15}H_{25}N_3Ti$	$C_{15}H_{21}N_4Ti$	$C_{19}H_{32}N_4Ti$
Formula weight	323.30	305.26	364.39
Space Group	P2(1)2(1)2(1)	P2(1)/c	P2(1)/c
a (Å)	9.832(2)	10.3208(17)	9.9440(14)
b (Å)	11.565(2)	12.3848(19)	15.266(2)
c (Å)	15.177(3)	25.325(4)	13.696(2)
α (°)	90	90	90
β (°)	90	93.708(3)	93.252(3)
γ (°)	90	90	90
Volume ($Å^3$)	1725.8(6)	3230.3(9)	2075.8(5)
Z	4	8	4
μ (mm^{-1})	0.497	0.526	0.419
$D_{calc.}$ ($g\ cm^{-3}$)	1.244	1.255	1.166
$R(F_0)$ (I > 2s)	0.0524	0.0622	0.0876
$R_w(F_0)$ (I > 2s)	0.1297	0.1030	0.2273

(10 mL) and chilled to –35 °C. A 5 mL solution of H_2dpma (0.600 g, 3.1704 mmol) in Et_2O was added dropwise. After 30 min the volatiles were removed, and a yellow powder remained. X-ray quality crystals were obtained from pentane/Et_2O at –35 °C in 97.1 % yield (0.955 g), m 52 °C dec. ^{1}H NMR (300 MHz, $CDCl_3$): δ 6.89 (m, 2H), 6.07 (m, 2H), 5.90 (m, 2H), 4.03 (d, J = 14 Hz, 2H), 3.75 (d, J = 14 Hz, 2H), 3.30 (s, 12H), 2.49 (s, 3H). ^{13}C NMR ($CDCl_3$): δ 137.40, 126.64, 107.62, 102.54, 57.90, 47.18, 45.90, 42.82. MS (70 eV): *m/z*(%) 323.4(0.18) [M^+]. Anal. Calcd. for $C_{15}H_{25}N_5Ti$: C, 55.73; H, 7.80; N, 21.66. Found: C, 55.64;H, 7.52; N, 21.38.

Ti(dppm)(NMe_2)$_2$ (26). A solution of 2.242 g Ti(NMe_2)$_4$ (10 mmol) in 20 mL ether was added to a near frozen solution of H_2dppm (2.303g, 10 mmol) in 20 mL ether. The reaction was allowed to warm to box temperature, and stirred for 3h. The volatiles were removed in vacuo, and the orange solid was recrystallized toluene/pentane. The title compound was collected as an orange powder in 68% yield (2.48 g). ^{1}H (C_6D_6, 300 MHz): δ = 6.95 (m, 2H, 5*H*-pyrrolyl), 6.32 (m, 2H, 4*H*-pyrrolyl), 6.28 (m, 2H, 3*H*-pyrrolyl), 2.96 (s, 12H, N(CH_3)$_2$), 2.16 (m, 4H, $CH_2CH_2CH_3$), 1.45 (m, 4H, $CH_2CH_2CH_3$), 0.90 (t, 6H, $CH_2CH_2CH_3$). ^{13}C (C_6D_6): δ = 161.5 (2*C*-pyrrole), 126.1 (5*C*-pyrrole), 111.9 (4*C*-pyrrole), 109.6 (3*C*-pyrrole), 47.6 (N(CH_3)$_2$), 47.0 (CPr^n_2), 40.8 ($CH_2CH_2CH_3$), 18.2 ($CH_2CH_2CH_3$), 15.0 ($CH_2CH_2CH_3$). Anal. Calcd. for $C_{19}H_{32}N_4Ti$: C, 62.63; H, 8.85; N, 15.38. Found: C, 62.91; H, 9.21; N, 15.25.

Representative procedure for hydroamination reactions. All manipulations of the solutions were done in a glove box under an atmosphere of dry nitrogen. In a 5 mL volumetric flask was loaded Ti(NMe_2)$_2$(dpma) (0.2 M solution in toluene, 0.2 mmol, 1 mL), amine (6 mmol, 3 equiv), dodecane (454 μL, 2 mmol, 1 equiv), and alkyne (2 mmol, 1 equiv). The solution was diluted to 5 mL with toluene and transferred to a pressure tube. A stirbar was added, and the tube was fitted with a Teflon stopper. The tube was removed from the drybox and heated in an oil bath. Reactions were run until no alkyne was detected or production of product ceased as determined by GC analysis. Most yields are

of ketones and aldehydes produced by hydrolysis of imine. This was done by stirring the imine solution with an equal volume of 10% HCl. The product was extracted with CH_2Cl_2 (3 x 5 mL) and analyzed by GC. Yields are versus dodecane internal standard. In the case of PhN=C(Me)Ph, CyN=C(Me)Ph, and Bu^tN=C(Me)Ph, the imines were prepared and yields obtained directly versus dodecane internal standard.

Procedure for the kinetic measurements. All manipulations of the solutions were done in an inert atmosphere glove box. In a 2 mL volumetric flask were loaded catalyst (0.1 equiv, 0.500 mL, 0.2 M solution), aniline (10 equiv, 10 mmol), dodecane (1 equiv, 1 mmol), and 1-phenylpropyne (1 equiv, 1 mmol). The solution was diluted to 2 mL with solvent and transferred to a pressure tube. The tube was removed from the glove box and heated in an oil bath at 75 °C. The relative 1-phenylpropyne versus dodecane concentration was monitored as a function of time by GC-FID.

Reaction of excess phenylacetylene with $Ti(NMe_2)_2$(dpma). In an inert atmosphere dry box, a 250 mL round-bottom flask was loaded with a stir bar, toluene (30 mL), phenylacetylene (8.237 g, 75 mmol), and $Ti(NMe_2)_2$(dpma) (0.1616g, 0.5 mmol). The tube was fitted with a stopper and removed from the box. The reaction was heated to 75 °C with stirring for 5 days. The toluene was removed under reduced pressure, and the resulting solid was purified by column chromatography utilizing silica gel (4.5 x 40 cm) and 2:1 hexanes/CH_2Cl_2. The first band contained the majority of the material and was determined to be 1,3,5-triphenylbenzene by ^1H NMR, ^{13}C NMR, and mass spectrometry. The reaction yielded 3.5 g (46%) of purified compound.

Procedure for hydroamination of 1-hexyne with *p*-toluidine followed by reduction. In an inert atmosphere dry box, a 250 mL flask was loaded with a stir bar, *p*-toluidine (12.86 g, 120 mmol), 1-hexyne (4.93 g, 60 mmol), toluene (50 mL), and $Ti(NMe_2)_2$(dpma) (0.388g, 1.2 mmol). The flask was sealed, removed from the dry box, and heated to 75 °C with stirring. The reaction was heated for 28 h, then additional *p*-toluidine (6.43 g, 60 mmol) was added, followed by heating for 37 h. Most of the toluene

was removed in vacuo, and 80 mL of dry THF was added to the solution. The flask was cooled in an ice water bath, and $LiAlH_4$ (6 g, 158 mmol) was added slowly. The reaction was refluxed for 61 h under N_2. The flask was cooled to room temperature, and $NaHCO_3$ (30 g) was added followed by stirring for 5 min. The mixture was filtered, and the solids were washed with ether (3 × 50 mL). The solution was washed with 70 mL of water. The aqueous layer was extracted with ether (3 × 30 mL), and all the organic solutions were combined. The solution was dried with Na_2SO_4 and solvent was removed in vacuo. To the residue was added 50 mL of pentane. Cooling to –25 °C caused *p*-toluidine to crystallize, which was removed by filtration. The product was distilled (65-67 °C, 0.25 mmHg) to give pure 9.4 g (82 %) of 2-(*p*-tolylamino)hexane.

General considerations for single crystal x-ray diffraction. Single crystals of **1-4** were grown at –35 °C in an MBraun inert atmosphere glove box. All but a small portion of the mother liquor was removed, and the crystals were removed from the glovebox in a sealed vial. The crystals were rapidly coated in Paratone N and mounted on a glass fiber. The mounted crystal was placed under a cold stream of nitrogen from an Oxford "Cryostream" low-temperature device. Data were collected on a Bruker-AXS, Inc. SMART CCD diffractometer utilizing a PC running Windows NT. The data collection was done on a Bruker-AXS, Inc. 3-circle goniometer (χ set to 54.78°). The source was a water-cooled Mo x-ray tube (λ = 0.71073 Å) operating at 50 kV/40 mA. A single crystal graphite monochromator selected the wavelength of light prior to being columated. The cell was determined using ω–θ scans (–0.3° scan width) with 3 sets of 20 frames. The initial cell was found by repeated least squares and Bravais lattice analysis. Full data sets were collected using ω–θ scans in four runs. The fourth run duplicates the first 50 frames of the first run to allow analysis of peak intensity changes resulting from crystal degradation; no correction was necessary for any of the structures reported. Absorption corrections were applied to the data. Using the initial cell, data were integrated to hkl/ intensity data using the Bruker-AXS, Inc. program package SAINT. The final unit cell was

determined by SAINT using all the observed data. The structures were solved and refined using the SHELXTL program developed by G. M. Sheldrick and Bruker-AXS, Inc. A full listing of atomic coordinates, bond lengths, bond angles, and thermal parameters for all the structures have been deposited at the Cambridge Crystallographic Data Centre and can be found in the Appendix I. Additional data pertaining to the collection and processing of the four structures can be found in Table 6-6. In Table 2-3, $R1 = \Sigma||F_0|-|F_c||/\Sigma|F_o|$ and $wR2 = \{\Sigma w(F_0^2-F_c^2)^2/\Sigma w(F_o^2)^2\}^{1/2}$. A partial listing of geometrical parameters for all four data sets may be found in Table 6-6.

BIBLIOGRAPHY

1. Lindoy, L. F. *Chemistry of Macrocyclic Ligand Complexes*. ed.; Cambridge University Press: 1992.

2. March, J. *Advanced Organic Chemistry*. 4th ed.; John Wiley and Sons: New York, 1992.

3. Jones, R. A. B., G. P. *The Chemistry of Pyrroles*. ed.; Academic Press: London, 1977.

4. Raines, S.; Kovacs, C. A. *J. Heterocyclic Chem.* **1970,** *7*, 223.

5. Littler, B. J.; Miller, M. A.; Hung, C. H.; Wagner, R. W.; O'Shea, D. F.; Boyle, P. D.; Lindsey, J. S. *J. Org. Chem.* **1999,** *64*, 1391.

6. Alder, K.; Windemuth, E. *Ber.* **1938,** *71B*, 1939.

7. Adolfsson, H.; Nordstrom, K.; Warnmark, K.; Moberg, C. *Tetrahedron.-Asymmetr.* **1996,** *7*, 1967.

8. (a) Buchmeiser, M. R. *Chem. Rev.* **2000**, *100*, 1565. (b) Phillips, A. J.; Abell, A. D. *Aldrichimica Acta* **1999**, *32*, 75. (c) Schrock, R. R. *Tetrahedron* **1999**, *55*, 8141. (d) Schrock, R. R. Olefin Metathesis by Well-Defined Complexes of Molybdenum and Tungsten. In *Topics in Organometallic Chemistry*, Fürstner, A. Ed.; Springer: Berlin, 1998; Vol. 1. (e) Jamieson, J. Y.; Schrock, R. R.; Davis, W. M.; Bonitatebus, P. J.; Zhu, S. S.; Hoveyda, A. H. *Organometallics* **2000**, *19*, 925. (f) Adams, J. A.; Ford, J. G.; Stamatos, P. J.; Hoveyda, A. H. *J. Org. Chem.* **1999**, *64*, 9690. (g) Nugent, W. A.; Feldman, J.; Calabrese, J. C. *J. Am. Chem. Soc.* **1995**, *117*, 8992. (h) La, D. S.; Alexander, J. B.; Cefalo, D. R.; Graf, D. D.; Hoveyda, A. H.; Schrock, R. R. *J. Am. Chem. Soc.* **1998**, *120*, 9720. (i) Alexander, J. B.; La, D. S.; Cefalo, D. R.; Hoveyda, A. H.; Schrock, R. R. *J. Am. Chem. Soc.* **1998**, *120*, 4041. (j) Fujimura, O.; Grubbs, R. H. *J. Org. Chem.* **1998**, *63*, 824. (k) Schrock, R. R. *Acc. Chem. Res.* **1990**, *23*, 158.

9. Bennett, J. L.; Wolczanski, P. T. *J. Am. Chem. Soc.* **1997**, *119*, 10696.

10. For examples see (a) Cao, C.; Ciszewski, J. T.; Odom, A. L. *Organometallics* **2001**, *20*, 5011-5013 and *Organometallics* **2002**, *21*, 5148. (b) Shi, Y.; Ciszewski, J. T.; Odom, A. L. *Organometallics* **2001**, *20*, 3967-3969 and *Organometallics* **2002**, *21*, 5148. (c) Hill, J. E.; Profilet, R. D.; Fanwick, P. E.; Rothwell, I. P. *Angew. Chem. Int. Ed.* **1990**, *29*, 664. (d) Tillack, A.; Castro, I. G.; Hartung, C. G.; Beller, M. *Angew. Chem. Int. Ed.* **2002**, *41*, 2541. (e) Pohlki, F.; Heutling, A.; Bytschkov, I.; Hotopp, T.; Doye, S. *Synlett* **2002**, 799. (f) Haak, E.; Bytschkov, I.; Doye, S. *Angew. Chem. Int. Ed.* **1999**, *38*, 3389. (g) Johnson, J. S.; Bergman, R. G. *J. Am. Chem. Soc.* **2001**, *123*, 2923. (h) Ackermann, L.; Bergman, R. G. *Org. Lett.* **2002**, *4*, 1475. (i)

Ong, T.-G.; Yap, G. P. A.; Richeson, D. S. *J. Am. Chem. Soc.* **2003**, *125*, 8100. (j) Ackermann, L.; Bergman, R. G.; Loy, R. N. *J. Am. Chem. Soc.* **2003**, *125*, 11956. (k) Cao, C.; Shi, Y.; Odom, A. L. *J. Am. Chem. Soc.* **2003**, *125*, 2880.

11. For a few examples see (a) Bruno, J. W.; Li, X. J. *Organometallics* **2000**, *19*, 4672. (b) Zuckerman, R. L.; Bergman, R. G. *Organometallics* **2000**, *19*, 4795. (c) Bashall, A.; Collier, P. E.; Gade L. H.; McPartlin, M.; Mountford P.; Pugh, S. M.; Radojevic, S.; Schubart, M.; Scowen, I. J.; Trosch, D. J. M. *Organometallics* **2000**, *19*, 4784. (d) McInnes J. M.; Mountford, P. *J. Chem. Soc., Chem. Communications* **1998** 1669. (e) Cantrell, G. K.; Meyer, T. Y. *J. Am. Chem. Soc.* **120**, 8035.

12. Wigley, D. E.; Organoimido Complexes of the Transition Metals. In *Progress in Inorganic Chemistry*; Karlin, K.D. Ed.; John Wiley & Sons, Inc.: New York, 1994; Vol. 42, 239.

13. Haymore, B. L.; Maatta, E. A.; Wentworth, R. A. D. *J. Am. Chem. Soc.*, **1979**, *101*, 2063.

14. (a) Barrie, P.; Coffey, T. A.; Forster, G. D.; Hogarth, G. *J. Chem. Soc., Dalton Trans.* **1999**, 4519. (b) Strong, J. B.; Yap, G. P. A.; Ostrander, R.; Liable-Sands, L. M.; Rheingold, A. L.; Thouvenot, R.; Gouzerh, P.; Maatta, E. A. *J. Am. Chem. Soc.* **2000**, *122*, 639.

15. Bradley, D. C.; Hodge, S. R.; Runnacles, J. D.; Hughes, M.; Mason, J.; Richards, R. L. *J. Chem. Soc., Dalton Trans.* **1992**, 1663.

16. Lin, Z.; Hall, M. B. *Coord. Chem. Rev.* **1993**, *123*, 149.

17. For the sake of simplicity, a few of the canonical valence bond forms are given. A more complete discussion involving all of the limiting structures as applied to imido bonding is found in Cundari, T. R. *Chem. Rev.* **2000**, *100*, 807 and references therein.

18. Parkin, G.; van Asselt, A.; Leahy, D. J.; Whinnery, L.; Huya, N. G.; Quan, R. W.; Henling, L. M.; Schaefer, W. P.; Santarsiero, B. D.; Bercaw, J. E. *Inorg. Chem.* **1992**, *31*, 82.

19. Antiñolo, A.; Espinosa, P.; Fajardo, M.; Gómez-Sal, P.; López-Mardomingo, C.; Martin-Alonso, A.; Otero, A. *J. Chem. Soc., Dalton Trans.* **1995**, 1007-1013.

20. Jørgensen, K. A. *Inorg. Chem.* **1993**, *32*, 1521.

21. Chernega, A. N.; Green, M. L. H.; Suárez, A. G. *J. Chem. Soc., Dalton Trans.* **1993**, 3031.

22. McCarty, C. G. *syn-anti* Isomerization and rearrangements. In *The Chemistry of the Carbon-Nitrogen Double Bond*; Patai, S Ed.; The Chemistry of Functional Groups; Interscience Publishers: London, 1970, 365.

23. (a) *Cyclic Organonitrogen Stereodynamics*, Lambert, J. B.; Takeuchi, Y. Eds.; VCH Publishers, Inc.: New York, 1992. (b) Guerra, A.; Lunazzi, L. *J. Org. Chem.* **1995**, *60*, 7959. (c) Kontoyianni, M.; Hoffman, A. J.; Bowen, J. P. *J. Comp. Chem.* **1992**, *13*, 57.

24. For an example of recent calculations on oxo systems, see Gisdakis, P.; Rosch, N. *J. Am. Chem. Soc.* **2001**, *123*, 697.

25. Li, Y.; Turnas, A.; Ciszewski, J. T.; Odom, A. L. *Inorg. Chem.* **2002**, *41*, 6298.

26. Schrock, R. R.; Seidel, S. W.; Schrodi, Y.; Davis, W. M. *Organometallics* **1999**, *18*, 428.

27. Lam, H.-W.; Wilkinson, G.; Hussain-Bates, B.; Hursthouse, M. B. *J. Chem. Soc., Dalton Trans.* **1993**, 781.

28. For additional systems involving nonexchanging bent and linear imidos on the NMR timescale, see (a) Danopoulos, A. A.; Wilkinson, G.; Hussain, B.; Hursthouse, M. B. *J. Chem. Soc., Chem. Comm.* **1989**, 896. (b) Danopoulos, A. A.; Leung, W.-H.; Wilkinson, G.; Hussain-Bates, B.; Hursthouse, M. B. *Polyhedron* **1990**, *9*, 2625.

29. Meijboom, N.; Schaverien, C. J.; Orpen, A. G. *Organometallics* **1990**, *9*, 774.

30. Fox, H. H.; Yap, K. B.; Robbins, J.; Cai, S.; Schrock, R. R. *Inorg. Chem.* **1992**, *31*, 2287.

31. Nugent, W. A.; Harlow, R. L. *Inorg. Chem.* **1980**, *19*, 777.

32. (a) Alvarez, S.; Llunell, M. *Dalton Trans.* **2000**, 3288. (b) Addison, A. W.; Rao, T. N.; Reedijk, J.; van Rijn, J.; Verschoor, G. C. *Dalton Trans.* **1984**, 1349. (c) Zabrodsky, H.; Peleg, S.; Avnir, D. *J. Am. Chem. Soc.* **1992**, *114*, 7843.

33. Minoretti, A.; Aue, W. P.; Reinhold, M.; Ernst, R. R. *J. Magnetic Resonance* **1980**, *40*, 175.

34. (a) Nugent, W. A.; McKinney, R. J.; Kasowski, R. V.; Van-Catledge, F. A. *Inorg. Chim. Acta* **1982**, *65*, L91. (b) Ashcroft, B. R.; Clark, G. R.; Nielson, A. J.; Rickard, C. E. F. *Polyhedron* **1986**, *5*, 2081. (c) Nugent, W. A.; Mayer, J. M. *Metal-Ligand Multiple Bonds*, Interscience: NewYork, 1988, 133.

35. The values for the dpma complexes reported were obtained by taking the average of the C_α resonances minus the average of the C_β resonances in each of the spectra.

This was done for comparison purposes with other bis(imido) complexes where the imidos are quickly exchanging.

36. For a discussion and an extensive listing of applications in organic chemistry of NMR as it relates to charge densities see Emsley, J. W.; Feeney, J.; Sutcliffe, L. H. *High Resolution Nuclear Magnetic Resonance Spectroscopy*, Pergamon Press: Oxford, 1966. A brief discussion on paramagnetic contributions to the ^{14}N NMR chemical shift and relevant references are found in this book.

37. (a) Gasteiger, J.; Marsili, M. *Org. Mag. Res.* **1981**, *15*, 353. (b) Spiesecke, H.; Schneider, W. G. *J. Chem. Phys.* **1961**, *35*, 722. (c) Cavanaugh, J. R.; Dailey, B. P. *J. Chem. Phys.* **1961**, *14*, 1099. (d) Dailey, B. P.; Shoolery, J. N. *J. Am. Chem. Soc.* **1955**, *77*, 3977.

38. For a discussion of Pauling electronegativities versus transition metal oxidation states see Sanderson, R. T. *Inorg. Chem.* **1986**, *25*, 3518. The same procedure using optical electronegativities provides plots of equally good linearity. For a discussion of optical electronegativity, see Jørgensen, C. K. Electron Transfer Spectra in *Prog. Inorg. Chem.* **1971**, *12*, 101. For a similar correlation between optical electronegativity and $\Delta\delta$ values see reference 34c.

39. Sundermeyer, J.; Putterlik, J.; Foth, M.; Field, J. S.; Ramesar, N. *Chem. Ber.* **1994**, *127*, 1201. Tp* is *tris*(3,5-dimethyl-1-pyrazolyl)hydroborate.

40. For chromium and molybdenum, R is Bu^t. For tungsten, R is Ph.

41. Radius, U.; Sundermeyer, J. *Chem. Ber.* **1992**, *125*, 2183-2186.

42. Coles, M. P.; Dalby, C. I.; Gibson, V. C.; Clegg, W; Elsegood, M. R. J. *Chem. Comm.* **1995**, 1709.

43. For a similar discussion on *bis*(1-adamantylimido)chromium(VI) complexes see Coles, M. P.; Gibson, V. C.; Clegg, W.; Elsegood, M. R. J. *Polyhedron* **1998**, 2483.

44. Similar results are found when series of molybdenum complexes are examined, see Cole, S. C.; Coles, M. P.; Hitchcock, P. B. *Dalton Trans.* **2002**, 4168.

45. An alternative measure of linear versus bent comparison would be to use $\Delta\delta_{\alpha\beta(linear)} - \Delta\delta_{\alpha\beta(bent)}$. The solution numbers using this method would be in the order Cr > W > Mo with values of 1.2, 0.7, and 0.1 respectively. However, the result is similar in that the $\Delta\delta$ values due to changing the imido environment are far smaller (< 1.2 ppm) than changing the metal or ligands on the metal.

46. Le Ny, J. P.; Osborn, J. A. *Organometallics*, **1991**, *10*, 1546.

47. ^{14}N NMR spectra are referenced to the ammonia scale with NH_3 as 0.00 ppm. On this scale, neat nitromethane has a resonance at 380.4 ppm. Another common scale uses ammonium as the reference, which appears at ~21 ppm on the ammonia scale.

48. (a) Webb, G. A.; Witanowski, M. Theoretical Background to Nitrogen NMR. In *Nitrogen NMR*, Witanowski, M.; Webb, G. A. Eds; Plenum Press: London, 1973. (b) Mason, J. *Multinuclear NMR*, Plenum Press: New York, 1987.

49. (a) Mason, J. *Chem. Rev.* **1981**, *81*, 205. (b) Donovan-Mtunzi, S.; Richards, R. L.; Mason, J. *J. Chem. Soc., Dalton Trans.* **1984**, 1329. (c) Dilworth, J. R.; Donovan-Mtunzi, S.; Kan C. T.; Richards, R. L.; Mason, J. *Inorg. Chim. Acta* **1981**, *53*, L161. (d) Odom, A. L.; Cummins, C. C. *Organometallics* **1996**, *15*, 898.

50. For discussion of similar effects in ^{17}O NMR metal-oxo shifts see (a) Kidd, R. G. *Can. J. Chem.* **1967**, *45*, 605. (b) Klemperer, W. G. *Angew. Chem. Int. Ed.* **1978**, *17*, 246. (c) Miller, K. F.; Wentworth, R. A. D. *Inorg. Chem.* **1979**, *18*, 984.

51. Witanowski, M.; Stefaniak, L.; Januszewski, H.; Grabowski, Z. *Tetrahedron* **1972**, *28*, 637.

52. (a) Steffey, B. D; Fanwick, P. E., Rothwell, I. P. *Polyhedron* **1990**, *9*, 963. For similar examples of early metal alkoxides with little or no correlation between bond distance and angle, see (b) Howard, W. A.; Trnka, T. M.; Parkin, G. *Inorg. Chem.* **1995**, *34*, 5900. (c) Wolczanski, P. T. *Polyhedron* **1995**, *14*, 3335. For systems where alkoxide bond angle does seem to correlate with bond distance, see (d) Tomaszewski, R.; Arif, A. M.; Ernst, R. D. *J. Chem. Soc., Dalton Trans.* **1999**, 1883. (e) Huffman, J. C.; Moloy, K. G.; Marsella, J. A.; Caulton, K. G. *J. Am. Chem. Soc.* **1980**, *102*, 3009. For a recent computational study supporting Ti–OR triple bonding, see (f) Dobado, J. A.; Molina, J. M.; Uggla, R.; Sundberg, M. R. *Inorg. Chem.* **2000**, *39*, 2831. For an excellent experimental study comparing π-bonding in a variety of monoanionic ligands to a common metal fragment, see (g) Lukens, W. W., Jr.; Smith, M. R., III; Andersen, R. A. *J. Am. Chem. Soc.* **1996**, *118*, 1719.

53. Jandciu, E. W.; Legzdins, P.; McNeil, W. S.; Patrick, B. O.; Smith, K. M. *Chem. Commun.* **2000**, 1809.

54. Imido bond angle has recently been correlated with ^{95}Mo NMR shielding as well. Minelli, M.; Hoang, M. L.; Kraus, M.; Kucera, G.; Loertscher, J.; Reynolds, M.; Timm, N.; Chiang, M. Y.; Powell, D. *Inorg. Chem.* **2002**, *41*, 5954.

55. For a reference demonstrating through SCF-Xα-SW analysis the high electron density on even linear imido nitrogens, see Schofield, M. H.; Kee, T. P.; Anhaus, J. T.; Schrock, R. R.; Johnson, K. H.; Davis, W. M. *Inorg. Chem.* **1991**, *30*, 3595.

56. Similar arguments relating bond order and bond polarity are put forth in Reference 41c, Chapter 2.

57. Coffey, T. A.; Forster, G. D.; Hogarth, G.; Sella, A. *Polyhedron* **1993**, *12*, 2741.

58. For an interesting reactivity study on an imido with an extremely small angle, see Gountchev, T. I.; Tilley, T. D. *J. Am. Chem. Soc.* **1997**, *119*, 12831.

59. Hay, P. J.; Wadt, W. R. *J. Chem. Phys.* **1985**, *82*, 284.

60. Gordon, M. S.; Binkley, J. S.; Pople, J. A.; Pietro, W. J.; Hehre, W. J. *J. Am. Chem. Soc.* **1983**, *104*, 2797.

61. Becke, A. D. *J. Chem. Phys.* **1993**, *98*, 1372.

62. Gaussian 98, Revision A.11.1, Frisch, M. J.; Trucks, G. W.; Schlegel, H. B.; Scuseria, G. E.; Robb, M. A.; Cheeseman, J. R.; Zakrzewski, V. G.; Montgomery, J. A., Jr.; Stratmann, R. E.; Burant, J. C.; Dapprich, S.; Millam, J. M.; Daniels, A. D.; Kudin, K. N.; Strain, M. C.; Farkas, O.; Tomasi, J.; Barone, V.; Cossi, M.; Cammi, R.; Mennucci, B.; Pomelli, C.; Adamo, C.; Clifford, S.; Ochterski, J.; Petersson, G. A.; Ayala, P. Y.; Cui, Q.; Morokuma, K.; Salvador, P.; Dannenberg, J. J.; Malick, D. K.; Rabuck, A. D.; Raghavachari, K.; Foresman, J. B.; Cioslowski, J.; Ortiz, J. V.; Baboul, A. G.; Stefanov, B. B.; Liu, G.; Liashenko, A.; Piskorz, P.; Komaromi, I.; Gomperts, R.; Martin, R. L.; Fox, D. J.; Keith, T.; Al-Laham, M. A.; Peng, C. Y.; Nanayakkara, A.; Challacombe, M.; Gill, P. M. W.; Johnson, B.; Chen, W.; Wong, M. W.; Andres, J. L.; Gonzalez, C.; Head-Gordon, M.; Replogle, E. S.; Pople, J. A., Gaussian, Inc., Pittsburgh, PA, 2001.

63. Schoettel, G.; Kress, J.; Osborn, J. A. *J. Chem. Soc., Chem. Commun.* **1989**, 1062.

64. Schrock, R. R. *Acc. Chem. Res.* **1986**, *19*, 342.

65. Schrock, R. R. *Acc. Chem. Res.* **1990**, *23*, 158.

66. Tsang, W. C. P.; Hultzsch, K. C.; Alexander, J. B.; Bonitatebus, P. J.; Schrock, R. R.; Hoveyda, A. H. *J. Am. Chem. Soc.* **2003**, *125*, 6337.

67. Tsang, W. C. P.; Hultzsch, K. C.; Alexander, J. B.; Bonitatebus, P. J.; Schrock, R. R.; Hoveyda, A. H. *J. Am. Chem. Soc.* **2003**, *125*, 2652.

68. Tsang, W. C. P.; Jernelius, J. A.; Cortez, G. A.; Weatherhead, G. S.; Schrock, R. R.; Hoveyda, A. H. *J. Am. Chem. Soc.* **2003**, *125*, 2591.

69. Schrock, R. R.; Hoveyda, A. H. *Angew. Chem Int. Ed. Eng.* **2003**, *42*, 4592.

70. Schrock, R. R.; Jamieson, J. Y.; Araujo, J. P.; Bonitatebus, P. J.; Sinha, A.; Pia, L.; Lopez, H. *J. Organomet. Chem.* **2003**, *684*, 56.

71. Schrock, R. R.; Jamieson, J. Y.; Dolman, S. J.; Miller, S. A.; Bonitatebus, P. J.; Hoveyda, A. H. *Organometallics* **2002**, *21*, 409.

72. Hultzsch, K. C.; Jernelius, J. A.; Hoveyda, A. H.; Schrock, R. R. *Angew. Chem. Int. Ed.* **2002**, *41*, 589.

73. Cochran, F. V.; Schrock, R. R. *Abstr. Pap. Am. Chem. Soc.* **2000**, *220*, U529.

74. Gibson, V. C.; Marshall, E. L.; Redshaw, C.; Clegg, W.; Elsegood, M. R. J. *J. Chem. Soc. Dalton* **1996**, 4197.

75. Trnka, T. M.; Grubbs, R. H. *Acc. Chem. Res.* **2001**, *34*, 18.

76. Huang, J.; Stevens, E. D.; Nolan, S. P.; Petersen, J. L. *J. Am. Chem. Soc.* **1999**, *121*, 2674.

77. Huang, J.; Schanz, H.-J.; Stevens, E. D.; Nolan, S. P. *Organometallics* **1999**, *18*, 5375.

78. Scholl, M.; Trnka, T. M.; Morgan, J. P.; Grubbs, R. H. *Tet. Let.* **1999**, *40*, 2247.

79. Furstner, A.; Ackermann, L.; Gabor, B.; Goddard, R.; Lehmann, C. W.; Mynott, R.; Stelzer, F.; Thiel, O. R. *Chem. Eur. J.* **2001**, *7*, 3236.

80. Jafarpour, L.; Nolan, S. P. *Org. Lett.* **2000**, *2*, 4075.

81. Jafarpour, L.; Nolan, S. P. *Organometallics* **2000**, *19*, 2055.

82. Jafarpour, L.; Heck, M.-P.; Baylon, C.; Lee, H. M.; Mioskowski, C.; Nolan, S. P. *Organometallics* **2002**, *21*, 671.

83. Jafarpour, L.; Hillier, A. C.; Nolan, S. P. *Organometallics* **2002**, *21*, 442.

84. Sanford, M. S.; Henling, L. M.; Day, M. W.; Grubbs, R. H. *Angew. Chem. Int. Ed. Eng.* **2000**, *39*, 3451.

85. (a) Shi, Y.; Ciszewski, J. T.; Odom, A. L. *Organometallics* **2001**, *20*, 3967. (b) Cao, C.; Ciszewski, J. T.; Odom, A. L. *Organometallics* **2001**, *20*, 5011. (c) Shi, Y.; Hall, C.; Ciszewski, J. T.; Cao, C.; Odom, A. L. *Chem. Commun.* **2003**, 586. (d) Cao, C.; Shi, Y.; Odom, A. L. *Org. Lett.* **2003**, *4*, 2853. (e) Li, Y.; Shi, Y.; Odom, A. L. *J. Am. Chem. Soc.* **2004**, *126*, 1794.

86. Schrock, R. R.; Murdzek, J. S.; Bazan, G. C.; Robbins, J.; Dimare, M.; Oregan, M. *J. Am. Chem. Soc.* **1990**, *112*, 3875.

87. Wilhelm, T. E.; Belderrain, T. R.; Brown, S. N.; Grubbs, R. H. *Organometallics* **1997**, *16*, 3867.

88. Nolan, S. P.; Belderrain, T. R.; Grubbs, R. H. *Organometallics* **1997**, *16*, 5569.

89. The history of olefin metathesis was recently highlighted, see A. M. Rouhi, *Chemical and Engineering News* **2002**, *80*, 29. A. M. Rouhi, *Chemical and Engineering News* 2002, *80*, 34.

90. Ivin, K. J.; Mol, J. C. *Olefin Metathesis and Metathesis Polymerization*, Academic Press: San Diego, 1997.

91. Schrock, R. R. *J. Am. Chem. Soc.* **1974**, *97*, 6577.

92. Schrock, R. R. *Chem. Rev.* **2002**, *102*, 145.

93. Oskam, J. H.; Fox, H. H.; Yap, K. B.; McConville, D. H.; O'Dell, R.; Lichtenstein, B. J.; Schrock, R. R. *J. Organomet. Chem.* **1993**, *459*, 185.

94. For examples, see Alexander, J. B.; La, D. S.; Cefalo, D. R.; Hoveyda, A. H.; Schrock, R. R. *J. Am. Chem. Soc.* **1998**, *120*, 4041. La, D. S.; Alexander, J. B.; Cefalo, D. R.; Graf, D. D.; Hoveyda, A. H.; Schrock, R. R. *J. Am. Chem. Soc.* **1998**, *120*, 9720.

95. Hultzsch, K. C.; Jernelius, J. A.; Hoveyda, A. H.; Schrock, R. R. *Angew. Chem. Int. Ed.* **2002**, *41*, 589.

96. Fürstner, A.; Krause, H.; Ackermann, L.; Lehmann, C. W. *Chem. Commun.* **2001**, 2240.

97. Bielawski, C. W.; Benitez, D.; Grubbs R. H. *Science*, **2002**, *297*, 2041. Bielawski, C. W.; Benitez, D.; Grubbs, R. H. *J. Am. Chem. Soc.*, **2003**, *125*, 8424.

98. Hultzsch, K. C.; Jernelius, J. A.; Hoveyda, A. H.; Schrock, R. R., *Angew. Chem. Int. Ed.* **2002**, *41*, 589.

99. For examples, see Kriley, C. E.; Kerschner, J. L.; Fanwick, P. E.; Rothwell, I. P. *Organometallics*, **1993**, *12*, 2051. Yeh, W.-Y.; Ho, C.-L.; Chiang, M. Y.; Chen, I-T. *Organometallics*, **1997**, *16*, 2698. Kershner, J. L.; Fanwick, P. E.; Rothwell, I. P. *J. Am. Chem. Soc.*, **1988**, *110*, 8235.

100. For seminal examples, see Simeling, U.; Kölling, L.; Stammler, A.; Stammler, H.-G.; Kaminski, E.; Fink, G. *Chem. Commun.*, **2000**, 1177;. Kretzchmar, E. A.; Kipke, J.; Sundermeyer, J. *Chem. Commun.*, **1999**, 2381. Redshaw, C.; Gibson, V. C.; Clegg, W.; Edwards, A. J.; Miles, B. *J. Chem. Soc., Dalton Trans.*, **1997**, 3343. Gibson, V.C.; Redshaw, C.; Clegg, W.; Elsegood, M. R. J. *J. Chem. Soc., Dalton*

Trans., **1996**, 4513; Lentz, M. R.; Fanwick, P.E.; Rothwell, I. P. *Chem. Commun.*, **2002**, 2482.

101. Vani, P. V. S. N.; Chida, A. S.; Srinivasan, R.; Chandrasekharam, M.; Singh, A. K. *Synth. Commun.*, **2001**, *31*, 219.

102. Zhu, L.; Wehmeyer, R. M.; Rieke, R. D. *J. Org. Chem.*, **1991**, *56*, 1145.

103. Hurd, C. D.; Jenkins, W. W. *J. Org. Chem.*, **1957**, *22*, 1418. Strazzolini, P.; Giumanini, A. G.; Runcio, A.; Scuccato, M. *J. Org. Chem.* **1998**, *63*, 952. Mellor, A. G.; Mittoo, S.; Parkes, R.; Millar, R. W. *Tetrahedron*, **2000**, *56*, 8019.

104. Tepe, J. J.; Madalengoitia, J. S.; Slunt, K. M.; Werbovetz, K. W.; Spoors, P. G.; Macdonald, T. L. *J. Med. Chem.*, **1996**, *39*, 2188. Razafimbelo, J.; Baudouin, G.; Tillequin, F.; Renard, P.; *Chem. Pharm. Bull.*, **1998**, *46*, 34. Fletcher, R. J.; Lampard, C.; Murphy, J. A.; Lewis, N. *J. Chem. Soc., Perkin Trans. 1*, **1995**, 623.

105. Schrock, R. R.; Murdzek, J. S.; Bazan, G. C.; Robbins, J.; DiMare, M.; O'Regan, M. *J. Am. Chem. Soc.*, **1990**, *112*, 3875.

106. Schrock, R. R. *Chem. Rev.* **2002**, *102*, 145.

107. Grubbs, R. H. ed. *Handbook of Olefin Metathesis* Wiley-VCH: Weinheim, 2003.

108. Nugent, W. A.; Feldman, J.; Calabrese, J. C. *J. Am. Chem. Soc.* **1995**, *117*, 8992.

109. Johnson, L. K.; Grubbs, R. H.; Ziller, J. W. *J. Am. Chem. Soc.* **1993**, *115*, 8130.

110. For a review, see Müller, T. E.; Beller, M. *Chem. Rev.* **1998**, *98*, 675.

111. (a) Shi, Y.; Ciszewski, J. T.; Odom, A. L. *Organometallics* **2001**, *20*, 3967. (b) Cao, C.; Ciszewski, J. T.; Odom, A. L. *Organometallics* **2001**, *20*, 5011. (c) Shi, Y.; Hall, C.; Ciszewski, J. T.; Cao, C.; Odom, A. L. *Chem. Commun.* **2003**, 586. (d) Cao, C.; Shi, Y.; Odom, *Org. Lett.* **2003**, *4*, 2853. (e) Li, Y.; Shi, Y.; Odom, A. L. *J. Am. Chem. Soc.* **2004**, *126*, 1794.

112. Cao, C.; Shi, Y.; Odom, A. L. *J. Am. Chem. Soc.* **2003**, *125*, 2880.

113. For seminal mechanistic studies on Group-4 metal catalyzed hydroamination, see (a) Baranger, A. M.; Walsh, P. J.; Bergman, R. G. *J. Am. Chem. Soc.* **1993**, *115*, 2753. (b) Walsh, P. J.; Baranger, A. M.; Bergman, R. G. *J. Am. Chem. Soc.* **1992**, *114*, 1708.

114. For an isolable azatitanacyclobutene, see Ward, B. D.; Maisse-François, A.; Mountford, P.; Gade, L. H. *Chem. Commun.* **2004**, 704.

115. Nugent, W. A.; Mayer, J. M. *Metal-Ligand Multiple Bonds*, John Wiley & Sons: New York, 1988.

116. Schrock, R. R.; Mudzek, J. S.; Bazan, G. C.; Robbins, J.; DiMare, M.; O'Regan, M. B. *J. Am. Chem. Soc.* **1990**, *112*, 3875.

117. The ring-strain in the triple-bond of cyclooctyne is estimated by hydrogenation (cyclooctyne to *cis*-cyclooctene versus 4-octyne to *cis*-4-octene) to be ~10 kcal/mol. Turner, R. B.; Jarret, A. D.; Goebel, P.; Mallon, B. J. *J. Am. Chem. Soc.* **1973**, *95*, 790.

118. Cyclooctyne is readily prepared on >10 g scales. Brandsma, L.; Verkruijsse, H. D. *Synthesis* **1978**, 290. At –35 °C under an inert atmosphere, pure cyclooctyne has been stored without noticeable decomposition for months.

119. Schrock, R. R.; Crowe, W. E.; Bazan, G. C.; DiMare, M.; O'Regan, M. B.; Schofield, M. H. *Organometallics* **1991**, *10*, 1832.

120. Gordon, A. J.; Ford, R. A. *The Chemist's Companion*, John Wiley & Sons: New York, 1972.

121. Schrock, R. R.; DePue, R. T.; Feldman, J.; Yap, K. B.; Yang, D. C.; Davis, W. M.; Park, L.; DiMare, M.; Schofield, M.; Anhaus, J.; Walborsky, E.; Evitt, E.; Krüger, C.; Betz, P. *Organometallics* **1990**, *9*, 2262.

122. Kress, J.; Wesolek, M.; Osborn, J. A. *Chem. Commun.* **1982**, 514.

123. Fox, H. H.; Yap, K. B.; Robbins, J. J.; Cai, S.; Schrock, R. R. *Inorg. Chem.* **1992**, *31*, 2287.

124. Brandsma, L.; Verkruijsse, H. D. *Synthesis* **1978**, 290.

125. Two recent reviews: Nobis, M.; Driebe-Hölscher, B. *Angew. Chem. Int. Ed.* **2001**, *40*, 3983. Müller, T. E.; Beller, M. *Chem. Rev.* **1998**, *98*, 675.

126. Pez, G. P.; Galle, J. E. *Pure Appl. Chem.* **1985**, *57*, 1917.

127. (a) Johnson, J. S.; Bergman, R. G. *J. Am. Chem. Soc.* **2001**, *123*, 2923. (b) Haak, E.; Siebeneicher, H.; Doye, S. *Org. Lett.*, **2000**, *2*, 1935. (c) Haak, E.; Bytschkov, I.; Doye, S. *Angew. Chem., Int. Ed.* **1999**, *38*, 3389. (d) Siebeneicher, H.; Doye, S. *J. Prak. Chem. – Chem Ztg.* **2000**, *342*, 102. (e) McGrane, P. L.; Livinghouse, T. *J. Am. Chem. Soc.* **1993**, *115*, 11485. (f) Walsh, P. J.; Baranger, A. M.; Bergman, R. G. *J. Am. Chem. Soc.* **1992**, *114*, 1708.

128. (a) Kawatsura, M.; Hartwig, J. F. *J. Am. Chem. Soc.* **2000**, *122*, 9546. (b) Tokunaga, M.; Eckert, M.; Wakatsuki, Y. *Angew. Chem. Int. Ed.* **1999**, *38*, 3222. (c) Beller, M.;

Trauthwein, H.; Eichberger, M.; Breindl, C.; Müller, T. E.; Zapf, A. *J. Organomet. Chem.* **1998**, *566*, 277.

129. Straub, T.; Frank, W.; Reiss, G. J.; Eisen, M. S. *J. Chem. Soc., Dalton Trans.* **1996**, 2541.

130. (a) Molander, G. A.; Dowdy, E. D. *J. Org. Chem.* **1999**, *64*, 6515. (b) Li, Y. W.; Marks, T. J. *J. Am. Chem. Soc.* **1998**, *120*, 1757. (c) Li, Y.; Marks, T. J. *J. Am. Chem. Soc.* **1996**, *118*, 9295.

131. For metallocene-based systems, terminal imines are almost certainly the active species reacting with alkyne. We currently have no evidence for such a species in our system. However, it should be noted that $Ti(NMe_2)_4$ is known to produce isolable bridging imido complexes on reaction with primary amines, see Thorn, D. L.; Nugent, W. A.; Harlow, R. L. *J. Am. Chem. Soc.* **1981**, *103*, 357. Excess of amine during the reactions conditions may support monomeric species for reaction with alkynes.

132. (a) Fairfax, D.; Stein, M.; Livinghouse, T.; Jensen, M. *Organometallics* **1997**, *16*, 1523. (b) McGrane, P. L.; Livinghouse, T. *J. Am. Chem. Soc.* **1993**, *115*, 11485. (c) McGrane, P. L.; Jensen, M.; Livinghouse, T. *J. Am. Chem. Soc.* **1992**, **114**, 5459. (d) McGrane, P. L.; Livinghouse, T. *J. Org. Chem.* **1992**, *57*, 1323.

133. Hill, J. E.; Profilet, R. D.; Fanwick, P. E.; Rothwell, I. P. *Angew. Chem. Int Ed. Eng.* **1990**, *29*, 664.

134. (a) Pohlki, F.; Bytschkov, I.; Siebeneicher, H.; Heutling, A.; Konig, W. A.; Doye, S. *Eur. J. Org. Chem.* **2004**, 1967. (b) Heutling, A.; Pohlki, F.; Doye, S. *Chem.-Eur. J.* **2004**, *10*, 3059. (c) Doye, S. *Synlett* **2004**, 1653. (d) Siebeneicher, H.; Bytschkov, I.; Doye, S. *Angew. Chem. Int. Ed.* **2003**, *42*, 3042. (e) Pohlki, F.; Doye, S. *Chem. Soc. Rev.* **2003**, *32*, 104. (f) Bytschkov, I.; Siebeneicher, H.; Doye, S. *Eur. J. Org. Chem.* **2003**, 2888. (g) Bytschkov, I.; Doye, S. *Eur. J. Org. Chem.* **2003**, 935. (h) Siebeneicher, H.; Doye, S. *Eur. J. Org. Chem.* **2002**, 1213. (i) Pohlki, F.; Heutling, A.; Bytschkov, I.; Hotopp, T.; Doye, S. *Synlett.* **2002**, 799. (j) Heutling, A.; Doye, S. *J. Org. Chem.* **2002**, *67*, 1961. (k) Haak, E.; Bytschkov, I.; Doye, S. *Eur. J. Org. Chem.* **2002**, 457. (l) Bytschkov, T.; Doye, S. *Tetrahedron Lett.* **2002**, *43*, 3715. (m) Bytschkov, I.; Doye, S. *Eur. J. Org. Chem.* **2001**, 4411. (n) Sieibeneicher, H.; Doye, S. *J. Prak. Chem-Chem. Ztg.* **2000**, *342*, 102. (o) Haak, E.; Siebeneicher, H.; Doye, S. *Org. Lett.* **2000**, *2*, 1935. (p) Haak, E.; Bytschkov, I.; Doye, S. *Angew. Chem. Int. Ed. Eng.* **1999**, *38*, 3389.

135. Johnson, J. S.; Bergman, R. G. *J. Am. Chem. Soc.* **2001**, *123*, 2923.

136. Tillack, A.; Castro, I. G.; Hartung, C. G.; Beller, M. *Angew. Chem. Int. Ed.* **2002**, *41*, 2541.

137. Ackermann, L.; Bergman, R. G. *Org. Lett.* **2002,** *4*, 1475.

138. Novak, A.; Blake, A. J.; Wilson, C.; Love, J. B. *Chem. Commun.* **2002**, 2796.

139. Seo, W. S.; Cho, Y. J.; Yoon, S. C.; Park, J. T.; Park, Y. *J. Organomet. Chem.* **2001,** *640*, 79.

140. A possible explanation for the selectivities in this reaction involves synthesis of a metallocyclobutane intermediate due to 1,3-hydrogen shift. Trösch, D. J. M.; Collier, P. E.; Bashall, A.; Gade, L. H.; McPartlin, M.; Mountford, P.; Radojevic, S. *Organometallics* **2001**, *20*, 3308.

141. For other early transition metal cyclotrimerizations of alkynes (a) Strickler, J. R.; Bruck, M. A.; Wigley, D. E. *J. Am. Chem. Soc.* **1990**, *112*, 2814. (b) Smith, D. P.; Strickler, J. R.; Gray, S. D.; Bruck, M. A.; Holmes, R. S.; Wigley, D. E. *Organometallics* **1992**, *11*, 1275. (c) Hartung, J. B.; Pedersen, S. F. *Organometallics* **1990**, *9*, 1414.

142. Benati, L.; Montevecchi, P. C.; Spagnolo, P. *Tetrahedron* **1986**, *42*, 1145.

APPENDIX

COMPLETE CRYSTAL DATA AND STRUCTURE REFINEMENT DATA

Table A-1.1. Crystal data and structure refinement for H_2dpma.

Identification code	jtcat1	
Empirical formula	$C_{11}H_{15}N_3$	
Formula weight	189.26	
Temperature	173 K	
Wavelength	0.71073 Å	
Crystal system	Trigonal	
Space group	P3(1)	
Unit cell dimensions	a = 14.094(4) Å	α= 90°.
	b = 14.094(4) Å	β= 90°.
	c = 9.288(3) Å	γ = 120°.
Volume	1597.7(8) $Å^3$	
Z	6	
Density (calculated)	1.180 Mg/m^3	
Absorption coefficient	0.073 mm^{-1}	
F(000)	612	
Crystal size	0.19 x 0.13 x 0.11 mm^3	
Theta range for data collection	1.67 to 23.30°.	
Index ranges	-15<=h<=15, -15<=k<=15, -10<=l<=8	
Reflections collected	7273	
Independent reflections	2705 [R(int) = 0.1179]	
Completeness to theta = 23.30°	99.7 %	
Absorption correction	Empirical	
Max. and min. transmission	0.9982 and 0.3890	
Refinement method	Full-matrix least-squares on F^2	
Data / restraints / parameters	2705 / 1 / 256	
Goodness-of-fit on F^2	1.097	
Final R indices [I>2sigma(I)]	R1 = 0.0988, wR2 = 0.2636	
R indices (all data)	R1 = 0.1030, wR2 = 0.2664	
Absolute structure parameter	8(7)	
Extinction coefficient	0.026(7)	
Largest diff. peak and hole	0.358 and -0.292 $e.Å^{-3}$	

Table A-1.2. Atomic coordinates (x 10^4) and equivalent isotropic displacement parameters ($Å^2$ x 10^3)for H_2dpma. U(eq) is defined as one third of the trace of the orthogonalized U^{ij} tensor.

	x	y	z	U(eq)		x	y	z	U(eq)
N(1A)	4488(5)	3637(5)	8021(7)	35(2)	N(1B)	5712(5)	8526(5)	-1455(7)	34(2)
N(2A)	5254(5)	6919(5)	4861(8)	38(2)	N(2B)	7450(5)	9279(5)	3487(7)	31(2)
N(3A)	5029(5)	4423(5)	4744(6)	28(1)	N(3B)	7958(5)	10217(5)	106(6)	27(1)
C(11A)	4748(7)	3923(7)	9426(10)	42(2)	C(11B)	4918(6)	7454(6)	-1516(9)	37(2)
C(12A)	5867(7)	4507(7)	9533(10)	46(2)	C(12B)	5411(6)	6821(6)	-1524(9)	35(2)
C(13A)	6294(7)	4570(8)	8163(9)	44(2)	C(13B)	6575(6)	7588(5)	-1470(8)	30(2)
C(14A)	5430(6)	4037(7)	7218(9)	35(2)	C(14B)	6722(6)	8619(6)	-1427(8)	30(2)
C(21A)	4929(6)	7512(6)	3996(11)	41(2)	C(21B)	7643(6)	9662(6)	4883(9)	37(2)
C(22A)	5042(6)	7302(7)	2622(11)	44(2)	C(22B)	8693(7)	10551(7)	4915(10)	44(2)
C(23A)	5481(6)	6562(7)	2633(10)	42(2)	C(23B)	9080(7)	10689(7)	3501(10)	42(2)
C(24A)	5549(6)	6346(6)	4026(10)	38(2)	C(24B)	8313(6)	9885(6)	2633(8)	31(2)
C(31A)	5408(6)	3823(7)	5652(9)	39(2)	C(31B)	7743(6)	9711(6)	-1359(8)	29(2)
C(32A)	5935(6)	5605(6)	4693(9)	37(2)	C(32B)	8305(6)	9617(6)	1095(8)	31(2)
C(33A)	4805(7)	3959(7)	3292(9)	44(2)	C(33B)	8839(7)	11359(7)	-6(10)	45(2)

Table A-1.3. Bond lengths [Å] and angles [°] for H_2dpma.

N(1A)-C(11A)	1.362(11)	N(1B)-C(11B)	1.359(10)
N(1A)-C(14A)	1.374(10)	N(1B)-C(14B)	1.363(9)
N(2A)-C(24A)	1.327(11)	N(2B)-C(24B)	1.342(10)
N(2A)-C(21A)	1.392(11)	N(2B)-C(21B)	1.378(10)
N(3A)-C(33A)	1.462(11)	N(3B)-C(33B)	1.464(10)
N(3A)-C(31A)	1.472(10)	N(3B)-C(32B)	1.486(9)
N(3A)-C(32A)	1.510(9)	N(3B)-C(31B)	1.495(9)
C(11A)-C(12A)	1.369(12)	C(11B)-C(12B)	1.379(11)
C(12A)-C(13A)	1.391(12)	C(12B)-C(13B)	1.445(11)
C(13A)-C(14A)	1.379(11)	C(13B)-C(14B)	1.362(10)
C(14A)-C(31A)	1.483(11)	C(14B)-C(31B)	1.492(10)
C(21A)-C(22A)	1.338(13)	C(21B)-C(22B)	1.381(11)
C(22A)-C(23A)	1.453(13)	C(22B)-C(23B)	1.399(13)
C(23A)-C(24A)	1.344(12)	C(23B)-C(24B)	1.370(11)
C(24A)-C(32A)	1.528(12)	C(24B)-C(32B)	1.475(11)

C(11A)-N(1A)-C(14A)	109.7(7)	C(11B)-N(1B)-C(14B)	110.4(6)
C(24A)-N(2A)-C(21A)	109.0(7)	C(24B)-N(2B)-C(21B)	111.6(6)
C(33A)-N(3A)-C(31A)	109.3(6)	C(33B)-N(3B)-C(32B)	109.3(6)
C(33A)-N(3A)-C(32A)	109.8(6)	C(33B)-N(3B)-C(31B)	108.5(6)
C(31A)-N(3A)-C(32A)	107.6(6)	C(32B)-N(3B)-C(31B)	109.7(5)
N(1A)-C(11A)-C(12A)	107.8(8)	N(1B)-C(11B)-C(12B)	108.5(7)
C(11A)-C(12A)-C(13A)	107.7(8)	C(11B)-C(12B)-C(13B)	105.5(6)
C(14A)-C(13A)-C(12A)	108.1(7)	C(14B)-C(13B)-C(12B)	108.1(6)
N(1A)-C(14A)-C(13A)	106.7(7)	N(1B)-C(14B)-C(13B)	107.5(6)
N(1A)-C(14A)-C(31A)	122.1(7)	N(1B)-C(14B)-C(31B)	121.5(6)
C(13A)-C(14A)-C(31A)	131.1(7)	C(13B)-C(14B)-C(31B)	131.0(7)
C(22A)-C(21A)-N(2A)	107.8(7)	N(2B)-C(21B)-C(22B)	106.7(7)
C(21A)-C(22A)-C(23A)	107.0(7)	C(21B)-C(22B)-C(23B)	105.8(7)
C(24A)-C(23A)-C(22A)	105.9(8)	C(24B)-C(23B)-C(22B)	110.2(7)
N(2A)-C(24A)-C(23A)	110.2(8)	N(2B)-C(24B)-C(23B)	105.6(7)
N(2A)-C(24A)-C(32A)	120.4(8)	N(2B)-C(24B)-C(32B)	121.4(6)
C(23A)-C(24A)-C(32A)	129.4(8)	C(23B)-C(24B)-C(32B)	133.1(8)
N(3A)-C(31A)-C(14A)	115.0(6)	C(14B)-C(31B)-N(3B)	113.0(6)
N(3A)-C(32A)-C(24A)	111.9(6)	C(24B)-C(32B)-N(3B)	114.6(6)

Table A-1.4. Anisotropic displacement parameters ($Å^2$ x 10^3) for H_2dpma.
The anisotropic displacement factor exponent takes the form:
$-2\pi^2[h^2 a^{*2}U^{11} + ... + 2 h k a^* b^* U^{12}]$

	U^{11}	U^{22}	U^{33}	U^{23}	U^{13}	U^{12}
N(1A)	28(3)	42(4)	34(4)	-6(3)	-8(3)	17(3)
N(2A)	30(3)	33(3)	39(4)	-6(3)	3(3)	6(3)
N(3A)	28(3)	30(3)	21(3)	-2(3)	3(3)	12(3)
C(11A)	39(5)	41(4)	40(6)	1(4)	3(4)	15(4)
C(12A)	39(5)	58(6)	40(6)	-5(4)	-9(4)	24(4)
C(13A)	34(4)	68(6)	37(5)	9(4)	-3(4)	31(4)
C(14A)	31(4)	44(4)	31(5)	0(4)	6(4)	20(4)
C(21A)	27(4)	26(4)	63(7)	-1(4)	3(4)	8(3)
C(22A)	27(4)	39(4)	55(6)	8(4)	-16(4)	9(4)
C(23A)	29(4)	36(4)	49(6)	0(4)	-3(4)	7(4)
C(24A)	24(4)	31(4)	43(5)	4(4)	-5(4)	4(3)
C(31A)	37(4)	44(5)	42(5)	1(4)	-3(4)	26(4)
C(32A)	21(4)	39(4)	33(5)	3(3)	1(3)	0(3)
C(33A)	36(4)	52(5)	36(5)	-3(4)	-2(4)	16(4)

N(1B)	34(3)	31(3)	35(4)	4(3)	1(3)	15(3)
N(2B)	24(3)	30(3)	30(4)	-8(3)	-6(3)	7(3)
N(3B)	31(3)	23(3)	30(4)	-2(3)	-5(2)	17(3)
C(11B)	23(4)	35(4)	48(5)	-2(4)	4(3)	12(3)
C(12B)	38(4)	25(4)	46(5)	3(3)	-5(4)	18(3)
C(13B)	36(4)	28(4)	32(4)	4(3)	-4(3)	20(3)
C(14B)	30(4)	36(4)	26(4)	-2(3)	-3(3)	19(3)
C(21B)	30(4)	35(4)	35(5)	2(4)	-1(4)	8(3)
C(22B)	38(5)	42(5)	41(5)	1(4)	-2(4)	10(4)
C(23B)	30(4)	40(5)	43(6)	1(4)	-8(4)	8(4)
C(24B)	28(4)	34(4)	29(4)	-1(3)	-9(3)	15(3)
C(31B)	34(4)	34(4)	20(4)	1(3)	-1(3)	17(3)
C(32B)	30(4)	29(4)	33(4)	-4(3)	-3(3)	15(3)
C(33B)	51(5)	35(4)	42(6)	-4(4)	-1(4)	17(4)

Table A-1.5. Hydrogen coordinates (x 10^4) and isotropic displacement parameters ($Å^2$ x 10^3) for H_2dpma.

	x	y	z	U(eq)		x	y	z	U(eq)
H(1A)	3833	3262	7686	42	H(1B)	5593	9068	-1437	41
H(2A)	5263	6923	5787	46	H(2B)	6851	8720	3199	37
H(11A)	4254	3752	10180	50	H(11B)	4167	7192	-1547	44
H(12A)	6269	4807	10370	55	H(12B)	5068	6060	-1557	42
H(13A)	7033	4912	7925	53	H(13B)	7127	7409	-1466	36
H(21A)	4678	7973	4316	50	H(21B)	7159	9376	5654	44
H(22A)	4872	7576	1813	53	H(22B)	9065	10972	5713	53
H(23A)	5674	6294	1838	51	H(23B)	9761	11246	3193	50
H(31C)	6141	4012	5349	46	H(31A)	7685	10200	-2042	35
H(31D)	4934	3044	5487	46	H(31B)	8360	9629	-1644	35
H(32A)	6541	5660	4134	45	H(32C)	7815	8837	967	37
H(32B)	6197	5855	5662	45	H(32D)	9035	9778	825	37
H(33D)	5452	3985	2913	66	H(33A)	9513	11381	-244	67
H(33E)	4598	4375	2683	66	H(33B)	8919	11722	897	67
H(33F)	4220	3212	3329	66	H(33C)	8663	11721	-745	67

Table A-2.1. Crystal data and structure refinement for H_2dpna.

Identification code	jtc16t	
Empirical formula	$C_{18}H_{23}N_3$	
Formula weight	281.39	
Temperature	173(2) K	
Wavelength	0.71073 Å	
Crystal system	Triclinic	
Space group	P-1	
Unit cell dimensions	a = 7.6219(9) Å	α= 72.509(2)°.
	b = 9.8910(12) Å	β= 83.640(2)°.
	c = 10.9370(13) Å	γ = 77.710(3)°.
Volume	767.41(16) $Å^3$	
Z	2	
Density (calculated)	1.218 Mg/m^3	
Absorption coefficient	0.073 mm^{-1}	
F(000)	304	
Crystal size	0.86 x 0.75 x 0.28 mm^3	
Theta range for data collection	1.95 to 23.27°.	
Index ranges	-8<=h<=8, -8<=k<=10, -11<=l<=12	
Reflections collected	3523	
Independent reflections	2203 [R(int) = 0.0606]	
Completeness to theta = 23.27°	99.6 %	
Absorption correction	Empirical	
Max. and min. transmission	0.8654 and 0.6448	
Refinement method	Full-matrix least-squares on F^2	
Data / restraints / parameters	2203 / 0 / 282	
Goodness-of-fit on F^2	0.949	
Final R indices [I>2sigma(I)]	R1 = 0.0536, wR2 = 0.1209	
R indices (all data)	R1 = 0.1026, wR2 = 0.1394	
Largest diff. peak and hole	0.400 and -0.219 $e.Å^{-3}$	

Table A-2.2. Atomic coordinates (x 10^4) and equivalent isotropic displacement parameters ($Å^2$ x 10^3) for H_2dpna. U(eq) is defined as one third of the trace of the orthogonalized U^{ij} tensor.

	x	y	z	U(eq)		x	y	z	U(eq)
N(1)	4033(3)	3336(3)	4574(2)	28(1)	C(31)	1845(4)	5695(3)	4073(3)	29(1)
N(2)	-883(3)	8973(3)	3511(3)	40(1)	C(32)	2449(4)	8095(3)	3708(3)	31(1)
N(3)	3177(3)	6635(2)	3535(2)	27(1)	C(33)	3652(4)	6715(4)	2165(3)	30(1)
C(11)	4337(4)	2031(3)	4304(3)	33(1)	C(34)	5380(4)	7264(4)	1663(3)	34(1)
C(12)	2996(4)	2053(4)	3574(3)	38(1)	C(35)	5756(5)	7479(5)	198(3)	45(1)
C(13)	1838(4)	3415(4)	3391(3)	34(1)	C(36)	7696(5)	6666(4)	99(3)	53(1)
C(14)	2507(3)	4184(3)	4011(2)	26(1)	C(37)	7555(5)	5100(4)	643(4)	53(1)
C(21)	-2071(5)	9944(4)	2656(3)	45(1)	C(38)	7228(5)	4859(5)	1894(4)	63(1)
C(22)	-1108(5)	10555(4)	1600(4)	50(1)	C(39)	7121(4)	6244(4)	2221(3)	40(1)
C(23)	724(5)	9963(4)	1809(3)	42(1)	C(40)	8508(5)	6895(5)	1181(4)	53(1)
C(24)	839(4)	8977(3)	2997(3)	33(1)					

Table A-2.3. Bond lengths [Å] and angles [°] for H_2dpna.

N(1)-C(14)	1.366(3)	C(22)-C(23)	1.410(5)
N(1)-C(11)	1.376(4)	C(23)-C(24)	1.369(4)
N(2)-C(24)	1.369(4)	C(24)-C(32)	1.490(4)
N(2)-C(21)	1.377(4)	C(33)-C(34)	1.515(4)
N(3)-C(31)	1.478(3)	C(34)-C(39)	1.546(4)
N(3)-C(33)	1.484(4)	C(34)-C(35)	1.554(4)
N(3)-C(32)	1.493(4)	C(35)-C(36)	1.534(5)
C(11)-C(12)	1.358(4)	C(36)-C(40)	1.489(5)
C(12)-C(13)	1.416(4)	C(36)-C(37)	1.506(5)
C(13)-C(14)	1.360(4)	C(37)-C(38)	1.321(5)
C(14)-C(31)	1.491(4)	C(38)-C(39)	1.500(5)
C(21)-C(22)	1.349(5)	C(39)-C(40)	1.552(5)
C(14)-N(1)-C(11)	109.3(3)	N(3)-C(31)-C(14)	112.9(2)
C(24)-N(2)-C(21)	109.6(3)	C(24)-C(32)-N(3)	118.1(2)
C(31)-N(3)-C(33)	111.0(2)	N(3)-C(33)-C(34)	113.8(3)
C(31)-N(3)-C(32)	109.2(2)	C(33)-C(34)-C(39)	115.5(3)
C(33)-N(3)-C(32)	111.6(2)	C(33)-C(34)-C(35)	112.9(3)
C(12)-C(11)-N(1)	107.9(3)	C(39)-C(34)-C(35)	102.1(3)
C(11)-C(12)-C(13)	107.2(3)	C(36)-C(35)-C(34)	103.6(3)

C(14)-C(13)-C(12)	107.9(3)	C(40)-C(36)-C(37)	100.4(3)
C(13)-C(14)-N(1)	107.6(3)	C(40)-C(36)-C(35)	101.7(3)
C(13)-C(14)-C(31)	129.5(3)	C(37)-C(36)-C(35)	104.0(3)
N(1)-C(14)-C(31)	122.9(3)	C(38)-C(37)-C(36)	107.1(4)
C(22)-C(21)-N(2)	107.8(3)	C(37)-C(38)-C(39)	108.6(4)
C(21)-C(22)-C(23)	107.8(3)	C(38)-C(39)-C(34)	107.0(3)
C(24)-C(23)-C(22)	108.0(3)	C(38)-C(39)-C(40)	98.3(3)
C(23)-C(24)-N(2)	106.8(3)	C(34)-C(39)-C(40)	99.1(3)
C(23)-C(24)-C(32)	130.1(3)	C(36)-C(40)-C(39)	94.9(3)
N(2)-C(24)-C(32)	123.0(3)		

Table A-2.4. Anisotropic displacement parameters H_2dpna. The anisotropic displacement factor exponent takes the form: $-2\pi^2[h^2 a^{*2}U^{11} + ... + 2 h k a^* b^* U^{12}]$

	U^{11}	U^{22}	U^{33}	U^{23}	U^{13}	U^{12}
N(1)	33(2)	28(2)	27(1)	-10(1)	-6(1)	-6(1)
N(2)	36(2)	40(2)	41(2)	-13(1)	1(2)	-2(1)
N(3)	26(1)	26(2)	28(1)	-8(1)	1(1)	-5(1)
C(11)	37(2)	26(2)	37(2)	-9(2)	-7(2)	-2(2)
C(12)	50(2)	33(2)	40(2)	-17(2)	-9(2)	-12(2)
C(13)	32(2)	40(2)	32(2)	-10(2)	-10(2)	-5(2)
C(14)	26(2)	28(2)	24(2)	-6(1)	1(1)	-6(2)
C(21)	32(2)	48(2)	58(2)	-26(2)	-11(2)	9(2)
C(22)	57(3)	37(2)	51(2)	-8(2)	-17(2)	4(2)
C(23)	40(2)	34(2)	48(2)	-5(2)	-5(2)	-8(2)
C(24)	31(2)	27(2)	42(2)	-14(2)	-2(2)	-5(2)
C(31)	24(2)	33(2)	29(2)	-8(2)	-1(2)	-6(2)
C(32)	31(2)	27(2)	36(2)	-10(2)	-5(2)	-6(2)
C(33)	28(2)	32(2)	29(2)	-8(2)	-2(1)	-2(2)
C(34)	31(2)	33(2)	36(2)	-10(2)	7(1)	-9(2)
C(35)	40(2)	52(3)	34(2)	-1(2)	2(2)	-10(2)
C(36)	49(2)	70(3)	31(2)	-11(2)	9(2)	-4(2)
C(37)	55(2)	56(3)	56(2)	-29(2)	24(2)	-23(2)
C(38)	39(2)	45(3)	90(3)	-2(2)	5(2)	-3(2)
C(39)	34(2)	54(3)	32(2)	-13(2)	-2(2)	-8(2)
C(40)	26(2)	80(3)	55(2)	-27(2)	7(2)	-11(2)

Table A-2.5. Hydrogen coordinates (x 10^4) and isotropic displacement parameters ($Å^2$ x 10^3) for (H_2dpna).

	x	y	z	U(eq)		x	y	z	U(eq)
H(1)	4680(40)	3520(30)	5090(30)	40(10)	H(39)	7380(40)	6230(30)	3090(30)	43(9)
H(2)	-1190(40)	8490(30)	4300(30)	47(10)	H(31A)	730(30)	6090(30)	3630(20)	22(7)
H(11)	5370(30)	1320(30)	4610(20)	26(8)	H(32A)	2200(30)	7940(30)	4700(20)	26(7)
H(12)	2790(40)	1340(40)	3230(30)	52(10)	H(33A)	3860(30)	5700(30)	2080(20)	31(8)
H(13)	810(30)	3750(30)	2910(20)	17(7)	H(35A)	5580(40)	8520(40)	-290(30)	60(11)
H(21)	-3380(40)	10080(30)	2840(30)	55(10)	H(40A)	9760(40)	6320(40)	1320(30)	61(10)
H(22)	-1640(40)	11260(40)	870(30)	63(11)	H(31B)	1560(30)	5740(30)	4980(30)	28(8)
H(23)	1730(40)	10160(30)	1230(30)	45(10)	H(32B)	3510(30)	8610(30)	3420(20)	26(7)
H(34)	5310(40)	8190(40)	1810(30)	58(11)	H(33B)	2620(30)	7350(30)	1620(20)	30(7)
H(36)	8350(40)	6910(30)	-750(30)	54(10)	H(35B)	5020(50)	7020(40)	-190(30)	79(13)
H(37)	7550(60)	4440(50)	30(40)	130(17)	H(40B)	8400(50)	8010(50)	960(40)	101(16)
H(38)	6920(50)	3870(50)	2520(40)	99(14)					

Table A-3.1. Crystal data and structure refinement for H_2dmpm.

Identification code	jtc51t	
Empirical formula	$C_{22}H_{28}N_4$	
Formula weight	348.48	
Temperature	173(2) K	
Wavelength	0.71073 Å	
Crystal system	Triclinic	
Space group	P-1	
Unit cell dimensions	a = 8.434(3) Å	α= 99.838(7)°.
	b = 9.197(3) Å	β= 95.449(7)°.
	c = 13.232(4) Å	γ = 97.257(7)°.
Volume	996.0(6) Å^3	
Z	2	
Density (calculated)	1.162 Mg/m^3	
Absorption coefficient	0.070 mm^{-1}	
F(000)	376	
Crystal size	0.38 x 0.54 x 0.98 mm^3	
Theta range for data collection	1.57 to 23.29°.	
Index ranges	-9<=h<=7, -9<=k<=10, -14<=l<=13	
Reflections collected	4583	
Independent reflections	2863 [R(int) = 0.0648]	
Completeness to theta = 23.29°	99.3 %	
Absorption correction	None	
Refinement method	Full-matrix least-squares on F^2	
Data / restraints / parameters	2863 / 0 / 348	
Goodness-of-fit on F^2	0.917	
Final R indices [I>2sigma(I)]	R1 = 0.0405, wR2 = 0.0811	
R indices (all data)	R1 = 0.0715, wR2 = 0.0906	
Extinction coefficient	0.052(3)	
Largest diff. peak and hole	0.190 and -0.152 e.Å^{-3}	

Table A-3.2. Atomic coordinates (x 10^4) and equivalent isotropic displacement parameters ($Å^2$ x 10^3)for H_2dmpm. U(eq) is defined as one third of the trace of the orthogonalized U^{ij} tensor.

	x	y	z	U(eq)		x	y	z	U(eq)
N(1A)	1215(2)	2513(2)	8133(2)	31(1)	N(1B)	5141(2)	3726(2)	8660(1)	29(1)
N(2A)	4069(2)	181(2)	7422(1)	32(1)	N(2B)	3262(2)	2812(2)	6101(1)	32(1)
C(11A)	1373(3)	3799(3)	8852(2)	37(1)	C(11B)	6008(3)	2884(2)	9202(2)	32(1)
C(12A)	1748(3)	3457(3)	9793(2)	41(1)	C(12B)	7307(3)	2620(2)	8701(2)	36(1)
C(13A)	1833(3)	1916(3)	9642(2)	36(1)	C(13B)	7232(3)	3316(2)	7831(2)	34(1)
C(14A)	1494(2)	1342(2)	8609(2)	28(1)	C(14B)	5880(2)	4009(2)	7816(1)	27(1)
C(21A)	4839(3)	-163(2)	6570(2)	38(1)	C(21B)	1706(3)	2473(3)	5636(2)	37(1)
C(22A)	3742(3)	-954(2)	5799(2)	42(1)	C(22B)	1018(3)	3736(3)	5802(2)	41(1)
C(23A)	2238(3)	-1088(2)	6191(2)	37(1)	C(23B)	2196(3)	4878(3)	6387(2)	37(1)
C(24A)	2462(3)	-375(2)	7200(2)	29(1)	C(24B)	3576(3)	4280(2)	6571(1)	28(1)
C(31A)	1330(3)	-234(2)	8018(2)	34(1)	C(31B)	5224(2)	4977(2)	7106(1)	30(1)
C(32A)	-409(3)	-714(3)	7489(3)	54(1)	C(32B)	6385(3)	5176(3)	6287(2)	46(1)
C(33A)	1702(4)	-1282(3)	8772(2)	55(1)	C(33B)	5110(4)	6511(3)	7737(2)	44(1)

Table A-3.3. Bond lengths [Å] and angles [°] for H_2dmpm.

N(1A)-C(11A)	1.369(3)	N(1B)-C(11B)	1.372(3)
N(1A)-C(14A)	1.371(2)	N(1B)-C(14B)	1.376(2)
N(2A)-C(21A)	1.364(3)	N(2B)-C(24B)	1.368(2)
N(2A)-C(24A)	1.372(3)	N(2B)-C(21B)	1.370(3)
C(11A)-C(12A)	1.354(3)	C(11B)-C(12B)	1.360(3)
C(12A)-C(13A)	1.409(3)	C(12B)-C(13B)	1.410(3)
C(13A)-C(14A)	1.368(3)	C(13B)-C(14B)	1.375(3)
C(14A)-C(31A)	1.508(3)	C(14B)-C(31B)	1.514(3)
C(21A)-C(22A)	1.350(3)	C(21B)-C(22B)	1.357(3)
C(22A)-C(23A)	1.414(3)	C(22B)-C(23B)	1.415(3)
C(23A)-C(24A)	1.367(3)	C(23B)-C(24B)	1.367(3)
C(24A)-C(31A)	1.510(3)	C(24B)-C(31B)	1.509(3)
C(31A)-C(33A)	1.539(3)	C(31B)-C(33B)	1.531(3)
C(31A)-C(32A)	1.540(3)	C(31B)-C(32B)	1.546(3)
C(11A)-N(1A)-C(14A)	110.0(2)	C(11B)-N(1B)-C(14B)	110.27(19)
C(21A)-N(2A)-C(24A)	110.0(2)	C(24B)-N(2B)-C(21B)	110.27(19)

C(12A)-C(11A)-N(1A)	107.9(2)	C(12B)-C(11B)-N(1B)	107.4(2)
C(11A)-C(12A)-C(13A)	107.3(2)	C(11B)-C(12B)-C(13B)	107.9(2)
C(14A)-C(13A)-C(12A)	108.5(2)	C(14B)-C(13B)-C(12B)	108.09(19)
C(13A)-C(14A)-N(1A)	106.4(2)	C(13B)-C(14B)-N(1B)	106.38(18)
C(13A)-C(14A)-C(31A)	131.4(2)	C(13B)-C(14B)-C(31B)	131.94(18)
N(1A)-C(14A)-C(31A)	122.12(18)	N(1B)-C(14B)-C(31B)	121.62(18)
C(22A)-C(21A)-N(2A)	108.0(2)	C(22B)-C(21B)-N(2B)	107.6(2)
C(21A)-C(22A)-C(23A)	107.4(2)	C(21B)-C(22B)-C(23B)	107.4(2)
C(24A)-C(23A)-C(22A)	108.1(2)	C(24B)-C(23B)-C(22B)	108.2(2)
C(23A)-C(24A)-N(2A)	106.48(19)	C(23B)-C(24B)-N(2B)	106.6(2)
C(23A)-C(24A)-C(31A)	131.8(2)	C(23B)-C(24B)-C(31B)	131.60(19)
N(2A)-C(24A)-C(31A)	121.53(18)	N(2B)-C(24B)-C(31B)	121.66(18)
C(14A)-C(31A)-C(24A)	111.81(16)	C(24B)-C(31B)-C(14B)	110.97(15)
C(14A)-C(31A)-C(33A)	109.37(18)	C(24B)-C(31B)-C(33B)	109.07(19)
C(24A)-C(31A)-C(33A)	108.78(18)	C(14B)-C(31B)-C(33B)	109.41(18)
C(14A)-C(31A)-C(32A)	109.20(18)	C(24B)-C(31B)-C(32B)	109.37(17)
C(24A)-C(31A)-C(32A)	108.58(19)	C(14B)-C(31B)-C(32B)	109.09(19)
C(33A)-C(31A)-C(32A)	109.1(2)	C(33B)-C(31B)-C(32B)	108.9(2)

Table A-3.4. Anisotropic displacement parameters ($Å^2 \times 10^3$) for H_2dmpm.
The anisotropic displacement factor exponent takes the form:
$-2\pi^2[h^2 a^{*2}U^{11} + ... + 2 h k a^* b^* U^{12}]$

	U^{11}	U^{22}	U^{33}	U^{23}	U^{13}	U^{12}
N(1A)	24(1)	34(1)	35(1)	6(1)	5(1)	5(1)
N(2A)	27(1)	32(1)	37(1)	2(1)	6(1)	2(1)
C(11A)	22(1)	31(1)	55(2)	-1(1)	12(1)	2(1)
C(12A)	25(1)	48(2)	44(2)	-8(1)	10(1)	-2(1)
C(13A)	24(1)	48(2)	37(1)	11(1)	8(1)	4(1)
C(14A)	17(1)	34(1)	35(1)	11(1)	7(1)	5(1)
C(21A)	38(2)	34(1)	51(2)	14(1)	18(1)	12(1)
C(22A)	56(2)	37(1)	37(1)	6(1)	19(1)	11(1)
C(23A)	38(2)	31(1)	39(1)	3(1)	1(1)	2(1)
C(24A)	28(1)	24(1)	37(1)	7(1)	5(1)	3(1)
C(31A)	30(1)	32(1)	42(1)	9(1)	11(1)	2(1)
C(32A)	33(2)	46(2)	73(2)	-11(2)	16(2)	-7(1)
C(33A)	75(2)	43(2)	61(2)	25(1)	38(2)	22(2)
N(1B)	19(1)	34(1)	34(1)	9(1)	3(1)	4(1)
N(2B)	31(1)	28(1)	37(1)	7(1)	0(1)	8(1)

C(11B)	28(1)	34(1)	35(1)	12(1)	-1(1)	2(1)
C(12B)	24(1)	37(1)	48(2)	8(1)	-2(1)	8(1)
C(13B)	25(1)	39(1)	40(1)	9(1)	8(1)	4(1)
C(14B)	24(1)	27(1)	29(1)	3(1)	2(1)	-1(1)
C(21B)	34(2)	36(2)	37(1)	10(1)	-5(1)	-1(1)
C(22B)	32(2)	45(2)	46(1)	14(1)	-5(1)	5(1)
C(23B)	39(2)	29(1)	43(1)	6(1)	2(1)	11(1)
C(24B)	30(1)	24(1)	28(1)	6(1)	3(1)	4(1)
C(31B)	29(1)	30(1)	31(1)	9(1)	1(1)	-1(1)
C(32B)	35(2)	56(2)	46(2)	20(1)	1(1)	-7(1)
C(33B)	51(2)	31(1)	46(2)	6(1)	-9(2)	0(1)

Table A-3.5. Hydrogen coordinates (x 10^4) and isotropic displacement parameters ($Å^2$ x 10^3) for H_2dmpm.

	x	y	z	U(eq)		x	y	z	U(eq)
H(1A)	1100(20)	2470(20)	7480(14)	23(6)	H(1B)	4230(30)	3990(20)	8841(16)	48(7)
H(2A)	4490(30)	740(20)	8003(15)	39(7)	H(2B)	3920(30)	2130(20)	6140(15)	44(7)
H(11A)	1250(20)	4720(20)	8620(15)	45(7)	H(11B)	5640(20)	2600(20)	9854(15)	45(6)
H(12A)	1930(20)	4120(20)	10440(15)	38(6)	H(12B)	8100(30)	2050(20)	8939(14)	41(6)
H(13A)	2110(30)	1360(20)	10180(16)	49(7)	H(13B)	8020(30)	3350(20)	7307(14)	46(6)
H(21A)	5990(30)	140(20)	6592(16)	58(7)	H(21B)	1300(30)	1430(20)	5243(14)	47(6)
H(22A)	3920(20)	-1350(20)	5108(15)	36(6)	H(22B)	-50(30)	3820(20)	5531(16)	47(7)
H(23A)	1240(30)	-1550(20)	5814(15)	43(6)	H(23B)	2040(20)	5870(20)	6642(14)	37(6)
H(32A)	-730(30)	-30(30)	6959(18)	72(9)	H(32D)	5990(30)	5850(20)	5855(17)	56(7)
H(32B)	-540(30)	-1750(30)	7097(17)	70(8)	H(32E)	7420(30)	5640(20)	6626(15)	46(7)
H(32C)	-1100(30)	-600(20)	8060(17)	61(7)	H(32F)	6460(30)	4150(30)	5802(17)	61(7)
H(33A)	1590(30)	-2330(30)	8361(17)	66(8)	H(33D)	4450(30)	6500(20)	8323(16)	44(6)
H(33B)	970(30)	-1240(20)	9309(18)	67(8)	H(33E)	4740(30)	7160(30)	7290(18)	62(8)
H(33C)	2910(30)	-960(30)	9163(18)	77(9)	H(33F)	6160(30)	6940(20)	8084(16)	50(7)

Table A-4.1. Crystal data and structure refinement for $Cr(NBu^t)_2(dpma)$

Identification code	$Cr(NBu^t)_2(dpma)$	
Empirical formula	$C_{19}H_{31}CrN_5$	
Formula weight	81.49	
Temperature	173(2) K	
Wavelength	0.71073 Å	
Crystal system	Monoclinic	
Space group	P21/c	
Unit cell dimensions	a = 10.2007(2) Å	α = 90 °
	b = 9.4695(3) Å	β = 94.638(2) °
	c = 21.7312(5) Å	γ = 90 °
Volume	2092.26(9) $Å^3$	
Z	4	
Density (calculated)	1.211 Mg/m^3	
Absorption coefficient	0.557 mm^{-1}	
F(000)	816	
Crystal size	0.53 x 0.26 x 0.26 mm	
Theta range for data collection	1.88 to 28.24 deg.	
Index ranges	-12<=h<=13, -11<=k<=12, -28<=l<=28	
Reflections collected / unique	12878 / 4936 [R(int) = 0.0553]	
Completeness to theta = 28.24	95.1%	
Refinement method	Full-matrix least-squares on F^2	
Data / restraints / parameters	4936 / 0 / 227	
Goodness-of-fit on F^2	0.929	
Final R indices [I>2sigma(I)]	R1 = 0.0433, wR2 = 0.0961	
R indices (all data)	R1 = 0.0853, wR2 = 0.1071	
Extinction coefficient	0.0000(5)	
Largest diff. peak and hole	0.510 and -0.295 $e.A^{-3}$	

Table A-4.2. Atomic coordinates (x 10^4), equivalent isotropic displacement parameters ($Å^2$ x 10^3), and occupancies for $Cr(NBu^t)_2(dpma)$. U(eq) is defined as one third of the trace of the orthogonalized U^{ij} tensor.

	x	y	z	U(eq)		x	y	z	U(eq)
Cr	2216(1)	7791(1)	1209(1)	29(1)	C(11)	-252(2)	5870(3)	1011(1)	43(1)
N(1)	412(2)	7021(2)	1265(1)	37(1)	C(32)	2190(3)	10319(3)	2022(1)	46(1)
N(5)	2914(2)	6261(2)	1143(1)	32(1)	C(33)	1800(3)	8099(3)	2545(1)	46(1)
N(2)	3787(2)	8849(2)	1575(1)	35(1)	C(53)	3079(3)	4338(3)	406(1)	53(1)
N(3)	1487(2)	8939(2)	1976(1)	34(1)	C(52)	4939(2)	4930(3)	1201(1)	49(1)
C(14)	-464(2)	7760(3)	1588(1)	37(1)	C(23)	4762(3)	10700(3)	2069(1)	45(1)
N(4)	2026(2)	8641(2)	550(1)	34(1)	C(12)	-1512(2)	5875(3)	1175(1)	47(1)
C(50)	3429(2)	4853(2)	1067(1)	35(1)	C(31)	39(3)	9102(3)	1868(1)	45(1)
C(24)	3580(3)	10032(2)	1921(1)	39(1)	C(43)	3705(3)	8355(3)	-169(1)	55(1)
C(40)	2305(2)	8822(2)	-94(1)	38(1)	C(42)	1324(3)	7921(4)	-491(1)	66(1)
C(21)	5105(2)	8790(3)	1499(1)	40(1)	C(51)	2843(3)	3887(3)	1534(1)	57(1)
C(13)	-1662(2)	7078(3)	1541(1)	46(1)	C(41)	2127(4)	10393(3)	-248(1)	71(1)
C(22)	5723(3)	9908(3)	1799(1)	45(1)					

Table A-4.3. Bond lengths [Å] and angles [deg] for $Cr(NBu^t)_2(dpma)$

Cr-N(5)	1.6256(18)	C(14)-C(31)	1.482(4)
Cr-N(4)	1.6409(18)	N(4)-C(40)	1.458(3)
Cr-N(1)	1.993(2)	C(50)-C(51)	1.524(3)
Cr-N(2)	1.9994(19)	C(50)-C(53)	1.531(3)
Cr-N(3)	2.1717(18)	C(50)-C(52)	1.546(3)
N(1)-C(14)	1.372(3)	C(24)-C(23)	1.376(3)
N(1)-C(11)	1.375(3)	C(24)-C(32)	1.477(3)
N(5)-C(50)	1.448(3)	C(40)-C(43)	1.517(4)
N(2)-C(21)	1.369(3)	C(40)-C(42)	1.528(4)
N(2)-C(24)	1.375(3)	C(40)-C(41)	1.533(3)
N(3)-C(33)	1.484(3)	C(21)-C(22)	1.370(3)
N(3)-C(31)	1.485(3)	C(13)-C(12)	1.405(4)
N(3)-C(32)	1.490(3)	C(22)-C(23)	1.400(4)
C(14)-C(13)	1.379(3)	C(11)-C(12)	1.362(3)
N(5)-Cr-N(4)	112.48(9)	C(13)-C(14)-C(31)	135.0(2)
N(5)-Cr-N(1)	95.27(8)	C(40)-N(4)-Cr	151.10(16)

N(4)-Cr-N(1)	100.86(9)	N(5)-C(50)-C(51)	108.09(19)
N(5)-Cr-N(2)	98.00(8)	N(5)-C(50)-C(53)	109.94(19)
N(4)-Cr-N(2)	97.83(8)	C(51)-C(50)-C(53)	111.1(2)
N(1)-Cr-N(2)	150.85(8)	N(5)-C(50)-C(52)	107.49(19)
N(5)-Cr-N(3)	133.88(8)	C(51)-C(50)-C(52)	109.9(2)
N(4)-Cr-N(3)	113.64(8)	C(53)-C(50)-C(52)	110.2(2)
N(1)-Cr-N(3)	76.15(8)	N(2)-C(24)-C(23)	109.3(2)
N(2)-Cr-N(3)	75.94(7)	N(2)-C(24)-C(32)	115.0(2)
C(14)-N(1)-C(11)	106.8(2)	C(23)-C(24)-C(32)	135.6(2)
C(14)-N(1)-Cr	119.18(16)	N(4)-C(40)-C(43)	109.10(19)
C(11)-N(1)-Cr	133.89(17)	N(4)-C(40)-C(42)	107.9(2)
C(50)-N(5)-Cr	175.28(16)	C(43)-C(40)-C(42)	110.8(2)
C(21)-N(2)-C(24)	107.14(19)	N(4)-C(40)-C(41)	107.1(2)
C(21)-N(2)-Cr	134.05(15)	C(43)-C(40)-C(41)	110.8(2)
C(24)-N(2)-Cr	118.16(16)	C(42)-C(40)-C(41)	111.0(2)
C(33)-N(3)-C(31)	109.43(18)	N(2)-C(21)-C(22)	109.3(2)
C(33)-N(3)-C(32)	110.16(19)	C(14)-C(13)-C(12)	106.6(2)
C(31)-N(3)-C(32)	112.74(19)	C(21)-C(22)-C(23)	107.6(2)
C(33)-N(3)-Cr	107.90(14)	C(12)-C(11)-N(1)	109.7(2)
C(31)-N(3)-Cr	109.18(14)	C(24)-C(32)-N(3)	106.91(19)
C(32)-N(3)-Cr	107.29(14)	C(24)-C(23)-C(22)	106.7(2)
N(1)-C(14)-C(13)	109.5(2)	C(11)-C(12)-C(13)	107.4(2)
N(1)-C(14)-C(31)	115.4(2)	C(14)-C(31)-N(3)	106.41(19)

Table A-4.4. Anisotropic displacement parameters ($A^2 \times 10^3$) for $Cr(NBu^t)_2(dpma)$. The anisotropic displacement factor exponent takes the form:

$-2\pi^2[h^2 a^{*2} U^{11} + ... + 2 h k a^* b^* U^{12}]$

	U^{11}	U^{22}	U^{33}	U^{23}	U^{13}	U^{12}
Cr	33(1)	25(1)	29(1)	-1(1)	2(1)	1(1)
N(1)	35(1)	39(1)	37(1)	1(1)	5(1)	1(1)
N(5)	29(1)	26(1)	39(1)	-5(1)	1(1)	-3(1)
N(2)	43(1)	26(1)	35(1)	-5(1)	1(1)	-2(1)
N(3)	44(1)	27(1)	33(1)	3(1)	8(1)	5(1)
C(14)	37(1)	41(1)	34(1)	11(1)	6(1)	7(1)
N(4)	38(1)	29(1)	35(1)	2(1)	0(1)	-3(1)
C(50)	41(1)	22(1)	41(1)	-1(1)	0(1)	2(1)
C(24)	54(2)	28(1)	34(1)	-4(1)	4(1)	-1(1)

C(40)	50(2)	32(1)	31(1)	3(1)	5(1)	5(1)
C(21)	37(2)	34(1)	47(1)	-5(1)	-2(1)	1(1)
C(13)	33(1)	61(2)	45(1)	25(1)	7(1)	7(1)
C(22)	41(2)	43(2)	49(2)	0(1)	-9(1)	-9(1)
C(11)	40(2)	49(2)	42(1)	-6(1)	2(1)	-9(1)
C(32)	63(2)	27(1)	50(2)	-9(1)	13(1)	2(1)
C(33)	63(2)	44(2)	31(1)	5(1)	7(1)	-2(1)
C(53)	66(2)	41(2)	52(2)	-15(1)	-4(1)	4(1)
C(52)	44(2)	38(2)	63(2)	-11(1)	-3(1)	11(1)
C(23)	62(2)	30(1)	40(1)	-7(1)	-6(1)	-12(1)
C(12)	37(2)	55(2)	47(2)	10(1)	-6(1)	-9(1)
C(31)	49(2)	38(2)	51(2)	7(1)	16(1)	13(1)
C(43)	56(2)	62(2)	50(2)	12(1)	17(1)	12(2)
C(42)	74(2)	80(2)	42(2)	-13(2)	-7(1)	-6(2)
C(51)	63(2)	40(2)	68(2)	19(1)	1(2)	-3(1)
C(41)	111(3)	42(2)	63(2)	22(2)	26(2)	18(2)

Table A-4.5. Hydrogen coordinates (x 10^4), isotropic displacement parameters (A^2 x 10^3), and occupancies for $Cr(NBu^t)_2(dpma)$.

	x	y	z	U(eq)		x	y	z	U(eq)
H(21A)	5517	8100	1279	48	H(12A)	-2156	5205	1065	56
H(13A)	-2421	7360	1717	55	H(31A)	-348	9276	2254	54
H(22A)	6619	10105	1820	54	H(31B)	-175	9887	1591	54
H(11A)	106	5191	765	52	H(43A)	3800	7375	-62	83
H(32A)	1811	10969	1711	55	H(43B)	4302	8907	98	83
H(32B)	2122	10735	2426	55	H(43C)	3899	8488	-590	83
H(33A)	1496	8591	2892	69	H(42A)	1461	6942	-390	99
H(33B)	2735	7965	2608	69	H(42B)	1450	8068	-919	99
H(33C)	1374	7196	2503	69	H(42C)	444	8186	-413	99
H(53A)	3456	4964	121	80	H(51A)	1906	3851	1450	86
H(53B)	2140	4324	323	80	H(51B)	3054	4248	1943	86
H(53C)	3421	3403	359	80	H(51C)	3202	2955	1503	86
H(52A)	5299	5556	911	73	H(41A)	2756	10937	5	106
H(52B)	5310	4005	1163	73	H(41B)	1253	10682	-170	106
H(52C)	5147	5277	1612	73	H(41C)	2260	10545	-675	106
H(23A)	4895	11518	2302	53					

Table A-5.1. Crystal data and structure refinement for $Mo(dpma)(NBu^t)_2$.

Identification code	alo2m	
Empirical formula	$C_{19}H_{31}MoN_5$	
Formula weight	425.43	
Temperature	173(2) K	
Wavelength	0.71073 Å	
Crystal system	Monoclinic	
Space group	P2(1)/n	
Unit cell dimensions	a = 9.451(5) Å	α= 90°
	b = 10.175(5) Å	β= 93.569(9)°
	c = 22.217(11) Å	γ = 90°
Volume	2132.4(17) $Å^3$	
Z	4	
Density (calculated)	1.325 Mg/m^3	
Absorption coefficient	0.626 mm^{-1}	
F(000)	888	
Crystal size	0.42 x 0.23 x 0.11 mm	
Theta range for data collection	1.84 to 23.32°	
Index ranges	-10<=h<=10, -7<=k<=11, -24<=l<=24	
Reflections collected	9490	
Independent reflections	3082 [R(int) = 0.3237]	
Completeness to theta = 23.32°	99.5 %	
Absorption correction	None	
Refinement method	Full-matrix least-squares on F^2	
Data / restraints / parameters	3082 / 0 / 227	
Goodness-of-fit on F^2	0.931	
Final R indices [I>2sigma(I)]	R1 = 0.0723, wR2 = 0.1020	
R indices (all data)	R1 = 0.1697, wR2 = 0.1225	
Extinction coefficient	0.0000(3)	
Largest diff. peak and hole	0.550 and -0.580 $e.Å^{-3}$	

Table A-5.2. Atomic coordinates (x 10^4) and equivalent isotropic displacement parameters ($Å^2$ x 10^3) for Mo(dpma)$(NBu^t)_2$. U(eq) is defined as one third of the trace of the orthogonalized U^{ij} tensor.

	x	y	z	U(eq)		x	y	z	U(eq)
Mo	9029(1)	8510(1)	1426(1)	27(1)	C(24)	6234(9)	8680(9)	719(4)	38(2)
N(1)	9194(7)	8822(6)	2347(3)	34(2)	C(31)	7286(11)	10402(8)	2174(4)	57(3)
N(2)	7492(7)	7913(6)	780(3)	28(2)	C(32)	6158(10)	9818(8)	1131(4)	45(3)
N(3)	6879(7)	9379(6)	1711(3)	36(2)	C(33)	6007(10)	8380(9)	2008(4)	56(3)
N(4)	9768(7)	9943(5)	1166(3)	31(2)	C(40)	10896(9)	10821(8)	1009(4)	30(2)
N(5)	10220(7)	7221(5)	1401(3)	27(2)	C(41)	11786(11)	11131(8)	1587(4)	65(3)
C(11)	10065(9)	8334(8)	2830(4)	41(2)	C(42)	10185(11)	12097(7)	752(4)	54(3)
C(12)	9687(11)	8834(9)	3357(4)	58(3)	C(43)	11810(9)	10185(7)	538(4)	44(2)
C(13)	8610(12)	9738(9)	3220(4)	56(3)	C(50)	11400(9)	6270(7)	1378(4)	32(2)
C(14)	8334(11)	9718(8)	2605(4)	48(3)	C(51)	12770(9)	6925(7)	1603(4)	48(3)
C(21)	7295(11)	6868(8)	394(3)	41(2)	C(52)	11469(10)	5828(8)	734(4)	49(3)
C(22)	5971(11)	6948(10)	109(4)	53(3)	C(53)	11053(10)	5111(7)	1782(4)	46(3)
C(23)	5309(11)	8063(10)	313(4)	56(3)					

Table A-5.3. Bond lengths [Å] and angles [°] for Mo(dpma)$(NBu^t)_2$.

Mo-N(4)	1.731(6)	C(11)-C(12)	1.346(11)
Mo-N(5)	1.732(6)	C(12)-C(13)	1.392(12)
Mo-N(1)	2.066(6)	C(13)-C(14)	1.375(11)
Mo-N(2)	2.069(6)	C(14)-C(31)	1.504(12)
Mo-N(3)	2.339(7)	C(21)-C(22)	1.369(12)
N(1)-C(14)	1.370(10)	C(22)-C(23)	1.385(12)
N(1)-C(11)	1.402(9)	C(23)-C(24)	1.369(11)
N(2)-C(21)	1.372(8)	C(24)-C(32)	1.481(11)
N(2)-C(24)	1.422(10)	C(40)-C(41)	1.523(10)
N(3)-C(33)	1.487(10)	C(40)-C(43)	1.541(11)
N(3)-C(32)	1.488(10)	C(40)-C(42)	1.555(10)
N(3)-C(31)	1.498(10)	C(50)-C(52)	1.505(11)
N(4)-C(40)	1.450(10)	C(50)-C(51)	1.513(11)
N(5)-C(50)	1.480(9)	C(50)-C(53)	1.530(10)
N(4)-Mo-N(5)	110.5(3)	C(52)-C(50)-C(51)	111.0(7)
N(4)-Mo-N(1)	101.2(3)	N(5)-C(50)-C(53)	107.1(7)

N(5)-Mo-N(1)	98.0(3)	C(52)-C(50)-C(53)	110.5(6)
N(4)-Mo-N(2)	107.2(3)	C(51)-C(50)-C(53)	110.9(6)
N(5)-Mo-N(2)	100.6(3)	C(40)-N(4)-Mo	156.5(6)
N(1)-Mo-N(2)	137.6(3)	C(50)-N(5)-Mo	171.6(5)
N(4)-Mo-N(3)	98.5(3)	C(12)-C(11)-N(1)	111.0(8)
N(5)-Mo-N(3)	150.8(3)	C(11)-C(12)-C(13)	106.8(8)
N(1)-Mo-N(3)	71.8(3)	C(14)-C(13)-C(12)	107.4(9)
N(2)-Mo-N(3)	73.4(3)	N(1)-C(14)-C(13)	110.2(8)
C(14)-N(1)-C(11)	104.5(7)	N(1)-C(14)-C(31)	115.2(8)
C(14)-N(1)-Mo	120.4(5)	C(13)-C(14)-C(31)	134.5(9)
C(11)-N(1)-Mo	135.1(6)	C(22)-C(21)-N(2)	109.2(8)
C(21)-N(2)-C(24)	106.5(7)	C(21)-C(22)-C(23)	108.4(8)
C(21)-N(2)-Mo	136.4(6)	C(24)-C(23)-C(22)	107.9(9)
C(24)-N(2)-Mo	116.9(5)	C(23)-C(24)-N(2)	107.9(8)
C(33)-N(3)-C(32)	110.7(7)	C(23)-C(24)-C(32)	135.4(9)
C(33)-N(3)-C(31)	107.2(7)	N(2)-C(24)-C(32)	116.2(7)
C(32)-N(3)-C(31)	118.1(6)	N(3)-C(31)-C(14)	104.3(6)
C(33)-N(3)-Mo	112.1(5)	C(24)-C(32)-N(3)	105.2(6)
C(32)-N(3)-Mo	103.8(5)	N(4)-C(40)-C(41)	107.5(7)
C(31)-N(3)-Mo	104.9(5)	N(4)-C(40)-C(43)	110.9(6)
C(43)-C(40)-C(42)	110.4(7)	C(41)-C(40)-C(43)	110.8(8)
N(5)-C(50)-C(52)	107.8(6)	N(4)-C(40)-C(42)	107.2(7)
N(5)-C(50)-C(51)	109.4(6)	C(41)-C(40)-C(42)	109.9(6)

Table A-5.4. Anisotropic displacement parameters ($Å^2 \times 10^3$) for Mo(dpma)$(NBu^t)_2$. The anisotropic displacement factor exponent takes the form:

$-2\pi^2[\, h^2 a^{*2} U^{11} + \ldots + 2\, h\, k\, a^*\, b^*\, U^{12}\,]$

	U^{11}	U^{22}	U^{33}	U^{23}	U^{13}	U^{12}
Mo	30(1)	24(1)	25(1)	0(1)	-2(1)	1(1)
N(1)	47(5)	28(4)	27(4)	-3(3)	10(4)	8(3)
N(2)	27(4)	35(4)	24(4)	-1(3)	8(3)	-8(3)
N(3)	32(5)	15(4)	60(5)	-15(4)	1(4)	3(3)
N(4)	31(5)	30(4)	32(4)	2(3)	-8(3)	-7(3)
N(5)	26(4)	29(4)	25(4)	0(3)	-13(3)	-3(3)
C(11)	41(6)	47(6)	34(5)	8(5)	-11(4)	-5(5)
C(12)	88(9)	66(7)	19(5)	-3(5)	-5(5)	10(6)
C(13)	74(9)	75(7)	20(6)	-7(5)	10(5)	6(6)

C(14)	58(7)	45(6)	41(6)	3(5)	0(5)	5(5)
C(21)	63(7)	41(6)	20(5)	-1(4)	3(5)	-8(5)
C(22)	55(8)	86(8)	18(5)	-10(5)	-5(5)	-38(6)
C(23)	35(6)	104(9)	29(5)	-7(6)	-2(5)	-4(6)
C(24)	31(6)	55(6)	29(5)	8(5)	0(4)	1(5)
C(31)	65(8)	44(6)	64(7)	-15(5)	17(6)	3(5)
C(32)	30(6)	49(6)	55(6)	14(5)	1(5)	13(4)
C(33)	50(7)	74(7)	45(6)	-11(6)	15(5)	4(6)
C(40)	32(6)	33(5)	25(5)	4(4)	-1(4)	-10(4)
C(41)	73(8)	71(7)	47(6)	-3(5)	-23(6)	-36(6)
C(42)	78(8)	33(5)	51(6)	10(5)	2(6)	-4(5)
C(43)	44(7)	46(6)	43(6)	3(5)	7(5)	-11(5)
C(50)	28(5)	28(5)	40(5)	-1(4)	4(4)	6(4)
C(51)	42(7)	41(6)	62(7)	10(4)	-3(5)	3(4)
C(52)	56(7)	51(6)	42(6)	-7(5)	17(5)	18(5)
C(53)	50(7)	32(5)	56(6)	5(5)	10(5)	6(4)

Table A-5.5. Hydrogen coordinates (x 10^4) and isotropic displacement parameters ($Å^2$ x 10^3) for Mo(dpma)$(NBu^t)_2$.

	x	y	z	U(eq)		x	y	z	U(eq)
H(11A)	10805	7743	2791	49	H(42A)	9620	12483	1050	81
H(12A)	10072	8617	3740	70	H(42B)	9592	11889	398	81
H(13A)	8160	10260	3494	67	H(42C)	10905	12709	648	81
H(21A)	7955	6210	335	49	H(43A)	12241	9399	703	66
H(22A)	5583	6354	-174	64	H(43B)	12535	10790	434	66
H(23A)	4397	8343	194	67	H(43C)	11223	9970	184	66
H(31A)	6466	10694	2380	69	H(51A)	12967	7648	1344	72
H(31B)	7717	11156	1991	69	H(51B)	13531	6300	1603	72
H(32A)	5180	10053	1186	54	H(51C)	12680	7242	2006	72
H(32B)	6639	10573	972	54	H(52A)	11687	6566	487	73
H(33A)	5137	8775	2117	84	H(52B)	10571	5465	594	73
H(33B)	6522	8057	2363	84	H(52C)	12193	5172	710	73
H(33C)	5801	7665	1734	84	H(53A)	10182	4710	1631	69
H(41A)	12221	10338	1743	97	H(53B)	10955	5418	2185	69
H(41B)	11190	11493	1879	97	H(53C)	11805	4476	1782	69
H(41C)	12508	11755	1502	97					

Table A-6.1. Crystal data and structure refinement for $W(dpma)(NBu^t)_2$.

Identification code	alo	
Empirical formula	$C_{19}H_{31}N_5W$	
Formula weight	513.34	
Temperature	173(2) K	
Wavelength	0.71073 Å	
Crystal system	Monoclinic	
Space group	P2(1)/n	
Unit cell dimensions	a = 9.4181(11) Å	α= 90°
	b = 10.2171(12) Å	β= 93.271(2)°
	c = 22.190(3) Å	γ = 90°
Volume	2131.8(4) $Å^3$	
Z	4	
Density (calculated)	1.599 Mg/m^3	
Absorption coefficient	5.429 mm^{-1}	
F(000)	1016	
Crystal size	0.43 x 0.25 x 0.19 mm^3	
Theta range for data collection	1.84 to 23.26°	
Index ranges	-9<=h<=10, -10<=k<=11, -20<=l<=24	
Reflections collected	9456	
Independent reflections	3074 [R(int) = 0.0355]	
Completeness to theta = 23.26°	99.9 %	
Absorption correction	Empirical	
Max. and min. transmission	1.0000 and 0.5215	
Refinement method	Full-matrix least-squares on F^2	
Data / restraints / parameters	3074 / 0 / 227	
Goodness-of-fit on F^2	1.090	
Final R indices [I>2sigma(I)]	R1 = 0.0192, wR2 = 0.0466	
R indices (all data)	R1 = 0.0212, wR2 = 0.0473	
Extinction coefficient	0.00089(11)	
Largest diff. peak and hole	0.690 and -0.368 $e.Å^{-3}$	

Table A-6.2. Atomic coordinates (x 10^4) and equivalent isotropic displacement parameters ($Å^2$ x 10^3) for W(dpma)$(NBu^t)_2$. U(eq) is defined as one third of the trace of the orthogonalized U^{ij} tensor.

	x	y	z	U(eq)		x	y	z	U(eq)
W	4007(1)	6522(1)	1438(1)	20(1)	C(24)	1230(4)	6326(4)	718(2)	29(1)
N(1)	4190(3)	6219(3)	2358(1)	25(1)	C(31)	1148(4)	5204(4)	1147(2)	33(1)
N(2)	2461(3)	7069(3)	786(1)	24(1)	C(32)	2261(4)	4662(4)	2186(2)	32(1)
N(3)	1862(3)	5675(3)	1725(1)	25(1)	C(33)	950(4)	6672(4)	2001(2)	33(1)
N(4)	4758(3)	5084(3)	1171(1)	24(1)	C(40)	5870(4)	4171(4)	1010(2)	28(1)
N(5)	5194(3)	7845(3)	1412(1)	23(1)	C(41)	6752(5)	3853(5)	1587(2)	51(1)
C(11)	5032(4)	6737(4)	2826(2)	31(1)	C(42)	6793(4)	4785(4)	547(2)	37(1)
C(12)	4670(5)	6204(4)	3358(2)	42(1)	C(43)	5127(5)	2939(4)	752(2)	46(1)
C(13)	3575(5)	5293(4)	3229(2)	41(1)	C(50)	6354(4)	8774(4)	1375(2)	26(1)
C(14)	3305(4)	5305(4)	2616(2)	30(1)	C(51)	7739(4)	8110(4)	1590(2)	38(1)
C(21)	2288(4)	8116(4)	402(2)	30(1)	C(52)	6072(4)	9943(4)	1782(2)	38(1)
C(22)	982(5)	8049(5)	104(2)	40(1)	C(53)	6422(5)	9210(5)	719(2)	45(1)
C(23)	305(4)	6912(5)	307(2)	38(1)					

Table A-6.3. Bond lengths [Å] and angles [°] for W(dpma)$(NBu^t)_2$.

W-N(4)	1.748(3)	C(11)-C(12)	1.361(6)
W-N(5)	1.757(3)	C(12)-C(13)	1.407(6)
W-N(1)	2.063(3)	C(13)-C(14)	1.369(5)
W-N(2)	2.070(3)	C(14)-C(32)	1.484(5)
W-N(3)	2.321(3)	C(21)-C(22)	1.365(6)
N(1)-C(11)	1.375(5)	C(22)-C(23)	1.411(6)
N(1)-C(14)	1.397(5)	C(23)-C(24)	1.364(6)
N(2)-C(21)	1.371(5)	C(24)-C(31)	1.495(5)
N(2)-C(24)	1.387(5)	C(40)-C(42)	1.519(5)
N(3)-C(32)	1.487(5)	C(40)-C(41)	1.522(6)
N(3)-C(33)	1.487(5)	C(40)-C(43)	1.535(6)
N(3)-C(31)	1.494(5)	C(50)-C(51)	1.523(6)
N(4)-C(40)	1.462(5)	C(50)-C(53)	1.526(5)
N(5)-C(50)	1.453(5)	C(50)-C(52)	1.530(5)
N(4)-W-N(5)	111.40(14)	C(11)-C(12)-C(13)	107.8(4)
N(4)-W-N(1)	101.33(12)	C(14)-C(13)-C(12)	106.7(4)

N(5)-W-N(1)	97.53(12)	C(13)-C(14)-N(1)	109.4(4)
N(4)-W-N(2)	105.80(13)	C(13)-C(14)-C(32)	135.5(4)
N(5)-W-N(2)	101.10(12)	N(1)-C(14)-C(32)	114.9(3)
N(1)-W-N(2)	138.42(11)	N(2)-C(21)-C(22)	109.5(4)
N(4)-W-N(3)	98.89(12)	C(21)-C(22)-C(23)	107.3(4)
N(5)-W-N(3)	149.51(12)	C(24)-C(23)-C(22)	106.9(4)
N(1)-W-N(3)	72.36(11)	C(23)-C(24)-N(2)	109.3(4)
N(2)-W-N(3)	72.78(11)	C(23)-C(24)-C(31)	135.1(4)
C(11)-N(1)-C(14)	106.3(3)	N(2)-C(24)-C(31)	115.1(3)
C(11)-N(1)-W	134.5(3)	N(3)-C(31)-C(24)	105.2(3)
C(14)-N(1)-W	119.2(2)	C(14)-C(32)-N(3)	105.5(3)
C(21)-N(2)-C(24)	106.9(3)	N(4)-C(40)-C(42)	110.3(3)
C(21)-N(2)-W	134.3(3)	N(4)-C(40)-C(41)	107.1(3)
C(24)-N(2)-W	118.6(2)	C(42)-C(40)-C(41)	110.6(4)
C(32)-N(3)-C(33)	108.8(3)	N(4)-C(40)-C(43)	107.3(3)
C(32)-N(3)-C(31)	116.8(3)	C(42)-C(40)-C(43)	110.6(3)
C(33)-N(3)-C(31)	109.4(3)	C(41)-C(40)-C(43)	110.8(4)
C(32)-N(3)-W	105.0(2)	N(5)-C(50)-C(51)	108.9(3)
C(33)-N(3)-W	112.9(2)	N(5)-C(50)-C(53)	108.5(3)
C(31)-N(3)-W	103.9(2)	C(51)-C(50)-C(53)	110.3(3)
C(40)-N(4)-W	158.2(3)	N(5)-C(50)-C(52)	108.7(3)
C(50)-N(5)-W	170.4(3)	C(51)-C(50)-C(52)	109.7(3)
C(12)-C(11)-N(1)	109.8(4)	C(53)-C(50)-C(52)	110.7(3)

Table A-6.4. Anisotropic displacement parameters ($Å^2$ x 10^3) for $W(dpma)(NBu^t)_2$.

The anisotropic displacement factor exponent takes the form:

$-2\pi^2[\, h^2\, a^{*2} U^{11} + \ldots + 2\, h\, k\, a^*\, b^*\, U^{12}\,]$

	U^{11}	U^{22}	U^{33}	U^{23}	U^{13}	U^{12}
W	20(1)	19(1)	21(1)	1(1)	1(1)	0(1)
N(1)	29(2)	26(2)	20(2)	-2(1)	2(1)	2(1)
N(2)	23(2)	29(2)	20(2)	0(1)	1(1)	5(1)
N(3)	23(2)	24(2)	29(2)	6(1)	5(1)	-3(1)
N(4)	26(2)	23(2)	25(2)	4(1)	2(1)	0(1)
N(5)	26(2)	25(2)	18(2)	2(1)	1(1)	1(1)
C(11)	35(2)	34(2)	25(2)	-3(2)	-3(2)	3(2)
C(12)	54(3)	44(3)	27(2)	0(2)	-2(2)	6(2)
C(13)	57(3)	41(3)	26(2)	10(2)	10(2)	13(2)

C(14)	33(2)	25(2)	33(2)	5(2)	6(2)	4(2)
C(21)	38(2)	32(2)	19(2)	2(2)	1(2)	7(2)
C(22)	43(3)	55(3)	19(2)	3(2)	-4(2)	15(2)
C(23)	25(2)	60(3)	27(2)	-6(2)	-2(2)	3(2)
C(24)	21(2)	41(2)	26(2)	-5(2)	1(2)	-5(2)
C(31)	25(2)	39(2)	35(2)	-6(2)	1(2)	-10(2)
C(32)	32(2)	26(2)	40(2)	7(2)	8(2)	-1(2)
C(33)	29(2)	39(2)	31(2)	3(2)	8(2)	1(2)
C(40)	32(2)	23(2)	28(2)	-2(2)	-3(2)	10(2)
C(41)	57(3)	54(3)	39(3)	3(2)	-10(2)	27(2)
C(42)	33(2)	36(2)	43(2)	-7(2)	5(2)	6(2)
C(43)	61(3)	22(2)	55(3)	-4(2)	3(2)	5(2)
C(50)	27(2)	21(2)	30(2)	0(2)	4(2)	-5(2)
C(51)	30(2)	34(2)	52(3)	-8(2)	2(2)	-5(2)
C(52)	36(2)	27(2)	51(3)	-6(2)	5(2)	-4(2)
C(53)	51(3)	45(3)	39(3)	9(2)	10(2)	-18(2)

Table A-6.5. Hydrogen coordinates (x 10^4) and isotropic displacement parameters ($Å^2$ x 10^3) for W(dpma)(NBu^t)$_2$.

	x	y	z	U(eq)		x	y	z	U(eq)
H(11A)	5743	7357	2785	37	H(42A)	7233	5562	713	55
H(12A)	5074	6407	3739	50	H(42B)	6214	5005	191	55
H(13A)	3122	4780	3507	49	H(42C)	7514	4174	443	55
H(21A)	2958	8770	353	36	H(43A)	4590	3157	385	69
H(22A)	608	8643	-180	47	H(43B)	4499	2598	1039	69
H(23A)	-600	6618	184	45	H(43C)	5828	2290	669	69
H(31A)	165	4973	1204	39	H(51A)	7917	7382	1331	58
H(31B)	1634	4444	997	39	H(51B)	7665	7803	1996	58
H(32A)	1432	4377	2391	39	H(51C)	8507	8725	1578	58
H(32B)	2684	3909	2000	39	H(52A)	6065	9655	2193	57
H(33A)	80	6271	2111	49	H(52B)	5167	10322	1662	57
H(33B)	739	7361	1715	49	H(52C)	6806	10585	1745	57
H(33C)	1442	7029	2354	49	H(53A)	6593	8464	470	67
H(41A)	7208	4635	1741	76	H(53B)	7180	9830	688	67
H(41B)	7461	3214	1503	76	H(53C)	5536	9610	586	67
H(41C)	6145	3510	1882	76					

Table A-7.1. Crystal data and structure refinement for $Mo(dpma)(Ndip)_2$.

Identification code	jtc11	
Empirical formula	$C_{35}H_{47}MoN_5$	
Formula weight	633.72	
Temperature	173(2) K	
Wavelength	0.71073 Å	
Crystal system	Orthorhombic	
Space group	Fdd2	
Unit cell dimensions	a = 19.415(5) Å	α= 90°
	b = 61.473(17) Å	β= 90°
	c = 11.280(3) Å	γ = 90°
Volume	13463(6) $Å^3$	
Z	16	
Density (calculated)	1.251 Mg/m^3	
Absorption coefficient	0.419 mm^{-1}	
F(000)	5344	
Crystal size	0.25 x 0.25 x 0.11 mm^3	
Theta range for data collection	1.32 to 23.33°.	
Index ranges	-19<=h<=21, -67<=k<=68, -12<=l<=12	
Reflections collected	15135	
Independent reflections	4654 [R(int) = 0.0921]	
Completeness to theta = 23.33°	99.6 %	
Absorption correction	None	
Max. and min. transmission	0.9553 and 0.9024	
Refinement method	Full-matrix least-squares on F^2	
Data / restraints / parameters	4654 / 1 / 379	
Goodness-of-fit on F^2	0.977	
Final R indices [I>2sigma(I)]	R1 = 0.0431, wR2 = 0.0886	
R indices (all data)	R1 = 0.0673, wR2 = 0.0953	
Absolute structure parameter	0.06(5)	
Largest diff. peak and hole	0.318 and -0.493 $e.Å^{-3}$	

Table A-7.2. Atomic coordinates (x 10^4) and equivalent isotropic displacement parameters ($Å^2$ x 10^3) for Mo(dpma)(Ndip)$_2$. U(eq) is defined as one third of the trace of the orthogonalized U^{ij} tensor.

	x	y	z	U(eq)		x	y	z	U(eq)
Mo(1)	3194(1)	508(1)	8050(1)	22(1)	C(45)	981(4)	497(1)	10776(6)	42(2)
N(1)	4160(3)	492(1)	8820(4)	25(1)	C(46)	1434(3)	457(1)	9855(6)	29(2)
N(2)	2659(3)	405(1)	6558(5)	26(1)	C(51)	3286(3)	1014(1)	7674(5)	26(2)
N(3)	3698(2)	190(1)	7439(4)	22(1)	C(52)	2817(3)	1153(1)	8266(6)	30(2)
N(5)	3215(2)	786(1)	7815(5)	26(1)	C(53)	2904(4)	1374(1)	8089(8)	50(2)
N(4)	2632(3)	441(1)	9208(4)	24(1)	C(54)	3425(5)	1452(1)	7368(8)	60(3)
C(11)	4554(3)	643(1)	9440(6)	37(2)	C(55)	3881(4)	1316(1)	6838(7)	50(2)
C(12)	5054(3)	536(1)	10056(6)	35(2)	C(56)	3833(4)	1096(1)	6969(6)	33(2)
C(13)	4987(3)	313(1)	9819(6)	30(2)	C(421)	3138(4)	568(1)	11518(6)	49(2)
C(14)	4435(3)	290(1)	9059(5)	25(2)	C(422)	3327(6)	790(1)	11954(12)	130(5)
C(21)	2198(4)	499(1)	5800(6)	32(2)	C(423)	3380(4)	404(1)	12398(11)	97(4)
C(22)	1926(3)	344(1)	5079(6)	38(2)	C(461)	1200(3)	390(1)	8648(6)	38(2)
C(23)	2227(3)	142(1)	5393(7)	41(2)	C(462)	1220(4)	145(1)	8506(7)	72(3)
C(24)	2671(3)	187(1)	6295(5)	24(2)	C(463)	486(4)	470(1)	8341(8)	73(3)
C(31)	4083(3)	101(1)	8479(5)	23(2)	C(521)	2241(4)	1060(1)	9003(7)	41(2)
C(32)	3129(3)	48(1)	7013(5)	29(2)	C(522)	1598(4)	1032(2)	8258(9)	84(3)
C(33)	4188(3)	236(1)	6464(6)	39(2)	C(523)	2092(4)	1196(1)	10123(7)	61(2)
C(41)	2140(4)	482(1)	10107(6)	28(2)	C(561)	4324(4)	943(1)	6361(7)	44(2)
C(42)	2379(4)	544(1)	11249(6)	38(2)	C(562)	4007(5)	867(1)	5169(6)	67(3)
C(43)	1885(4)	583(1)	12124(6)	43(2)	C(563)	5037(4)	1042(1)	6111(8)	66(3)
C(44)	1205(4)	559(1)	11899(6)	44(2)					

Table A-7.3. Bond lengths [Å] and angles [°] for Mo(dpma)(Ndip)$_2$.

Mo(1)-N(5)	1.728(4)	C(41)-C(42)	1.421(9)
Mo(1)-N(4)	1.751(5)	C(42)-C(43)	1.398(9)
Mo(1)-N(1)	2.070(5)	C(42)-C(421)	1.510(10)
Mo(1)-N(2)	2.076(5)	C(43)-C(44)	1.353(9)
Mo(1)-N(3)	2.290(5)	C(44)-C(45)	1.394(10)
N(1)-C(14)	1.377(7)	C(45)-C(46)	1.382(9)
N(1)-C(11)	1.388(8)	C(46)-C(461)	1.494(9)
N(2)-C(21)	1.367(8)	C(51)-C(52)	1.415(8)
N(2)-C(24)	1.367(7)	C(51)-C(56)	1.418(8)

N(3)-C(33)	1.480(8)	C(52)-C(53)	1.383(8)
N(3)-C(32)	1.490(7)	C(52)-C(521)	1.506(9)
N(3)-C(31)	1.496(7)	C(53)-C(54)	1.384(10)
N(5)-C(51)	1.422(7)	C(54)-C(55)	1.357(9)
N(4)-C(41)	1.417(8)	C(55)-C(56)	1.366(8)
C(11)-C(12)	1.363(8)	C(56)-C(561)	1.504(9)
C(12)-C(13)	1.404(8)	C(421)-C(422)	1.494(10)
C(13)-C(14)	1.380(8)	C(421)-C(423)	1.495(11)
C(14)-C(31)	1.500(8)	C(461)-C(463)	1.511(9)
C(21)-C(22)	1.359(8)	C(461)-C(462)	1.512(9)
C(22)-C(23)	1.417(8)	C(521)-C(522)	1.515(11)
C(23)-C(24)	1.363(8)	C(521)-C(523)	1.542(9)
C(24)-C(32)	1.477(8)	C(561)-C(563)	1.539(9)
C(41)-C(46)	1.408(10)	C(561)-C(562)	1.552(10)
N(5)-Mo(1)-N(4)	111.2(2)	C(24)-C(32)-N(3)	106.4(5)
N(5)-Mo(1)-N(1)	95.1(2)	C(46)-C(41)-N(4)	119.5(6)
N(4)-Mo(1)-N(1)	103.9(2)	C(46)-C(41)-C(42)	122.0(7)
N(5)-Mo(1)-N(2)	101.0(2)	N(4)-C(41)-C(42)	118.4(7)
N(4)-Mo(1)-N(2)	102.8(2)	C(43)-C(42)-C(41)	117.5(7)
N(1)-Mo(1)-N(2)	141.17(19)	C(43)-C(42)-C(421)	120.7(7)
N(5)-Mo(1)-N(3)	141.8(2)	C(41)-C(42)-C(421)	121.9(7)
N(4)-Mo(1)-N(3)	106.9(2)	C(44)-C(43)-C(42)	121.2(7)
N(1)-Mo(1)-N(3)	72.47(17)	C(43)-C(44)-C(45)	120.4(7)
N(2)-Mo(1)-N(3)	73.11(19)	C(46)-C(45)-C(44)	122.2(7)
C(14)-N(1)-C(11)	106.8(5)	C(45)-C(46)-C(41)	116.6(6)
C(14)-N(1)-Mo(1)	118.4(4)	C(45)-C(46)-C(461)	122.7(6)
C(11)-N(1)-Mo(1)	132.8(4)	C(41)-C(46)-C(461)	120.7(6)
C(21)-N(2)-C(24)	106.9(5)	C(52)-C(51)-C(56)	122.2(6)
C(21)-N(2)-Mo(1)	134.7(5)	C(52)-C(51)-N(5)	118.7(5)
C(24)-N(2)-Mo(1)	117.7(4)	C(56)-C(51)-N(5)	119.0(5)
C(33)-N(3)-C(32)	110.4(5)	C(53)-C(52)-C(51)	116.4(6)
C(33)-N(3)-C(31)	109.3(4)	C(53)-C(52)-C(521)	122.9(6)
C(32)-N(3)-C(31)	114.0(4)	C(51)-C(52)-C(521)	120.7(5)
C(33)-N(3)-Mo(1)	109.8(4)	C(52)-C(53)-C(54)	121.1(7)
C(32)-N(3)-Mo(1)	106.3(3)	C(55)-C(54)-C(53)	121.4(6)
C(31)-N(3)-Mo(1)	106.9(3)	C(54)-C(55)-C(56)	121.2(7)
C(51)-N(5)-Mo(1)	175.2(5)	C(55)-C(56)-C(51)	117.6(6)
C(41)-N(4)-Mo(1)	155.8(5)	C(55)-C(56)-C(561)	121.8(7)
C(12)-C(11)-N(1)	109.2(6)	C(51)-C(56)-C(561)	120.5(6)
C(11)-C(12)-C(13)	107.9(6)	C(422)-C(421)-C(423)	108.7(7)

C(14)-C(13)-C(12)	106.7(6)	C(422)-C(421)-C(42)	113.4(7)
N(1)-C(14)-C(13)	109.4(5)	C(423)-C(421)-C(42)	112.0(6)
N(1)-C(14)-C(31)	115.9(5)	C(46)-C(461)-C(463)	113.4(6)
C(13)-C(14)-C(31)	134.6(6)	C(46)-C(461)-C(462)	111.4(6)
C(22)-C(21)-N(2)	109.4(6)	C(463)-C(461)-C(462)	108.9(6)
C(21)-C(22)-C(23)	107.7(6)	C(52)-C(521)-C(522)	110.5(6)
C(24)-C(23)-C(22)	105.7(6)	C(52)-C(521)-C(523)	112.7(6)
C(23)-C(24)-N(2)	110.4(6)	C(522)-C(521)-C(523)	111.3(6)
C(23)-C(24)-C(32)	132.3(6)	C(56)-C(561)-C(563)	114.0(6)
N(2)-C(24)-C(32)	117.3(5)	C(56)-C(561)-C(562)	109.5(6)
N(3)-C(31)-C(14)	106.5(5)	C(563)-C(561)-C(562)	108.5(7)

Table A-7.4. Anisotropic displacement parameters ($Å^2 \times 10^3$) for $Mo(dpma)(Ndip)_2$.

The anisotropic displacement factor exponent takes the form:

$-2\pi^2[h^2 a^{*2}U^{11} + ... + 2 h k a^* b^* U^{12}]$

	U^{11}	U^{22}	U^{33}	U^{23}	U^{13}	U^{12}
Mo(1)	22(1)	24(1)	20(1)	0(1)	1(1)	2(1)
N(1)	26(3)	19(3)	30(3)	-4(3)	-1(3)	2(3)
N(2)	28(4)	27(3)	23(3)	2(3)	-1(3)	2(3)
N(3)	18(3)	29(3)	19(3)	-4(2)	2(2)	-6(2)
N(5)	18(3)	37(3)	23(4)	3(2)	1(3)	4(3)
N(4)	17(3)	38(3)	18(3)	-1(3)	0(2)	-9(3)
C(11)	38(5)	31(4)	41(5)	-5(4)	2(4)	-5(4)
C(12)	29(4)	41(4)	34(4)	-3(3)	-11(3)	-9(4)
C(13)	20(4)	39(4)	29(4)	3(3)	7(3)	3(3)
C(14)	21(4)	30(4)	23(4)	-5(3)	1(3)	2(3)
C(21)	35(5)	33(4)	27(5)	4(4)	2(4)	8(4)
C(22)	40(5)	45(4)	27(4)	5(4)	-9(3)	10(4)
C(23)	44(4)	42(4)	36(5)	-10(4)	-6(4)	-3(4)
C(24)	23(4)	36(4)	14(4)	-1(3)	-3(3)	4(3)
C(31)	18(4)	26(3)	24(4)	0(3)	2(3)	-3(3)
C(32)	27(4)	34(4)	24(4)	-5(3)	1(3)	-2(3)
C(33)	38(5)	46(4)	31(4)	-4(4)	7(4)	-1(4)
C(41)	33(5)	26(4)	23(4)	3(3)	5(3)	0(3)
C(42)	46(5)	35(5)	34(5)	-3(4)	7(4)	-12(4)
C(43)	54(6)	51(5)	24(4)	-3(4)	8(4)	-10(4)
C(44)	52(6)	53(5)	28(5)	4(4)	19(4)	19(4)

C(45)	26(4)	61(5)	39(5)	12(4)	14(4)	10(4)
C(46)	23(4)	37(4)	27(4)	6(3)	4(3)	4(3)
C(51)	34(4)	22(3)	23(4)	1(3)	-1(3)	5(3)
C(52)	34(4)	24(4)	32(5)	-6(3)	-3(4)	5(3)
C(53)	60(5)	32(4)	56(5)	6(5)	2(6)	15(4)
C(54)	81(7)	19(4)	80(6)	12(4)	18(6)	8(4)
C(55)	54(5)	33(5)	64(6)	8(4)	15(5)	9(4)
C(56)	37(5)	24(4)	39(5)	8(3)	2(4)	4(3)
C(421)	59(6)	77(6)	12(3)	1(4)	3(4)	-17(5)
C(422)	132(10)	46(6)	211(13)	5(7)	-116(10)	-31(6)
C(423)	45(6)	68(6)	177(12)	7(7)	-10(7)	-10(5)
C(461)	24(4)	65(5)	26(4)	6(4)	1(3)	-1(4)
C(462)	74(7)	87(6)	54(6)	-26(5)	-24(5)	15(5)
C(463)	55(5)	101(7)	64(7)	9(6)	-27(5)	12(5)
C(521)	45(5)	29(4)	49(5)	0(4)	10(4)	14(4)
C(522)	62(7)	116(7)	74(8)	-8(7)	9(6)	-10(5)
C(523)	73(6)	60(5)	51(6)	-3(4)	25(5)	10(5)
C(561)	56(5)	39(4)	39(5)	8(4)	14(5)	4(4)
C(562)	83(7)	69(6)	48(6)	-13(5)	13(5)	-3(5)
C(563)	54(6)	57(5)	88(7)	16(5)	28(5)	15(5)

Table A-7.5. Hydrogen coordinates (x 10^4) and isotropic displacement parameters ($Å^2$ x 10^3) for Mo(dpma)(Ndip)$_2$.

	x	y	z	U(eq)		x	y	z	U(eq)
H(11)	4487	792	9435	44	H(42B)	3368	261	12045	145
H(12)	5382	600	10547	42	H(42C)	3086	406	13081	145
H(13)	5262	202	10117	36	H(461)	1521	452	8071	46
H(21)	2088	646	5781	38	H(46A)	1647	90	8813	107
H(22)	1601	367	4485	45	H(46B)	1182	109	7681	107
H(23)	2139	7	5054	49	H(46C)	843	81	8934	107
H(31A)	4419	-6	8221	27	H(46E)	162	414	8907	110
H(31B)	3768	32	9030	27	H(46D)	364	420	7562	110
H(32A)	3311	-70	6535	34	H(46F)	480	626	8359	110
H(32B)	2880	-14	7678	34	H(521)	2385	915	9266	49
H(33A)	4543	332	6743	58	H(52C)	1457	1170	7949	126
H(33B)	3948	303	5817	58	H(52B)	1236	972	8740	126
H(33C)	4392	102	6200	58	H(52A)	1694	934	7614	126
H(43)	2027	626	12877	52	H(52F)	2519	1238	10486	92

H(44)	886	585	12496	53	H(52D)	1827	1111	10672	92
H(45)	511	481	10641	50	H(52E)	1837	1324	9908	92
H(53)	2609	1471	8460	59	H(561)	4386	815	6869	53
H(54)	3463	1601	7245	72	H(56F)	3577	795	5317	100
H(55)	4233	1374	6376	60	H(56E)	4317	768	4785	100
H(421)	3390	543	10778	59	H(56D)	3930	990	4667	100
H(42D)	3114	815	12710	195	H(56B)	4999	1149	5494	99
H(42E)	3170	897	11398	195	H(56C)	5348	929	5864	99
H(42F)	3818	800	12035	195	H(56A)	5210	1109	6818	99
H(42A)	3844	437	12632	145					

Table A-8.1. Crystal data and structure refinement for $Mo(dpCHIRA)(NBu^t)_2$.

Identification code	jtcxx3t	
Empirical formula	$C_{29}H_{49}MoN_5$	
Formula weight	563.67	
Temperature	173(2) K	
Wavelength	0.71073 Å	
Crystal system	Orthorhombic	
Space group	P2(1)2(1)2(1)	
Unit cell dimensions	a = 9.852(3) Å	a= 90°
	b = 16.642(4) Å	b= 90°
	c = 18.190(5) Å	g = 90°
Volume	2982.4(13) $Å^3$	
Z	4	
Density (calculated)	1.255 Mg/m^3	
Absorption coefficient	0.464 mm^{-1}	
F(000)	1200	
Crystal size	0.06 x 0.08 x 0.51 mm^3	
Theta range for data collection	1.66 to 23.36°.	
Index ranges	-10<=h<=10, -18<=k<=14, -18<=l<=20	
Reflections collected	13801	
Independent reflections	4323 [R(int) = 0.1614]	
Completeness to theta = 23.36°	99.7 %	
Absorption correction	Empirical	
Max. and min. transmission	1.0000 and 0.7001	
Refinement method	Full-matrix least-squares on F^2	
Data / restraints / parameters	4323 / 0 / 317	
Goodness-of-fit on F^2	0.976	
Final R indices [I>2sigma(I)]	R1 = 0.0640, wR2 = 0.0932	
R indices (all data)	R1 = 0.1216, wR2 = 0.1077	
Absolute structure parameter	-0.18(7)	
Extinction coefficient	0.00125(14)	
Largest diff. peak and hole	0.444 and -0.502 $e.Å^{-3}$	

Table A-8.2. Atomic coordinates (x 10^4) and equivalent isotropic displacement parameters ($Å^2$ x 10^3) for Mo(dpCHIRA)(NBu^t)$_2$. U(eq) is defined as one third of the trace of the orthogonalized U^{ij} tensor.

	x	y	z	U(eq)		x	y	z	U(eq)
Mo(1)	9670(1)	9877(1)	5187(1)	26(1)	C(35)	6818(9)	9871(5)	6244(4)	32(2)
N(1)	8110(6)	10050(4)	4441(3)	26(2)	C(36)	5560(9)	10157(5)	5852(4)	34(2)
N(2)	10233(8)	9214(3)	6101(3)	23(2)	C(360)	5467(10)	11074(4)	5865(4)	52(3)
N(3)	8477(7)	8671(3)	5110(4)	25(2)	C(37)	4316(9)	9781(5)	6186(4)	42(3)
N(4)	10958(7)	9652(3)	4557(3)	23(2)	C(38)	4393(8)	8870(5)	6262(5)	31(2)
N(5)	9861(7)	10844(3)	5542(3)	26(2)	C(39)	5670(9)	8626(5)	6679(4)	31(2)
C(11)	7555(11)	10701(6)	4071(6)	37(3)	C(390)	5698(9)	7718(4)	6863(5)	31(2)
C(12)	6756(12)	10459(6)	3515(6)	51(4)	C(391)	4481(11)	7460(5)	7324(5)	57(3)
C(13)	6806(11)	9598(6)	3502(6)	48(3)	C(392)	6974(11)	7499(5)	7301(5)	51(3)
C(14)	7625(11)	9392(6)	4081(6)	34(3)	C(40)	12038(9)	9840(6)	4041(5)	34(2)
C(21)	10774(8)	9355(5)	6783(5)	28(2)	C(41)	12701(11)	10653(5)	4236(6)	49(4)
C(22)	10983(8)	8672(5)	7163(5)	31(2)	C(42)	13098(11)	9173(6)	4093(6)	55(3)
C(23)	10564(9)	8040(5)	6704(5)	29(2)	C(43)	11413(10)	9856(6)	3285(4)	57(3)
C(24)	10098(9)	8379(4)	6082(5)	23(2)	C(50)	10079(10)	11643(4)	5844(5)	34(3)
C(31)	8192(9)	8598(5)	4320(4)	25(2)	C(51)	9413(12)	11688(5)	6597(5)	75(4)
C(32)	9484(10)	8078(4)	5378(5)	36(3)	C(52)	9464(13)	12235(4)	5328(5)	76(4)
C(33)	7127(9)	8581(4)	5513(4)	32(3)	C(53)	11588(11)	11778(6)	5928(6)	70(4)
C(34)	6964(9)	8959(5)	6275(5)	31(3)					

Table A-8.3. Bond lengths [Å] and angles [°] for Mo(dpCHIRA)(NBu^t)$_2$.

Mo(1)-N(5)	1.745(5)	C(23)-C(24)	1.345(10)
Mo(1)-N(4)	1.750(7)	C(24)-C(32)	1.502(11)
Mo(1)-N(1)	2.070(6)	C(33)-C(34)	1.530(10)
Mo(1)-N(2)	2.072(6)	C(34)-C(35)	1.526(11)
Mo(1)-N(3)	2.331(6)	C(34)-C(39)	1.573(11)
N(1)-C(14)	1.362(11)	C(35)-C(36)	1.506(10)
N(1)-C(11)	1.387(10)	C(36)-C(37)	1.504(11)
N(2)-C(21)	1.370(9)	C(36)-C(360)	1.529(9)
N(2)-C(24)	1.397(8)	C(37)-C(38)	1.524(10)
N(3)-C(31)	1.468(9)	C(38)-C(39)	1.523(10)
N(3)-C(32)	1.482(10)	C(39)-C(390)	1.548(10)
N(3)-C(33)	1.527(10)	C(390)-C(391)	1.524(12)
N(4)-C(40)	1.452(10)	C(390)-C(392)	1.532(11)

N(5)-C(50)	1.454(8)	C(40)-C(43)	1.506(11)
C(11)-C(12)	1.343(13)	C(40)-C(42)	1.528(12)
C(12)-C(13)	1.434(10)	C(40)-C(41)	1.544(13)
C(13)-C(14)	1.370(14)	C(50)-C(52)	1.490(11)
C(14)-C(31)	1.500(12)	C(50)-C(53)	1.511(13)
C(21)-C(22)	1.346(9)	C(50)-C(51)	1.520(11)
C(22)-C(23)	1.404(10)		
N(5)-Mo(1)-N(4)	111.2(3)	C(23)-C(24)-N(2)	111.3(7)
N(5)-Mo(1)-N(1)	101.2(3)	C(23)-C(24)-C(32)	135.7(7)
N(4)-Mo(1)-N(1)	98.0(2)	N(2)-C(24)-C(32)	113.0(7)
N(5)-Mo(1)-N(2)	99.5(3)	N(3)-C(31)-C(14)	106.5(7)
N(4)-Mo(1)-N(2)	102.6(3)	N(3)-C(32)-C(24)	109.2(6)
N(1)-Mo(1)-N(2)	143.1(3)	N(3)-C(33)-C(34)	119.1(7)
N(5)-Mo(1)-N(3)	150.6(3)	C(35)-C(34)-C(33)	112.6(7)
N(4)-Mo(1)-N(3)	98.2(3)	C(35)-C(34)-C(39)	106.9(7)
N(1)-Mo(1)-N(3)	72.9(3)	C(33)-C(34)-C(39)	111.3(7)
N(2)-Mo(1)-N(3)	74.0(3)	C(36)-C(35)-C(34)	114.2(7)
C(14)-N(1)-C(11)	104.8(7)	C(37)-C(36)-C(35)	110.4(7)
C(14)-N(1)-Mo(1)	117.6(6)	C(37)-C(36)-C(360)	111.1(7)
C(11)-N(1)-Mo(1)	136.0(6)	C(35)-C(36)-C(360)	111.0(7)
C(21)-N(2)-C(24)	103.3(6)	C(36)-C(37)-C(38)	114.2(7)
C(21)-N(2)-Mo(1)	137.7(5)	C(39)-C(38)-C(37)	110.6(7)
C(24)-N(2)-Mo(1)	119.0(5)	C(38)-C(39)-C(390)	112.5(7)
C(31)-N(3)-C(32)	113.3(7)	C(38)-C(39)-C(34)	110.0(7)
C(31)-N(3)-C(33)	107.2(7)	C(390)-C(39)-C(34)	115.5(7)
C(32)-N(3)-C(33)	111.1(6)	C(391)-C(390)-C(392)	107.0(7)
C(31)-N(3)-Mo(1)	103.0(4)	C(391)-C(390)-C(39)	112.3(7)
C(32)-N(3)-Mo(1)	102.5(5)	C(392)-C(390)-C(39)	111.0(7)
C(33)-N(3)-Mo(1)	119.6(4)	N(4)-C(40)-C(43)	107.1(7)
C(40)-N(4)-Mo(1)	155.2(6)	N(4)-C(40)-C(42)	107.7(8)
C(50)-N(5)-Mo(1)	177.7(6)	C(43)-C(40)-C(42)	110.4(8)
C(12)-C(11)-N(1)	111.3(9)	N(4)-C(40)-C(41)	110.5(8)
C(11)-C(12)-C(13)	107.0(10)	C(43)-C(40)-C(41)	111.6(8)
C(14)-C(13)-C(12)	104.9(10)	C(42)-C(40)-C(41)	109.5(8)
N(1)-C(14)-C(13)	112.0(9)	N(5)-C(50)-C(52)	107.9(7)
N(1)-C(14)-C(31)	116.0(9)	N(5)-C(50)-C(53)	108.6(8)
C(13)-C(14)-C(31)	131.5(9)	C(52)-C(50)-C(53)	111.4(8)
C(22)-C(21)-N(2)	112.3(7)	N(5)-C(50)-C(51)	108.8(7)
C(21)-C(22)-C(23)	106.4(8)	C(52)-C(50)-C(51)	111.1(8)
C(24)-C(23)-C(22)	106.7(7)	C(53)-C(50)-C(51)	109.0(9)

Table A-8.4. Anisotropic displacement parameters ($Å^2 x\ 10^3$) for Mo(dpCHIRA)(NBu^t)$_2$.

The anisotropic displacement factor exponent takes the form:

$-2\pi^2[\ h^2\ a^{*2}U^{11} + ... + 2\ h\ k\ a^*\ b^*\ U^{12}\ ]$

	U^{11}	U^{22}	U^{33}	U^{23}	U^{13}	U^{12}
Mo(1)	21(1)	25(1)	31(1)	2(1)	-1(1)	-2(1)
N(1)	25(5)	23(4)	29(4)	0(4)	5(3)	0(4)
N(2)	13(5)	33(4)	25(4)	-3(3)	-6(4)	-3(3)
N(3)	29(5)	29(4)	17(4)	-2(4)	9(4)	6(3)
N(4)	17(5)	45(5)	7(4)	0(3)	-4(3)	2(3)
N(5)	23(5)	29(4)	25(4)	-9(3)	-4(4)	-1(3)
C(11)	34(9)	26(6)	49(8)	12(5)	-5(7)	-7(5)
C(12)	58(11)	66(8)	30(8)	10(6)	-11(7)	12(6)
C(13)	27(9)	61(8)	54(9)	-7(6)	-1(7)	-1(6)
C(14)	28(8)	49(7)	25(8)	7(6)	-3(6)	-10(6)
C(21)	8(6)	29(5)	46(7)	6(5)	5(5)	-3(4)
C(22)	23(7)	37(6)	34(6)	3(5)	-6(5)	6(4)
C(23)	12(7)	32(5)	44(6)	23(5)	7(5)	13(4)
C(24)	1(7)	30(5)	38(6)	2(4)	4(5)	-4(4)
C(31)	28(7)	31(6)	16(6)	-7(5)	4(5)	-22(5)
C(32)	33(7)	25(4)	52(8)	7(4)	5(6)	3(5)
C(33)	39(7)	26(5)	32(6)	-2(4)	8(5)	-13(4)
C(34)	24(7)	44(6)	25(6)	-1(5)	-10(5)	1(5)
C(35)	29(6)	33(6)	33(6)	-6(5)	-4(5)	9(6)
C(36)	32(7)	30(5)	40(5)	6(5)	3(5)	-2(5)
C(360)	34(7)	58(6)	65(7)	-8(5)	5(7)	8(6)
C(37)	44(8)	50(6)	32(6)	3(5)	1(5)	-3(5)
C(38)	6(7)	48(6)	40(6)	5(5)	-1(5)	0(5)
C(39)	22(7)	49(6)	23(6)	0(4)	5(5)	-6(5)
C(390)	27(8)	37(6)	29(6)	-1(4)	4(5)	-2(4)
C(391)	47(10)	71(7)	53(8)	6(5)	25(7)	-13(6)
C(392)	68(10)	49(6)	36(8)	4(5)	-4(7)	-11(6)
C(40)	32(7)	45(6)	23(6)	8(6)	8(5)	-7(6)
C(41)	42(9)	57(8)	49(8)	2(6)	14(7)	-16(6)
C(42)	33(8)	72(8)	61(9)	-7(7)	2(7)	2(6)
C(43)	51(8)	67(7)	52(7)	13(6)	15(6)	-1(7)
C(50)	33(10)	23(5)	47(7)	-8(4)	-9(6)	-2(4)
C(51)	99(12)	60(7)	65(8)	-38(6)	39(8)	-3(7)
C(52)	113(11)	18(5)	95(9)	-2(6)	-30(10)	3(6)
C(53)	58(10)	61(8)	91(10)	-22(7)	-6(8)	-23(7)

Table A-8.5. Hydrogen coordinates (x 10^4) and isotropic displacement parameters ($Å^2$ x 10^3) for Mo(dpCHIRA)$(NBu^t)_2$.

	x	y	z	U(eq)		x	y	z	U(eq)
H(11A)	7715	11235	4192	44	H(39C)	4529	6893	7415	85
H(12A)	6264	10788	3198	62	H(39D)	3659	7582	7063	85
H(13A)	6376	9254	3172	57	H(39E)	4490	7744	7783	85
H(21A)	10974	9865	6963	33	H(39F)	6981	6932	7397	77
H(22A)	11335	8628	7635	37	H(39G)	6976	7787	7759	77
H(23A)	10602	7494	6810	35	H(39H)	7766	7641	7023	77
H(31A)	7540	8172	4232	30	H(41A)	12029	11070	4218	74
H(31B)	9018	8477	4052	30	H(41B)	13410	10769	3890	74
H(32A)	10189	8003	5012	44	H(41C)	13077	10625	4723	74
H(32B)	9045	7564	5462	44	H(42A)	12700	8673	3942	83
H(33A)	6943	8011	5561	39	H(42B)	13411	9129	4591	83
H(33B)	6425	8804	5200	39	H(42C)	13851	9298	3777	83
H(34A)	7766	8827	6570	37	H(43A)	11176	9319	3141	85
H(35A)	6807	10078	6742	38	H(43B)	12053	10075	2941	85
H(35B)	7607	10093	5999	38	H(43C)	10612	10184	3292	85
H(36A)	5618	9984	5338	41	H(51A)	9818	11296	6916	112
H(36B)	6280	11299	5660	78	H(51B)	8460	11581	6550	112
H(36C)	5362	11255	6363	78	H(51C)	9543	12215	6799	112
H(36D)	4699	11244	5579	78	H(52A)	9881	12183	4853	113
H(37A)	3536	9916	5885	50	H(52B)	9608	12769	5511	113
H(37B)	4170	10013	6669	50	H(52C)	8508	12135	5286	113
H(38A)	3599	8677	6523	37	H(53A)	12013	11760	5454	105
H(38B)	4400	8626	5778	37	H(53B)	11964	11366	6237	105
H(39A)	5629	8906	7152	38	H(53C)	11744	12294	6149	105
H(39B)	5697	7412	6403	37					

Table A-9.1. Crystal data and structure refinement for Mo(dpma)(Ndip)(=CHCMe$_2$Ph).

Identification code	jtc9	
Empirical formula	$C_{33}H_{42}MoN_4$	
Formula weight	590.65	
Temperature	173(2) K	
Wavelength	0.71073 Å	
Crystal system	Monoclinic	
Space group	P2(1)/n	
Unit cell dimensions	a = 9.7242(17) Å	α= 90°
	b = 16.088(2) Å	β= 100.005(12)°
	c = 19.984(3) Å	γ = 90°
Volume	3078.7(8) Å^3	
Z	4	
Density (calculated)	1.274 Mg/m^3	
Absorption coefficient	0.453 mm^{-1}	
F(000)	1240	
Crystal size	0.43 x 0.31 x 0.29 mm^3	
Theta range for data collection	1.63 to 23.31°.	
Index ranges	-10<=h<=10, -10<=k<=17, -22<=l<=21	
Reflections collected	13730	
Independent reflections	4433 [R(int) = 0.0325]	
Completeness to theta = 23.31°	99.8 %	
Absorption correction	Empirical	
Max. and min. transmission	0.8160 and 0.7072	
Refinement method	Full-matrix least-squares on F^2	
Data / restraints / parameters	4433 / 0 / 344	
Goodness-of-fit on F^2	1.043	
Final R indices [I>2sigma(I)]	R1 = 0.0252, wR2 = 0.0600	
R indices (all data)	R1 = 0.0374, wR2 = 0.0638	
Extinction coefficient	0.00053(13)	
Largest diff. peak and hole	0.254 and -0.250 e.Å^{-3}	

Table A-9.2. Atomic coordinates (x 10^4) and equivalent isotropic displacement parameters ($Å^2$ x 10^3) for Mo(dpma)(Ndip)(=CHCMe$_2$Ph). U(eq) is defined as one third of the trace of the orthogonalized U^{ij} tensor.

	x	y	z	U(eq)		x	y	z	U(eq)
Mo	9450(1)	1724(1)	840(1)	27(1)	C(43)	9961(3)	4868(2)	1664(2)	49(1)
N(1)	11176(2)	1181(1)	519(1)	36(1)	C(44)	11084(3)	5197(2)	1414(2)	50(1)
N(2)	8032(2)	1511(1)	1488(1)	32(1)	C(45)	11724(3)	4735(2)	976(1)	45(1)
N(3)	10565(2)	937(1)	1734(1)	32(1)	C(46)	11303(3)	3932(2)	791(1)	32(1)
N(4)	9783(2)	2770(1)	925(1)	29(1)	C(51)	7237(3)	2159(2)	-530(1)	33(1)
C(5)	8147(2)	1651(2)	17(1)	30(1)	C(52)	7880(3)	2093(2)	-1181(1)	31(1)
C(11)	11560(3)	1033(2)	-104(1)	43(1)	C(53)	7223(3)	1711(2)	-1769(1)	35(1)
C(12)	12842(3)	664(2)	-7(2)	53(1)	C(54)	7846(3)	1684(2)	-2345(1)	42(1)
C(13)	13289(3)	572(2)	695(2)	49(1)	C(55)	9133(3)	2024(2)	-2336(1)	45(1)
C(14)	12260(3)	895(2)	1004(1)	40(1)	C(56)	9823(3)	2391(2)	-1749(1)	48(1)
C(21)	6603(3)	1541(2)	1435(1)	36(1)	C(57)	9197(3)	2426(2)	-1182(1)	43(1)
C(22)	6243(3)	1438(2)	2057(1)	43(1)	C(58)	5742(3)	1805(2)	-633(1)	45(1)
C(23)	7486(3)	1344(2)	2526(1)	42(1)	C(59)	7173(3)	3076(2)	-321(1)	48(1)
C(24)	8559(3)	1391(2)	2169(1)	34(1)	C(421)	8169(3)	3745(2)	1740(2)	44(1)
C(31)	12085(3)	1004(2)	1726(1)	45(1)	C(422)	8333(3)	3736(2)	2509(2)	73(1)
C(32)	10113(3)	1306(2)	2345(1)	41(1)	C(423)	6885(3)	4253(2)	1439(2)	60(1)
C(33)	10127(3)	49(2)	1670(2)	50(1)	C(461)	12036(3)	3407(2)	328(1)	39(1)
C(41)	10171(3)	3602(2)	1069(1)	30(1)	C(462)	13304(3)	2974(2)	729(2)	51(1)
C(42)	9463(3)	4075(2)	1494(1)	38(1)	C(463)	12427(4)	3898(2)	-266(2)	74(1)

Table A-9.3. Bond lengths [Å] and angles [°] for Mo(dpma)(Ndip)(=CHCMe$_2$Ph).

Mo-N(4)	1.716(2)	C(41)-C(42)	1.405(3)
Mo-C(5)	1.898(2)	C(41)-C(46)	1.420(3)
Mo-N(2)	2.0789(19)	C(42)-C(43)	1.387(4)
Mo-N(1)	2.089(2)	C(42)-C(421)	1.524(4)
Mo-N(3)	2.303(2)	C(43)-C(44)	1.383(4)
N(1)-C(11)	1.381(3)	C(44)-C(45)	1.377(4)
N(1)-C(14)	1.382(3)	C(45)-C(46)	1.386(4)
N(2)-C(21)	1.376(3)	C(46)-C(461)	1.519(4)
N(2)-C(24)	1.381(3)	C(51)-C(59)	1.536(4)
N(3)-C(31)	1.486(3)	C(51)-C(52)	1.541(3)
N(3)-C(32)	1.489(3)	C(51)-C(58)	1.542(3)

N(3)-C(33)	1.489(3)	C(52)-C(53)	1.382(3)
N(4)-C(41)	1.407(3)	C(52)-C(57)	1.388(3)
C(5)-C(51)	1.519(3)	C(53)-C(54)	1.391(4)
C(11)-C(12)	1.365(4)	C(54)-C(55)	1.363(4)
C(12)-C(13)	1.404(4)	C(55)-C(56)	1.378(4)
C(13)-C(14)	1.367(4)	C(56)-C(57)	1.377(4)
C(14)-C(31)	1.492(4)	C(421)-C(422)	1.518(4)
C(21)-C(22)	1.359(3)	C(421)-C(423)	1.526(4)
C(22)-C(23)	1.404(4)	C(461)-C(462)	1.519(4)
C(23)-C(24)	1.364(4)	C(461)-C(463)	1.527(4)
C(24)-C(32)	1.497(4)		
N(4)-Mo-C(5)	103.45(10)	N(2)-C(24)-C(32)	115.5(2)
N(4)-Mo-N(2)	103.53(8)	N(3)-C(31)-C(14)	106.4(2)
C(5)-Mo-N(2)	96.60(9)	N(3)-C(32)-C(24)	105.9(2)
N(4)-Mo-N(1)	107.04(8)	C(42)-C(41)-N(4)	119.8(2)
C(5)-Mo-N(1)	99.16(9)	C(42)-C(41)-C(46)	121.9(2)
N(2)-Mo-N(1)	141.04(8)	N(4)-C(41)-C(46)	118.3(2)
N(4)-Mo-N(3)	114.05(8)	C(43)-C(42)-C(41)	117.4(2)
C(5)-Mo-N(3)	142.38(9)	C(43)-C(42)-C(421)	120.9(2)
N(2)-Mo-N(3)	72.45(7)	C(41)-C(42)-C(421)	121.7(2)
N(1)-Mo-N(3)	73.35(8)	C(44)-C(43)-C(42)	121.8(3)
C(11)-N(1)-C(14)	106.4(2)	C(45)-C(44)-C(43)	119.7(3)
C(11)-N(1)-Mo	134.92(19)	C(44)-C(45)-C(46)	121.9(3)
C(14)-N(1)-Mo	118.67(17)	C(45)-C(46)-C(41)	117.2(2)
C(21)-N(2)-C(24)	106.2(2)	C(45)-C(46)-C(461)	122.2(2)
C(21)-N(2)-Mo	135.73(17)	C(41)-C(46)-C(461)	120.6(2)
C(24)-N(2)-Mo	117.69(16)	C(5)-C(51)-C(59)	111.5(2)
C(31)-N(3)-C(32)	114.6(2)	C(5)-C(51)-C(52)	107.4(2)
C(31)-N(3)-C(33)	109.8(2)	C(59)-C(51)-C(52)	109.7(2)
C(32)-N(3)-C(33)	109.4(2)	C(5)-C(51)-C(58)	108.3(2)
C(31)-N(3)-Mo	106.63(15)	C(59)-C(51)-C(58)	108.0(2)
C(32)-N(3)-Mo	104.53(15)	C(52)-C(51)-C(58)	111.9(2)
C(33)-N(3)-Mo	111.81(16)	C(53)-C(52)-C(57)	117.4(2)
C(41)-N(4)-Mo	172.83(17)	C(53)-C(52)-C(51)	123.7(2)
C(51)-C(5)-Mo	143.84(19)	C(57)-C(52)-C(51)	119.0(2)
C(12)-C(11)-N(1)	109.3(3)	C(52)-C(53)-C(54)	121.0(2)
C(11)-C(12)-C(13)	107.7(3)	C(55)-C(54)-C(53)	120.4(3)
C(14)-C(13)-C(12)	106.8(3)	C(54)-C(55)-C(56)	119.6(3)
C(13)-C(14)-N(1)	109.8(3)	C(57)-C(56)-C(55)	119.9(3)
C(13)-C(14)-C(31)	134.2(3)	C(56)-C(57)-C(52)	121.7(3)

N(1)-C(14)-C(31)	116.0(2)	C(422)-C(421)-C(42)	112.5(2)
C(22)-C(21)-N(2)	110.0(2)	C(422)-C(421)-C(423)	109.8(2)
C(21)-C(22)-C(23)	107.2(2)	C(42)-C(421)-C(423)	110.6(2)
C(24)-C(23)-C(22)	107.0(2)	C(462)-C(461)-C(46)	110.9(2)
C(23)-C(24)-N(2)	109.7(2)	C(462)-C(461)-C(463)	111.0(2)
C(23)-C(24)-C(32)	134.8(2)	C(46)-C(461)-C(463)	113.1(2)

Table A-9.4. Anisotropic displacement parameters ($Å^2 x\ 10^3$) for Mo(dpma)(Ndip)(=CHCMe$_2$Ph). The anisotropic displacement factor exponent takes the form: $-2\pi^2[\ h^2\ a^{*2}U^{11} + ... + 2\ h\ k\ a^*\ b^*\ U^{12}\ ]$

	U^{11}	U^{22}	U^{33}	U^{23}	U^{13}	U^{12}
Mo	27(1)	27(1)	27(1)	0(1)	7(1)	-2(1)
N(1)	34(1)	35(1)	41(1)	-5(1)	12(1)	-3(1)
N(2)	32(1)	34(1)	31(1)	5(1)	9(1)	-1(1)
N(3)	31(1)	26(1)	38(1)	0(1)	3(1)	-1(1)
N(4)	27(1)	30(1)	29(1)	1(1)	7(1)	-3(1)
C(5)	31(1)	31(2)	31(1)	-4(1)	14(1)	-5(1)
C(11)	44(2)	42(2)	47(2)	-13(1)	20(1)	-11(2)
C(12)	44(2)	47(2)	76(2)	-18(2)	32(2)	-6(2)
C(13)	31(2)	39(2)	80(2)	-7(2)	13(2)	0(1)
C(14)	27(2)	37(2)	55(2)	-2(1)	7(1)	-3(1)
C(21)	31(2)	40(2)	38(2)	3(1)	9(1)	-2(1)
C(22)	40(2)	46(2)	46(2)	3(1)	20(1)	-1(1)
C(23)	58(2)	42(2)	31(2)	3(1)	19(2)	-2(2)
C(24)	43(2)	31(2)	28(1)	2(1)	6(1)	-4(1)
C(31)	32(2)	45(2)	54(2)	4(2)	-2(1)	2(1)
C(32)	48(2)	44(2)	30(2)	3(1)	1(1)	-2(2)
C(33)	53(2)	32(2)	67(2)	6(2)	12(2)	1(2)
C(41)	29(1)	26(2)	33(1)	4(1)	-3(1)	-2(1)
C(42)	34(2)	28(2)	50(2)	-2(1)	6(1)	1(1)
C(43)	42(2)	35(2)	71(2)	-11(2)	14(2)	2(2)
C(44)	46(2)	27(2)	75(2)	-5(2)	6(2)	-8(2)
C(45)	37(2)	40(2)	56(2)	12(2)	5(1)	-10(2)
C(46)	31(1)	33(2)	31(1)	7(1)	-2(1)	-5(1)
C(51)	36(2)	36(2)	28(1)	-3(1)	5(1)	-1(1)
C(52)	33(2)	31(2)	27(1)	2(1)	0(1)	1(1)
C(53)	31(1)	40(2)	33(2)	-2(1)	-2(1)	1(1)
C(54)	48(2)	45(2)	30(2)	-3(1)	-2(1)	8(2)

C(55)	55(2)	50(2)	31(2)	8(1)	13(1)	12(2)
C(56)	44(2)	62(2)	41(2)	9(2)	11(1)	-14(2)
C(57)	47(2)	50(2)	28(2)	-1(1)	1(1)	-15(2)
C(58)	35(2)	61(2)	38(2)	-1(1)	8(1)	1(2)
C(59)	63(2)	42(2)	36(2)	-1(1)	2(1)	10(2)
C(421)	41(2)	31(2)	65(2)	-10(2)	21(2)	-1(1)
C(422)	45(2)	105(3)	67(2)	25(2)	9(2)	-6(2)
C(423)	36(2)	75(2)	66(2)	-12(2)	5(2)	-7(2)
C(461)	35(2)	50(2)	31(1)	4(1)	6(1)	-14(1)
C(462)	42(2)	65(2)	48(2)	-13(2)	8(1)	3(2)
C(463)	90(3)	90(3)	47(2)	14(2)	25(2)	-14(2)

Table A-9.5. Hydrogen coordinates (x 10^4) and isotropic displacement parameters ($Å^2$ x 10^3) for Mo(dpma)(Ndip)(=CHCMe$_2$Ph).

	x	y	z	U(eq)		x	y	z	U(eq)
H(5A)	8015	1092	-94	36	H(57)	9669	2678	-790	51
H(11A)	11027	1164	-524	51	H(58A)	5377	1857	-218	67
H(12A)	13332	502	-346	63	H(58B)	5759	1229	-758	67
H(13A)	14125	337	909	59	H(58C)	5158	2108	-988	67
H(21A)	5976	1620	1032	44	H(59B)	8095	3310	-253	72
H(22A)	5341	1432	2154	51	H(59C)	6806	3112	94	72
H(23A)	7564	1263	2992	51	H(59A)	6579	3377	-672	72
H(31A)	12594	577	2010	54	H(42A)	8016	3172	1578	53
H(31B)	12433	1543	1895	54	H(42E)	9142	3415	2696	109
H(32A)	10547	1844	2448	49	H(42F)	7518	3491	2640	109
H(32B)	10370	946	2736	49	H(42G)	8441	4294	2679	109
H(33A)	10612	-259	2050	75	H(42B)	6081	4037	1599	89
H(33B)	10350	-176	1257	75	H(42C)	6741	4219	952	89
H(33C)	9139	11	1661	75	H(42D)	7025	4823	1576	89
H(43A)	9528	5188	1955	59	H(46A)	11379	2973	133	46
H(44A)	11404	5729	1540	60	H(46E)	13032	2669	1098	77
H(45A)	12461	4967	800	54	H(46F)	13995	3380	906	77
H(53)	6352	1468	-1781	42	H(46G)	13687	2597	437	77
H(54)	7382	1432	-2739	50	H(46B)	12886	3537	-540	111
H(55)	9544	2010	-2723	53	H(46C)	13045	4344	-94	111
H(56)	10709	2614	-1736	58	H(46D)	11598	4122	-537	111

Table A-10.1. Crystal data and structure refinement for Mo(NBu^t)(dpma)(=CHCMe$_2$Ph) •pentane.

Identification code	at7tn	
Empirical formula	$C_{27.50}H_{41}MoN_4$	
Formula weight	523.58	
Temperature	173(2) K	
Wavelength	0.71073 Å	
Crystal system	Triclinic	
Space group	P-1	
Unit cell dimensions	a = 12.0651(19) Å	α= 96.541(3)°
	b = 14.139(2) Å	β= 102.773(3)°
	c = 19.318(3) Å	γ = 114.526(3)°
Volume	2844.3(8) Å^3	
Z	4	
Density (calculated)	1.223 Mg/m^3	
Absorption coefficient	0.481 mm^{-1}	
F(000)	1104	
Crystal size	0.37 x 0.23 x 0.18 mm^3	
Theta range for data collection	1.63 to 23.31°.	
Index ranges	-13<=h<=13, -15<=k<=15, -13<=l<=21	
Reflections collected	13157	
Independent reflections	8170 [R(int) = 0.0644]	
Completeness to theta = 23.31°	99.3 %	
Absorption correction	None	
Refinement method	Full-matrix least-squares on F^2	
Data / restraints / parameters	8170 / 0 / 601	
Goodness-of-fit on F^2	1.014	
Final R indices [I>2sigma(I)]	R1 = 0.0806, wR2 = 0.2252	
R indices (all data)	R1 = 0.1337, wR2 = 0.2518	
Extinction coefficient	0.0056(9)	
Largest diff. peak and hole	3.142 and -0.612 e.Å^{-3}	

Table A-10.2. Atomic coordinates (x 10^4) and equivalent isotropic displacement parameters ($Å^2$x 10^3) for Mo(dpma)(NBu^t)(=CHCMe$_2$Ph)•pentane. U(eq) is defined as one third of the trace of the orthogonalized U^{ij} tensor.

	x	y	z	U(eq)		x	y	z	U(eq)
Mo(1)	6368(1)	3443(1)	10258(1)	41(1)	Mo(2)	1825(1)	3253(1)	4471(1)	41(1)
N(1A)	6827(8)	4766(6)	9800(5)	46(2)	N(1B)	3090(8)	4104(7)	3912(5)	50(2)
N(2A)	5952(9)	2791(7)	11149(4)	52(2)	N(2B)	964(8)	3302(7)	5319(4)	46(2)
N(3A)	6863(7)	4857(6)	11179(4)	39(2)	N(3B)	2586(7)	5020(6)	4996(4)	40(2)
N(4A)	7347(8)	2973(7)	10068(5)	53(2)	N(4B)	523(8)	2437(6)	3742(4)	48(2)
C(4A)	8510(12)	2819(10)	10107(7)	65(3)	C(4B)	-651(10)	2017(9)	3135(6)	58(3)
C(5A)	4767(11)	2511(8)	9567(6)	59(3)	C(5B)	2555(9)	2373(8)	4760(5)	45(3)
C(11A)	6956(11)	4939(10)	9140(7)	67(3)	C(11B)	3322(11)	3830(9)	3278(6)	56(3)
C(12A)	7321(11)	5993(11)	9121(7)	71(4)	C(12B)	4160(11)	4717(11)	3127(6)	71(4)
C(13A)	7488(13)	6552(11)	9823(8)	82(4)	C(13B)	4480(10)	5600(9)	3693(6)	56(3)
C(14A)	7090(14)	5730(11)	10201(7)	83(4)	C(14B)	3819(10)	5191(9)	4152(6)	49(3)
C(21A)	5566(16)	1805(10)	11280(8)	99(5)	C(21B)	-10(10)	2574(9)	5500(7)	58(3)
C(22A)	5377(14)	1786(10)	11940(8)	83(4)	C(22B)	-182(11)	3045(10)	6087(7)	62(3)
C(23A)	5683(13)	2806(10)	12254(7)	72(4)	C(23B)	703(11)	4106(10)	6296(6)	53(3)
C(24A)	6005(13)	3424(9)	11771(6)	64(3)	C(24B)	1421(10)	4234(8)	5829(6)	46(3)
C(31A)	6580(20)	5656(15)	10933(9)	153(9)	C(31B)	3817(11)	5678(9)	4892(6)	62(3)
C(32A)	6230(20)	4548(13)	11738(10)	140(8)	C(32B)	2652(10)	5155(8)	5766(6)	54(3)
C(33A)	8236(17)	5263(16)	11528(10)	173(10)	C(33B)	1633(11)	5307(9)	4590(6)	57(3)
C(41A)	9438(16)	3369(19)	10858(9)	157(9)	C(41B)	-1670(11)	990(10)	3268(7)	79(4)
C(42A)	8120(20)	1577(15)	9935(15)	187(12)	C(42B)	-298(12)	1756(11)	2439(7)	82(4)
C(43A)	9115(16)	3325(16)	9563(9)	131(7)	C(43B)	-1085(15)	2894(11)	3083(9)	112(6)
C(51A)	4055(15)	1522(9)	8962(8)	97(5)	C(51B)	2478(10)	1264(8)	4684(6)	49(3)
C(52A)	3312(11)	1774(8)	8317(6)	54(3)	C(52B)	3771(9)	1371(7)	4625(6)	43(3)
C(53A)	3958(16)	2394(11)	7906(9)	91(5)	C(53B)	4646(12)	1287(9)	5180(6)	60(3)
C(54A)	3390(30)	2678(16)	7360(11)	126(8)	C(54B)	5778(13)	1397(11)	5116(8)	78(4)
C(55A)	2140(30)	2321(18)	7183(11)	138(12)	C(55B)	6107(13)	1580(10)	4507(9)	71(4)
C(56A)	1446(17)	1715(14)	7531(13)	121(8)	C(56B)	5284(14)	1665(9)	3937(7)	73(4)
C(57A)	2082(13)	1430(10)	8141(8)	79(4)	C(57B)	4115(11)	1583(8)	4000(6)	55(3)
C(58A)	4800(30)	1100(20)	8779(12)	290(20)	C(58B)	2177(12)	852(9)	5365(7)	73(4)
C(59A)	3160(30)	709(17)	9281(12)	260(20)	C(59B)	1399(12)	494(10)	4001(7)	83(4)
C(1S)	7600(20)	761(15)	7633(11)	139(8)	C(4S)	8428(14)	4365(14)	7503(8)	105(5)
C(2S)	7160(20)	1440(20)	7315(10)	168(10)	C(5S)	7911(11)	2522(10)	7495(6)	51(3)
C(3S)	7464(15)	3117(16)	7250(8)	118(7)					

Table A-10.3. Bond lengths [Å] and angles [°] for Mo(dpma)(NBu^t)(=CHCMe$_2$Ph)•pentane.

Mo(1)-N(4A)	1.661(9)	Mo(2)-N(4B)	1.711(8)
Mo(1)-C(5A)	1.896(11)	Mo(2)-C(5B)	1.867(10)
Mo(1)-N(1A)	2.079(8)	Mo(2)-N(1B)	2.108(9)
Mo(1)-N(2A)	2.104(8)	Mo(2)-N(2B)	2.134(9)
Mo(1)-N(3A)	2.291(8)	Mo(2)-N(3B)	2.285(8)
N(1A)-C(11A)	1.357(14)	N(1B)-C(11B)	1.364(13)
N(1A)-C(14A)	1.360(15)	N(1B)-C(14B)	1.374(13)
N(2A)-C(21A)	1.348(14)	N(2B)-C(21B)	1.350(13)
N(2A)-C(24A)	1.387(13)	N(2B)-C(24B)	1.370(12)
N(3A)-C(31A)	1.408(17)	N(3B)-C(32B)	1.457(12)
N(3A)-C(32A)	1.462(17)	N(3B)-C(31B)	1.463(13)
N(3A)-C(33A)	1.469(18)	N(3B)-C(33B)	1.471(12)
N(4A)-C(4A)	1.494(14)	N(4B)-C(4B)	1.464(12)
C(4A)-C(43A)	1.493(17)	C(4B)-C(43B)	1.538(17)
C(4A)-C(41A)	1.51(2)	C(4B)-C(42B)	1.548(16)
C(4A)-C(42A)	1.59(2)	C(4B)-C(41B)	1.559(16)
C(5A)-C(51A)	1.498(16)	C(5B)-C(51B)	1.520(13)
C(11A)-C(12A)	1.375(16)	C(11B)-C(12B)	1.357(16)
C(12A)-C(13A)	1.417(18)	C(12B)-C(13B)	1.416(16)
C(13A)-C(14A)	1.414(16)	C(13B)-C(14B)	1.342(14)
C(14A)-C(31A)	1.66(2)	C(14B)-C(31B)	1.515(14)
C(21A)-C(22A)	1.346(17)	C(21B)-C(22B)	1.348(15)
C(22A)-C(23A)	1.358(16)	C(22B)-C(23B)	1.377(15)
C(23A)-C(24A)	1.359(15)	C(23B)-C(24B)	1.359(14)
C(24A)-C(32A)	1.509(18)	C(24B)-C(32B)	1.557(15)
C(51A)-C(58A)	1.35(3)	C(51B)-C(59B)	1.535(14)
C(51A)-C(59A)	1.52(3)	C(51B)-C(52B)	1.535(14)
C(51A)-C(52A)	1.533(17)	C(51B)-C(58B)	1.554(15)
C(52A)-C(57A)	1.302(16)	C(52B)-C(53B)	1.383(14)
C(52A)-C(53A)	1.369(17)	C(52B)-C(57B)	1.386(14)
C(53A)-C(54A)	1.32(2)	C(53B)-C(54B)	1.344(16)
C(54A)-C(55A)	1.33(3)	C(54B)-C(55B)	1.341(17)
C(55A)-C(56A)	1.29(3)	C(55B)-C(56B)	1.364(17)
C(56A)-C(57A)	1.45(2)	C(56B)-C(57B)	1.400(16)
C(1S)-C(2S)	1.41(3)	C(3S)-C(5S)	1.26(2)
C(2S)-C(5S)	1.37(2)	C(3S)-C(4S)	1.60(2)
N(4A)-Mo(1)-C(5A)	104.1(5)	N(4B)-Mo(2)-C(5B)	104.2(4)

N(4A)-Mo(1)-N(1A)	102.4(4)	N(4B)-Mo(2)-N(1B)	99.6(4)
C(5A)-Mo(1)-N(1A)	99.0(4)	C(5B)-Mo(2)-N(1B)	99.0(4)
N(4A)-Mo(1)-N(2A)	101.5(4)	N(4B)-Mo(2)-N(2B)	101.6(4)
C(5A)-Mo(1)-N(2A)	96.1(4)	C(5B)-Mo(2)-N(2B)	98.8(4)
N(1A)-Mo(1)-N(2A)	147.6(3)	N(1B)-Mo(2)-N(2B)	148.0(3)
N(4A)-Mo(1)-N(3A)	127.0(4)	N(4B)-Mo(2)-N(3B)	130.0(3)
C(5A)-Mo(1)-N(3A)	128.9(4)	C(5B)-Mo(2)-N(3B)	125.8(4)
N(1A)-Mo(1)-N(3A)	74.2(3)	N(1B)-Mo(2)-N(3B)	74.2(3)
N(2A)-Mo(1)-N(3A)	74.0(3)	N(2B)-Mo(2)-N(3B)	73.8(3)
C(11A)-N(1A)-C(14A)	105.3(9)	C(11B)-N(1B)-C(14B)	105.8(9)
C(11A)-N(1A)-Mo(1)	134.5(8)	C(11B)-N(1B)-Mo(2)	133.8(8)
C(14A)-N(1A)-Mo(1)	120.2(8)	C(14B)-N(1B)-Mo(2)	120.2(7)
C(21A)-N(2A)-C(24A)	104.8(10)	C(21B)-N(2B)-C(24B)	105.8(9)
C(21A)-N(2A)-Mo(1)	134.6(8)	C(21B)-N(2B)-Mo(2)	134.2(8)
C(24A)-N(2A)-Mo(1)	120.5(7)	C(24B)-N(2B)-Mo(2)	120.0(7)
C(31A)-N(3A)-C(32A)	107.4(13)	C(32B)-N(3B)-C(31B)	111.8(8)
C(31A)-N(3A)-C(33A)	111.5(14)	C(32B)-N(3B)-C(33B)	110.9(8)
C(32A)-N(3A)-C(33A)	106.9(13)	C(31B)-N(3B)-C(33B)	108.4(8)
C(31A)-N(3A)-Mo(1)	113.5(8)	C(32B)-N(3B)-Mo(2)	110.0(6)
C(32A)-N(3A)-Mo(1)	113.5(8)	C(31B)-N(3B)-Mo(2)	111.9(6)
C(33A)-N(3A)-Mo(1)	103.9(8)	C(33B)-N(3B)-Mo(2)	103.7(6)
C(4A)-N(4A)-Mo(1)	161.9(8)	C(4B)-N(4B)-Mo(2)	163.2(7)
C(43A)-C(4A)-N(4A)	108.8(10)	N(4B)-C(4B)-C(43B)	108.5(9)
C(43A)-C(4A)-C(41A)	108.7(13)	N(4B)-C(4B)-C(42B)	106.1(9)
N(4A)-C(4A)-C(41A)	108.7(11)	C(43B)-C(4B)-C(42B)	109.8(11)
C(43A)-C(4A)-C(42A)	110.2(14)	N(4B)-C(4B)-C(41B)	108.6(9)
N(4A)-C(4A)-C(42A)	109.4(11)	C(43B)-C(4B)-C(41B)	112.5(11)
C(41A)-C(4A)-C(42A)	111.0(14)	C(42B)-C(4B)-C(41B)	111.1(10)
C(51A)-C(5A)-Mo(1)	145.1(11)	C(51B)-C(5B)-Mo(2)	149.0(8)
N(1A)-C(11A)-C(12A)	111.4(11)	C(12B)-C(11B)-N(1B)	109.7(10)
C(11A)-C(12A)-C(13A)	107.6(11)	C(11B)-C(12B)-C(13B)	107.5(10)
C(12A)-C(13A)-C(14A)	103.2(12)	C(14B)-C(13B)-C(12B)	105.5(10)
N(1A)-C(14A)-C(13A)	112.1(11)	C(13B)-C(14B)-N(1B)	111.4(9)
N(1A)-C(14A)-C(31A)	113.9(11)	C(13B)-C(14B)-C(31B)	132.5(11)
C(13A)-C(14A)-C(31A)	132.3(14)	N(1B)-C(14B)-C(31B)	115.8(9)
C(22A)-C(21A)-N(2A)	111.9(12)	N(2B)-C(21B)-C(22B)	109.6(11)
C(21A)-C(22A)-C(23A)	106.2(11)	C(21B)-C(22B)-C(23B)	108.7(10)
C(22A)-C(23A)-C(24A)	108.6(11)	C(24B)-C(23B)-C(22B)	105.4(10)
C(23A)-C(24A)-N(2A)	108.5(10)	C(23B)-C(24B)-N(2B)	110.5(10)
C(23A)-C(24A)-C(32A)	134.4(12)	C(23B)-C(24B)-C(32B)	135.5(10)
N(2A)-C(24A)-C(32A)	116.7(11)	N(2B)-C(24B)-C(32B)	114.0(9)

N(3A)-C(31A)-C(14A)	101.3(12)	N(3B)-C(31B)-C(14B)	107.9(9)
N(3A)-C(32A)-C(24A)	108.3(12)	N(3B)-C(32B)-C(24B)	107.4(8)
C(58A)-C(51A)-C(59A)	105.6(19)	C(5B)-C(51B)-C(59B)	110.3(9)
C(58A)-C(51A)-C(5A)	113.8(15)	C(5B)-C(51B)-C(52B)	107.1(8)
C(59A)-C(51A)-C(5A)	104.3(16)	C(59B)-C(51B)-C(52B)	110.6(9)
C(58A)-C(51A)-C(52A)	113.6(17)	C(5B)-C(51B)-C(58B)	108.2(9)
C(59A)-C(51A)-C(52A)	111.1(16)	C(59B)-C(51B)-C(58B)	108.6(10)
C(5A)-C(51A)-C(52A)	108.1(10)	C(52B)-C(51B)-C(58B)	112.1(9)
C(57A)-C(52A)-C(53A)	117.6(13)	C(53B)-C(52B)-C(57B)	117.1(10)
C(57A)-C(52A)-C(51A)	123.1(13)	C(53B)-C(52B)-C(51B)	123.0(10)
C(53A)-C(52A)-C(51A)	119.3(13)	C(57B)-C(52B)-C(51B)	119.9(10)
C(54A)-C(53A)-C(52A)	122.9(18)	C(54B)-C(53B)-C(52B)	121.7(12)
C(55A)-C(54A)-C(53A)	119(2)	C(55B)-C(54B)-C(53B)	121.6(12)
C(56A)-C(55A)-C(54A)	122(2)	C(54B)-C(55B)-C(56B)	119.8(12)
C(55A)-C(56A)-C(57A)	118.0(19)	C(55B)-C(56B)-C(57B)	119.5(12)
C(52A)-C(57A)-C(56A)	120.0(15)	C(52B)-C(57B)-C(56B)	120.3(11)
C(5S)-C(2S)-C(1S)	120(2)	C(3S)-C(5S)-C(2S)	119.3(17)
C(5S)-C(3S)-C(4S)	114.8(14)		

Table A-10.4. Anisotropic displacement parameters ($Å^2$ x 10^3) for Mo(dpma)(NBut)(=CHCMe2Ph)•pentane. The anisotropic displacement factor exponent takes the form: $-2\pi^2[h^2 a^{*2}U^{11} + ... + 2 h k a^* b^* U^{12}]$

	U^{11}	U^{22}	U^{33}	U^{23}	U^{13}	U^{12}
Mo(1)	45(1)	39(1)	35(1)	2(1)	5(1)	19(1)
Mo(2)	37(1)	39(1)	37(1)	-5(1)	6(1)	13(1)
N(1A)	54(6)	42(5)	38(5)	4(4)	9(4)	20(5)
N(2A)	78(7)	39(5)	39(5)	6(4)	16(5)	29(5)
N(3A)	40(5)	38(5)	34(5)	8(4)	1(4)	18(4)
N(4A)	60(6)	50(6)	50(6)	11(4)	24(5)	24(5)
N(1B)	44(5)	55(6)	42(6)	-2(4)	10(4)	18(5)
N(2B)	35(5)	46(5)	45(5)	3(4)	4(4)	14(4)
N(3B)	29(5)	46(5)	32(5)	-3(4)	6(4)	10(4)
N(4B)	41(5)	45(5)	44(5)	-9(4)	4(4)	14(4)
C(4A)	71(9)	85(9)	65(9)	32(7)	32(7)	50(8)
C(5A)	72(8)	42(7)	40(7)	6(5)	-3(6)	15(6)
C(11A)	76(9)	59(8)	57(9)	10(7)	23(7)	23(7)
C(12A)	66(8)	88(11)	61(9)	38(8)	18(7)	33(8)

C(13A)	108(11)	55(8)	88(11)	35(8)	34(9)	36(8)
C(14A)	110(12)	71(10)	40(8)	8(7)	15(8)	19(8)
C(21A)	169(16)	39(8)	74(10)	8(7)	60(11)	20(9)
C(22A)	121(12)	54(9)	75(10)	24(7)	48(9)	30(8)
C(23A)	103(10)	66(9)	42(7)	11(7)	24(7)	33(8)
C(24A)	88(9)	50(7)	50(8)	11(6)	21(7)	26(7)
C(31A)	230(20)	155(17)	76(12)	-35(11)	-31(14)	145(18)
C(32A)	240(20)	96(13)	116(15)	22(11)	104(17)	75(15)
C(33A)	109(15)	162(19)	151(18)	-108(15)	-19(13)	36(14)
C(41A)	101(13)	320(30)	94(14)	50(17)	28(11)	140(18)
C(42A)	210(20)	136(18)	350(40)	130(20)	170(20)	137(18)
C(43A)	111(14)	210(20)	138(16)	93(15)	90(13)	95(14)
C(51A)	118(12)	26(7)	91(11)	-5(7)	-29(10)	15(8)
C(52A)	55(8)	40(6)	35(7)	-7(5)	-4(6)	4(6)
C(53A)	112(12)	68(10)	104(13)	25(10)	56(11)	38(9)
C(54A)	250(30)	85(14)	63(14)	28(11)	67(16)	86(19)
C(55A)	230(30)	85(17)	63(13)	-25(11)	-43(18)	90(20)
C(56A)	61(11)	73(13)	150(20)	-56(12)	-47(12)	19(10)
C(57A)	49(9)	70(9)	81(10)	-20(8)	15(8)	6(7)
C(58A)	430(50)	200(30)	150(20)	-140(20)	-190(30)	260(30)
C(59A)	310(40)	107(16)	130(20)	65(16)	-80(20)	-60(20)
C(4B)	42(7)	56(7)	43(7)	-7(6)	-9(5)	5(6)
C(5B)	39(6)	41(6)	40(6)	-1(5)	6(5)	10(5)
C(11B)	57(7)	59(8)	45(7)	0(6)	16(6)	24(6)
C(12B)	55(8)	103(11)	34(7)	3(7)	18(6)	19(8)
C(13B)	47(7)	65(8)	51(7)	13(6)	19(6)	17(6)
C(14B)	43(6)	55(7)	41(7)	-3(6)	15(5)	17(6)
C(21B)	47(7)	53(7)	69(9)	15(6)	25(6)	14(6)
C(22B)	59(8)	77(9)	65(9)	33(7)	34(7)	34(7)
C(23B)	61(8)	71(9)	47(7)	15(6)	30(6)	41(7)
C(24B)	54(7)	51(7)	39(6)	4(5)	10(6)	32(6)
C(31B)	54(7)	51(7)	62(8)	-6(6)	11(6)	16(6)
C(32B)	54(7)	47(7)	52(8)	-6(5)	13(6)	20(6)
C(33B)	63(8)	51(7)	52(7)	0(6)	11(6)	26(6)
C(41B)	44(7)	79(9)	70(9)	-10(7)	-4(7)	6(7)
C(42B)	66(9)	93(10)	53(9)	-6(7)	-2(7)	22(8)
C(43B)	108(12)	80(11)	110(13)	-7(9)	-35(10)	50(10)
C(51B)	46(6)	37(6)	52(7)	-5(5)	8(5)	16(5)
C(52B)	45(6)	22(5)	52(7)	-4(5)	13(6)	8(5)
C(53B)	77(9)	65(8)	47(8)	18(6)	21(7)	37(7)
C(54B)	75(10)	96(11)	81(11)	32(9)	17(8)	57(9)

C(55B)	66(9)	65(9)	108(12)	23(8)	46(9)	45(7)
C(56B)	103(11)	57(8)	56(9)	5(6)	40(8)	28(8)
C(57B)	58(8)	49(7)	45(7)	8(6)	8(6)	16(6)
C(58B)	76(9)	60(8)	87(10)	27(7)	46(8)	23(7)
C(59B)	65(9)	74(9)	75(9)	-36(7)	-11(7)	29(7)
C(1S)	210(20)	122(16)	109(16)	37(13)	77(16)	85(17)
C(2S)	170(20)	170(20)	72(14)	16(15)	15(14)	1(19)
C(3S)	80(12)	168(19)	42(9)	-5(11)	14(8)	5(13)
C(4S)	85(11)	154(16)	65(10)	2(10)	10(8)	56(12)
C(5S)	50(7)	69(9)	33(7)	8(6)	10(6)	27(7)

Table A-10.5. Hydrogen coordinates (x 10^4) and isotropic displacement parameters ($Å^2$x 10^3) for Mo(dpma)(NBu^t)(=CHCMe$_2$Ph)•pentane.

	x	y	z	U(eq)		x	y	z	U(eq)
H(5A)	4195	2772	9628	71	H(5B)	3323	2822	5116	54
H(11A)	6816	4412	8749	80	H(11B)	2961	3140	2992	67
H(12A)	7438	6286	8720	85	H(12B)	4468	4742	2725	85
H(13A)	7787	7282	9994	98	H(13B)	5032	6313	3738	67
H(14A)	7960	5887	10469	100	H(21B)	-489	1858	5258	70
H(21A)	5444	1209	10953	119	H(22B)	-797	2709	6313	74
H(22A)	5093	1193	12141	100	H(23B)	791	4624	6675	64
H(23A)	5675	3043	12721	86	H(31A)	4504	5695	5273	74
H(24A)	6917	3651	11986	77	H(31B)	3938	6404	4912	74
H(31C)	7045	6330	11294	184	H(32A)	2701	5843	5951	65
H(31D)	5677	5446	10807	184	H(32B)	3403	5122	6047	65
H(32C)	5425	4580	11618	168	H(33A)	811	4861	4635	86
H(32D)	6762	5033	12208	168	H(33B)	1599	5206	4084	86
H(33D)	8706	5691	11242	260	H(33C)	1867	6043	4784	86
H(33E)	8429	4673	11560	260	H(41A)	-1472	407	3166	118
H(33F)	8471	5691	12008	260	H(41B)	-2498	815	2953	118
H(41D)	10023	4080	10857	236	H(41C)	-1669	1114	3767	118
H(41E)	9902	2975	10996	236	H(42A)	237	2409	2331	122
H(41F)	8980	3402	11201	236	H(42B)	-1061	1363	2037	122
H(42D)	7490	1219	10170	281	H(42C)	151	1335	2517	122
H(42E)	8856	1472	10113	281	H(43A)	-1155	3144	3547	167
H(42F)	7766	1289	9417	281	H(43B)	-1899	2607	2720	167
H(43D)	8487	3068	9093	197	H(43C)	-471	3477	2949	167
H(43E)	9791	3145	9534	197	H(53B)	4447	1150	5608	72

H(43F)	9456	4087	9710	197	H(54B)	6347	1344	5504	93
H(53A)	4833	2626	8015	110	H(55B)	6893	1650	4474	85
H(54A)	3867	3121	7103	152	H(56B)	5498	1777	3509	88
H(55A)	1742	2514	6794	166	H(57B)	3566	1670	3620	66
H(56A)	567	1468	7394	146	H(58A)	2799	1363	5799	109
H(57A)	1611	1002	8406	94	H(58B)	2206	181	5351	109
H(58D)	4279	453	8403	428	H(58C)	1342	756	5367	109
H(58E)	5212	934	9200	428	H(59A)	591	337	4082	124
H(58F)	5431	1600	8604	428	H(59C)	1471	-156	3902	124
H(59D)	2671	40	8926	392	H(59B)	1462	820	3592	124
H(59E)	2587	961	9412	392	H(3S1)	6711	2997	7402	142
H(59F)	3642	611	9708	392	H(3S2)	7196	2911	6721	142
H(1S1)	8465	975	7632	209	H(4S1)	8588	4607	8016	157
H(1S2)	7073	37	7357	209	H(4S2)	8060	4752	7239	157
H(1S3)	7560	810	8126	209	H(4S3)	9217	4486	7405	157
H(2S1)	6942	1206	6790	202	H(5S1)	8192	2750	8023	62
H(2S2)	6367	1313	7424	202	H(5S2)	8665	2656	7342	62

Table A-11.1. Crystal data and structure refinement for Mo(dmpm)(Ndip)(=CHCMe$_2$Ph).

Identification code	at9a	
Empirical formula	$C_{33}H_{41}MoN_3$	
Formula weight	575.63	
Temperature	173(2) K	
Wavelength	0.71073 Å	
Crystal system	Orthorhombic	
Space group	Pna2(1)	
Unit cell dimensions	a = 26.218(6) Å	α= 90°
	b = 11.061(2) Å	β= 90°
	c = 10.104(2) Å	γ = 90°
Volume	2930.3(11) Å^3	
Z	4	
Density (calculated)	1.305 Mg/m^3	
Absorption coefficient	0.473 mm^{-1}	
F(000)	1208	
Crystal size	0.14 x 0.18 x 0.21 mm^3	
Theta range for data collection	1.55 to 23.27°.	
Index ranges	-26<=h<=29, -11<=k<=12, -11<=l<=11	
Reflections collected	12902	
Independent reflections	4192 [R(int) = 0.1590]	
Completeness to theta = 23.27°	99.7 %	
Absorption correction	Empirical	
Max. and min. transmission	0.8150 and 0.6157	
Refinement method	Full-matrix least-squares on F^2	
Data / restraints / parameters	4192 / 1 / 343	
Goodness-of-fit on F^2	0.853	
Final R indices [I>2sigma(I)]	R1 = 0.0571, wR2 = 0.0876	
R indices (all data)	R1 = 0.1281, wR2 = 0.1034	
Absolute structure parameter	-0.01(7)	
Extinction coefficient	0.00014(12)	
Largest diff. peak and hole	0.458 and -0.367 e.Å^{-3}	

Table A-11.2. Atomic coordinates (x 10^4) and equivalent isotropic displacement parameters ($Å^2$ x 10^3) for Mo(dmpm)(Ndip)(=CHCMe$_2$Ph). U(eq) is defined as one third of the trace of the orthogonalized U^{ij} tensor.

	x	y	z	U(eq)		x	y	z	U(eq)
Mo(1)	540(1)	3532(1)	3604(1)	21(1)	C(44)	1971(4)	-42(10)	5695(13)	47(4)
N(1)	-240(3)	4578(6)	3770(12)	23(2)	C(45)	1901(4)	992(10)	6411(11)	43(3)
N(2)	227(3)	2747(6)	1916(8)	22(2)	C(46)	1587(4)	1898(8)	5896(10)	23(3)
N(4)	1026(3)	2573(6)	4103(6)	16(2)	C(51)	1458(4)	5287(8)	2618(10)	21(3)
C(5)	915(3)	4846(8)	2823(9)	24(3)	C(52)	1833(4)	4211(9)	2602(11)	29(3)
C(11)	46(4)	4917(9)	4803(11)	30(3)	C(53)	1817(4)	3424(10)	1527(12)	45(3)
C(12)	126(4)	3968(10)	5681(10)	34(3)	C(54)	2161(5)	2465(10)	1476(15)	59(4)
C(13)	-135(5)	2960(11)	5180(11)	30(3)	C(55)	2499(5)	2248(11)	2481(19)	76(6)
C(14)	-350(3)	3373(9)	3995(8)	23(3)	C(56)	2519(4)	3054(11)	3460(20)	60(4)
C(21)	450(4)	2413(7)	733(9)	21(2)	C(57)	2191(3)	4039(8)	3623(19)	46(3)
C(22)	108(4)	1823(8)	-57(10)	26(3)	C(58)	1572(4)	6185(8)	3759(18)	52(4)
C(23)	-355(4)	1806(8)	658(10)	36(3)	C(59)	1492(4)	5957(9)	1307(10)	45(3)
C(24)	-266(4)	2349(10)	1814(12)	27(3)	C(421)	1208(4)	479(9)	2606(11)	33(3)
C(30)	-628(4)	2620(8)	2969(10)	27(3)	C(422)	1535(4)	-300(8)	1628(11)	37(3)
C(31)	-822(3)	1421(8)	3560(20)	49(3)	C(423)	678(3)	-68(8)	2671(10)	43(3)
C(32)	-1098(4)	3351(9)	2485(9)	41(3)	C(461)	1485(4)	3033(8)	6683(9)	27(3)
C(41)	1352(4)	1701(9)	4651(10)	22(3)	C(462)	1964(4)	3584(9)	7278(10)	50(3)
C(42)	1450(4)	628(9)	3916(11)	23(4)	C(463)	1105(4)	2751(9)	7786(10)	55(4)
C(43)	1762(4)	-229(9)	4485(11)	35(3)					

Table A-11.3. Bond lengths [Å] and angles [°] for Mo(dmpm)(Ndip)(=CHCMe$_2$Ph).

Mo(1)-N(4)	1.731(7)	C(30)-C(32)	1.553(12)
Mo(1)-C(5)	1.924(9)	C(41)-C(46)	1.418(13)
Mo(1)-N(2)	2.082(8)	C(41)-C(42)	1.423(13)
Mo(1)-C(11)	2.344(9)	C(42)-C(43)	1.379(12)
Mo(1)-N(1)	2.357(6)	C(42)-C(421)	1.477(15)
Mo(1)-C(14)	2.375(8)	C(43)-C(44)	1.354(14)
Mo(1)-C(12)	2.413(10)	C(44)-C(45)	1.366(14)
Mo(1)-C(13)	2.464(12)	C(45)-C(46)	1.397(12)
N(1)-C(11)	1.339(14)	C(46)-C(461)	1.509(12)
N(1)-C(14)	1.383(10)	C(51)-C(59)	1.521(12)

N(2)-C(24)	1.371(11)	C(51)-C(52)	1.545(13)
N(2)-C(21)	1.380(11)	C(51)-C(58)	1.551(16)
N(4)-C(41)	1.403(10)	C(52)-C(53)	1.392(13)
C(5)-C(51)	1.519(12)	C(52)-C(57)	1.407(17)
C(11)-C(12)	1.389(12)	C(53)-C(54)	1.393(14)
C(12)-C(13)	1.403(14)	C(54)-C(55)	1.369(17)
C(13)-C(14)	1.400(12)	C(55)-C(56)	1.33(2)
C(14)-C(30)	1.515(11)	C(56)-C(57)	1.399(13)
C(21)-C(22)	1.366(11)	C(421)-C(423)	1.516(12)
C(22)-C(23)	1.413(12)	C(421)-C(422)	1.568(12)
C(23)-C(24)	1.334(14)	C(461)-C(462)	1.518(12)
C(24)-C(30)	1.533(14)	C(461)-C(463)	1.527(12)
C(30)-C(31)	1.540(12)		
N(4)-Mo(1)-C(5)	102.0(4)	N(1)-C(14)-Mo(1)	72.3(4)
N(4)-Mo(1)-N(2)	105.9(3)	C(13)-C(14)-Mo(1)	76.7(6)
C(5)-Mo(1)-N(2)	100.4(3)	C(30)-C(14)-Mo(1)	113.5(6)
N(4)-Mo(1)-C(11)	131.0(4)	C(22)-C(21)-N(2)	110.9(9)
C(5)-Mo(1)-C(11)	90.0(3)	C(21)-C(22)-C(23)	105.7(9)
N(2)-Mo(1)-C(11)	118.6(4)	C(24)-C(23)-C(22)	107.0(9)
N(4)-Mo(1)-N(1)	156.6(4)	C(23)-C(24)-N(2)	112.0(10)
C(5)-Mo(1)-N(1)	95.8(3)	C(23)-C(24)-C(30)	130.3(10)
N(2)-Mo(1)-N(1)	85.5(4)	N(2)-C(24)-C(30)	117.6(10)
C(11)-Mo(1)-N(1)	33.1(3)	C(14)-C(30)-C(24)	109.4(8)
N(4)-Mo(1)-C(14)	129.0(3)	C(14)-C(30)-C(31)	111.6(10)
C(5)-Mo(1)-C(14)	128.8(4)	C(24)-C(30)-C(31)	109.2(9)
N(2)-Mo(1)-C(14)	73.6(3)	C(14)-C(30)-C(32)	108.1(8)
C(11)-Mo(1)-C(14)	54.5(3)	C(24)-C(30)-C(32)	110.6(8)
N(1)-Mo(1)-C(14)	34.0(3)	C(31)-C(30)-C(32)	107.9(8)
N(4)-Mo(1)-C(12)	101.5(3)	N(4)-C(41)-C(46)	120.6(9)
C(5)-Mo(1)-C(12)	115.8(4)	N(4)-C(41)-C(42)	118.5(9)
N(2)-Mo(1)-C(12)	128.2(3)	C(46)-C(41)-C(42)	120.9(9)
C(11)-Mo(1)-C(12)	33.9(3)	C(43)-C(42)-C(41)	117.5(10)
N(1)-Mo(1)-C(12)	56.5(4)	C(43)-C(42)-C(421)	123.5(11)
C(14)-Mo(1)-C(12)	55.0(3)	C(41)-C(42)-C(421)	118.9(10)
N(4)-Mo(1)-C(13)	100.5(3)	C(44)-C(43)-C(42)	120.8(11)
C(5)-Mo(1)-C(13)	145.7(4)	C(43)-C(44)-C(45)	123.5(11)
N(2)-Mo(1)-C(13)	98.0(4)	C(44)-C(45)-C(46)	118.8(11)
C(11)-Mo(1)-C(13)	55.7(4)	C(45)-C(46)-C(41)	118.4(9)
N(1)-Mo(1)-C(13)	57.0(3)	C(45)-C(46)-C(461)	120.3(10)
C(14)-Mo(1)-C(13)	33.6(3)	C(41)-C(46)-C(461)	121.2(9)

C(12)-Mo(1)-C(13)	33.4(3)	C(5)-C(51)-C(59)	109.3(8)
C(11)-N(1)-C(14)	105.0(9)	C(5)-C(51)-C(52)	110.5(8)
C(11)-N(1)-Mo(1)	72.9(5)	C(59)-C(51)-C(52)	109.2(8)
C(14)-N(1)-Mo(1)	73.7(4)	C(5)-C(51)-C(58)	106.6(8)
C(24)-N(2)-C(21)	104.4(8)	C(59)-C(51)-C(58)	108.9(8)
C(24)-N(2)-Mo(1)	124.6(7)	C(52)-C(51)-C(58)	112.2(8)
C(21)-N(2)-Mo(1)	130.8(7)	C(53)-C(52)-C(57)	120.5(11)
C(41)-N(4)-Mo(1)	169.7(6)	C(53)-C(52)-C(51)	118.1(10)
C(51)-C(5)-Mo(1)	141.0(7)	C(57)-C(52)-C(51)	121.4(10)
N(1)-C(11)-C(12)	111.8(9)	C(52)-C(53)-C(54)	119.1(12)
N(1)-C(11)-Mo(1)	74.0(5)	C(55)-C(54)-C(53)	121.6(13)
C(12)-C(11)-Mo(1)	75.7(6)	C(56)-C(55)-C(54)	117.4(14)
C(11)-C(12)-C(13)	107.3(10)	C(55)-C(56)-C(57)	125.7(17)
C(11)-C(12)-Mo(1)	70.3(6)	C(56)-C(57)-C(52)	115.4(16)
C(13)-C(12)-Mo(1)	75.3(7)	C(42)-C(421)-C(423)	113.6(10)
C(14)-C(13)-C(12)	104.2(10)	C(42)-C(421)-C(422)	113.0(9)
C(14)-C(13)-Mo(1)	69.7(6)	C(423)-C(421)-C(422)	108.1(8)
C(12)-C(13)-Mo(1)	71.3(7)	C(46)-C(461)-C(462)	113.3(8)
N(1)-C(14)-C(13)	111.8(10)	C(46)-C(461)-C(463)	109.2(8)
N(1)-C(14)-C(30)	121.2(9)	C(462)-C(461)-C(463)	109.3(8)
C(13)-C(14)-C(30)	126.8(10)		

Table A-11.4. Anisotropic displacement parameters ($Å^2$ x 10^3) for Mo(dmpm)(Ndip)(=CHCMe$_2$Ph). The anisotropic displacement factor exponent takes the form: $-2\pi^2[h^2 a^{*2}U^{11} + ... + 2 h k a^* b^* U^{12}]$

	U^{11}	U^{22}	U^{33}	U^{23}	U^{13}	U^{12}
Mo(1)	20(1)	21(1)	22(1)	-1(1)	0(1)	3(1)
N(1)	17(4)	20(4)	31(6)	3(6)	-3(6)	4(3)
N(2)	29(6)	12(5)	27(6)	2(4)	11(5)	-9(4)
N(4)	17(5)	12(4)	20(5)	3(3)	2(4)	1(4)
C(5)	11(6)	32(7)	29(6)	0(5)	-1(5)	7(5)
C(11)	21(7)	34(7)	36(8)	-12(6)	11(6)	-3(5)
C(12)	32(7)	50(8)	20(7)	14(6)	3(6)	20(6)
C(13)	30(9)	42(9)	18(8)	5(7)	-8(6)	15(7)
C(14)	6(5)	35(7)	28(9)	1(6)	2(4)	-5(5)
C(21)	20(7)	24(6)	20(6)	3(5)	-2(6)	1(5)
C(22)	25(7)	30(7)	22(7)	5(5)	3(6)	5(5)

C(23)	28(7)	46(8)	34(7)	-5(6)	-2(6)	-17(5)
C(24)	19(7)	38(8)	24(8)	2(6)	4(6)	-4(6)
C(30)	11(7)	33(6)	38(7)	4(5)	3(5)	-6(5)
C(31)	47(6)	53(6)	48(6)	19(11)	21(12)	-19(6)
C(32)	31(7)	66(9)	26(6)	-4(7)	-8(5)	-2(7)
C(41)	24(6)	15(7)	26(6)	10(5)	2(5)	-5(5)
C(42)	6(6)	24(6)	40(12)	-2(6)	-10(6)	-4(5)
C(43)	31(7)	18(7)	57(9)	-2(6)	-4(7)	3(6)
C(44)	43(9)	30(8)	68(10)	11(8)	-11(8)	12(6)
C(45)	48(8)	39(8)	44(8)	11(7)	-17(7)	6(6)
C(46)	15(6)	23(7)	31(7)	-1(5)	4(5)	-5(5)
C(51)	25(7)	20(6)	19(6)	2(5)	3(5)	1(5)
C(52)	27(7)	20(6)	40(8)	6(6)	14(6)	-10(6)
C(53)	38(8)	30(7)	67(9)	7(8)	12(7)	-17(7)
C(54)	45(9)	20(8)	111(14)	-11(8)	39(9)	5(7)
C(55)	36(10)	30(9)	162(18)	46(10)	29(11)	9(8)
C(56)	35(7)	62(8)	81(11)	36(14)	0(13)	0(7)
C(57)	25(6)	60(7)	55(8)	25(14)	20(12)	-4(5)
C(58)	45(6)	47(7)	63(10)	-14(9)	-10(10)	-2(5)
C(59)	33(8)	45(8)	57(9)	6(6)	-6(6)	-2(6)
C(421)	28(8)	23(7)	47(9)	8(6)	6(6)	-1(6)
C(422)	32(8)	20(7)	60(9)	-3(6)	-2(7)	1(6)
C(423)	43(8)	40(7)	46(7)	23(6)	-10(6)	-18(6)
C(461)	21(6)	35(7)	23(7)	11(6)	-1(5)	-3(5)
C(462)	53(8)	50(7)	47(8)	-12(7)	-4(6)	2(7)
C(463)	67(9)	47(8)	50(8)	19(6)	-3(7)	0(7)

Table A-11.5. Hydrogen coordinates (x 10^4) and isotropic displacement parameters ($Å^2$x 10^3) for Mo(dmpm)(Ndip)(=CHCMe$_2$Ph).

	x	y	z	U(eq)		x	y	z	U(eq)
H(5)	688	5394	2445	29	H(58A)	1317	6808	3769	77
H(11)	176	5692	4919	36	H(58C)	1902	6542	3625	77
H(12)	316	3997	6456	41	H(52B)	1568	5761	4588	77
H(13)	-160	2192	5550	36	H(59A)	1374	5441	607	67
H(21)	787	2569	505	25	H(59B)	1840	6183	1143	67
H(22)	168	1499	-892	31	H(59C)	1284	6670	1343	67
H(23)	-663	1478	376	43	H(421)	1174	1286	2217	39

H(31A)	-537	909	3759	74	H(42A)	1885	-44	1670	56
H(31B)	-1038	1024	2925	74	H(42B)	1410	-196	743	56
H(31C)	-1011	1581	4350	74	H(42C)	1512	-1137	1872	56
H(32A)	-1308	3559	3229	61	H(42D)	704	-913	2879	64
H(32B)	-1291	2870	1874	61	H(42E)	512	28	1831	64
H(32C)	-984	4076	2052	61	H(42F)	483	334	3345	64
H(43)	1831	-943	4034	42	H(461)	1330	3631	6091	32
H(44)	2172	-650	6057	57	H(46A)	2098	3051	7942	75
H(45)	2060	1092	7226	52	H(46B)	1882	4349	7671	75
H(53)	1580	3537	854	54	H(46C)	2214	3699	6596	75
H(54)	2160	1959	741	70	H(46D)	1266	2246	8437	82
H(55)	2707	1566	2479	91	H(46E)	816	2338	7422	82
H(56)	2774	2951	4091	72	H(46F)	996	3491	8193	82
H(57)	2208	4546	4356	56					

Table A-12.1. Crystal data and structure refinement for Ru(dpma)(PCy_3)(=CHCH=CMe_2) •toluene.

Identification code	jtcx9t	
Empirical formula	$C_{41}H_{62}N_3PRu$	
Formula weight	728.98	
Temperature	173(2) K	
Wavelength	0.71073 Å	
Crystal system	Triclinic	
Space group	P-1	
Unit cell dimensions	a = 9.6514(12) Å	α= 69.938(2)°
	b = 13.3909(16) Å	β= 76.147(2)°
	c = 19.128(2) Å	γ = 74.182(2)°
Volume	2204.9(5) $Å^3$	
Z	2	
Density (calculated)	1.098 Mg/m^3	
Absorption coefficient	0.419 mm^{-1}	
F(000)	776	
Crystal size	0.19 x 0.23 x 0.56 mm^3	
Theta range for data collection	1.66 to 23.26°	
Index ranges	-10<=h<=10, -14<=k<=14, -21<=l<=21	
Reflections collected	19115	
Independent reflections	6339 [R(int) = 0.0608]	
Completeness to theta = 23.26°	99.9 %	
Absorption correction	Empirical	
Max. and min. transmission	0.9193 and 0.8148	
Refinement method	Full-matrix least-squares on F^2	
Data / restraints / parameters	6339 / 0 / 416	
Goodness-of-fit on F^2	1.121	
Final R indices [I>2sigma(I)]	R1 = 0.0980, wR2 = 0.2979	
R indices (all data)	R1 = 0.1251, wR2 = 0.3206	
Extinction coefficient	0.009(2)	
Largest diff. peak and hole	3.625 and -0.489 $e.Å^{-3}$	

Table A-12.2. Atomic coordinates (x 10^4) and equivalent isotropic displacement parameters ($Å^2$ x 10^3) for Ru(dpma)(PCy_3)(=CHCH=CMe_2)•toluene. U(eq) is defined as one third of the trace of the orthogonalized U^{ij} tensor.

	x	y	z	U(eq)		x	y	z	U(eq)
Ru	7369(1)	-613(1)	7031(1)	31(1)	C(113)	9367(18)	-2200(30)	9212(11)	164(14)
P	6109(3)	10(2)	8043(1)	31(1)	C(114)	8750(40)	-3169(17)	9515(11)	156(14)
N(1)	6205(12)	-1798(8)	7205(5)	47(2)	C(115)	7180(30)	-2881(11)	9776(9)	96(7)
N(2)	9101(9)	191(7)	6724(5)	36(2)	C(116)	6370(20)	-2078(12)	9141(9)	93(6)
N(3)	9026(11)	-1727(7)	6546(5)	43(2)	C(121)	6473(14)	1291(9)	8053(6)	42(3)
C(1)	6253(12)	320(9)	6306(6)	40(3)	C(122)	5715(16)	2295(10)	7519(7)	60(4)
C(2)	6497(13)	1309(9)	5751(6)	42(3)	C(123)	6240(30)	3282(11)	7437(8)	96(7)
C(3)	5721(11)	1914(10)	5183(6)	40(3)	C(124)	6000(30)	3475(12)	8195(9)	128(9)
C(4)	6098(16)	2966(11)	4664(8)	65(4)	C(125)	6810(30)	2494(12)	8744(9)	97(7)
C(5)	4500(15)	1631(14)	5021(9)	80(5)	C(126)	6311(19)	1481(11)	8840(7)	69(4)
C(11)	4803(16)	-1892(12)	7286(7)	58(4)	C(131)	4144(12)	-10(13)	8344(6)	59(4)
C(12)	4720(20)	-2838(15)	7221(8)	82(5)	C(132)	3492(14)	217(19)	9104(7)	96(7)
C(13)	6160(30)	-3403(13)	7095(8)	90(7)	C(133)	1976(17)	-110(30)	9366(8)	165(14)
C(14)	7049(18)	-2738(11)	7080(7)	58(4)	C(134)	953(16)	600(30)	8788(9)	150(12)
C(21)	9365(12)	1213(10)	6520(6)	41(3)	C(135)	1613(14)	470(20)	8021(8)	103(8)
C(22)	10817(13)	1206(13)	6193(6)	54(3)	C(136)	3142(13)	693(14)	7757(7)	65(4)
C(23)	11489(13)	136(13)	6197(7)	57(4)	C(80S)	2030(30)	4280(20)	6999(14)	124(10)
C(24)	10433(11)	-453(10)	6518(6)	42(3)	C(81S)	2460(30)	4917(18)	7259(14)	121(8)
C(31)	8676(19)	-2842(10)	6951(7)	70(5)	C(82S)	1830(20)	5040(20)	8023(18)	126(9)
C(32)	10434(13)	-1618(10)	6653(7)	54(3)	C(83S)	820(40)	4708(19)	8385(15)	140(10)
C(33)	9012(15)	-1448(10)	5722(6)	52(3)	C(84S)	320(50)	4070(30)	8040(30)	310(40)
C(111)	6970(11)	-1031(8)	8831(6)	36(2)	C(85S)	810(30)	3900(30)	7340(20)	171(15)
C(112)	8593(15)	-1272(15)	8569(8)	92(6)	C(86S)	2750(50)	4010(30)	6346(16)	240(20)

Table A-12.3. Bond lengths [Å] and angles [°] for Ru(dpma)(PCy_3)(=CHCH=CMe_2) •toluene.

Ru-C(1)	1.854(11)	C(24)-C(32)	1.491(18)
Ru-N(1)	2.078(10)	C(111)-C(112)	1.507(17)
Ru-N(2)	2.092(9)	C(111)-C(116)	1.539(17)
Ru-N(3)	2.141(9)	C(112)-C(113)	1.58(2)
Ru-P	2.313(3)	C(113)-C(114)	1.45(4)

P-C(121)	1.849(11)	C(114)-C(115)	1.46(3)
P-C(131)	1.850(12)	C(115)-C(116)	1.535(19)
P-C(111)	1.852(10)	C(121)-C(122)	1.505(16)
N(1)-C(11)	1.360(16)	C(121)-C(126)	1.576(16)
N(1)-C(14)	1.364(17)	C(122)-C(123)	1.49(2)
N(2)-C(21)	1.366(14)	C(123)-C(124)	1.51(2)
N(2)-C(24)	1.391(14)	C(124)-C(125)	1.52(2)
N(3)-C(32)	1.474(16)	C(125)-C(126)	1.50(2)
N(3)-C(33)	1.492(14)	C(131)-C(132)	1.536(18)
N(3)-C(31)	1.516(16)	C(131)-C(136)	1.543(17)
C(1)-C(2)	1.423(15)	C(132)-C(133)	1.56(2)
C(2)-C(3)	1.361(15)	C(133)-C(134)	1.55(3)
C(3)-C(5)	1.458(18)	C(134)-C(135)	1.50(2)
C(3)-C(4)	1.500(17)	C(135)-C(136)	1.517(18)
C(11)-C(12)	1.34(2)	C(80S)-C(81S)	1.32(3)
C(12)-C(13)	1.40(3)	C(80S)-C(85S)	1.34(4)
C(13)-C(14)	1.38(2)	C(80S)-C(86S)	1.39(4)
C(14)-C(31)	1.51(2)	C(81S)-C(82S)	1.49(4)
C(21)-C(22)	1.391(16)	C(82S)-C(83S)	1.15(3)
C(22)-C(23)	1.40(2)	C(83S)-C(84S)	1.47(5)
C(23)-C(24)	1.359(17)	C(84S)-C(85S)	1.38(5)
C(1)-Ru-N(1)	89.5(4)	C(21)-C(22)-C(23)	107.4(12)
C(1)-Ru-N(2)	98.2(4)	C(24)-C(23)-C(22)	105.9(11)
N(1)-Ru-N(2)	160.6(4)	C(23)-C(24)-N(2)	111.7(11)
C(1)-Ru-N(3)	109.1(4)	C(23)-C(24)-C(32)	132.2(11)
N(1)-Ru-N(3)	80.4(4)	N(2)-C(24)-C(32)	116.1(10)
N(2)-Ru-N(3)	80.2(4)	C(14)-C(31)-N(3)	108.9(10)
C(1)-Ru-P	98.7(3)	N(3)-C(32)-C(24)	110.3(9)
N(1)-Ru-P	97.4(3)	C(112)-C(111)-C(116)	111.2(13)
N(2)-Ru-P	99.0(2)	C(112)-C(111)-P	108.1(8)
N(3)-Ru-P	152.0(3)	C(116)-C(111)-P	114.2(8)
C(121)-P-C(131)	110.8(7)	C(111)-C(112)-C(113)	109.8(12)
C(121)-P-C(111)	103.6(5)	C(114)-C(113)-C(112)	115(2)
C(131)-P-C(111)	103.8(5)	C(113)-C(114)-C(115)	110.3(15)
C(121)-P-Ru	115.7(4)	C(114)-C(115)-C(116)	112.1(16)
C(131)-P-Ru	119.0(5)	C(115)-C(116)-C(111)	109.2(12)
C(111)-P-Ru	101.4(3)	C(122)-C(121)-C(126)	109.9(10)
C(11)-N(1)-C(14)	105.4(11)	C(122)-C(121)-P	114.1(9)
C(11)-N(1)-Ru	139.4(9)	C(126)-C(121)-P	118.1(8)
C(14)-N(1)-Ru	114.0(9)	C(123)-C(122)-C(121)	112.4(13)

C(21)-N(2)-C(24)	105.1(9)	C(122)-C(123)-C(124)	110.2(14)
C(21)-N(2)-Ru	140.8(7)	C(123)-C(124)-C(125)	110.2(14)
C(24)-N(2)-Ru	112.7(7)	C(126)-C(125)-C(124)	111.3(16)
C(32)-N(3)-C(33)	108.9(9)	C(125)-C(126)-C(121)	110.7(11)
C(32)-N(3)-C(31)	114.2(10)	C(132)-C(131)-C(136)	109.6(11)
C(33)-N(3)-C(31)	110.0(9)	C(132)-C(131)-P	114.3(9)
C(32)-N(3)-Ru	106.6(7)	C(136)-C(131)-P	116.1(9)
C(33)-N(3)-Ru	110.9(7)	C(131)-C(132)-C(133)	107.6(13)
C(31)-N(3)-Ru	106.2(7)	C(134)-C(133)-C(132)	109.6(17)
C(2)-C(1)-Ru	129.5(9)	C(135)-C(134)-C(133)	110.3(16)
C(3)-C(2)-C(1)	127.3(11)	C(134)-C(135)-C(136)	113.1(14)
C(2)-C(3)-C(5)	125.2(11)	C(135)-C(136)-C(131)	111.0(12)
C(2)-C(3)-C(4)	120.1(11)	C(81S)-C(80S)-C(85S)	120(3)
C(5)-C(3)-C(4)	114.7(11)	C(81S)-C(80S)-C(86S)	122(3)
C(12)-C(11)-N(1)	112.4(16)	C(85S)-C(80S)-C(86S)	117(3)
C(11)-C(12)-C(13)	105.8(15)	C(80S)-C(81S)-C(82S)	122(2)
C(14)-C(13)-C(12)	106.9(14)	C(83S)-C(82S)-C(81S)	123(3)
N(1)-C(14)-C(13)	109.5(16)	C(82S)-C(83S)-C(84S)	113(3)
N(1)-C(14)-C(31)	116.7(11)	C(85S)-C(84S)-C(83S)	129(3)
C(13)-C(14)-C(31)	133.9(15)	C(80S)-C(85S)-C(84S)	112(3)
N(2)-C(21)-C(22)	110.0(11)		

Table A-12.4. Anisotropic displacement parameters ($Å^2$ x 10^3) for Ru(dpma)(PCy_3)(=CHCH=CMe_2)•toluene. The anisotropic displacement factor exponent takes the form: $-2\pi^2[h^2 a^{*2}U^{11} + ... + 2 h k a^* b^* U^{12}]$

	U^{11}	U^{22}	U^{33}	U^{23}	U^{13}	U^{12}
Ru	34(1)	34(1)	25(1)	-10(1)	-3(1)	-7(1)
P	29(1)	37(2)	23(1)	-6(1)	-4(1)	-6(1)
N(1)	67(7)	39(6)	35(5)	-9(4)	-8(5)	-17(5)
N(2)	31(5)	50(6)	29(5)	-18(4)	-2(4)	-6(4)
N(3)	55(6)	43(6)	30(5)	-18(4)	-5(4)	0(5)
C(1)	36(6)	53(7)	32(6)	-18(5)	5(5)	-12(5)
C(2)	50(7)	45(7)	31(6)	-6(5)	-10(5)	-13(5)
C(3)	32(6)	54(7)	34(6)	-17(5)	-2(5)	-6(5)
C(4)	73(9)	57(9)	49(8)	10(7)	-22(7)	-10(7)
C(5)	51(8)	98(12)	67(10)	21(9)	-19(7)	-25(8)
C(11)	78(10)	72(9)	38(7)	-3(6)	-9(6)	-56(8)

C(12)	128(16)	96(13)	45(9)	-20(9)	-1(9)	-75(13)
C(13)	200(20)	46(9)	49(9)	-11(7)	-4(11)	-76(12)
C(14)	94(11)	50(8)	32(7)	-5(6)	-10(7)	-27(8)
C(21)	41(6)	52(7)	35(6)	-9(5)	-5(5)	-23(6)
C(22)	45(7)	92(11)	32(6)	-15(7)	1(5)	-34(7)
C(23)	34(7)	96(11)	38(7)	-19(7)	-4(5)	-13(7)
C(24)	28(6)	65(8)	29(6)	-19(6)	0(5)	0(6)
C(31)	134(15)	25(7)	40(7)	-11(6)	-22(8)	7(7)
C(32)	44(7)	59(8)	44(7)	-19(6)	-7(6)	17(6)
C(33)	71(9)	46(7)	34(6)	-13(6)	-6(6)	-4(6)
C(111)	36(6)	34(6)	35(6)	-8(5)	-8(5)	-4(5)
C(112)	46(8)	112(13)	54(9)	15(9)	-4(7)	32(9)
C(113)	46(10)	270(30)	59(12)	31(16)	-20(8)	52(15)
C(114)	260(30)	85(15)	47(11)	-12(10)	-42(15)	96(19)
C(115)	220(20)	21(7)	60(10)	15(7)	-78(13)	-23(10)
C(116)	167(18)	53(9)	74(11)	19(8)	-70(12)	-53(11)
C(121)	57(7)	36(6)	28(6)	-8(5)	-1(5)	-10(5)
C(122)	83(10)	40(7)	38(7)	-6(6)	1(7)	0(7)
C(123)	200(20)	32(8)	46(8)	-5(6)	-20(11)	-11(10)
C(124)	280(30)	33(8)	57(10)	-7(7)	-32(14)	-21(12)
C(125)	200(20)	55(10)	56(9)	-21(8)	-38(12)	-37(11)
C(126)	109(12)	50(8)	36(7)	-13(6)	1(7)	-10(8)
C(131)	28(6)	110(12)	29(6)	-11(7)	-6(5)	-10(7)
C(132)	33(7)	220(20)	33(7)	-46(10)	5(6)	-14(10)
C(133)	45(9)	420(40)	22(8)	-54(15)	14(7)	-69(16)
C(134)	31(8)	350(40)	53(10)	-69(16)	4(7)	-19(14)
C(135)	32(7)	240(20)	37(8)	-34(11)	-8(6)	-35(11)
C(136)	32(6)	127(13)	28(6)	-18(7)	-1(5)	-13(7)
C(80S)	150(20)	115(18)	114(19)	-63(15)	-85(18)	53(16)
C(81S)	123(18)	109(17)	124(18)	-48(15)	46(15)	-53(14)
C(82S)	65(13)	111(18)	170(30)	-9(17)	-18(15)	-15(12)
C(83S)	170(30)	75(15)	130(20)	1(14)	0(20)	-9(16)
C(84S)	290(50)	210(40)	430(70)	-190(50)	260(50)	-190(40)
C(85S)	73(15)	200(30)	280(40)	-130(30)	10(20)	-48(18)
C(86S)	410(60)	170(30)	120(20)	-40(20)	-160(30)	90(30)

Table A-12.5. Hydrogen coordinates (x 10^4) and isotropic displacement parameters ($Å^2$ x 10^3) for Ru(dpma)(PCy_3)(=CHCH=CMe_2)•toluene.

	x	y	z	U(eq)		x	y	z	U(eq)
H(1A)	5410	111	6306	48	H(11O)	6493	-2400	8740	111
H(2A)	7275	1571	5778	50	H(12B)	7512	1248	7846	50
H(4A)	6895	3100	4814	97	H(12C)	5874	2184	7029	72
H(4B)	5266	3548	4688	97	H(12D)	4674	2411	7703	72
H(4C)	6376	2923	4156	97	H(12E)	5725	3908	7091	116
H(5A)	4328	952	5378	121	H(12F)	7276	3187	7229	116
H(5B)	4727	1563	4520	121	H(12G)	4969	3601	8392	153
H(5C)	3642	2189	5059	121	H(12H)	6357	4115	8136	153
H(11A)	3993	-1360	7377	70	H(12I)	7847	2396	8560	117
H(12A)	3875	-3072	7254	98	H(12J)	6633	2623	9230	117
H(13A)	6465	-4093	7032	108	H(12K)	5298	1543	9081	82
H(21A)	8675	1823	6590	49	H(12L)	6888	863	9163	82
H(22A)	11261	1801	6007	65	H(13B)	4079	-761	8428	71
H(23A)	12460	-118	6016	68	H(13C)	3381	981	9047	115
H(31A)	9153	-3331	6649	84	H(13D)	4129	-206	9473	115
H(31B)	9030	-3139	7430	84	H(13E)	2093	-870	9411	198
H(32A)	11216	-1910	6305	65	H(13F)	1552	-8	9857	198
H(32B)	10605	-2032	7162	65	H(13G)	16	389	8946	180
H(33A)	9762	-1958	5517	78	H(13H)	794	1359	8765	180
H(33B)	9188	-728	5473	78	H(13I)	993	965	7659	124
H(33C)	8079	-1480	5646	78	H(13J)	1643	-264	8032	124
H(11E)	6792	-712	9244	43	H(13K)	3102	1456	7675	78
H(11F)	8972	-621	8446	110	H(13L)	3544	536	7281	78
H(11G)	8797	-1499	8118	110	H(80S)	3174	5298	6958	145
H(11H)	10390	-2411	9012	197	H(81S)	2271	5409	8216	151
H(11I)	9314	-1916	9620	197	H(82S)	373	4830	8844	168
H(11J)	9227	-3673	9933	187	H(83S)	-430	3725	8339	374
H(11K)	8918	-3526	9130	187	H(84S)	344	3577	7132	206
H(11L)	7026	-2559	10180	116	H(86A)	3577	4354	6141	365
H(11M)	6789	-3535	9978	116	H(86B)	2102	4262	5984	365
H(11N)	5331	-1910	9333	111	H(86C)	3082	3238	6462	365

Table A-13.1. Crystal data and structure refinement for $Mo(NR)(OTf)_2(DME)$.

Identification code	alo3	
Empirical formula	$C_{18}H_{25}F_6MoNO_8S_2$	
Formula weight	657.45	
Temperature	173(2) K	
Wavelength	0.71073 A	
Crystal system	Monoclinic	
space group	P2(1)/n	
Unit cell dimensions	a = 12.694(15) A	$\alpha = 90^\circ$
b	b = 15.77(3) A	$\beta = 92.93(16)^\circ$
c	c = 12.87(2) A	$\gamma = 90^\circ$
Volume	2573(8) A^3	
Z	4	
Calculated density	1.697 Mg/m^3	
Absorption coefficient	0.758 mm^{-1}	
F(000)	1328	
Crystal size	0.14 x 0.19 x 0.37 mm	
Theta range for data collection	2.04 to 24.48°	
Limiting indices	-10<=h<=14, -15<=k<=17, -14<=l<=13	
Reflections collected / unique	11661 / 3709 [R(int) = 0.2521]	
Completeness to theta = 24.48	86.9 %	
Absorption correction	None	
Refinement method	Full-matrix least-squares on F^2	
Data / restraints / parameters	3709 / 0 / 325	
Goodness-of-fit on F^2	1.001	
Final R indices [I>2sigma(I)]	R1 = 0.1008, wR2 = 0.2300	
R indices (all data)	R1 = 0.2080, wR2 = 0.3187	
Largest diff. peak and hole	1.813 and -2.866 $e.A^{-3}$	

Table A-13.2. Atomic coordinates (x 10^4) and equivalent isotropic displacement parameters ($Å^2$ x 10^3) for $Mo(NR)(OTf)_2(DME)$. U(eq) is defined as one third of the trace of the orthogonalized U^{ij} tensor.

	x	y	z	U(eq)		x	y	z	U(eq)
Mo	7718(1)	4616(1)	5922(1)	28(1)	C(1')	7501(15)	5432(18)	2436(14)	54(7)
S(1)	7047(4)	4717(4)	3479(3)	43(2)	C(1)	6475(13)	4028(12)	5902(12)	35(5)
S(2)	7549(4)	4294(4)	8500(4)	45(2)	C(2)	6054(14)	3072(13)	5928(13)	39(5)
O(11)	7766(8)	5020(7)	4315(8)	30(3)	C(2')	8640(20)	4516(19)	9299(16)	66(7)
O(12)	7295(11)	3960(10)	3040(9)	64(4)	C(3)	6915(13)	2433(14)	5984(13)	44(5)
O(13)	5986(9)	4948(12)	3708(10)	73(5)	C(4)	7712(13)	2348(17)	5006(13)	55(6)
O(21)	7855(8)	4837(7)	7553(8)	28(3)	C(10)	9210(13)	3055(15)	5864(14)	40(5)
O(22)	7522(13)	3370(13)	8308(11)	88(6)	C(11)	10180(13)	3068(15)	6321(13)	43(6)
O(23)	6699(13)	4692(13)	9103(12)	104(8)	C(12)	10755(14)	2348(15)	6283(14)	41(5)
O(31)	6782(8)	5855(8)	6093(8)	30(3)	C(13)	10438(15)	1603(16)	5780(14)	50(6)
O(32)	8890(8)	5796(9)	5900(8)	34(3)	C(14)	9458(15)	1597(15)	5336(14)	48(6)
N(1)	8594(10)	3792(12)	5865(10)	45(5)	C(15)	8815(14)	2335(16)	5382(14)	45(6)
F(11)	7401(9)	6256(9)	2759(8)	59(3)	C(21)	5407(15)	2953(18)	4939(15)	76(9)
F(12)	8487(9)	5317(8)	2146(8)	58(3)	C(22)	5270(14)	3005(15)	6886(16)	59(7)
F(13)	6916(9)	5330(9)	1613(8)	74(4)	C(31')	7359(12)	6544(14)	5704(13)	38(5)
F(21)	9517(10)	4187(13)	8800(11)	112(7)	C(32)	9873(13)	5661(15)	6414(16)	54(6)
F(22)	8517(11)	4041(8)	10197(8)	74(4)	C(32')	8410(13)	6566(14)	6144(14)	42(5)
F(23)	8770(15)	5284(13)	9506(12)	124(7)	C(311)	6155(13)	6037(15)	7058(13)	47(6)

Table A-13.3. Bond lengths [Å] and angles [°] for $Mo(NR)(OTf)_2(DME)$.

Mo-N(1)	1.714(18)	F(11)-C(1')	1.37(3)
Mo-C(1)	1.828(19)	F(12)-C(1')	1.34(2)
Mo-O(21)	2.125(11)	F(13)-C(1')	1.27(2)
Mo-O(11)	2.168(11)	F(21)-C(2')	1.41(3)
Mo-O(31)	2.303(12)	F(22)-C(2')	1.39(3)
Mo-O(32)	2.384(13)	F(23)-C(2')	1.25(3)
S(1)-O(12)	1.363(15)	C(1)-C(2)	1.60(3)
S(1)-O(13)	1.440(13)	C(2)-C(3)	1.49(3)
S(1)-O(11)	1.456(12)	C(2)-C(21)	1.49(2)
S(1)-C(1')	1.87(2)	C(2)-C(22)	1.63(3)
S(2)-O(22)	1.48(2)	C(3)-C(4)	1.66(2)
S(2)-O(23)	1.498(15)	C(4)-C(15)	1.46(2)

S(2)-O(21)	1.556(12)	C(10)-C(11)	1.34(2)
S(2)-C(2')	1.72(2)	C(10)-C(15)	1.38(3)
O(31)-C(31')	1.42(2)	C(11)-C(12)	1.35(3)
O(31)-C(311)	1.536(19)	C(12)-C(13)	1.39(3)
O(32)-C(32)	1.398(18)	C(13)-C(14)	1.34(2)
O(32)-C(32')	1.40(2)	C(14)-C(15)	1.42(3)
N(1)-C(10)	1.40(2)	C(31')-C(32')	1.42(2)
N(1)-Mo-C(1)	100.2(8)	C(10)-N(1)-Mo	172.9(14)
N(1)-Mo-O(21)	98.4(5)	F(13)-C(1')-F(12)	105.4(17)
C(1)-Mo-O(21)	97.2(6)	F(13)-C(1')-F(11)	108.3(19)
N(1)-Mo-O(11)	97.6(5)	F(12)-C(1')-F(11)	108.5(17)
C(1)-Mo-O(11)	101.6(6)	F(13)-C(1')-S(1)	109.4(15)
O(21)-Mo-O(11)	152.7(4)	F(12)-C(1')-S(1)	116.5(16)
N(1)-Mo-O(31)	170.4(6)	F(11)-C(1')-S(1)	108.5(14)
C(1)-Mo-O(31)	89.0(6)	C(2)-C(1)-Mo	140.0(12)
O(21)-Mo-O(31)	77.5(4)	C(3)-C(2)-C(21)	109.1(18)
O(11)-Mo-O(31)	83.2(4)	C(3)-C(2)-C(1)	113.2(15)
N(1)-Mo-O(32)	100.6(6)	C(21)-C(2)-C(1)	105.7(16)
C(1)-Mo-O(32)	159.1(6)	C(3)-C(2)-C(22)	113.3(15)
O(21)-Mo-O(32)	82.2(4)	C(21)-C(2)-C(22)	107.9(15)
O(11)-Mo-O(32)	73.2(4)	C(1)-C(2)-C(22)	107.2(15)
O(31)-Mo-O(32)	70.4(4)	F(23)-C(2')-F(22)	111.3(19)
O(12)-S(1)-O(13)	123.0(10)	F(23)-C(2')-F(21)	111(2)
O(12)-S(1)-O(11)	116.4(8)	F(22)-C(2')-F(21)	108(2)
O(13)-S(1)-O(11)	108.8(8)	F(23)-C(2')-S(2)	114.7(19)
O(12)-S(1)-C(1')	98.4(11)	F(22)-C(2')-S(2)	105.4(18)
O(13)-S(1)-C(1')	108.7(10)	F(21)-C(2')-S(2)	106.5(15)
O(11)-S(1)-C(1')	97.4(8)	C(2)-C(3)-C(4)	119.5(16)
O(22)-S(2)-O(23)	119.2(11)	C(15)-C(4)-C(3)	111.2(14)
O(22)-S(2)-O(21)	114.6(8)	C(11)-C(10)-C(15)	121.1(19)
O(23)-S(2)-O(21)	113.0(8)	C(11)-C(10)-N(1)	119(2)
O(22)-S(2)-C(2')	108.2(12)	C(15)-C(10)-N(1)	119.7(16)
O(23)-S(2)-C(2')	100.7(13)	C(10)-C(11)-C(12)	117(2)
O(21)-S(2)-C(2')	97.5(10)	C(11)-C(12)-C(13)	125.6(19)
S(1)-O(11)-Mo	124.2(7)	C(14)-C(13)-C(12)	116(2)
S(2)-O(21)-Mo	132.3(7)	C(13)-C(14)-C(15)	120(2)
C(31')-O(31)-C(311)	116.2(14)	C(10)-C(15)-C(14)	119.8(18)
C(31')-O(31)-Mo	109.8(10)	C(10)-C(15)-C(4)	117.4(19)
C(311)-O(31)-Mo	121.8(10)	C(14)-C(15)-C(4)	123(2)
C(32)-O(32)-C(32')	114.4(14)	O(31)-C(31')-C(32')	111.7(15)

C(32)-O(32)-Mo	114.7(12)	O(32)-C(32')-C(31')	107.4(16)
C(32')-O(32)-Mo	113.2(10)		

Table A-13.4. Anisotropic displacement parameters ($Å^2$ x 10^3) for $Mo(NR)(OTf)_2(DME)$. The anisotropic displacement factor exponent takes the form: $-2\pi^2 [h^2 a^{*2} U^{11} + ... + 2 h k a^* b^* U^{12}]$

	U^{11}	U^{22}	U^{33}	U^{23}	U^{13}	U^{12}
Mo	24(1)	43(1)	17(1)	1(1)	-4(1)	2(1)
S(1)	37(3)	70(5)	22(3)	-3(3)	-14(2)	-7(3)
S(2)	50(3)	60(4)	23(3)	7(3)	-5(2)	-1(3)
O(11)	41(7)	17(7)	30(7)	4(6)	-3(5)	2(6)
O(12)	92(12)	64(12)	32(8)	-26(8)	-23(7)	2(9)
O(13)	20(8)	141(16)	57(9)	47(10)	-9(6)	2(8)
O(21)	28(6)	25(8)	30(7)	-5(5)	-10(5)	-4(5)
O(22)	109(14)	112(17)	41(9)	-6(10)	-32(8)	-15(12)
O(23)	83(12)	160(20)	69(11)	79(12)	42(9)	76(13)
O(31)	28(7)	42(9)	20(6)	0(6)	1(5)	13(6)
O(32)	22(6)	58(10)	20(6)	-1(6)	-9(5)	5(6)
N(1)	11(7)	105(16)	16(8)	-12(9)	-7(6)	-9(9)
F(11)	78(9)	51(10)	44(7)	3(6)	-25(6)	-10(7)
F(12)	58(8)	75(10)	39(7)	1(6)	4(5)	-1(7)
F(13)	67(8)	114(12)	37(7)	19(7)	-30(6)	-22(8)
F(21)	56(9)	200(20)	75(10)	42(11)	-18(8)	22(10)
F(22)	134(12)	55(10)	30(7)	10(6)	-28(7)	3(8)
F(23)	185(18)	100(16)	78(11)	13(10)	-85(11)	-40(13)
C(1')	35(12)	100(20)	27(11)	10(13)	-13(9)	-19(13)
C(1)	41(11)	41(14)	21(9)	1(9)	-19(8)	30(9)
C(2)	33(11)	50(15)	32(11)	4(9)	-17(8)	-4(10)
C(2')	90(19)	70(20)	31(13)	-6(14)	-39(12)	4(16)
C(3)	32(11)	63(16)	35(11)	9(11)	-6(8)	-4(10)
C(4)	45(12)	90(20)	25(11)	8(11)	-10(9)	-1(12)
C(10)	21(10)	68(17)	29(11)	0(10)	2(8)	22(11)
C(11)	22(10)	84(19)	25(10)	8(10)	1(8)	8(10)
C(12)	24(11)	59(17)	41(12)	12(11)	-6(8)	12(10)
C(13)	35(12)	80(19)	37(12)	13(12)	16(9)	13(12)
C(14)	50(13)	59(16)	33(11)	11(11)	1(10)	-1(11)

C(15)	29(11)	75(18)	32(11)	6(12)	6(9)	10(11)
C(21)	46(14)	130(30)	48(14)	24(14)	-19(11)	-20(14)
C(22)	33(12)	72(18)	71(15)	26(13)	-13(10)	-6(11)
C(31')	24(10)	61(15)	28(10)	15(10)	0(8)	-6(10)
C(32)	24(11)	76(18)	60(14)	2(12)	-11(9)	2(10)
C(32')	23(10)	70(17)	32(11)	-7(11)	-1(8)	3(10)
C(311)	33(11)	81(19)	29(11)	-2(11)	7(8)	-7(11)

Table A-13.5. Hydrogen coordinates (x 10^4) and isotropic displacement parameters (A^2 x 10^3) for $Mo(NR)(OTf)_2(DME)$.

	x	y	z	U(eq)		x	y	z	U(eq)
H(1A)	5909	4403	5864	42	H(22B)	4686	3386	6765	89
H(3A)	6593	1882	6078	53	H(22C)	5649	3155	7525	89
H(3B)	7351	2549	6609	53	H(31A)	7006	7071	5861	45
H(4A)	7550	1831	4622	66	H(31B)	7377	6496	4954	45
H(4B)	7595	2823	4535	66	H(32A)	10295	6164	6369	81
H(11A)	10448	3553	6651	52	H(32B)	10222	5197	6094	81
H(12A)	11419	2351	6622	50	H(32C)	9776	5531	7131	81
H(13B)	10880	1134	5752	60	H(32D)	8793	7037	5859	50
H(14A)	9200	1113	4998	57	H(32E)	8406	6636	6893	50
H(21A)	5144	2382	4904	115	H(31C)	5823	6582	6987	71
H(21B)	5835	3057	4359	115	H(31D)	6624	6033	7667	71
H(21C)	4825	3342	4917	115	H(31E)	5625	5608	7123	71
H(22A)	5012	2435	6935	89					

Table A-14.1. Crystal data and structure refinement for $MoCl_2(NAr)(=C_8H_{12}=C_8H_{12}=NAr)$.

Identification code	jtcx10t	
Empirical formula	$C_{40}H_{58}Cl_2MoN_2$	
Formula weight	733.72	
Temperature	173(2) K	
Wavelength	0.71073 Å	
Crystal system	Monoclinic	
Space group	P2(1)/n	
Unit cell dimensions	a = 10.487(3) Å	α = 90°
	b = 17.824(3) Å	β = 100.66°
	c = 20.347(7) Å	γ = 90°
Volume	3737.8(17) $Å^3$	
Z	4	
Calculated density	1.304 Mg/m^3	
Absorption coefficient	0.523 mm^{-1}	
F(000)	1552	
Crystal size	0.17 x 0.19 x 0.24 mm	
Theta range for data collection	1.53 to 23.24°	
Limiting indices	-11<=h<=11, -19<=k<=19, -22<=l<=22	
Reflections collected / unique	31846 / 5361 [R(int) = 0.1619]	
Completeness to theta = 23.24	99.9 %	
Absorption correction	Empirical	
Max. and min. transmission	0.9914 and 0.8827	
Refinement method	Full-matrix least-squares on F^2	
Data / restraints / parameters	5361 / 0 / 407	
Goodness-of-fit on F^2	0.891	
Final R indices [I>2sigma(I)]	R1 = 0.0521, wR2 = 0.0902	
R indices (all data)	R1 = 0.1203, wR2 = 0.1077	
Extinction coefficient	0.00035(11)	
Largest diff. peak and hole	0.791 and -0.842 $e.A^{-3}$	

Table A-14.2. Atomic coordinates (x 10^4) and equivalent isotropic displacement parameters ($Å^2$ x 10^3) for $MoCl_2(NAr)(=C_8H_{12}=C_8H_{12}=NAr)$. U(eq) is defined as one third of the trace of the orthogonalized U^{ij} tensor.

	x	y	z	U(eq)		x	y	z	U(eq)
Mo	6521(1)	7754(1)	7496(1)	25(1)	C(13)	6005(6)	8836(4)	9873(3)	36(2)
Cl(1)	7417(2)	6509(1)	7354(1)	38(1)	C(14)	5564(6)	8252(4)	10216(3)	46(2)
Cl(2)	8743(2)	8090(1)	7955(1)	39(1)	C(15)	5222(6)	7582(4)	9893(3)	44(2)
N(1)	5947(4)	7957(2)	8223(2)	24(1)	C(16)	5300(6)	7476(4)	9219(3)	37(2)
N(2)	4878(4)	7346(3)	6791(2)	24(1)	C(21)	3611(6)	7090(3)	6902(3)	24(2)
C(1A)	6261(6)	8665(3)	6975(3)	25(2)	C(22)	2689(6)	7642(4)	6970(3)	31(2)
C(1B)	5162(5)	7351(3)	6190(3)	24(2)	C(23)	1502(6)	7396(4)	7112(3)	38(2)
C(2A)	6818(6)	8363(3)	6436(3)	26(2)	C(24)	1229(6)	6650(4)	7168(3)	40(2)
C(2B)	6435(5)	7682(4)	6126(3)	26(2)	C(25)	2140(6)	6123(4)	7070(3)	35(2)
C(3A)	7984(6)	8785(3)	6273(3)	35(2)	C(26)	3342(6)	6316(3)	6931(3)	26(2)
C(3B)	7300(6)	7265(4)	5734(3)	37(2)	C(121)	6682(6)	9398(3)	8861(3)	31(2)
C(4A)	7714(8)	9258(4)	5639(3)	63(3)	C(122)	5795(6)	10085(4)	8808(3)	51(2)
C(4B)	6841(8)	6758(6)	5197(5)	136(5)	C(123)	8050(6)	9619(4)	9196(3)	53(2)
C(5A)	6638(10)	9817(8)	5609(7)	170(8)	C(161)	4884(7)	6730(4)	8887(3)	44(2)
C(5B)	5985(8)	7058(5)	4547(4)	78(3)	C(162)	5434(7)	6064(4)	9302(4)	75(3)
C(6A)	5980(18)	10080(7)	5958(5)	236(11)	C(163)	3399(7)	6665(4)	8738(3)	66(2)
C(6B)	5194(9)	7749(5)	4626(3)	73(3)	C(221)	2920(6)	8473(3)	6903(3)	36(2)
C(7A)	5339(7)	9966(4)	6518(3)	50(2)	C(222)	1931(6)	8821(4)	6342(3)	58(2)
C(7B)	4022(7)	7596(4)	4967(3)	55(2)	C(223)	2929(6)	8874(4)	7574(3)	60(2)
C(8A)	6069(6)	9481(3)	7089(3)	35(2)	C(261)	4299(6)	5708(3)	6821(3)	30(2)
C(8B)	4216(6)	7076(3)	5587(3)	35(2)	C(262)	4826(6)	5280(3)	7456(3)	44(2)
C(11)	5781(6)	8071(4)	8881(3)	27(2)	C(263)	3662(6)	5156(3)	6267(3)	42(2)
C(12)	6144(6)	8761(4)	9203(3)	28(2)					

Table A-14.3. Bond lengths [Å] and angles [°] for $MoCl_2(NAr)(=C_8H_{12}=C_8H_{12}=NAr)$.

Mo-N(1)	1.736(5)	C(7B)-C(8B)	1.549(8)
Mo-C(1A)	1.932(6)	C(11)-C(16)	1.406(8)
Mo-N(2)	2.154(5)	C(11)-C(12)	1.412(8)
Mo-Cl(2)	2.4192(18)	C(12)-C(13)	1.404(7)
Mo-Cl(1)	2.4478(17)	C(12)-C(121)	1.496(8)
Mo-C(2A)	2.486(6)	C(13)-C(14)	1.379(8)
N(1)-C(11)	1.396(7)	C(14)-C(15)	1.379(8)

N(2)-C(1B)	1.311(6)	C(15)-C(16)	1.401(8)
N(2)-C(21)	1.462(7)	C(16)-C(161)	1.519(8)
C(1A)-C(2A)	1.439(8)	C(21)-C(22)	1.404(8)
C(1A)-C(8A)	1.492(7)	C(21)-C(26)	1.411(8)
C(1B)-C(2B)	1.487(7)	C(22)-C(23)	1.399(8)
C(1B)-C(8B)	1.509(7)	C(22)-C(221)	1.512(8)
C(2A)-C(2B)	1.393(8)	C(23)-C(24)	1.368(8)
C(2A)-C(3A)	1.523(7)	C(24)-C(25)	1.381(8)
C(2B)-C(3B)	1.510(7)	C(25)-C(26)	1.385(8)
C(3A)-C(4A)	1.523(8)	C(26)-C(261)	1.522(8)
C(3B)-C(4B)	1.430(9)	C(121)-C(123)	1.522(8)
C(4A)-C(5A)	1.498(12)	C(121)-C(122)	1.529(8)
C(4B)-C(5B)	1.550(11)	C(161)-C(162)	1.509(8)
C(5A)-C(6A)	1.175(12)	C(161)-C(163)	1.535(9)
C(5B)-C(6B)	1.511(10)	C(221)-C(222)	1.525(8)
C(6A)-C(7A)	1.440(12)	C(221)-C(223)	1.541(8)
C(6B)-C(7B)	1.543(10)	C(261)-C(262)	1.514(7)
C(7A)-C(8A)	1.535(8)	C(261)-C(263)	1.551(8)
N(1)-Mo-C(1A)	104.9(2)	C(5B)-C(6B)-C(7B)	113.7(7)
N(1)-Mo-N(2)	106.1(2)	C(6A)-C(7A)-C(8A)	116.0(7)
C(1A)-Mo-N(2)	84.4(2)	C(6B)-C(7B)-C(8B)	118.5(6)
N(1)-Mo-Cl(2)	94.63(16)	C(1A)-C(8A)-C(7A)	119.5(5)
C(1A)-Mo-Cl(2)	91.85(18)	C(1B)-C(8B)-C(7B)	115.8(5)
N(2)-Mo-Cl(2)	159.23(13)	N(1)-C(11)-C(16)	118.6(6)
N(1)-Mo-Cl(1)	119.40(15)	N(1)-C(11)-C(12)	120.0(6)
C(1A)-Mo-Cl(1)	135.70(19)	C(16)-C(11)-C(12)	121.3(6)
N(2)-Mo-Cl(1)	83.83(13)	C(13)-C(12)-C(11)	117.8(6)
Cl(2)-Mo-Cl(1)	84.65(6)	C(13)-C(12)-C(121)	119.6(6)
N(1)-Mo-C(2A)	140.2(2)	C(11)-C(12)-C(121)	122.6(6)
C(1A)-Mo-C(2A)	35.3(2)	C(14)-C(13)-C(12)	121.6(6)
N(2)-Mo-C(2A)	77.43(18)	C(15)-C(14)-C(13)	119.6(6)
Cl(2)-Mo-C(2A)	87.75(14)	C(14)-C(15)-C(16)	121.8(6)
Cl(1)-Mo-C(2A)	100.43(15)	C(15)-C(16)-C(11)	117.9(6)
C(11)-N(1)-Mo	166.4(4)	C(15)-C(16)-C(161)	119.3(6)
C(1B)-N(2)-C(21)	121.0(5)	C(11)-C(16)-C(161)	122.8(6)
C(1B)-N(2)-Mo	109.1(4)	C(22)-C(21)-C(26)	122.3(6)
C(21)-N(2)-Mo	129.8(4)	C(22)-C(21)-N(2)	117.3(5)
C(2A)-C(1A)-C(8A)	124.7(5)	C(26)-C(21)-N(2)	120.4(5)
C(2A)-C(1A)-Mo	93.9(4)	C(23)-C(22)-C(21)	117.1(6)
C(8A)-C(1A)-Mo	138.0(4)	C(23)-C(22)-C(221)	119.3(6)

N(2)-C(1B)-C(2B)	116.5(5)	C(21)-C(22)-C(221)	123.5(6)
N(2)-C(1B)-C(8B)	121.8(5)	C(24)-C(23)-C(22)	122.0(6)
C(2B)-C(1B)-C(8B)	121.5(5)	C(23)-C(24)-C(25)	119.2(6)
C(2B)-C(2A)-C(1A)	123.2(5)	C(24)-C(25)-C(26)	122.7(6)
C(2B)-C(2A)-C(3A)	120.5(5)	C(25)-C(26)-C(21)	116.6(6)
C(1A)-C(2A)-C(3A)	115.9(5)	C(25)-C(26)-C(261)	120.2(6)
C(2B)-C(2A)-Mo	86.6(4)	C(21)-C(26)-C(261)	123.2(6)
C(1A)-C(2A)-Mo	50.8(3)	C(12)-C(121)-C(123)	113.2(5)
C(3A)-C(2A)-Mo	129.7(4)	C(12)-C(121)-C(122)	111.4(5)
C(2A)-C(2B)-C(1B)	119.7(5)	C(123)-C(121)-C(122)	109.6(5)
C(2A)-C(2B)-C(3B)	121.1(5)	C(162)-C(161)-C(16)	113.1(6)
C(1B)-C(2B)-C(3B)	119.2(5)	C(162)-C(161)-C(163)	108.7(6)
C(4A)-C(3A)-C(2A)	115.3(5)	C(16)-C(161)-C(163)	110.6(6)
C(4B)-C(3B)-C(2B)	124.3(6)	C(22)-C(221)-C(222)	111.6(5)
C(5A)-C(4A)-C(3A)	115.1(7)	C(22)-C(221)-C(223)	110.4(5)
C(3B)-C(4B)-C(5B)	119.6(8)	C(222)-C(221)-C(223)	111.5(5)
C(6A)-C(5A)-C(4A)	139.6(12)	C(262)-C(261)-C(26)	112.3(5)
C(6B)-C(5B)-C(4B)	115.6(7)	C(262)-C(261)-C(263)	109.9(5)
C(5A)-C(6A)-C(7A)	146.5(12)	C(26)-C(261)-C(263)	110.6(5)

Table A-14.4. Anisotropic displacement parameters ($Å^2$ x 10^3) for $MoCl_2(NAr)(=C_8H_{12}=C_8H_{12}=NAr)$. The anisotropic displacement factor exponent takes the form: $-2\pi^2 [h^2 a^{*2} U^{11} + ... + 2 h k a^* b^* U^{12}]$

	U^{11}	U^{22}	U^{33}	U^{23}	U^{13}	U^{12}
Mo	24(1)	27(1)	23(1)	0(1)	1(1)	1(1)
Cl(1)	32(1)	35(1)	43(1)	-2(1)	0(1)	9(1)
Cl(2)	27(1)	51(1)	34(1)	-3(1)	-4(1)	-2(1)
N(1)	27(3)	23(3)	22(3)	2(2)	4(2)	2(2)
N(2)	19(3)	20(3)	32(3)	2(3)	0(2)	1(2)
C(1A)	30(4)	22(4)	22(4)	0(3)	-2(3)	-1(3)
C(1B)	25(4)	14(4)	30(4)	-1(3)	-3(3)	5(3)
C(2A)	23(4)	29(4)	23(4)	-1(3)	-4(3)	-6(3)
C(2B)	22(4)	32(4)	21(4)	4(3)	0(3)	1(4)
C(3A)	29(4)	41(5)	37(4)	-10(4)	9(4)	-11(3)
C(3B)	38(4)	47(5)	25(4)	-9(4)	3(3)	1(4)
C(4A)	80(7)	77(6)	32(5)	5(4)	13(5)	-52(5)
C(4B)	59(7)	244(14)	94(8)	-99(9)	-19(6)	68(8)

C(5A)	59(7)	238(17)	229(17)	206(14)	64(9)	45(9)
C(5B)	61(6)	137(10)	36(5)	-5(6)	5(5)	-30(6)
C(6A)	480(30)	206(15)	54(7)	86(8)	131(12)	269(18)
C(6B)	106(8)	66(6)	34(5)	13(5)	-20(5)	-58(6)
C(7A)	67(6)	32(5)	43(5)	8(4)	-12(4)	0(4)
C(7B)	70(6)	47(5)	35(4)	-5(4)	-23(4)	4(4)
C(8A)	34(4)	39(5)	28(4)	1(3)	-3(3)	-4(4)
C(8B)	21(4)	43(5)	40(4)	-8(4)	3(3)	-11(3)
C(11)	25(4)	34(4)	22(4)	0(3)	7(3)	7(3)
C(12)	21(4)	37(5)	24(4)	-1(4)	-1(3)	11(3)
C(13)	35(4)	38(5)	33(5)	-6(4)	4(4)	-1(4)
C(14)	37(5)	65(6)	35(5)	-2(4)	9(4)	-8(4)
C(15)	56(5)	41(5)	40(5)	7(4)	20(4)	1(4)
C(16)	38(4)	44(5)	30(4)	0(4)	9(4)	1(3)
C(21)	21(4)	29(5)	22(4)	-1(3)	3(3)	-4(3)
C(22)	28(4)	32(5)	32(4)	-1(3)	3(3)	4(4)
C(23)	30(4)	38(5)	46(5)	-7(4)	6(4)	10(4)
C(24)	25(4)	58(6)	35(4)	-6(4)	2(3)	-4(4)
C(25)	33(5)	36(5)	36(4)	5(4)	4(4)	-2(4)
C(26)	25(4)	29(4)	23(4)	-2(3)	0(3)	1(3)
C(121)	44(5)	25(4)	25(4)	4(3)	7(4)	6(4)
C(122)	48(5)	44(5)	61(5)	1(4)	10(4)	9(4)
C(123)	40(5)	59(6)	62(6)	9(4)	18(4)	0(4)
C(161)	56(5)	39(5)	38(5)	0(4)	14(4)	-6(4)
C(162)	78(7)	41(6)	95(7)	-1(5)	-7(5)	16(5)
C(163)	77(7)	68(6)	45(5)	-11(4)	-12(5)	-5(5)
C(221)	28(4)	21(4)	57(5)	-2(4)	4(4)	8(3)
C(222)	51(5)	40(5)	77(6)	4(4)	-7(5)	9(4)
C(223)	56(6)	45(5)	73(6)	-21(4)	-3(5)	10(4)
C(261)	29(4)	20(4)	40(4)	4(3)	0(3)	-7(3)
C(262)	40(5)	34(5)	52(5)	4(4)	-10(4)	-7(4)
C(263)	40(5)	40(5)	49(5)	-4(4)	11(4)	-2(4)

Table A-14.5. Hydrogen coordinates (x 10^4) and isotropic displacement parameters ($Å^2$ x 10^3) for $MoCl_2(NAr)(=C_8H_{12}=C_8H_{12}=NAr)$.

	x	y	z	U(eq)		x	y	z	U(eq)
H(3AA)	8322	9111	6647	42	H(25A)	1938	5617	7097	42
H(3AB)	8656	8424	6231	42	H(12A)	6720	9236	8405	38
H(3BA)	7803	7644	5553	45	H(12E)	4933	9945	8597	76
H(3BB)	7910	6983	6059	45	H(12F)	6115	10465	8546	76
H(4AA)	8502	9525	5597	75	H(12G)	5781	10277	9248	76
H(4AB)	7505	8925	5258	75	H(12B)	8606	9188	9229	79
H(4BA)	6354	6367	5372	164	H(12C)	8037	9810	9636	79
H(4BB)	7594	6520	5073	164	H(12D)	8372	10000	8935	79
H(5AA)	7004	10259	5436	205	H(16A)	5192	6709	8461	52
H(5AB)	6001	9632	5237	205	H(16B)	6364	6098	9399	112
H(5BA)	6543	7169	4229	94	H(16C)	5180	5610	9059	112
H(5BB)	5397	6662	4357	94	H(16D)	5109	6059	9713	112
H(6AA)	5256	10254	5625	283	H(16E)	3153	6191	8528	99
H(6AB)	6468	10532	6102	283	H(16F)	3041	7064	8444	99
H(6BA)	4883	7965	4188	87	H(16G)	3074	6700	9148	99
H(6BB)	5752	8117	4888	87	H(22A)	3781	8536	6788	43
H(7AA)	4503	9735	6354	60	H(22E)	1949	8560	5931	88
H(7AB)	5177	10453	6698	60	H(22F)	2141	9340	6292	88
H(7BA)	3336	7383	4634	66	H(22G)	1080	8783	6450	88
H(7BB)	3711	8076	5098	66	H(22B)	3560	8642	7916	90
H(8AA)	6920	9702	7232	42	H(22C)	2086	8837	7691	90
H(8AB)	5615	9524	7462	42	H(22D)	3148	9393	7534	90
H(8BA)	3380	7002	5717	42	H(26A)	5031	5950	6669	36
H(8BB)	4509	6591	5459	42	H(26B)	5219	5625	7796	66
H(13A)	6215	9290	10090	43	H(26C)	5463	4924	7370	66
H(14A)	5499	8311	10663	55	H(26D)	4129	5019	7604	66
H(15A)	4931	7190	10128	53	H(26E)	4277	4776	6205	64
H(23A)	880	7749	7169	46	H(26F)	3392	5425	5856	64
H(24A)	440	6501	7272	48	H(26G)	2920	4925	6398	64

Table A-15.1. Crystal data and structure refinement for $WCl_2(NAr)(=C_8H_{12}=C_8H_{12}=NAr)$.

Identification code	kapil1t	
Empirical formula	$C_{40}H_{57}Cl_2N_2W$	
Formula weight	820.63	
Temperature	173(2) K	
Wavelength	0.71073 A	
Crystal system	Orthorhombic	
Space group	Pbca	
Unit cell dimensions	a = 17.040(3) Å	α = 90°
	b = 19.421(3) Å	β = 90°
	c = 22.704(3) Å	γ = 90°
Volume	7513.3(19) $Å^3$	
Z	8	
Calculated density	1.451 Mg/m^3	
Absorption coefficient	3.247 mm^{-1}	
F(000)	3352	
Crystal size	0.23 x 0.25 x 0.50 mm	
Theta range for data collection	1.79 to 23.28°.	
Limiting indices	-18<=h<=18, -21<=k<=21, -25<=l<=25	
Reflections collected / unique	61037 / 5405 [R(int) = 0.0500]	
Completeness to theta = 23.28°	100.0 %	
Absorption correction	Empirical	
Max. and min. transmission	0.8387 and 0.6216	
Refinement method	Full-matrix least-squares on F^2	
Data / restraints / parameters	5405 / 0 / 407	
Goodness-of-fit on F^2	1.056	
Final R indices [I>2sigma(I)]	R1 = 0.0206, wR2 = 0.0460	
R indices (all data)	R1 = 0.0354, wR2 = 0.0511	
Extinction coefficient	0.00021(2)	
Largest diff. peak and hole	0.751 and -0.507 $e.A^{-3}$	

Table A-15.2. Atomic coordinates (x 10^4) and equivalent isotropic displacement parameters ($Å^2$ x 10^3) for $WCl_2(NAr)(=C_8H_{12}=C_8H_{12}=NAr)$. U(eq) is defined as one third of the trace of the orthogonalized U^{ij} tensor.

	x	y	z	U(eq)		x	y	z	U(eq)
W	9278(1)	1225(1)	3781(1)	19(1)	C(13)	10127(2)	3547(2)	2632(2)	35(1)
N(1)	9474(2)	1934(2)	3339(1)	21(1)	C(14)	10157(3)	3348(2)	2048(2)	40(1)
N(2)	8069(2)	1074(1)	3606(1)	19(1)	C(15)	9964(2)	2682(2)	1898(2)	32(1)
Cl(1)	9395(1)	61(1)	3422(1)	32(1)	C(16)	9732(2)	2200(2)	2311(2)	24(1)
Cl(2)	10622(1)	1068(1)	4083(1)	32(1)	C(21)	7647(2)	1340(2)	3093(2)	22(1)
C(1B)	7759(2)	659(2)	3999(2)	20(1)	C(22)	7441(2)	2040(2)	3093(2)	25(1)
C(1A)	8961(2)	1572(2)	4549(2)	23(1)	C(23)	7105(2)	2308(2)	2581(2)	36(1)
C(2B)	8244(2)	457(2)	4499(2)	22(1)	C(24)	6975(2)	1903(2)	2094(2)	35(1)
C(2A)	8726(2)	925(2)	4802(2)	23(1)	C(25)	7164(2)	1213(2)	2112(2)	31(1)
C(3B)	8203(2)	-309(2)	4666(2)	27(1)	C(26)	7497(2)	908(2)	2607(2)	23(1)
C(3A)	9043(2)	746(2)	5411(2)	34(1)	C(121)	9924(2)	3299(2)	3716(2)	29(1)
C(4B)	7680(2)	-557(2)	5172(2)	35(1)	C(122)	10692(2)	3067(2)	4010(2)	36(1)
C(4A)	8510(3)	932(2)	5926(2)	47(1)	C(123)	9799(2)	4068(2)	3821(2)	38(1)
C(5B)	6796(2)	-451(2)	5096(2)	37(1)	C(161)	9555(2)	1466(2)	2132(2)	27(1)
C(5A)	8317(3)	1692(2)	6040(2)	51(1)	C(162)	10283(2)	1021(2)	2193(2)	39(1)
C(6B)	6554(3)	313(2)	5054(2)	38(1)	C(163)	9214(3)	1407(2)	1511(2)	47(1)
C(6A)	7880(3)	2075(2)	5548(2)	46(1)	C(221)	7535(2)	2501(2)	3632(2)	31(1)
C(7B)	6365(2)	567(2)	4436(2)	31(1)	C(222)	6779(3)	2534(2)	3988(2)	47(1)
C(7A)	8402(3)	2540(2)	5181(2)	39(1)	C(223)	7800(3)	3230(2)	3481(2)	46(1)
C(8B)	6941(2)	382(2)	3943(2)	24(1)	C(261)	7622(2)	126(2)	2596(2)	28(1)
C(8A)	9129(2)	2197(2)	4922(2)	30(1)	C(262)	8211(2)	-97(2)	2128(2)	38(1)
C(11)	9708(2)	2413(2)	2906(2)	22(1)	C(263)	6838(2)	-250(2)	2490(2)	35(1)
C(12)	9913(2)	3090(2)	3074(2)	25(1)					

Table A-15.3. Bond lengths [Å] and angles [°] for $WCl_2(NAr)(=C_8H_{12}=C_8H_{12}=NAr)$.

W-N(1)	1.736(3)	C(7A)-C(8A)	1.525(5)
W-C(1A)	1.944(4)	C(11)-C(12)	1.413(5)
W-N(2)	2.120(3)	C(11)-C(16)	1.414(5)
W-Cl(2)	2.4095(10)	C(12)-C(13)	1.387(5)
W-Cl(1)	2.4120(10)	C(12)-C(121)	1.514(5)
W-C(2A)	2.567(4)	C(13)-C(14)	1.382(5)

N(1)-C(11)	1.411(4)	C(14)-C(15)	1.376(5)
N(2)-C(1B)	1.315(4)	C(15)-C(16)	1.384(5)
N(2)-C(21)	1.462(4)	C(16)-C(161)	1.512(5)
C(1B)-C(2B)	1.458(5)	C(21)-C(22)	1.405(5)
C(1B)-C(8B)	1.500(5)	C(21)-C(26)	1.409(5)
C(1A)-C(2A)	1.438(5)	C(22)-C(23)	1.396(5)
C(1A)-C(8A)	1.507(5)	C(22)-C(221)	1.524(5)
C(2B)-C(2A)	1.404(5)	C(23)-C(24)	1.375(5)
C(2B)-C(3B)	1.536(5)	C(24)-C(25)	1.378(5)
C(2A)-C(3A)	1.526(5)	C(25)-C(26)	1.392(5)
C(3B)-C(4B)	1.532(5)	C(26)-C(261)	1.534(5)
C(3A)-C(4A)	1.524(6)	C(121)-C(123)	1.527(5)
C(4B)-C(5B)	1.529(6)	C(121)-C(122)	1.537(5)
C(4A)-C(5A)	1.534(6)	C(161)-C(162)	1.518(5)
C(5B)-C(6B)	1.543(5)	C(161)-C(163)	1.529(5)
C(5A)-C(6A)	1.536(6)	C(221)-C(222)	1.521(6)
C(6B)-C(7B)	1.522(5)	C(221)-C(223)	1.527(5)
C(6A)-C(7A)	1.515(6)	C(261)-C(262)	1.526(5)
C(7B)-C(8B)	1.531(5)	C(261)-C(263)	1.541(5)

N(1)-W-C(1A)	107.30(14)	C(7A)-C(6A)-C(5A)	113.8(4)
N(1)-W-N(2)	100.81(12)	C(6B)-C(7B)-C(8B)	117.5(3)
C(1A)-W-N(2)	86.94(13)	C(6A)-C(7A)-C(8A)	115.4(3)
N(1)-W-Cl(2)	94.70(9)	C(1B)-C(8B)-C(7B)	116.7(3)
C(1A)-W-Cl(2)	93.04(11)	C(1A)-C(8A)-C(7A)	114.6(3)
N(2)-W-Cl(2)	163.77(8)	N(1)-C(11)-C(12)	119.8(3)
N(1)-W-Cl(1)	122.11(10)	N(1)-C(11)-C(16)	118.7(3)
C(1A)-W-Cl(1)	130.59(11)	C(12)-C(11)-C(16)	121.5(3)
N(2)-W-Cl(1)	83.49(8)	C(13)-C(12)-C(11)	117.7(4)
Cl(2)-W-Cl(1)	84.24(3)	C(13)-C(12)-C(121)	121.5(3)
N(1)-W-C(2A)	140.57(12)	C(11)-C(12)-C(121)	120.7(3)
C(1A)-W-C(2A)	33.73(13)	C(14)-C(13)-C(12)	121.6(4)
N(2)-W-C(2A)	77.40(11)	C(15)-C(14)-C(13)	119.5(4)
Cl(2)-W-C(2A)	93.64(8)	C(14)-C(15)-C(16)	122.4(4)
Cl(1)-W-C(2A)	97.04(8)	C(15)-C(16)-C(11)	117.2(3)
C(11)-N(1)-W	168.6(3)	C(15)-C(16)-C(161)	120.9(3)
C(1B)-N(2)-C(21)	124.1(3)	C(11)-C(16)-C(161)	121.8(3)
C(1B)-N(2)-W	110.3(2)	C(22)-C(21)-C(26)	122.0(3)
C(21)-N(2)-W	125.4(2)	C(22)-C(21)-N(2)	117.7(3)
N(2)-C(1B)-C(2B)	117.8(3)	C(26)-C(21)-N(2)	120.2(3)
N(2)-C(1B)-C(8B)	122.4(3)	C(23)-C(22)-C(21)	117.6(4)

C(2B)-C(1B)-C(8B)	119.8(3)	C(23)-C(22)-C(221)	119.5(3)
C(2A)-C(1A)-C(8A)	122.2(3)	C(21)-C(22)-C(221)	122.8(3)
C(2A)-C(1A)-W	97.6(2)	C(24)-C(23)-C(22)	121.6(4)
C(8A)-C(1A)-W	136.8(3)	C(23)-C(24)-C(25)	119.6(4)
C(2A)-C(2B)-C(1B)	122.5(3)	C(24)-C(25)-C(26)	122.2(4)
C(2A)-C(2B)-C(3B)	122.2(3)	C(25)-C(26)-C(21)	117.0(3)
C(1B)-C(2B)-C(3B)	115.3(3)	C(25)-C(26)-C(261)	117.7(3)
C(2B)-C(2A)-C(1A)	122.2(3)	C(21)-C(26)-C(261)	125.2(3)
C(2B)-C(2A)-C(3A)	120.3(3)	C(12)-C(121)-C(123)	114.2(3)
C(1A)-C(2A)-C(3A)	117.4(3)	C(12)-C(121)-C(122)	110.5(3)
C(2B)-C(2A)-W	85.4(2)	C(123)-C(121)-C(122)	109.8(3)
C(1A)-C(2A)-W	48.65(18)	C(16)-C(161)-C(162)	110.4(3)
C(3A)-C(2A)-W	137.7(3)	C(16)-C(161)-C(163)	113.1(3)
C(4B)-C(3B)-C(2B)	121.0(3)	C(162)-C(161)-C(163)	110.6(3)
C(4A)-C(3A)-C(2A)	115.5(3)	C(222)-C(221)-C(22)	111.2(3)
C(5B)-C(4B)-C(3B)	116.6(3)	C(222)-C(221)-C(223)	109.3(3)
C(3A)-C(4A)-C(5A)	119.0(4)	C(22)-C(221)-C(223)	113.3(3)
C(4B)-C(5B)-C(6B)	113.6(3)	C(262)-C(261)-C(26)	112.6(3)
C(4A)-C(5A)-C(6A)	116.6(4)	C(262)-C(261)-C(263)	109.0(3)
C(7B)-C(6B)-C(5B)	115.2(3)	C(26)-C(261)-C(263)	110.6(3)

Table A-15.4. Anisotropic displacement parameters ($Å^2$ x 10^3) for $WCl_2(NAr)(=C_8H_{12}=C_8H_{12}=NAr)$. The anisotropic displacement factor exponent takes the form: $-2\pi^2 [h^2 a^{*2} U^{11} + ... + 2 h k a^* b^* U^{12}]$

	U^{11}	U^{22}	U^{33}	U^{23}	U^{13}	U^{12}
W	21(1)	15(1)	20(1)	2(1)	-2(1)	0(1)
N(1)	18(2)	22(2)	24(2)	-1(1)	-4(1)	3(1)
N(2)	21(2)	17(2)	19(2)	-1(1)	-3(1)	1(1)
Cl(1)	34(1)	20(1)	42(1)	-6(1)	-1(1)	4(1)
Cl(2)	25(1)	31(1)	42(1)	8(1)	-7(1)	2(1)
C(1B)	27(2)	12(2)	21(2)	-4(2)	2(2)	0(2)
C(1A)	19(2)	23(2)	26(2)	2(2)	-6(2)	-1(2)
C(2B)	23(2)	21(2)	22(2)	2(2)	1(2)	0(2)
C(2A)	22(2)	22(2)	25(2)	3(2)	-2(2)	0(2)
C(3B)	30(2)	21(2)	31(2)	3(2)	-6(2)	-1(2)
C(3A)	42(3)	29(2)	30(2)	8(2)	-14(2)	-14(2)
C(4B)	43(3)	26(2)	36(3)	12(2)	-9(2)	-9(2)

C(4A)	74(4)	42(3)	24(2)	7(2)	6(2)	-28(3)
C(5B)	45(3)	34(3)	32(3)	10(2)	5(2)	-10(2)
C(5A)	64(3)	66(3)	24(3)	-11(2)	14(2)	-26(3)
C(6B)	38(3)	40(3)	37(3)	-5(2)	8(2)	-3(2)
C(6A)	48(3)	52(3)	37(3)	-20(2)	10(2)	-3(2)
C(7B)	25(2)	24(2)	44(3)	2(2)	-1(2)	-3(2)
C(7A)	56(3)	32(3)	29(2)	-12(2)	-10(2)	0(2)
C(8B)	24(2)	20(2)	27(2)	4(2)	-5(2)	-2(2)
C(8A)	42(3)	25(2)	23(2)	1(2)	-5(2)	-13(2)
C(11)	17(2)	21(2)	27(2)	8(2)	0(2)	3(2)
C(12)	20(2)	20(2)	34(2)	3(2)	0(2)	2(2)
C(13)	36(3)	19(2)	49(3)	6(2)	3(2)	-4(2)
C(14)	50(3)	32(3)	37(3)	14(2)	6(2)	-4(2)
C(15)	33(3)	35(3)	28(2)	5(2)	3(2)	3(2)
C(16)	17(2)	25(2)	29(2)	7(2)	-1(2)	4(2)
C(21)	20(2)	24(2)	23(2)	3(2)	-3(2)	-2(2)
C(22)	24(2)	22(2)	30(2)	2(2)	-8(2)	0(2)
C(23)	41(3)	23(2)	45(3)	10(2)	-12(2)	4(2)
C(24)	35(3)	42(3)	29(2)	13(2)	-9(2)	0(2)
C(25)	32(2)	39(3)	22(2)	-3(2)	-6(2)	-5(2)
C(26)	21(2)	27(2)	21(2)	3(2)	-1(2)	-1(2)
C(121)	26(2)	22(2)	38(2)	0(2)	1(2)	-3(2)
C(122)	37(3)	30(2)	41(3)	-4(2)	-4(2)	2(2)
C(123)	39(3)	27(2)	47(3)	-9(2)	-1(2)	4(2)
C(161)	30(2)	29(2)	20(2)	1(2)	-1(2)	-1(2)
C(162)	38(3)	31(2)	47(3)	-7(2)	4(2)	2(2)
C(163)	62(3)	49(3)	29(2)	5(2)	-3(2)	-14(2)
C(221)	34(3)	20(2)	38(3)	0(2)	-14(2)	6(2)
C(222)	55(3)	43(3)	44(3)	-5(2)	0(2)	-12(2)
C(223)	45(3)	28(2)	66(3)	-11(2)	4(3)	-2(2)
C(261)	34(2)	29(2)	23(2)	-4(2)	-5(2)	1(2)
C(262)	41(3)	37(3)	37(3)	-11(2)	-1(2)	4(2)
C(263)	40(3)	30(2)	36(2)	-6(2)	-1(2)	-5(2)

Table A-15.5. Hydrogen coordinates (x 10^4) and isotropic displacement parameters ($Å^2$ x 10^3) for $WCl_2(NAr)(=C_8H_{12}=C_8H_{12}=NAr)$.

	x	y	z	U(eq)		x	y	z	U(eq)
H(3BA)	8043	-558	4316	33	H(12A)	9494	3054	3912	34
H(3BB)	8734	-456	4756	33	H(12E)	10761	2581	3952	54
H(3AA)	9146	255	5425	41	H(12F)	10671	3165	4424	54
H(3AB)	9541	981	5464	41	H(12G)	11126	3309	3836	54
H(4BA)	7775	-1044	5230	42	H(12B)	9317	4210	3639	57
H(4BB)	7842	-321	5528	42	H(12C)	10228	4321	3653	57
H(4AA)	8304	590	6168	56	H(12D)	9773	4156	4237	57
H(5BA)	6527	-659	5428	45	H(16A)	9161	1287	2407	32
H(5BB)	6627	-687	4742	45	H(16E)	10494	1070	2583	58
H(5AA)	8806	1934	6116	61	H(16F)	10669	1164	1910	58
H(5AB)	8004	1720	6396	61	H(16G)	10148	548	2125	58
H(6BA)	6096	385	5301	46	H(16B)	8759	1696	1479	70
H(6BB)	6975	593	5212	46	H(16C)	9070	938	1435	70
H(6AA)	7634	1740	5291	55	H(16D)	9601	1552	1229	70
H(6AB)	7467	2351	5723	55	H(22D)	7939	2294	3884	37
H(7BA)	6322	1065	4450	37	H(22E)	6619	2076	4093	71
H(7BB)	5853	389	4328	37	H(22F)	6376	2748	3756	71
H(7AA)	8570	2923	5425	47	H(22G)	6866	2799	4339	71
H(7AB)	8092	2727	4861	47	H(22A)	8279	3211	3259	69
H(8BA)	6972	-116	3919	28	H(22B)	7886	3485	3838	69
H(8BB)	6723	545	3573	28	H(22C)	7402	3455	3252	69
H(8AA)	9407	2532	4683	36	H(26G)	7824	-15	2982	34
H(8AB)	9473	2063	5242	36	H(26D)	8703	130	2194	58
H(13A)	10253	3998	2731	42	H(26E)	8015	24	1745	58
H(14A)	10306	3661	1759	48	H(26F)	8284	-587	2148	58
H(15A)	9991	2553	1504	38	H(26A)	6471	-125	2792	53
H(23A)	6967	2771	2569	44	H(26B)	6924	-738	2499	53
H(24A)	6760	2093	1754	42	H(26C)	6632	-121	2112	53
H(25A)	7065	942	1782	37					

Table A-16.1. Crystal data and structure refinement for $[W(=C_8H_{12}=C_8H_{12}=NAr)(O)(\mu\text{-}O)]_2$.

Identification code	kl11461t	
Empirical formula	$C_{16}H_{25}N_{0.50}O_{1.50}W_{0.50}$	
Formula weight	340.29	
Temperature	173(2) K	
Wavelength	0.71073 Å	
Crystal system	Triclinic	
space group	P-1	
Unit cell dimensions	a = 11.1553(16) Å	α = 118.851(9)°
	b = 12.7101(17) Å	β = 98.755(8)°
	c = 13.1510(14) Å	γ = 99.161(12)°
Volume	1554.8(3) $Å^3$	
Z	4	
Calculated density	1.454 Mg/m^3	
Absorption coefficient	3.745 mm^{-1}	
F(000)	694	
Crystal size	0.02 x 0.59 x 0.62 mm	
Theta range for data collection	1.83 to 23.25°	
Limiting indices	-12<=h<=12, -14<=k<=14, -14<=l<=14	
Reflections collected / unique	13507 / 4475 [R(int) = 0.0393]	
Completeness to theta = 23.25	100.0 %	
Absorption correction	None	
Refinement method	Full-matrix least-squares on F^2	
Data / restraints / parameters	4475 / 0 / 334	
Goodness-of-fit on F^2	1.023	
Final R indices [I>2sigma(I)]	R1 = 0.0219, wR2 = 0.0471	
R indices (all data)	R1 = 0.0276, wR2 = 0.0486	
Largest diff. peak and hole	0.669 and -0.540 $e.A^{-3}$	

Table A-16.2. Atomic coordinates (x 10^4) and equivalent isotropic displacement parameters ($Å^2$ x 10^3) for [W(=C_8H_{12}=C_8H_{12}=NAr)(O)(μ-O)]$_2$. U(eq) is defined as one third of the trace of the orthogonalized U^{ij} tensor.

	x	y	z	U(eq)		x	y	z	U(eq)
W	3839(1)	469(1)	241(1)	18(1)	C(4A)	4927(5)	5361(4)	2309(4)	44(1)
N	3439(3)	1163(3)	1853(3)	18(1)	C(4S)	2409(8)	1096(7)	5821(7)	112(3)
O(1)	2415(2)	-507(2)	-691(2)	25(1)	C(5)	236(4)	739(4)	2333(3)	28(1)
O(2)	5157(2)	-8(2)	931(2)	19(1)	C(5B)	7310(4)	2256(4)	3657(4)	41(1)
O(8S)	1340(4)	2659(4)	6641(4)	75(1)	C(5A)	3514(5)	5010(4)	1790(4)	43(1)
C(1)	2284(4)	630(4)	2041(3)	20(1)	C(6)	1343(4)	1254(4)	2175(3)	21(1)
C(1B)	4347(4)	2162(4)	2801(3)	20(1)	C(6B)	6805(4)	2335(4)	4715(4)	38(1)
C(1A)	4039(4)	2175(4)	467(3)	21(1)	C(6A)	3082(5)	4537(4)	444(4)	45(1)
C(1S)	325(7)	4229(7)	7641(9)	123(3)	C(7B)	5399(4)	1738(4)	4399(4)	39(1)
C(2)	2130(4)	-488(4)	2037(3)	22(1)	C(7A)	2615(4)	3125(4)	-424(4)	37(1)
C(2B)	5139(4)	2991(4)	2615(4)	23(1)	C(8B)	4461(4)	2328(4)	4035(4)	30(1)
C(2A)	4890(4)	3082(4)	1547(4)	24(1)	C(8A)	3573(4)	2357(4)	-568(4)	30(1)
C(2S)	501(8)	3310(9)	6521(8)	127(3)	C(21)	3114(4)	-1229(4)	1816(4)	27(1)
C(3)	1006(4)	-949(4)	2203(4)	30(1)	C(22)	3439(4)	-1564(4)	2784(4)	40(1)
C(3B)	6288(4)	3920(4)	3646(4)	33(1)	C(23)	2652(4)	-2410(4)	570(4)	38(1)
C(3A)	5541(4)	4300(4)	1658(4)	31(1)	C(61)	1469(4)	2443(4)	2145(4)	24(1)
C(3S)	1561(9)	1770(8)	5615(7)	116(3)	C(62)	386(4)	2327(4)	1203(4)	40(1)
C(4)	76(4)	-347(4)	2356(4)	29(1)	C(63)	1587(5)	3560(4)	3384(4)	46(1)
C(4B)	7447(4)	3415(4)	3575(4)	39(1)					

Table A-16.3. Bond lengths [Å] and angles [°] for [W(=C_8H_{12}=C_8H_{12}=NAr)(O)(μ-O)]$_2$.

W-O(1)	1.696(3)	C(2B)-C(3B)	1.523(5)
W-O(2)	1.940(2)	C(2A)-C(3A)	1.528(5)
W-O(2)#1	1.958(2)	C(3)-C(4)	1.367(6)
W-C(1A)	2.010(4)	C(3B)-C(4B)	1.528(6)
W-N	2.021(3)	C(3A)-C(4A)	1.543(6)
W-W#1	3.0475(5)	C(3S)-C(4S)	1.452(10)
N-C(1B)	1.368(5)	C(4)-C(5)	1.379(5)
N-C(1)	1.469(5)	C(4B)-C(5B)	1.514(6)
O(2)-W#1	1.958(2)	C(4A)-C(5A)	1.517(6)
O(8S)-C(3S)	1.370(8)	C(5)-C(6)	1.397(5)
O(8S)-C(2S)	1.383(8)	C(5B)-C(6B)	1.543(6)

C(1)-C(6)	1.396(5)	C(5A)-C(6A)	1.532(6)
C(1)-C(2)	1.401(5)	C(6)-C(61)	1.516(5)
C(1B)-C(2B)	1.403(5)	C(6B)-C(7B)	1.525(6)
C(1B)-C(8B)	1.515(5)	C(6A)-C(7A)	1.529(6)
C(1A)-C(2A)	1.381(5)	C(7B)-C(8B)	1.527(6)
C(1A)-C(8A)	1.517(5)	C(7A)-C(8A)	1.532(6)
C(1S)-C(2S)	1.440(10)	C(21)-C(23)	1.525(6)
C(2)-C(3)	1.392(5)	C(21)-C(22)	1.537(5)
C(2)-C(21)	1.530(5)	C(61)-C(62)	1.526(5)
C(2B)-C(2A)	1.454(5)	C(61)-C(63)	1.527(5)
O(1)-W-O(2)	124.84(12)	C(1B)-C(2B)-C(2A)	124.5(4)
O(1)-W-O(2)#1	99.07(11)	C(1B)-C(2B)-C(3B)	117.3(4)
O(2)-W-O(2)#1	77.15(11)	C(2A)-C(2B)-C(3B)	118.0(3)
O(1)-W-C(1A)	111.38(14)	C(1A)-C(2A)-C(2B)	124.1(4)
O(2)-W-C(1A)	123.69(13)	C(1A)-C(2A)-C(3A)	118.1(4)
O(2)#1-W-C(1A)	92.15(12)	C(2B)-C(2A)-C(3A)	117.6(3)
O(1)-W-N	100.55(12)	O(8S)-C(2S)-C(1S)	114.4(7)
O(2)-W-N	85.54(11)	C(4)-C(3)-C(2)	121.7(4)
O(2)#1-W-N	159.01(11)	C(2B)-C(3B)-C(4B)	112.4(3)
C(1A)-W-N	87.60(13)	C(2A)-C(3A)-C(4A)	112.8(4)
O(1)-W-W#1	117.71(9)	O(8S)-C(3S)-C(4S)	114.1(7)
O(2)-W-W#1	38.78(7)	C(3)-C(4)-C(5)	119.9(4)
O(2)#1-W-W#1	38.37(7)	C(5B)-C(4B)-C(3B)	114.7(4)
C(1A)-W-W#1	112.16(11)	C(5A)-C(4A)-C(3A)	113.8(4)
N-W-W#1	123.39(9)	C(4)-C(5)-C(6)	121.2(4)
C(1B)-N-C(1)	120.7(3)	C(4B)-C(5B)-C(6B)	114.9(4)
C(1B)-N-W	115.4(2)	C(4A)-C(5A)-C(6A)	115.4(4)
C(1)-N-W	123.9(2)	C(1)-C(6)-C(5)	117.6(4)
W-O(2)-W#1	102.85(11)	C(1)-C(6)-C(61)	123.1(3)
C(3S)-O(8S)-C(2S)	117.9(6)	C(5)-C(6)-C(61)	119.3(4)
C(6)-C(1)-C(2)	122.0(3)	C(7B)-C(6B)-C(5B)	115.5(4)
C(6)-C(1)-N	117.4(3)	C(7A)-C(6A)-C(5A)	117.3(4)
C(2)-C(1)-N	120.5(3)	C(6B)-C(7B)-C(8B)	118.9(4)
N-C(1B)-C(2B)	120.3(3)	C(6A)-C(7A)-C(8A)	118.1(4)
N-C(1B)-C(8B)	117.7(3)	C(1B)-C(8B)-C(7B)	115.7(3)
C(2B)-C(1B)-C(8B)	122.0(3)	C(1A)-C(8A)-C(7A)	117.1(3)
C(2A)-C(1A)-C(8A)	124.6(4)	C(23)-C(21)-C(2)	110.2(3)
C(2A)-C(1A)-W	111.6(3)	C(23)-C(21)-C(22)	110.2(3)
C(8A)-C(1A)-W	121.9(3)	C(2)-C(21)-C(22)	112.0(3)
C(3)-C(2)-C(1)	117.5(4)	C(6)-C(61)-C(62)	112.1(3)

C(3)-C(2)-C(21)	119.5(4)	C(6)-C(61)-C(63)	111.3(3)
C(1)-C(2)-C(21)	123.0(3)	C(62)-C(61)-C(63)	110.7(4)

Symmetry transformations used to generate equivalent atoms:

#1 -x+1,-y,-z

Table A-16.4. Anisotropic displacement parameters ($Å^2$ x 10^3) for $[W(=C_8H_{12}=C_8H_{12}=NAr)(O)(\mu\text{-}O)]_2$. The anisotropic displacement factor exponent takes the form: $-2\pi^2 [h^2 a^{*2} U^{11} + ... + 2 h k a^* b^* U^{12}]$

	U^{11}	U^{22}	U^{33}	U^{23}	U^{13}	U^{12}
W	17(1)	18(1)	17(1)	8(1)	5(1)	5(1)
N	17(2)	20(2)	22(2)	13(2)	8(2)	6(2)
O(1)	22(2)	30(2)	19(2)	10(1)	4(1)	3(1)
O(2)	22(2)	22(2)	17(2)	12(1)	9(1)	9(1)
O(8S)	70(3)	98(3)	53(3)	41(3)	7(2)	16(3)
C(1)	18(2)	26(2)	14(2)	10(2)	7(2)	5(2)
C(1B)	17(2)	22(2)	19(2)	8(2)	6(2)	7(2)
C(1A)	21(2)	26(2)	21(2)	14(2)	12(2)	11(2)
C(1S)	95(6)	93(6)	190(10)	80(7)	23(7)	40(5)
C(2)	26(2)	21(2)	21(2)	13(2)	7(2)	5(2)
C(2B)	23(2)	19(2)	21(2)	7(2)	5(2)	6(2)
C(2A)	25(2)	22(2)	27(3)	12(2)	13(2)	7(2)
C(2S)	110(7)	127(8)	138(9)	87(7)	-29(6)	19(6)
C(3)	33(3)	26(3)	31(3)	17(2)	9(2)	3(2)
C(3B)	32(3)	31(3)	24(3)	11(2)	1(2)	-4(2)
C(3A)	36(3)	26(3)	27(3)	14(2)	7(2)	0(2)
C(3S)	146(9)	121(8)	49(5)	34(5)	18(5)	-2(6)
C(4)	25(3)	34(3)	27(3)	16(2)	11(2)	2(2)
C(4B)	21(3)	56(3)	27(3)	17(3)	3(2)	-4(2)
C(4A)	68(4)	20(3)	39(3)	13(2)	18(3)	6(3)
C(4S)	119(7)	108(7)	66(5)	12(5)	50(5)	9(5)
C(5)	21(2)	32(3)	23(3)	9(2)	6(2)	7(2)
C(5B)	30(3)	51(3)	31(3)	14(3)	2(2)	15(2)
C(5A)	64(4)	25(3)	55(4)	23(3)	32(3)	23(3)
C(6)	22(2)	23(2)	14(2)	7(2)	4(2)	4(2)
C(6B)	37(3)	41(3)	26(3)	15(2)	-2(2)	7(2)
C(6A)	54(3)	41(3)	62(4)	37(3)	25(3)	23(3)
C(7B)	29(3)	50(3)	50(3)	40(3)	2(2)	3(2)

C(7A)	46(3)	39(3)	40(3)	29(3)	12(2)	19(2)
C(8B)	29(3)	34(3)	22(3)	12(2)	8(2)	1(2)
C(8A)	41(3)	27(3)	29(3)	19(2)	10(2)	9(2)
C(21)	28(3)	27(3)	36(3)	21(2)	13(2)	9(2)
C(22)	43(3)	44(3)	54(3)	38(3)	19(3)	18(2)
C(23)	49(3)	28(3)	45(3)	19(2)	19(3)	19(2)
C(61)	21(2)	24(2)	27(3)	12(2)	7(2)	5(2)
C(62)	37(3)	41(3)	47(3)	30(3)	4(2)	5(2)
C(63)	60(4)	27(3)	42(3)	10(2)	13(3)	12(3)

Table A-16.5. Hydrogen coordinates (x 10^4) and isotropic displacement parameters ($Å^2$ x 10^3) for $[W(=C_8H_{12}=C_8H_{12}=NAr)(O)(\mu\text{-}O)]_2$.

	x	y	z	U(eq)		x	y	z	U(eq)
H(1SA)	-266	4639	7483	184	H(6BA)	7263	1939	5052	45
H(1SB)	1116	4832	8144	184	H(6BB)	6987	3207	5336	45
H(1SC)	8	3828	8042	184	H(6AA)	2410	4899	325	54
H(2SA)	-308	2720	6012	152	H(6AB)	3779	4854	218	54
H(2SB)	798	3723	6114	152	H(7BA)	5118	1027	4429	47
H(3A)	883	-1686	2210	36	H(7AA)	2234	2974	-1213	44
H(3BA)	6098	4121	4405	39	H(7AB)	1953	2804	-167	44
H(3BB)	6474	4683	3630	39	H(8BA)	3637	1977	4064	36
H(3AA)	5515	4155	859	37	H(8BB)	4702	3215	4628	36
H(3AB)	6418	4557	2096	37	H(8AA)	3199	1540	-1287	36
H(3SA)	1913	2169	5217	140	H(8AB)	4298	2754	-703	36
H(3SB)	764	1177	5074	140	H(21A)	3884	-712	1843	33
H(4A)	-662	-669	2475	35	H(22A)	4058	-2027	2614	59
H(4BA)	7640	3230	2821	47	H(22B)	2693	-2061	2782	59
H(4BB)	8157	4063	4223	47	H(22C)	3770	-813	3560	59
H(4AA)	5096	5611	3152	52	H(23A)	2451	-2190	-27	58
H(4AB)	5316	6074	2269	52	H(23B)	1915	-2945	534	58
H(4SA)	2522	494	5066	168	H(23C)	3301	-2836	418	58
H(4SB)	2058	675	6193	168	H(61A)	2248	2598	1920	29
H(4SC)	3209	1672	6340	168	H(62A)	326	1620	431	60
H(5A)	-406	1137	2426	33	H(62B)	537	3070	1163	60
H(5BA)	8125	2085	3731	49	H(62C)	-388	2217	1421	60
H(5BB)	6745	1557	2911	49	H(63A)	2272	3618	3964	69
H(5AA)	3212	5735	2229	52	H(63B)	819	3455	3611	69
H(5AB)	3120	4369	1927	52	H(63C)	1744	4309	3356	69

Table A-17.1. Crystal data and structure refinement for $Ti(NMe_2)_2(dpma)$.

Identification code	j	
Empirical formula	$C_{15}H_{25}N_5Ti$	
Formula weight	323.30	
Temperature	173(2) K	
Wavelength	0.71073 Å	
Crystal system	Orthorhombic	
Space group	P2(1)2(1)2(1) (#19)	
Unit cell dimensions	a = 9.832(2) Å	α= 90°
	b = 11.565(2) Å	β= 90°
	c = 15.177(3) Å	γ = 90°
Volume	1725.8(6) $Å^3$	
Z	4	
Density (calculated)	1.244 Mg/m^3	
Absorption coefficient	0.497 mm^{-1}	
F(000)	688	
Crystal size	0.39 x 0.13 x 0.13 mm^3	
Theta range for data collection	2.21 to 28.35°	
Index ranges	-12<=h<=13, -15<=k<=14, -19<=l<=20	
Reflections collected	20760	
Independent reflections	4189 [R(int) = 0.0764]	
Completeness to theta = 28.35°	98.2 %	
Refinement method	Full-matrix least-squares on F^2	
Data / restraints / parameters	4189 / 0 / 191	
Goodness-of-fit on F^2	1.016	
Final R indices [I>2sigma(I)]	R1 = 0.0524, wR2 = 0.1297	
R indices (all data)	R1 = 0.0920, wR2 = 0.1465	
Absolute structure parameter	0.04(4)	
Extinction coefficient	0.0029(13)	
Largest diff. peak and hole	0.450 and -0.348 $e.Å^{-3}$	

Table A-17.2. Atomic coordinates (x 10^4) and equivalent isotropic displacement parameters ($Å^2$ x 10^3) for $Ti(NMe_2)_2$(dpma). U(eq) is defined as one third of the trace of the orthogonalized U^{ij} tensor.

	x	y	z	U(eq)		x	y	z	U(eq)
Ti	-7941(1)	-4923(1)	-2063(1)	27(1)	C(22)	-7046(5)	-8204(4)	-945(3)	48(1)
N(1)	-7709(4)	-3395(3)	-1443(2)	34(1)	C(23)	-5831(5)	-7567(4)	-790(3)	43(1)
N(2)	-7346(3)	-6404(3)	-1477(2)	34(1)	C(24)	-6061(4)	-6485(3)	-1126(2)	35(1)
N(3)	-5610(3)	-4732(2)	-1922(2)	32(1)	C(31)	-5295(4)	-3482(3)	-1812(3)	40(1)
N(4)	-9810(3)	-5138(3)	-1827(2)	35(1)	C(32)	-5256(4)	-5385(3)	-1115(3)	40(1)
N(5)	-7957(3)	-4866(3)	-3288(2)	36(1)	C(33)	-4876(4)	-5225(4)	-2685(3)	41(1)
C(11)	-8584(4)	-2710(4)	-959(3)	41(1)	C(41)	-10303(4)	-5333(4)	-937(3)	47(1)
C(12)	-7873(6)	-1870(3)	-528(3)	47(1)	C(42)	-10948(4)	-5175(4)	-2445(3)	52(1)
C(13)	-6481(5)	-2016(4)	-755(3)	40(1)	C(51)	-8074(6)	-3827(4)	-3796(3)	57(1)
C(14)	-6431(4)	-2942(3)	-1312(3)	35(1)	C(52)	-7942(6)	-5902(4)	-3835(3)	62(1)
C(21)	-7932(5)	-7486(3)	-1367(3)	47(1)					

Table A-17.3. Bond lengths [Å] and angles [°] for $Ti(NMe_2)_2$(dpma).

Ti-N(5)	1.859(3)	N(4)-C(41)	1.453(5)
Ti-N(4)	1.888(3)	N(4)-C(42)	1.460(5)
Ti-N(1)	2.015(3)	N(5)-C(51)	1.433(5)
Ti-N(2)	2.017(3)	N(5)-C(52)	1.457(5)
Ti-N(3)	2.312(3)	C(11)-C(12)	1.364(6)
N(1)-C(14)	1.377(5)	C(12)-C(13)	1.421(7)
N(1)-C(11)	1.381(5)	C(13)-C(14)	1.365(6)
N(2)-C(24)	1.375(5)	C(14)-C(31)	1.487(6)
N(2)-C(21)	1.388(5)	C(21)-C(22)	1.363(6)
N(3)-C(33)	1.479(4)	C(22)-C(23)	1.423(7)
N(3)-C(32)	1.480(5)	C(23)-C(24)	1.370(5)
N(3)-C(31)	1.488(5)	C(24)-C(32)	1.498(6)
N(5)-Ti-N(4)	100.74(13)	C(31)-N(3)-Ti	108.0(2)
N(5)-Ti-N(1)	115.95(14)	C(41)-N(4)-C(42)	109.7(3)
N(4)-Ti-N(1)	97.88(14)	C(41)-N(4)-Ti	121.4(3)
N(5)-Ti-N(2)	118.21(14)	C(42)-N(4)-Ti	128.9(3)
N(4)-Ti-N(2)	94.96(13)	C(51)-N(5)-C(52)	112.5(3)
N(1)-Ti-N(2)	120.37(12)	C(51)-N(5)-Ti	124.6(3)

N(5)-Ti-N(3)	95.59(12)	C(52)-N(5)-Ti	122.7(3)
N(4)-Ti-N(3)	163.58(12)	C(12)-C(11)-N(1)	110.2(4)
N(1)-Ti-N(3)	76.16(12)	C(11)-C(12)-C(13)	107.0(3)
N(2)-Ti-N(3)	75.67(12)	C(14)-C(13)-C(12)	106.2(4)
C(14)-N(1)-C(11)	105.8(3)	C(13)-C(14)-N(1)	110.8(4)
C(14)-N(1)-Ti	120.3(3)	C(13)-C(14)-C(31)	132.2(4)
C(11)-N(1)-Ti	133.0(3)	N(1)-C(14)-C(31)	116.9(3)
C(24)-N(2)-C(21)	105.8(3)	C(22)-C(21)-N(2)	109.9(4)
C(24)-N(2)-Ti	119.7(3)	C(21)-C(22)-C(23)	107.4(4)
C(21)-N(2)-Ti	134.3(3)	C(24)-C(23)-C(22)	105.8(4)
C(33)-N(3)-C(32)	109.6(3)	C(23)-C(24)-N(2)	111.0(4)
C(33)-N(3)-C(31)	111.2(3)	C(23)-C(24)-C(32)	133.2(4)
C(32)-N(3)-C(31)	110.7(3)	N(2)-C(24)-C(32)	115.6(3)
C(33)-N(3)-Ti	112.0(2)	C(14)-C(31)-N(3)	108.0(3)
C(32)-N(3)-Ti	105.1(2)	N(3)-C(32)-C(24)	107.5(3)

Table A-17.4. Anisotropic displacement parameters ($Å^2 x\ 10^3$) for $Ti(NMe_2)_2(dpma)$.

The anisotropic displacement factor exponent takes the form:

$-2\pi^2[\ h^2\ a^{*2}U^{11} + ...\ + 2\ h\ k\ a^*\ b^*\ U^{12}\ ]$

	U^{11}	U^{22}	U^{33}	U^{23}	U^{13}	U^{12}
Ti	29(1)	27(1)	26(1)	1(1)	-2(1)	0(1)
N(1)	38(2)	28(2)	36(2)	-1(1)	3(2)	2(1)
N(2)	32(2)	30(2)	40(2)	5(1)	-2(1)	-3(1)
N(3)	31(2)	32(2)	33(2)	-3(1)	3(1)	-2(1)
N(4)	31(1)	37(2)	38(2)	3(2)	-1(1)	-2(2)
N(5)	39(2)	42(2)	27(1)	-1(1)	-2(1)	3(2)
C(11)	40(2)	39(2)	43(2)	2(2)	9(2)	6(2)
C(12)	73(3)	30(2)	37(2)	-7(2)	13(2)	2(2)
C(13)	55(3)	36(2)	30(2)	-4(2)	1(2)	-13(2)
C(14)	44(2)	27(2)	34(2)	3(2)	3(2)	-3(2)
C(21)	50(2)	34(2)	55(3)	3(2)	8(2)	-1(2)
C(22)	64(3)	34(2)	44(2)	9(2)	8(3)	10(2)
C(23)	50(3)	43(2)	36(2)	8(2)	-2(2)	14(2)
C(24)	39(2)	38(2)	27(2)	7(2)	1(2)	8(2)
C(31)	39(2)	37(2)	42(2)	-4(2)	6(2)	-14(2)
C(32)	34(2)	53(3)	34(2)	-1(2)	-5(2)	1(2)
C(33)	31(2)	48(2)	44(2)	-4(2)	8(2)	2(2)

C(41)	45(2)	54(3)	44(2)	3(2)	9(2)	-5(2)
C(42)	34(2)	65(3)	58(3)	-3(3)	-10(2)	2(2)
C(51)	76(4)	54(3)	42(3)	7(2)	3(3)	0(3)
C(52)	82(4)	55(3)	48(3)	-11(2)	-21(3)	-1(3)

Table A-17.5. Hydrogen coordinates (x 10^4) and isotropic displacement parameters ($Å^2$ x 10^3) for $Ti(NMe_2)_2(dpma)$.

	x	y	z	U(eq)		x	y	z	U(eq)
H(11A)	-9521	-2807	-930	49	H(41A)	-11273	-5423	-947	71
H(12A)	-8231	-1308	-156	56	H(41B)	-10067	-4684	-573	71
H(13A)	-5751	-1571	-563	48	H(41C)	-9893	-6021	-703	71
H(21A)	-8800	-7691	-1553	56	H(42A)	-11780	-5293	-2126	79
H(22A)	-7206	-8969	-788	57	H(42B)	-10817	-5800	-2853	79
H(23A)	-5043	-7830	-516	52	H(42C)	-10996	-4458	-2762	79
H(31A)	-4447	-3388	-1493	47	H(51A)	-8055	-4015	-4412	86
H(31B)	-5201	-3116	-2383	47	H(51B)	-7328	-3322	-3659	86
H(32A)	-5478	-4935	-596	48	H(51C)	-8916	-3449	-3658	86
H(32B)	-4290	-5555	-1106	48	H(52A)	-7957	-5683	-4445	93
H(33A)	-3915	-5129	-2602	61	H(52B)	-8727	-6365	-3704	93
H(33B)	-5152	-4833	-3213	61	H(52C)	-7133	-6339	-3715	93
H(33C)	-5085	-6034	-2735	61					

Table A-18.1. Crystal data and structure refinement for $Ti(dmpm)(NMe_2)_2$.

Identification code	jtcvi64t	
Empirical formula	$C_{15}H_{21}N_4Ti$	
Formula weight	305.26	
Temperature	446(2) K	
Wavelength	0.71073 Å	
Crystal system	Monoclinic	
Space group	P2(1)/c	
Unit cell dimensions	a = 10.3208(17) Å	α= 90°
	b = 12.3848(19) Å	β= 93.708(3)°
	c = 25.325(4) Å	γ = 90°
Volume	3230.3(9) $Å^3$	
Z	8	
Density (calculated)	1.255 Mg/m^3	
Absorption coefficient	0.526 mm^{-1}	
F(000)	1288	
Crystal size	0.18 x 0.08 x 0.06 mm^3	
Theta range for data collection	1.61 to 23.29°	
Index ranges	-11<=h<=11, -13<=k<=13, -28<=l<=13	
Reflections collected	14599	
Independent reflections	4627 [R(int) = 0.2227]	
Completeness to theta = 23.29°	99.4 %	
Absorption correction	Empirical	
Max. and min. transmission	0.9499 and 0.5252	
Refinement method	Full-matrix least-squares on F^2	
Data / restraints / parameters	4627 / 0 / 373	
Goodness-of-fit on F^2	0.787	
Final R indices [I>2sigma(I)]	R1 = 0.0622, wR2 = 0.1030	
R indices (all data)	R1 = 0.1910, wR2 = 0.1295	
Largest diff. peak and hole	0.475 and -0.377 $e.Å^{-3}$	

Table A-18.2. Atomic coordinates (x 10^4) and equivalent isotropic displacement parameters ($Å^2$x 10^3) for Ti(dmpm)$(NMe_2)_2$. U(eq) is defined as one third of the trace of the orthogonalized U^{ij} tensor.

	x	y	z	U(eq)		x	y	z	U(eq)
Ti(1)	5274(1)	3345(1)	1809(1)	27(1)	Ti(2)	362(1)	2662(1)	9619(1)	28(1)
N(1A)	3397(5)	4260(5)	1767(2)	32(2)	N(1B)	2171(5)	3637(4)	9567(2)	32(2)
N(2A)	4220(5)	2010(4)	1599(2)	23(2)	N(2B)	1022(5)	1671(4)	9062(2)	27(2)
N(4A)	6051(5)	3723(4)	1176(2)	30(2)	N(4B)	-889(5)	3431(4)	9205(2)	29(2)
N(5A)	6671(5)	2908(4)	2256(2)	28(2)	N(5B)	-608(5)	1817(4)	10075(2)	31(2)
C(11A)	4352(7)	5028(5)	1907(3)	32(2)	C(11B)	1492(6)	4137(6)	9956(3)	32(2)
C(12A)	4905(7)	4827(6)	2420(3)	34(2)	C(12B)	1497(7)	3454(6)	10408(3)	39(2)
C(13A)	4229(7)	3883(6)	2614(3)	31(2)	C(13B)	2214(6)	2500(6)	10289(3)	27(2)
C(14A)	3336(7)	3575(6)	2199(3)	29(2)	C(14B)	2621(6)	2657(6)	9778(3)	24(2)
C(21A)	4454(7)	1175(6)	1278(3)	26(2)	C(21B)	351(7)	1102(6)	8663(3)	34(2)
C(22A)	3454(7)	451(5)	1229(3)	30(2)	C(22B)	1186(7)	459(5)	8405(3)	28(2)
C(23A)	2509(7)	883(5)	1547(3)	31(2)	C(23B)	2432(7)	609(5)	8655(3)	30(2)
C(24A)	2985(6)	1822(6)	1769(3)	23(2)	C(24B)	2320(7)	1361(5)	9049(3)	25(2)
C(30A)	2462(6)	2599(6)	2169(3)	27(2)	C(30B)	3318(6)	1891(6)	9423(3)	26(2)
C(31A)	1048(6)	2919(5)	1990(3)	42(2)	C(31B)	4301(6)	2531(5)	9108(3)	41(2)
C(32A)	2462(7)	2037(5)	2704(3)	43(2)	C(32B)	4077(6)	1064(5)	9761(3)	41(2)
C(41A)	5246(7)	4033(5)	705(3)	45(2)	C(41B)	-470(7)	4007(6)	8737(3)	52(3)
C(42A)	7430(6)	3900(5)	1104(3)	54(3)	C(42B)	-2286(6)	3556(5)	9254(3)	44(2)
C(51A)	7310(6)	1965(5)	2049(3)	39(2)	C(51B)	-1579(6)	1154(5)	9774(3)	46(2)
C(52A)	7255(7)	3136(6)	2775(3)	53(3)	C(52B)	-557(7)	1507(6)	10636(3)	49(2)

Table A-18.3. Bond lengths [Å] and angles [°] for Ti(dmpm)$(NMe_2)_2$.

Ti(1)-N(5A)	1.857(6)	Ti(2)-N(4B)	1.870(5)
Ti(1)-N(4A)	1.896(6)	Ti(2)-N(5B)	1.893(5)
Ti(1)-N(2A)	2.030(5)	Ti(2)-N(2B)	2.020(6)
Ti(1)-N(1A)	2.240(5)	Ti(2)-N(1B)	2.234(5)
Ti(1)-C(14A)	2.305(6)	Ti(2)-C(11B)	2.302(7)
Ti(1)-C(11A)	2.312(7)	Ti(2)-C(14B)	2.340(6)
Ti(1)-C(12A)	2.447(7)	Ti(2)-C(12B)	2.455(7)
Ti(1)-C(13A)	2.459(7)	Ti(2)-C(13B)	2.480(7)
N(1A)-C(14A)	1.390(8)	N(1B)-C(11B)	1.391(7)
N(1A)-C(11A)	1.399(8)	N(1B)-C(14B)	1.393(7)

N(2A)-C(21A)	1.348(7)	N(2B)-C(21B)	1.381(8)
N(2A)-C(24A)	1.390(7)	N(2B)-C(24B)	1.396(7)
N(4A)-C(41A)	1.460(8)	N(4B)-C(42B)	1.462(7)
N(4A)-C(42A)	1.463(7)	N(4B)-C(41B)	1.472(8)
N(5A)-C(52A)	1.437(8)	N(5B)-C(52B)	1.469(8)
N(5A)-C(51A)	1.456(7)	N(5B)-C(51B)	1.471(8)
C(11A)-C(12A)	1.407(9)	C(11B)-C(12B)	1.422(9)
C(12A)-C(13A)	1.462(9)	C(12B)-C(13B)	1.437(9)
C(13A)-C(14A)	1.404(9)	C(13B)-C(14B)	1.399(9)
C(14A)-C(30A)	1.507(9)	C(14B)-C(30B)	1.520(8)
C(21A)-C(22A)	1.367(8)	C(21B)-C(22B)	1.369(8)
C(22A)-C(23A)	1.410(8)	C(22B)-C(23B)	1.409(9)
C(23A)-C(24A)	1.368(8)	C(23B)-C(24B)	1.375(8)
C(24A)-C(30A)	1.522(8)	C(24B)-C(30B)	1.504(9)
C(30A)-C(32A)	1.524(8)	C(30B)-C(32B)	1.520(8)
C(30A)-C(31A)	1.552(8)	C(30B)-C(31B)	1.549(8)
N(5A)-Ti(1)-N(4A)	103.5(2)	N(4B)-Ti(2)-N(5B)	104.5(3)
N(5A)-Ti(1)-N(2A)	107.7(2)	N(4B)-Ti(2)-N(2B)	99.8(2)
N(4A)-Ti(1)-N(2A)	103.2(2)	N(5B)-Ti(2)-N(2B)	107.8(2)
N(5A)-Ti(1)-N(1A)	144.2(2)	N(4B)-Ti(2)-N(1B)	104.0(2)
N(4A)-Ti(1)-N(1A)	104.3(2)	N(5B)-Ti(2)-N(1B)	144.2(3)
N(2A)-Ti(1)-N(1A)	87.3(2)	N(2B)-Ti(2)-N(1B)	88.1(2)
N(5A)-Ti(1)-C(14A)	115.8(3)	N(4B)-Ti(2)-C(11B)	96.8(3)
N(4A)-Ti(1)-C(14A)	139.3(3)	N(5B)-Ti(2)-C(11B)	119.2(3)
N(2A)-Ti(1)-C(14A)	75.4(2)	N(2B)-Ti(2)-C(11B)	123.8(2)
N(1A)-Ti(1)-C(14A)	35.6(2)	N(1B)-Ti(2)-C(11B)	35.67(19)
N(5A)-Ti(1)-C(11A)	120.3(3)	N(4B)-Ti(2)-C(14B)	137.9(3)
N(4A)-Ti(1)-C(11A)	93.9(2)	N(5B)-Ti(2)-C(14B)	117.0(3)
N(2A)-Ti(1)-C(11A)	123.0(3)	N(2B)-Ti(2)-C(14B)	75.0(2)
N(1A)-Ti(1)-C(11A)	35.8(2)	N(1B)-Ti(2)-C(14B)	35.37(18)
C(14A)-Ti(1)-C(11A)	57.8(2)	C(11B)-Ti(2)-C(14B)	57.5(2)
N(5A)-Ti(1)-C(12A)	88.7(3)	N(4B)-Ti(2)-C(12B)	121.9(3)
N(4A)-Ti(1)-C(12A)	116.2(2)	N(5B)-Ti(2)-C(12B)	88.1(3)
N(2A)-Ti(1)-C(12A)	132.3(2)	N(2B)-Ti(2)-C(12B)	130.2(3)
N(1A)-Ti(1)-C(12A)	58.8(2)	N(1B)-Ti(2)-C(12B)	58.3(2)
C(14A)-Ti(1)-C(12A)	57.4(2)	C(11B)-Ti(2)-C(12B)	34.6(2)
C(11A)-Ti(1)-C(12A)	34.2(2)	C(14B)-Ti(2)-C(12B)	56.2(2)
N(5A)-Ti(1)-C(13A)	86.4(2)	N(4B)-Ti(2)-C(13B)	153.9(2)
N(4A)-Ti(1)-C(13A)	149.9(2)	N(5B)-Ti(2)-C(13B)	87.2(2)
N(2A)-Ti(1)-C(13A)	100.5(2)	N(2B)-Ti(2)-C(13B)	98.5(2)

N(1A)-Ti(1)-C(13A)	58.5(2)	N(1B)-Ti(2)-C(13B)	58.3(2)
C(14A)-Ti(1)-C(13A)	34.1(2)	C(11B)-Ti(2)-C(13B)	57.4(2)
C(11A)-Ti(1)-C(13A)	57.3(3)	C(14B)-Ti(2)-C(13B)	33.6(2)
C(12A)-Ti(1)-C(13A)	34.7(2)	C(12B)-Ti(2)-C(13B)	33.8(2)
C(14A)-N(1A)-C(11A)	106.3(6)	C(11B)-N(1B)-C(14B)	106.7(6)
C(14A)-N(1A)-Ti(1)	74.8(4)	C(11B)-N(1B)-Ti(2)	74.8(4)
C(11A)-N(1A)-Ti(1)	74.9(4)	C(14B)-N(1B)-Ti(2)	76.5(3)
C(21A)-N(2A)-C(24A)	105.2(6)	C(21B)-N(2B)-C(24B)	106.2(6)
C(21A)-N(2A)-Ti(1)	132.0(5)	C(21B)-N(2B)-Ti(2)	130.2(5)
C(24A)-N(2A)-Ti(1)	122.8(5)	C(24B)-N(2B)-Ti(2)	123.5(5)
C(41A)-N(4A)-C(42A)	111.5(6)	C(42B)-N(4B)-C(41B)	111.1(6)
C(41A)-N(4A)-Ti(1)	120.4(4)	C(42B)-N(4B)-Ti(2)	130.9(5)
C(42A)-N(4A)-Ti(1)	127.5(5)	C(41B)-N(4B)-Ti(2)	118.0(4)
C(52A)-N(5A)-C(51A)	108.3(6)	C(52B)-N(5B)-C(51B)	109.6(5)
C(52A)-N(5A)-Ti(1)	139.8(5)	C(52B)-N(5B)-Ti(2)	138.4(5)
C(51A)-N(5A)-Ti(1)	111.5(4)	C(51B)-N(5B)-Ti(2)	111.2(4)
N(1A)-C(11A)-C(12A)	110.6(7)	N(1B)-C(11B)-C(12B)	109.2(6)
N(1A)-C(11A)-Ti(1)	69.3(3)	N(1B)-C(11B)-Ti(2)	69.5(4)
C(12A)-C(11A)-Ti(1)	78.1(4)	C(12B)-C(11B)-Ti(2)	78.6(4)
C(11A)-C(12A)-C(13A)	106.1(7)	C(11B)-C(12B)-C(13B)	107.2(7)
C(11A)-C(12A)-Ti(1)	67.6(4)	C(11B)-C(12B)-Ti(2)	66.8(4)
C(13A)-C(12A)-Ti(1)	73.1(4)	C(13B)-C(12B)-Ti(2)	74.0(4)
C(14A)-C(13A)-C(12A)	105.7(7)	C(14B)-C(13B)-C(12B)	105.6(7)
C(14A)-C(13A)-Ti(1)	66.9(4)	C(14B)-C(13B)-Ti(2)	67.7(4)
C(12A)-C(13A)-Ti(1)	72.2(4)	C(12B)-C(13B)-Ti(2)	72.1(4)
N(1A)-C(14A)-C(13A)	111.3(6)	N(1B)-C(14B)-C(13B)	111.2(6)
N(1A)-C(14A)-C(30A)	120.4(7)	N(1B)-C(14B)-C(30B)	118.5(7)
C(13A)-C(14A)-C(30A)	128.2(7)	C(13B)-C(14B)-C(30B)	129.9(7)
N(1A)-C(14A)-Ti(1)	69.7(3)	N(1B)-C(14B)-Ti(2)	68.1(3)
C(13A)-C(14A)-Ti(1)	79.0(4)	C(13B)-C(14B)-Ti(2)	78.7(4)
C(30A)-C(14A)-Ti(1)	114.3(4)	C(30B)-C(14B)-Ti(2)	113.8(4)
N(2A)-C(21A)-C(22A)	113.2(6)	C(22B)-C(21B)-N(2B)	110.2(7)
C(21A)-C(22A)-C(23A)	104.2(6)	C(21B)-C(22B)-C(23B)	107.0(6)
C(24A)-C(23A)-C(22A)	108.3(6)	C(24B)-C(23B)-C(22B)	107.3(6)
C(23A)-C(24A)-N(2A)	109.2(6)	C(23B)-C(24B)-N(2B)	109.3(7)
C(23A)-C(24A)-C(30A)	132.6(6)	C(23B)-C(24B)-C(30B)	131.7(7)
N(2A)-C(24A)-C(30A)	118.1(6)	N(2B)-C(24B)-C(30B)	118.9(6)
C(14A)-C(30A)-C(24A)	107.7(5)	C(24B)-C(30B)-C(14B)	108.3(6)
C(14A)-C(30A)-C(32A)	110.8(6)	C(24B)-C(30B)-C(32B)	111.7(6)
C(24A)-C(30A)-C(32A)	108.9(6)	C(14B)-C(30B)-C(32B)	109.5(6)
C(14A)-C(30A)-C(31A)	111.0(6)	C(24B)-C(30B)-C(31B)	110.1(6)

C(24A)-C(30A)-C(31A)	109.6(6)	C(14B)-C(30B)-C(31B)	109.6(6)
C(32A)-C(30A)-C(31A)	108.7(6)	C(32B)-C(30B)-C(31B)	107.7(6)

Table A-18.4. Anisotropic displacement parameters ($Å^2$ x 10^3) for Ti(dmpm)(NMe_2)$_2$.

The anisotropic displacement factor exponent takes the form:

$-2\pi^2[\ h^2\ a^{*2}U^{11} + \ldots + 2\ h\ k\ a^*\ b^*\ U^{12}\ ]$

	U^{11}	U^{22}	U^{33}	U^{23}	U^{13}	U^{12}
Ti(1)	27(1)	26(1)	27(1)	-1(1)	6(1)	1(1)
N(1A)	25(4)	33(4)	39(5)	6(4)	4(4)	4(3)
N(2A)	30(4)	22(4)	17(4)	-2(3)	12(3)	3(3)
N(4A)	29(4)	28(4)	34(4)	3(3)	10(4)	-3(3)
N(5A)	30(4)	28(4)	27(4)	-15(3)	3(4)	1(3)
C(11A)	28(5)	21(5)	48(6)	-14(5)	5(5)	2(4)
C(12A)	31(5)	26(5)	48(7)	-6(5)	13(5)	9(4)
C(13A)	20(5)	36(5)	38(6)	-24(5)	8(5)	6(4)
C(14A)	37(5)	19(5)	34(6)	-4(5)	25(5)	1(4)
C(21A)	23(5)	30(5)	27(5)	-3(4)	2(4)	4(4)
C(22A)	35(5)	21(5)	33(6)	-11(4)	6(5)	8(4)
C(23A)	34(5)	29(5)	30(5)	-6(4)	6(5)	-13(4)
C(24A)	27(5)	22(5)	19(5)	-2(4)	10(4)	-1(4)
C(30A)	25(5)	35(5)	23(5)	6(5)	6(4)	3(4)
C(31A)	29(5)	46(6)	51(6)	-12(5)	12(5)	0(4)
C(32A)	59(6)	33(5)	37(6)	-5(4)	14(5)	0(4)
C(41A)	55(6)	54(6)	27(6)	4(5)	15(5)	-1(5)
C(42A)	36(6)	53(6)	74(7)	14(5)	24(5)	-7(4)
C(51A)	30(5)	36(5)	52(6)	1(5)	7(5)	1(4)
C(52A)	42(5)	75(7)	42(6)	-8(5)	-7(5)	16(5)
Ti(2)	26(1)	29(1)	29(1)	0(1)	7(1)	0(1)
N(1B)	26(4)	25(4)	46(5)	4(4)	10(4)	-5(3)
N(2B)	20(4)	25(4)	36(4)	-2(4)	1(4)	2(3)
N(4B)	19(4)	36(4)	31(4)	6(4)	4(3)	7(3)
N(5B)	35(4)	30(4)	28(4)	1(4)	10(4)	-9(3)
C(11B)	17(4)	44(6)	35(6)	-20(5)	10(5)	-6(4)
C(12B)	40(5)	32(5)	43(6)	-6(5)	-11(5)	-7(4)
C(13B)	27(5)	40(5)	13(5)	-12(5)	2(4)	-4(4)
C(14B)	15(4)	14(5)	43(6)	-3(5)	-4(4)	-2(4)
C(21B)	33(5)	40(5)	30(6)	-10(5)	2(5)	-2(4)

C(22B)	44(5)	24(5)	17(5)	-3(4)	6(5)	-5(4)
C(23B)	33(5)	27(5)	30(6)	6(4)	11(5)	3(4)
C(24B)	29(5)	18(5)	30(5)	3(4)	5(5)	-2(4)
C(30B)	21(4)	40(5)	18(5)	-3(4)	1(4)	1(4)
C(31B)	41(5)	41(5)	41(5)	0(5)	8(5)	-8(4)
C(32B)	39(5)	37(5)	47(6)	0(5)	14(5)	8(4)
C(41B)	52(6)	52(6)	53(7)	-4(5)	4(6)	1(4)
C(42B)	31(5)	47(6)	54(6)	-16(5)	-3(5)	16(4)
C(51B)	43(5)	45(6)	52(6)	7(5)	15(5)	-21(4)
C(52B)	64(6)	50(6)	37(6)	7(5)	19(5)	-1(5)

Table A-18.5. Hydrogen coordinates (x 10^4) and isotropic displacement parameters ($Å^2$ x 10^3) for Ti(dmpm)$(NMe_2)_2$.

	x	y	z	U(eq)		x	y	z	U(eq)
H(21A)	5219	1098	1106	32	H(21B)	-539	1148	8581	41
H(22A)	3407	-183	1031	36	H(22B)	970	9	8119	34
H(23A)	1701	582	1598	37	H(23B)	3191	262	8570	35
H(31D)	705	3382	2252	63	H(31A)	4754	2043	8890	62
H(31E)	523	2281	1951	63	H(31B)	4913	2889	9350	62
H(31F)	1039	3293	1658	63	H(31C)	3846	3058	8889	62
H(32D)	3326	1801	2809	64	H(32A)	3494	672	9971	61
H(32E)	1892	1424	2676	64	H(32B)	4715	1427	9990	61
H(32F)	2167	2531	2962	64	H(32C)	4502	571	9537	61
H(41D)	5361	4788	637	67	H(41A)	-910	3712	8424	78
H(41E)	4350	3893	761	67	H(41B)	451	3923	8717	78
H(41F)	5498	3621	407	67	H(41C)	-676	4759	8765	78
H(42D)	7697	3449	823	80	H(42A)	-2501	4310	9257	67
H(42E)	7928	3723	1426	80	H(42B)	-2522	3228	9577	67
H(42F)	7569	4643	1017	80	H(42C)	-2751	3212	8959	67
H(51A)	8219	2113	2029	59	H(51D)	-1372	404	9824	69
H(51B)	6931	1799	1703	59	H(51E)	-1577	1330	9405	69
H(51C)	7203	1361	2280	59	H(51F)	-2424	1295	9897	69
H(52D)	7134	2531	3003	80	H(52A)	-1390	1628	10774	74
H(52E)	6854	3764	2915	80	H(52B)	86	1934	10831	74
H(52F)	8167	3267	2752	80	H(52C)	-334	757	10670	74

Table A-19.1. Crystal data and structure refinement for $Ti(dppm)(NMe_2)_2$.

Identification code	shi60t	
Empirical formula	$C_{19}H_{32}N_4Ti$	
Formula weight	364.39	
Temperature	173(2) K	
Wavelength	0.71073 Å	
Crystal system	Monoclinic	
Space group	P2(1)/c	
Unit cell dimensions	a = 9.9440(14) Å	α= 90°
	b = 15.266(2) Å	β= 93.252(3)°
	c = 13.696(2) Å	γ = 90°
Volume	2075.8(5) $Å^3$	
Z	4	
Density (calculated)	1.166 Mg/m^3	
Absorption coefficient	0.419 mm^{-1}	
F(000)	784	
Crystal size	0.16 x 0.28 x 0.43 mm^3	
Theta range for data collection	2.00 to 23.28°	
Index ranges	-11<=h<=9, -13<=k<=16, -15<=l<=15	
Reflections collected	9353	
Independent reflections	2980 [R(int) = 0.2034]	
Completeness to theta = 23.28°	99.9 %	
Absorption correction	Empirical	
Max. and min. transmission	0.9830 and 0.6436	
Refinement method	Full-matrix least-squares on F^2	
Data / restraints / parameters	2980 / 0 / 223	
Goodness-of-fit on F^2	0.971	
Final R indices [I>2sigma(I)]	R1 = 0.0876, wR2 = 0.2273	
R indices (all data)	R1 = 0.1837, wR2 = 0.3346	
Largest diff. peak and hole	1.194 and -1.414 $e.Å^{-3}$	

Table A-19.2. Atomic coordinates (x 10^4) and equivalent isotropic displacement parameters ($Å^2$ x 10^3) for Ti(dppm)$(NMe_2)_2$. U(eq) is defined as one third of the trace of the orthogonalized U^{ij} tensor.

	x	y	z	U(eq)		x	y	z	U(eq)
Ti(1)	9038(2)	2369(1)	1725(1)	35(1)	C(24)	8014(10)	1046(5)	3156(6)	27(2)
N(1)	8063(9)	1184(5)	967(5)	36(2)	C(30)	6808(10)	977(5)	2453(6)	31(2)
N(2)	8902(8)	1711(4)	3018(5)	30(2)	C(31)	6519(10)	5(5)	2164(6)	36(2)
N(4)	10876(8)	2205(5)	1473(5)	38(2)	C(32)	5324(12)	-143(6)	1463(6)	50(3)
N(5)	8810(9)	3574(5)	1981(5)	38(2)	C(33)	5161(15)	-1110(7)	1185(9)	82(5)
C(11)	8158(12)	1814(7)	257(7)	48(3)	C(34)	5580(10)	1395(6)	2925(7)	40(3)
C(12)	7414(11)	2501(7)	364(7)	44(3)	C(35)	5001(11)	885(6)	3782(7)	42(3)
C(13)	6634(11)	2299(6)	1193(6)	38(3)	C(36)	3915(13)	1380(7)	4266(8)	67(4)
C(14)	7160(10)	1488(6)	1543(6)	31(2)	C(41)	11422(14)	1308(7)	1361(9)	72(4)
C(21)	9962(10)	1642(6)	3774(6)	35(2)	C(42)	11938(15)	2837(8)	1285(9)	77(4)
C(22)	9636(13)	967(6)	4372(6)	46(3)	C(51)	7877(11)	4277(6)	1688(7)	46(3)
C(23)	8414(11)	581(5)	3981(6)	37(3)	C(52)	9811(11)	3889(6)	2744(7)	48(3)

Table A-19.3. Bond lengths [Å] and angles [°] for Ti(dppm)$(NMe_2)_2$.

Ti(1)-N(5)	1.889(7)	N(5)-C(52)	1.482(12)
Ti(1)-N(4)	1.896(9)	C(11)-C(12)	1.296(14)
Ti(1)-N(2)	2.046(7)	C(12)-C(13)	1.444(14)
Ti(1)-N(1)	2.275(7)	C(13)-C(14)	1.416(12)
Ti(1)-C(14)	2.303(9)	C(14)-C(30)	1.529(12)
Ti(1)-C(11)	2.308(9)	C(21)-C(22)	1.367(13)
Ti(1)-C(12)	2.405(9)	C(22)-C(23)	1.427(14)
Ti(1)-C(13)	2.461(10)	C(23)-C(24)	1.374(11)
N(1)-C(14)	1.313(11)	C(24)-C(30)	1.498(13)
N(1)-C(11)	1.376(11)	C(30)-C(34)	1.551(13)
N(2)-C(24)	1.366(11)	C(30)-C(31)	1.559(11)
N(2)-C(21)	1.440(11)	C(31)-C(32)	1.501(13)
N(4)-C(42)	1.464(14)	C(32)-C(33)	1.530(13)
N(4)-C(41)	1.484(12)	C(34)-C(35)	1.547(12)
N(5)-C(51)	1.460(12)	C(35)-C(36)	1.503(14)
N(5)-Ti(1)-N(4)	106.8(4)	C(41)-N(4)-Ti(1)	120.2(7)
N(5)-Ti(1)-N(2)	107.6(3)	C(51)-N(5)-C(52)	110.2(7)

N(4)-Ti(1)-N(2)	101.8(3)	C(51)-N(5)-Ti(1)	138.3(7)
N(5)-Ti(1)-N(1)	143.8(3)	C(52)-N(5)-Ti(1)	111.3(6)
N(4)-Ti(1)-N(1)	101.7(3)	C(12)-C(11)-N(1)	115.0(10)
N(2)-Ti(1)-N(1)	87.6(3)	C(12)-C(11)-Ti(1)	78.2(6)
N(5)-Ti(1)-C(14)	118.9(4)	N(1)-C(11)-Ti(1)	71.2(5)
N(4)-Ti(1)-C(14)	133.4(3)	C(11)-C(12)-C(13)	104.6(8)
N(2)-Ti(1)-C(14)	73.4(3)	C(11)-C(12)-Ti(1)	70.0(6)
N(1)-Ti(1)-C(14)	33.3(3)	C(13)-C(12)-Ti(1)	74.9(5)
N(5)-Ti(1)-C(11)	118.4(4)	C(14)-C(13)-C(12)	104.4(9)
N(4)-Ti(1)-C(11)	96.6(4)	C(14)-C(13)-Ti(1)	66.7(5)
N(2)-Ti(1)-C(11)	122.3(3)	C(12)-C(13)-Ti(1)	70.6(6)
N(1)-Ti(1)-C(11)	34.9(3)	N(1)-C(14)-C(13)	111.0(8)
C(14)-Ti(1)-C(11)	55.0(3)	N(1)-C(14)-C(30)	120.3(8)
N(5)-Ti(1)-C(12)	88.8(3)	C(13)-C(14)-C(30)	128.7(9)
N(4)-Ti(1)-C(12)	118.8(4)	N(1)-C(14)-Ti(1)	72.2(5)
N(2)-Ti(1)-C(12)	129.6(3)	C(13)-C(14)-Ti(1)	79.0(6)
N(1)-Ti(1)-C(12)	57.5(3)	C(30)-C(14)-Ti(1)	115.5(5)
C(14)-Ti(1)-C(12)	57.3(3)	C(22)-C(21)-N(2)	107.3(8)
C(11)-Ti(1)-C(12)	31.8(3)	C(21)-C(22)-C(23)	108.2(8)
N(5)-Ti(1)-C(13)	88.4(3)	C(24)-C(23)-C(22)	107.2(8)
N(4)-Ti(1)-C(13)	150.5(3)	N(2)-C(24)-C(23)	109.9(8)
N(2)-Ti(1)-C(13)	97.2(3)	N(2)-C(24)-C(30)	117.6(7)
N(1)-Ti(1)-C(13)	56.6(3)	C(23)-C(24)-C(30)	132.5(9)
C(14)-Ti(1)-C(13)	34.4(3)	C(24)-C(30)-C(14)	106.1(7)
C(11)-Ti(1)-C(13)	54.0(4)	C(24)-C(30)-C(34)	108.9(7)
C(12)-Ti(1)-C(13)	34.5(3)	C(14)-C(30)-C(34)	110.6(7)
C(14)-N(1)-C(11)	104.7(8)	C(24)-C(30)-C(31)	111.1(7)
C(14)-N(1)-Ti(1)	74.5(5)	C(14)-C(30)-C(31)	109.0(6)
C(11)-N(1)-Ti(1)	73.8(5)	C(34)-C(30)-C(31)	111.1(8)
C(24)-N(2)-C(21)	107.3(7)	C(32)-C(31)-C(30)	115.7(8)
C(24)-N(2)-Ti(1)	124.1(5)	C(31)-C(32)-C(33)	111.9(9)
C(21)-N(2)-Ti(1)	125.2(6)	C(35)-C(34)-C(30)	116.4(8)
C(42)-N(4)-C(41)	108.5(9)	C(36)-C(35)-C(34)	112.9(8)
C(42)-N(4)-Ti(1)	131.1(8)		

Table A-19.4. Anisotropic displacement parameters ($Å^2 \times 10^3$) for $Ti(dppm)(NMe_2)_2$.

The anisotropic displacement factor exponent takes the form:

$-2\pi^2[h^2 a^{*2}U^{11} + ... + 2 h k a^* b^* U^{12}]$

	U^{11}	U^{22}	U^{33}	U^{23}	U^{13}	U^{12}
Ti(1)	53(1)	27(1)	25(1)	4(1)	-5(1)	-5(1)
N(1)	48(6)	33(5)	27(4)	-5(3)	8(4)	-8(4)
N(2)	36(5)	26(4)	28(4)	5(3)	2(4)	2(4)
N(4)	38(6)	40(5)	37(4)	6(4)	5(4)	-8(4)
N(5)	59(6)	26(4)	28(4)	8(3)	1(4)	-5(4)
C(11)	70(9)	41(7)	33(6)	1(5)	4(5)	-29(6)
C(12)	58(8)	39(6)	32(5)	16(5)	-19(5)	-23(6)
C(13)	48(7)	30(5)	34(5)	10(4)	-12(5)	1(5)
C(14)	30(6)	36(6)	24(5)	-1(4)	-15(5)	-11(5)
C(21)	31(6)	45(6)	27(5)	-8(4)	-11(4)	-8(5)
C(22)	90(9)	30(5)	15(4)	0(4)	-20(5)	9(6)
C(23)	65(8)	20(5)	25(5)	-2(4)	-2(5)	6(5)
C(24)	42(7)	18(5)	21(4)	5(4)	0(4)	8(5)
C(30)	54(7)	13(4)	24(5)	-1(3)	-1(5)	-6(4)
C(31)	56(7)	23(5)	29(5)	-3(4)	-2(5)	-11(5)
C(32)	84(9)	35(6)	31(5)	-6(4)	-9(6)	-9(6)
C(33)	127(13)	42(7)	72(8)	-10(6)	-39(8)	-23(8)
C(34)	41(7)	40(6)	37(5)	1(4)	-10(5)	-1(5)
C(35)	45(7)	46(6)	35(5)	-6(5)	3(5)	-10(5)
C(36)	82(10)	66(8)	55(7)	-9(6)	28(7)	-6(7)
C(41)	85(11)	43(7)	91(9)	2(6)	27(8)	4(7)
C(42)	101(12)	70(8)	59(8)	22(6)	2(8)	-17(8)
C(51)	50(8)	34(6)	55(6)	1(5)	8(6)	-5(5)
C(52)	53(8)	43(6)	47(6)	-6(5)	-2(6)	-19(6)

Table A-19.5. Hydrogen coordinates (x 10^4) and isotropic displacement parameters ($Å^2$ x 10^3) for Ti(dppm)$(NMe_2)_2$.

	x	y	z	U(eq)		x	y	z	U(eq)
H(11)	8715	1753	-262	57	H(35B)	5725	756	4265	51
H(12)	7389	3010	-9	53	H(36A)	4277	1919	4530	100
H(13)	5943	2627	1440	46	H(36B)	3582	1032	4783	100
H(21)	10727	1992	3843	42	H(36C)	3192	1507	3793	100
H(22)	10125	790	4937	55	H(41A)	11882	1273	765	108
H(23)	7971	104	4237	44	H(41B)	10697	893	1342	108
H(31A)	7310	-232	1875	43	H(41C)	12042	1178	1905	108
H(31B)	6385	-326	2755	43	H(42A)	12640	2798	1794	115
H(32A)	5430	200	876	60	H(42B)	11568	3418	1270	115
H(32B)	4516	57	1759	60	H(42C)	12303	2708	667	115
H(33A)	6000	-1331	974	123	H(51A)	7364	4439	2232	69
H(33B)	4480	-1167	664	123	H(51B)	7279	4079	1159	69
H(33C)	4902	-1437	1743	123	H(51C)	8376	4775	1480	69
H(34A)	5839	1974	3158	48	H(52A)	10310	4368	2491	72
H(34B)	4867	1469	2419	48	H(52B)	10418	3421	2930	72
H(35A)	4637	332	3539	51	H(52C)	9355	4081	3304	72